Eco-evolutionary dynamics in asexual populations : evolutionary rescue in Fisher's adaptive landscape

Yoann Anciaux

THÈSE POUR OBTENIR LE GRADE DE DOCTEUR DE L'UNIVERSITÉ DE MONTPELLIER

En biologie des populations et écologie

École doctorale GAIA

Unité de recherche ISEM

Dynamiques éco-évolutives en populations asexuées : Sauvetage évolutif dans le paysage adaptatif de Fisher

Présentée par Yoann Anciaux

Le 15 novembre 2017

Sous la direction de Ophélie Ronce et Guillaume Martin

Devant le jury composé de

Olivier Tenaillon, Directeur de recherche, INSERM	Rapporteur
Richard Gomulkiewicz, Professor, Washington state university	Rapporteur
Florence Débarre, Chargé de recherche, CNRS	Examinatrice
Sylvain Gandon, Directeur de recherche, CNRS	Examinateur
Ophélie Ronce, Directeur de recherche, CNRS	Directrice
Guillaume Martin, Chargé de recherche, CNRS	Co-directeur

UNIVERSITÉ DE MONTPELLIER

Résumé :

La capacité de persistance d'une population face à un changement environnemental stressant est une question complexe à l'interface entre l'écologie et l'évolution. Le processus par lequel une population échappe à l'extinction en s'adaptant aux nouvelles conditions environnementales stressantes est nommé sauvetage évolutif. Ce cas particulier de dynamique éco-évolutive est de plus en plus étudié autant théoriquement qu'expérimentalement, entre autres dans le contexte des changements environnementaux d'origines anthropiques. Cependant, les études modélisant ce processus négligent les interactions entre génotypes et environnements, qui impactent le potentiel évolutif des populations face aux changements environnementaux. Dans le cadre de cette thèse, j'ai développé des modèles intégrant ces interactions. Pour cela, j'ai modélisé le processus de sauvetage évolutif de populations à reproduction asexuée, face à des changements environnementaux abruptes, en utilisant le paysage adaptatif de Fisher (modèle géométrique de Fisher (1930)). Ce paysage nous a permis de modéliser ces interactions génotypes-environnements et leur impact sur la proportion de mutations pouvant sauver une population. A travers deux modèles, considérant soit le sauvetage d'une population par une mutation d'effet fort, soit par un grand nombre de mutations d'effets faibles, nous avons pu dégager des prédictions pour la probabilité de sauvetage évolutif en fonction des conditions environnementales et des caractéristiques de l'organisme étudié. Ces modèles peuvent être paramétrés sur des données d'évolution expérimentale et leurs prédictions comparées à des données de traitement antibiotiques visant des pathogènes asexués. Au-delà du sauvetage évolutif, les modèles développés nous ont également permis d'établir des outils permettant de modéliser d'autres dynamiques éco-évolutives, intégrant des interactions génotype-environnement et leurs effets sur la distribution d'effets des mutations.

Mots-clefs : Sauvetage évolutif – Paysages adaptatifs – Dynamiques éco-évolutives – Mutation – Asexué

Summary:

The ability of a population to persist when facing a stressing environmental change is a complex question at the interface between ecology and evolution. The process by which a population avoids extinction by adapting to the new stressing environmental conditions is termed evolutionary rescue. This particular case of eco-evolutionary dynamic is increasingly investigated both theoretically and experimentally, among other things in the context of the environmental changes caused by human activity. However, the studies modeling this process neglect the interactions between genotypes and environments that impact the evolutionary potential of the populations facing environmental changes. In the context of this thesis, I developed models integrating these interactions. To this end, I modeled the process of evolutionary rescue in asexual populations facing abrupt environmental changes, using the adaptive landscape of Fisher (Fisher's geometric model (1930)). This landscape allowed us to model the genotypes-environments interactions and their impact on the proportion of mutations needed to save a population. Using two models, considering either the rescue of a population by a single mutation of strong effect, orby a large number of mutations of small effect, we derived predictions for the probability of evolutionary rescue, which depends on the environmental conditions and the characteristics of the studied organism. These models can be parametrized on data from evolutionary experiments and their predictions compared to data of antibiotic treatments used against asexual pathogens. Beyond evolutionary rescue, the models developed in this thesis also give tools to model other eco-evolutionary dynamics, integrating genotype-environment interactions and their effects on the distribution of mutations effects.

Key-words: Evolutionary rescue – Adaptive landscapes – Eco-evolutionary dynamics – Mutation – Asexual

Remerciements

Trois ans !

Ces trois années ont représentées pour moi le périple houleux d'un jeune matelot, faisant des premières armes sur le navire de la thèse. L'arrivée à bon port de ce navire n'aurait jamais été possible sans l'ensemble des membres d'équipages qui m'ont accompagné au cours de cette thèse et à qui j'aimerais rendre hommage ici.

Trois années à l'ISEM, grâce à Guillaume Martin et Ophélie Ronce qui ont accepté de de m'encadrer, de me soutenir et de me guider au cours de ce périple.

J'aimerais tout d'abord remercier Guillaume qui a été à la fois mon capitaine et mon mentor au cours de ce périple. Guillaume m'a fait confiance pour débuter cette aventure dès mon stage de master et m'a fait découvrir la modélisation et ce *fameux modèle de Fisher*, puis m'a permis de débuter cette thèse. Par son enthousiasme, son esprit débordant de nouvelles idées, ses connaissances tant théoriques qu'expérimentales et son acharnement à dériver des formules mathématiques « plus simples », Guillaume m'a énormément appris au cours de cette thèse, tant au niveau méthodologique, qu'au niveau conceptuel.

J'aimerais aussi remercier Guillaume pour avoir toujours su garder le sourire et avoir su faire de n'importe quelle hypothèse mathématique un sujet de blague, afin de m'aider à rester optimiste. Et enfin j'aimerais le remercier lui et sa famille, Marie, Anouk et Thomas, d'avoir sacrifié tant de soirée et d'être resté tant de fois à la garderie pour m'aider à mener ma thèse à bien.

J'aimerais également remercier ma deuxième encadrante de thèse, Ophélie, qui a été la navigatrice de ce périple. Ophélie a toujours été présente afin de maintenir le cap et a su nous guider, Guillaume et moi, afin que nous évitions les nombreux écueils rencontrés au cours de ces trois ans. Elle a su également s'adapté à mon rythme de travail erratique et surtout à mon habitude de tout faire au dernier moment. J'aimerais aussi la remercier pour avoir élargie mon champ de vision scientifique par ses vastes connaissances dans tous les domaines de la biologie. Et enfin je souhaiterais rendre hommage à tous les efforts qu'elle fournit afin de rendre la science plus vivante au sein du labo, et grâce auxquels je suis maintenant un enthousiaste des conférences, quel que soit le sujet.

J'aimerais aussi remercier ceux qui m'ont fait confiance pour enseigner et m'ont donné goût à l'enseignement au cours de ces trois ans. Tout particulièrement à Sandrine Maurice et Céline Devault qui m'ont suivi depuis mon master et m'ont fait confiance pour passer de l'autre côté du bureau, à Pierrick Labbé avec qui je partage l'amour des shorts et qui m'a donné des responsabilités et m'a beaucoup appris et enfin à Eric Imbert et Agnès Mignot avec qui j'ai eu de passionnantes discussions sur l'éducation, l'administration et tout un tas d'autres sujets.

J'aimerais également remercier l'ensemble des membres d'équipage de métapop qui m'ont accueilli, écouté et accepté sans aucune restriction et qui ont su me soutenir tout au long de cette thèse à grand renfort de pause-café et de chocolat! J'aimerais tout particulièrement remercier les savoyards de l'équipe qui ont partagé avec moi la souffrance de vivre dans une région sans montagne ni neige!

J'aimerais remercier les doctorants de l'ISEM avec qui j'ai passé de super apéros devant l'ISEM, de super soirées et de super week-ends. L'esprit de communauté qui s'est installé entre les doctorants de l'ISEM m'a beaucoup aidé au cours de cette thèse et j'espère qu'il se perpétuera.

J'aimerais finalement remercier au sein de l'ISEM les membres de l'administration et tout particulièrement Fadela Tamoune, sans qui j'aurais vite été suffoqué par les démarches administratives des projets auxquels j'ai participé au cours de ma thèse.

Trois années loin de ma Savoie natale, qui est pourtant resté un sanctuaire ou j'ai toujours pu rentrer me ressourcer auprès de mes amis, des montagnes et de ma famille.

J'aimerais tout d'abord remercier mes parents qui m'ont soutenu dans tous les choix que j'ai fait jusqu'ici et qui continuent à me soutenir. Ils ont toujours été là quand j'avais besoin d'eux et spécialement au cours de ces trois ans et n'ont jamais rien attendu en retour et je les en remercie.

J'aimerais également remercier tous mes amis de Savoie qui ont su m'accueillir à chaque fois que je suis rentré et qui m'ont aidé à me rappeler que tous les soucis peuvent être oubliés sur les skis. Et j'aimerais également remercier tous mes amis de prépas qui sont souvent venus me rendre visite à Montpellier et qui m'ont rappelé que la thèse ce n'était qu'un moment à passer et qu'il y aurait un après.

Trois années à Montpellier avec mes amis, mes super colocs et Marjolaine.

Merci à Pierre, Paul, Adélaïde, Pachka d'avoir été mes mentors de thèse, de m'avoir poussé à sortir à la plage, à la pêche ou à l'apéro. Merci à Théo et Félise d'avoir été toujours aussi enthousiaste, joyeux et compatissants. Merci à Marine d'avoir été aussi patiente avec moi en cuisine. Merci à Paul et Coco de m'avoir fait oublier ma fin de thèse grâce aux jeux de rôles. Merci à Clémentine, Yoann et à tout ceux du rez-de-chaussée de l'ISEM qui m'ont soutenu pendant les moments difficiles et féliciter pour mes moments de réussite. Merci à Manon d'être restée une amie si fidèle et d'avoir toujours autant de caractère.

Merci à mes supers colocs avec qui j'ai passé trois ans dans un super appartement puis une super maison ! Grâce à Alain, Valentin, Marianne et Iago ces trois années à Montpellier sont passées beaucoup plus vite que prévue.

Merci Valentin d'avoir été le moteur des super projets de bricolage dans la maison, d'avoir toujours su relativiser sur les difficultés du boulot et d'être toujours aussi motivé, en particulier pour les fameuses potées !

Merci Marianne pour tous ces fous-rires, toutes ces idées loufoques, ces motivations de dernières minutes, ces recettes de cuisine au « pifomètre », ces après-midi DIY.

Merci Iago d'avoir toujours été ce fameux moteur diesel qui une fois partit mène les projets à bien, écoute d'une oreille bienveillante les tracas de chacun et aide sans compter dès qu'un problème survient.

Merci à Alain, qui a été à mes côtés depuis le début du master et a toujours su rester mon plus fidèle amis. Merci Alain pour avoir su partager avec moi depuis plus de cinq ans ta culture, ta sérénité, mais aussi ta joie de vivre, des folles soirées, des moments de tristesse, de joie ou de frustration.

Et enfin merci à Marjolaine qui a été pour moi le phare qui m'a guidé à bon port, le vent soufflant dans mes voiles, la mer qui m'a porté et le soleil qui m'a réchauffé. Merci d'avoir tout donné sans jamais rien demander et d'avoir su croire en moi quand je n'y croyais plus.

Trois années de travail, d'acharnement, de déception et de frustration. Trois années de joie, de rigolades, d'enthousiasme et de découverte. Mais surtout trois années partagées avec des gens qui m'ont soutenu, dirigés, aidés et aimés. Merci à tous ceux qui ont été présents pour moi durant ces trois ans et sans qui cette belle expérience aurait été tout autre.

_ _ _ _

Table des Matières

Remerciements ..... - 7 -
Table des Matières ..... - 11 -
Introduction ..... - 13 -
CHAPTER I Evolutionary rescue over a fitness landscape ..... - 43 -
CHAPTER I Appendix: Analytical derivation ..... - 77 -
CHAPTER II Population persistence under high mutation rate: from evolutionary rescue to lethal mutagenesis ..... - 101 -
CHAPTER II Appendix: Mathematical derivations and approximation ..... - 131 -
CHAPTER III Theoretical and empirical perspectives ..... - 145 -
Discussion ..... - 169 -

Introduction

I. L'écologie et l'évolution

La biologie est caractérisée par la longévité de ses problématiques (p.22 Mayr 1982). Comprendre les changements de diversité biologique dans le temps et dans l'espace est une des plus anciennes problématiques dans l'étude du vivant mais également une des plus actuelles. Cette question a soulevé et soulève encore actuellement des questionnements sociétaux sur la place et l'impact de l'Homme sur son environnement. L'écologie et l'évolution sont deux domaines dont la construction s'est faite autour du sujet de la diversité du vivant et dont les questionnements actuels convergent sur l'impact des activités anthropiques sur cette diversité, en utilisant des concepts issus d'un riche développement historique parallèle des deux domaines depuis plus d'un siècle.

"Research initiatives in ecology and evolution have periodically dated but never married" (Hendry 2016)

Les rencontres entre l'écologie et l'évolution tant sur des aspects théoriques que sur des aspects empiriques se sont multipliées ces dernières décennies avec l'avènement des études sur les dynamiques éco-évolutives, portant sur les interactions entre dynamiques écologiques et dynamiques évolutives sur des temps contemporains (Schoener 2011; Hendry 2016). En retraçant l'histoire de l'écologie et de l'évolution, la valeur de leur union est évidente. Des différences dans les conditions écologiques ont indiscutablement mené à de significatifs changements évolutifs, tout comme de grands changements évolutifs ont indéniablement entraînés des conséquences écologiques. L'objectif de cette introduction est de montrer l'intérêt d'associer des dynamiques écologiques et évolutives et plus particulièrement de mettre en évidence les apports de l'étude des dynamiques éco-évolutives au problème de la persistance des populations.

I.1. Aspects historiques

Au milieu du XIXème siècle, l'émergence des disciplines de l'écologie et de l'évolution fait suite à un siècle de description naturaliste prolixe, avec comme objectifs de comprendre et d'analyser les processus régissant l'incroyable diversité décrite au cours des grandes expéditions naturalistes. Charles Darwin et Alfred Wallace, célèbres pour leur contribution à la théorie de l'évolution, sont deux

parfait exemples de ces naturalistes ayant débuté la conceptualisation des processus expliquant la diversité des organismes dans le temps et dans l'espace (Mayhew 2006).

L'écologie et l'évolution se sont séparées à la fin du XIXème siècle. L'écologie s'est orientée vers la compréhension des interactions entre les êtres vivants et leur environnement tandis que l'évolution s'est focalisée sur les changements temporels dans les caractères héritables des êtres vivants. Au début du XXème siècle, les deux domaines se sont développés parallèlement sur un plan empirique avec le développement de la génétique en évolution (Galton, Pearson, Morgan) et la multiplication des observations en populations naturelles en écologie (Clements, Bonnier, Warming). Sur un plan théorique, les deux disciplines se sont développées en s'inspirant de la philosophie réductionniste de la physique statistique et de la mécanique, permettant des approches mécanistiques des processus biologiques (Delord 2009). De ce développement théorique émergèrent parallèlement la génétique des populations en évolution (Fisher, Wright, Haldane) et la dynamique des populations en écologie (Lotka, Volterra).

L'intégration des processus écologiques et évolutifs au sein d'une même théorie est difficilement envisageable au début du XXème siècle car ces deux théorisations parallèles des dynamiques des populations reposent sur des présupposés les rendant incompatibles. Premièrement, les processus évolutifs et écologiques sont supposés avoir un rôle sur des échelles de temps tellement différentes que l'évolution peut être ignorée dans des dynamiques écologiques contemporaines (Slobodkin 1961) tandis que les dynamiques écologiques peuvent être négligées sur des échelles évolutives. Cette différence dans la temporalité se traduit aussi par une conception différente du temps lui-même. En écologie le temps est similaire à la grandeur employée par les physiciens, un temps uniforme linéaire et absolu avec une orientation, mais qui reste réversible dans les équations fondamentales. Cette notion est opposée au temps historique, à l'accumulation d'événements au cours du temps, qui a une importance centrale sur l'aspect plus ou moins irréversible de l'évolution. Deuxièmement, l'écologie et l'évolution se sont également développées sur des échelles biologiques différentes se rejoignant à l'échelle de la population. L'évolution s'est focalisée sur des aspects populationnels, génétiques et moléculaires tandis que l'écologie s'est développée autour des populations, des communautés et des écosystèmes. À la fin des années 1930, l'incompréhension mutuelle entre évolution et écologie est telle que l'écologie est absente de la synthèse évolutive néo-darwinienne menée entre autres par R.A. Fisher, J.B.S Haldane, Sewall Wright, Theodosius Dobzhansky ou Julian Huxley.

Depuis cette séparation importante entre les théories écologiques et évolutives, de nombreuses approches se sont développées dans un but de convergence des deux domaines, dans l'objectif, *"si ce n'est d'accomplir une véritable unification de la biologie, du moins de souligner la complémentarité théorique entre ces deux interprétations des phénomènes macrobiologiques"* (Delord 2009). Au milieu du XXème siècle, une volonté de réunification des deux domaines à l'échelle des populations a donné lieu à l'émergence de la biologie des populations, convergence des disciplines jusqu'alors distinctes de la génétique des populations, de l'écologie des populations, de la biogéographie et d'études évolutives avec des objectifs théoriques relativement holistiques (Levins 1968). Certains écologistes et évolutionnistes ont souhaité changer ce paradigme de différence d'échelles temporelles et biologiques, en considérant des changements évolutifs substantiels sur des échelles de temps courtes (de l'ordre de quelques générations) interagissant directement avec des processus écologiques (pour une revue voir Pelletier *et al.* 2009). Ce développement a ensuite été soutenu par un grand nombre d'études empiriques en populations naturelles, considérant des processus écologiques et évolutifs contemporains (Hendry and Kinnison 1999; Stockwell *et al.* 2003; Schoener 2011; Hendry 2016).

"The fusion of population genetics with population ecology can be compared to a prearranged marriage between partners who speak different languages. Although both families agree that the marriage is advantageous, it is somewhat difficult to achieve because of cultural differences between geneticists and ecologists." (Roughgarden 1979)

Depuis le milieu du XXème siècle de nombreux développements théoriques et empiriques sont venus renforcer les interactions entre les domaines évolutifs et écologiques. Cette interface entre deux domaines s'est développée sous les noms d'écologie évolutive ou encore de dynamique éco-évolutive et regroupe, selon une définition large: les changements écologiques influençant les changements évolutifs (*éco vers évo*), les changements évolutifs influençant les changements écologiques (*évo vers éco*) et les boucles de rétroactions entre écologie et évolution. Ces trois différentes classes ne sont évidemment pas exclusives et n'ont qu'un but didactique.

Les relations *éco vers évo* font référence entre autres à l'impact de variables écologiques sur le potentiel évolutif de l'objet d'étude (Charmantier and Garant 2005; Hoffmann and Sgrò 2011). L'importance de la prise en compte de l'hétérogénéité de l'habitat, de la répartition spatiale des organismes et des capacités de dispersion sur l'évolution a également été mise en évidence au cours des dernières décennies par des modèles intégrant la dimension spatiale et la connectivité entre les

populations étudiées ainsi que par des études en population naturelle. La spéciation écologique est un exemple où des variables écologiques vont mener à une séparation évolutive de deux populations jusqu'à la spéciation. Les relations *évo vers éco* ont été développées plus récemment. Les changements évolutifs observés à des échelles génétiques, phénotypiques ou populationnelles impactent les interactions écologiques aux échelles des populations, des communautés voir même des écosystèmes (Pelletier *et al.* 2009). La **Figure 1,** modifiée de Hendry (2016) schématise les interactions éco vers évo au niveau intra (**Figure 1A**) et inter-populationnel (**Figure 1B**) et leur complémentarité avec les interactions évo vers éco formant des boucles de rétroaction (**Figure 1C**).

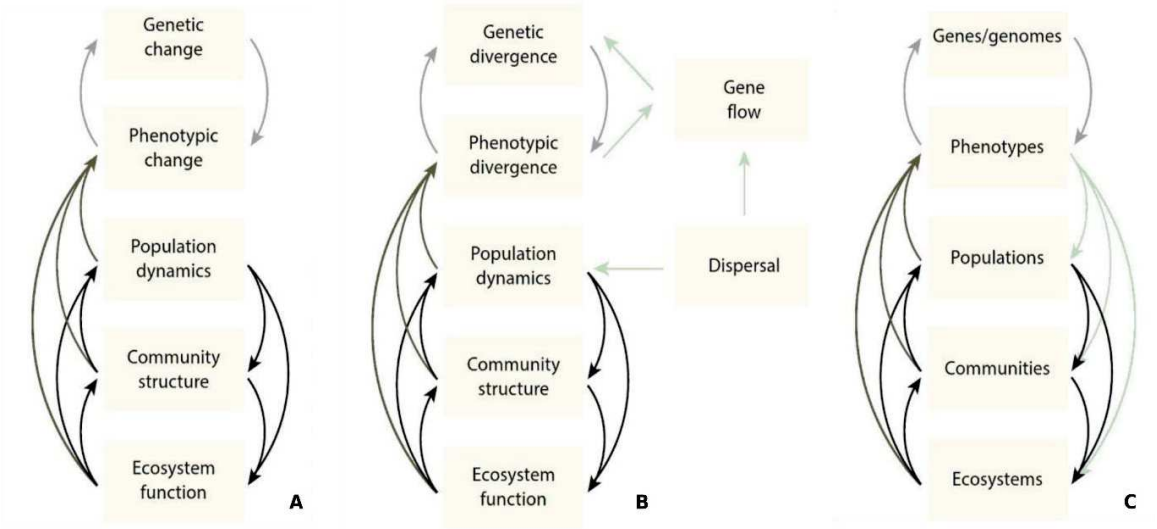

Figure 1 : *Représentation graphique des dynamiques éco-évolutives pour une (ou plusieurs) population(s) d'organismes focaux (3 premiers compartiments) en relation avec son (leur) environnement (2 derniers compartiments). Schéma des interactions éco vers évo au niveau intra (**A**) et inter-populationnel (**B**) et leur complémentarité avec les interactions évo vers éco formant des boucles de rétroactions (**C**). Les flèches représentent les interactions entre plusieurs compartiments.*

Les modèles évolutifs intégrant la démographie permettent ainsi d'étudier l'impact des différents traits d'histoire de vie et de la valeur sélective sur les variations démographiques des populations, au sein des communautés. Ces modèles ont été également développés récemment dans le cadre de l'étude du sauvetage évolutif, portant sur l'impact de l'adaptation d'une population à un nouvel environnement sur la probabilité de persistance de cette population. Ainsi, les relations unilatérales *éco vers évo* ou *évo vers éco* sont de plus en plus couplées dans les modèles, faisant intervenir des boucles de rétroaction liant écologie et évolution (Ferriere and Legendre 2013). Les différents modèles mettent l'accent plutôt sur la partie évolutive ou la partie écologique selon leur domaines d'origines. Les modèles de relations hôte-pathogène ont largement développé ces boucles

de rétroaction avec des phénomènes de densité-dépendance et de fréquence-dépendance (Pelletier *et al.* 2009). La modélisation de ces dynamiques nécessite d'intégrer des processus sur des échelles temporelles communes et des niveaux biologiques multiples tout en intégrant des processus stochastiques démographiques comme évolutifs. Au cours des dernières décennies, une littérature grandissante s'est intéressée aux relations étroites régissant les processus évolutifs et écologiques à l'échelle des populations. Ce récent développement tient autant à l'acquisition de données à l'interface entre ces deux domaines qu'aux développements théoriques intégrant des interactions éco-évolutives.

I.2. La biologie des populations

La population en écologie et en évolution

La différence d'échelle de temps entre les processus écologiques et évolutifs a longtemps été évoquée comme la principale difficulté pour lier ces deux domaines. Néanmoins, cette hypothèse de séparation des échelles de temps a été réfutée par de nombreuses études empiriques en populations naturelles ou en laboratoire, réalisées au cours des dernières décennies. La différence d'échelle biologique entre les processus écologiques et évolutifs semble par contre être une véritable difficulté. Les processus évolutifs sont étudiés à des échelles allant du génome à la (méta)population, alors que les processus écologiques sont étudiés à des échelles allant de l'individu à la communauté voire même à l'écosystème. Ainsi les dynamiques éco-évolutives se sont principalement développées au niveau populationnel, au sein duquel les deux domaines présentent chacun une littérature dense. Ce champ disciplinaire particulier est appelé dynamique des populations.

La population est un objet intéressant en termes de modélisation. Il est difficile de donner une définition stricte de ce que représente une population. La population se situe entre le niveau individuel et le niveau de l'espèce, et les individus qui la composent partagent une unité temporelle, démographique et géographique. Les limites du concept de population dépendent du problème étudié et sont souvent définis dans le but de réduire la complexité liée à la modélisation de ses dynamiques. Les problématiques éco-évolutives au niveau populationnel portent sur les processus liant la variance génétique et l'hétérogénéité environnementale temporelle et spatiale à la démographie et la répartition de cette population dans l'espace et dans le temps. Le niveau intermédiaire de la population par rapport aux communautés et aux gènes permet de rapprocher les échelles écologiques

et évolutives décrites précédemment. A cette échelle l'écologie et l'évolution sont toutes deux affectées par les taux de natalité et de mortalité, eux même influant sur la valeur sélective moyenne de la population qui est associée au taux de croissance de la population. Ce lien intuitif entre évolution et démographie remonte aux prémices des deux domaines, Darwin s'étant inspiré de la démographie de Malthus pour écrire *l'Origine des espèces*. A travers ce lien, les interactions entre les organismes au sein d'une population, mais également avec leur environnement biotique et abiotique, vont définir les pressions de sélection subies par les individus. De même, les différentes forces évolutives adaptatives ou non-adaptatives vont façonner la diversité des individus interagissant.

Modélisation en biologie des populations

Le domaine de la biologie des populations intègre simultanément la génétique, la physiologie, la structure d'âge et la répartition géographique d'espèces au sein de systèmes multi-espèces, changeant démographiquement et évoluant en interaction avec d'autres espèces dans des environnements hétérogènes. Comment modéliser des systèmes si complexes ?

Levins décrit dans "The strategy of model building in population biology" (Levins 1966), l'aspect stratégique de la construction de modèles en biologie des populations. La modélisation, en particulier en écologie et en évolution, répond pour Levins à un compromis entre généralisation, réalisme et précision, inhérent à toute approche modélisatrice de la diversité du vivant et tout particulièrement des approches intégratives à l'interface entre l'écologie et l'évolution. Trois stratégies sont alors possibles:

- Sacrifier la généralité et le réalisme à la précision. Ces modèles ont souvent une approche statistique d'un problème, permettant de prédire quantitativement la réponse d'un système aux variations de paramètres synthétiques. Ces modèles souvent utilisés pour leur intérêt pratique, comme par exemple dans la gestion des stocks halieutiques, sont souvent décriés, sous le terme de "Black Box", car trop peu mécanistiques pour permettre une compréhension claire des processus sous-jacents (D. S. Wilson (1988)).

- Sacrifier le réalisme et la précision à la généralité. Les modèles mathématiques développés dans la première moitié du XXème siècle tombent souvent dans cette catégorie de par l'utilisation d'hypothèses simplificatrices autant en écologie qu'en évolution. Ces modèles ont pour but final de développer des théories très générales mais parfois difficiles à appliquer empiriquement.

- Sacrifier la précision et la généralité au réalisme. Cette dernière approche mécanistique a pour but la compréhension des processus et la prédiction du futur, mais de manière qualitative. Levins et MacArthur se revendiquent de cette stratégie (Levins 1968).

Il est difficile de juger de manière générale de la supériorité d'une approche sur les autres. En revanche chaque stratégie répond à des objectifs dont dépend « l'utilité » du modèle pour traiter d'un sujet donné. Cette contingence de « l'utilité d'un modèle peut-être résumé par l'aphorisme de de Georges Box *"essentially, all models are wrong, but some are useful"* (Box and Draper 1987). Ainsi, les modèles et les hypothèses qui ne sont pas en adéquation avec la "réalité" des observations sont graduellement remplacés par ceux les reflétant mieux (Popper 1959). Cependant, la multiplicité des modèles en écologie et en évolution, et la difficulté des tests empiriques rendent difficile une unification théorique synthétique sous forme de "grandes lois". Les théories émergent alors de la multiplicité de modèles alternatifs traitant d'un même sujet avec des hypothèses très différentes. Cette stratégie est résumée avec humour par Levins: *"Then, if these models, despite their different assumptions, lead to similar results we have what we can call a robust theorem which is relatively free of the details of the model. Hence our truth is the intersection of independent lies."* (Levins 1966). Une théorie "satisfaisante" selon Levins est alors formée d'un groupe de modèles robustes et complémentaires liés par le phénomène cherchant à être décrit.

Le développement des modèles de dynamique des populations répond très bien aux stratégies décrites par Levins. La multiplicité des modèles étant imposée par la contradiction entre simplicité de modélisation et complexité de la diversité du vivant et de l'environnement. Cependant ce développement théorique n'a pas directement été suivi par un développement empirique des dynamiques éco-évolutives. Il a fallu attendre le développement de nouvelles méthodes de mesures simples et robustes de la sélection, de la valeur sélective et de la variance phénotypique dans les traits d'histoire de vie, à partir des années 1980, afin de déterminer des paramètres mesurables pour tester ces modèles théoriques. De même l'accumulation de jeux de donnée sur de longs pas de temps en population naturelle ou en laboratoire ont permis de tester et d'émettre de nouvelles hypothèses en dynamique des populations (Pelletier *et al.* 2009).

L'explosion récente d'études et de livres sur les dynamiques éco-évolutives (Ferrière *et al.* 2004; Mayhew 2006; Pianka 2011; Hendry 2016) ont permis d'explorer de nombreuses questions autour de la dynamique des populations et confortent l'importance de la prise en compte des relations entre écologie et évolution au sein de ces dynamiques (Schoener 2011; Kingsolver *et al.* 2012; Lowe

et al. 2017). Cependant, l'espace englobant l'ensemble de ces interactions reste encore largement inexploré. Des questions centrales autour de la dynamique des populations, des communautés et des écosystèmes restent encore ouvertes, au cœur des problématiques des deux domaines (pour une revue actuelle des cent questions centrales en écologie voir Sutherland *et al.* (2013), pour les questions centrales liant l'évolution et l'écologie voir Pelletier *et al.* (2009) et Lowe *et al.* (2017)).

II. Le sauvetage évolutif ou la dynamique des populations appliqué à la problématique de l'extinction

Décrire, comprendre et prédire la dynamique des populations est particulièrement important lorsque l'environnement change et stresse les organismes. Lorsque ce stress est suffisamment important pour qu'une population risque l'extinction, il est alors essentiel d'évaluer dans quelles conditions et avec quelle probabilité cette population persiste ou s'éteint. Pour que la population échappe à l'extinction, l'effondrement démographique d'une population doit être contrebalancé par une augmentation de sa taille ou par une fuite de la population de l'environnement stressant vers un nouvel environnement plus adéquat. Les changements démographiques et évolutifs opérant au sein d'une population peuvent alors impacter les dynamiques d'autres populations de la communauté et même le fonctionnement de l'écosystème. L'analyse des aspects évolutifs et démographiques, via la dynamique des populations, permet donc de comprendre comment des populations et éventuellement des communautés vont être modifiées dans l'espace et dans le temps par leur environnement mais également comment, en retour, celles-ci vont impacter l'environnement.

II.1. Qu'est-ce que le sauvetage évolutif

La persistance des populations est au cœur de plusieurs enjeux sociétaux. Dans le domaine de la conservation, la gestion des populations face aux changements environnementaux et plus particulièrement aux pressions anthropiques est une problématique appliquée, nécessitant des outils théoriques complexes. La dynamique des populations, selon la définition éco-évolutive évoquée dans la section précédente, est donc un outil essentiel pour répondre aux questions soulevées par la persistance des populations face aux changements environnementaux. Le sauvetage évolutif est le terme consacré, dans le cadre des dynamiques adaptatives, à l'étude des processus écologiques et évolutifs de la persistance des populations face à des changements environnementaux stressants. Il a été défini dans Gomulkiewicz et Holt (1995) en tant que processus d'adaptation permettant à la population de faire face à un risque démographique. La littérature sur le sujet, autant théorique

qu'empirique s'est grandement développée depuis une dizaine d'année (voir **Figure 2**), intégrant de multiples interactions (pour des revues voir Hoffmann and Sgrò (2011) et Gonzalez *et al.* (2013)) et des rétroactions éco-évolutives (e.g. Gonzalez *et al.* 2013; Osmond *et al.* 2017; Colautti *et al.* 2017; Moreno-Fenoll *et al.* 2017; Bay *et al.* 2017). Ainsi le sauvetage évolutif est désormais associé aux problématiques de dynamiques d'invasion (Gomulkiewicz *et al.* 2010), à la structuration des communautés (Osmond and Mazancourt 2013) , ou encore aux dynamiques épidémiologiques (Gandon *et al.* 2013).

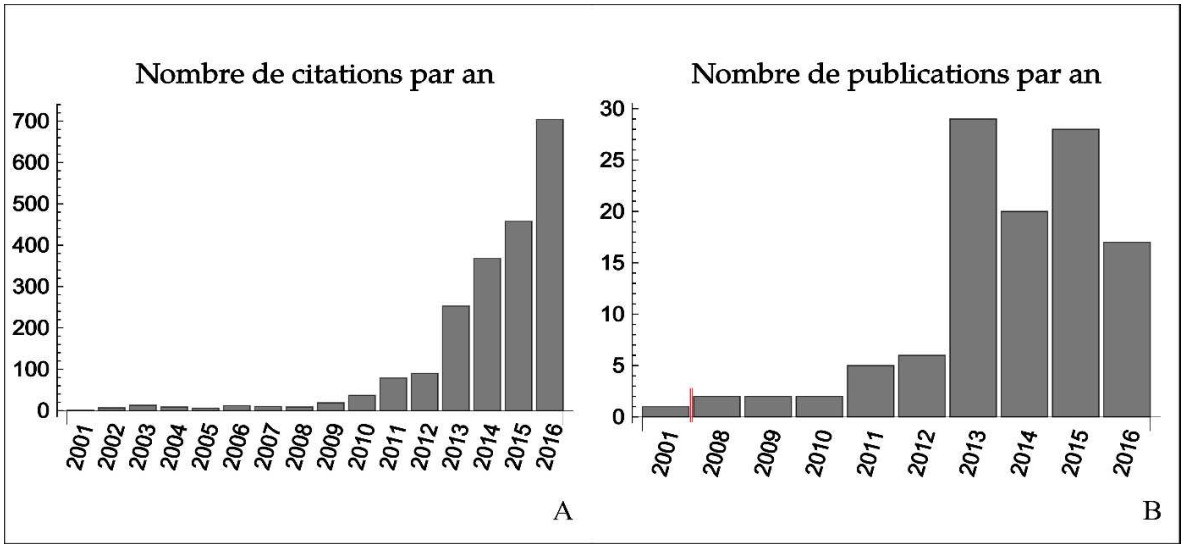

Figure 2 : *Nombre de citations (A) et nombres de publications (B) par an faisant référence au terme "Evolutionary Rescue". Les données ont été recueillies par une recherche via le portail Web of Science.*

Ce développement conceptuel et théorique s'est accompagné de démonstrations expérimentales (Bell and Collins 2008; Bell and Gonzalez 2009; Samani and Bell 2010; Agashe *et al.* 2011; Bell 2012; Lachapelle and Bell 2012; Bell 2013; Samani and Bell 2016) et d'études en populations naturelles des phénomènes de sauvetage évolutif (Gomulkiewicz and Shaw 2013; Gonzalez *et al.* 2013; Wal *et al.* 2013 p. 201). L'apparition de résistance aux traitements anti-pathogènes tels que les antibiotiques est un cas de sauvetage évolutif particulièrement pertinent et fournit de grandes quantités de données expérimentales, même si le dialogue entre écologie-évolution et médecine est encore peu développé (Alexander *et al.* 2014; Hiltunen *et al.* 2017).

II.2. Modélisation de la dynamique des populations en environnement changeant.

Historiquement l'étude du concept de sauvetage évolutif s'est d'abord focalisée au niveau théorique sur la capacité d'une population à persister face à un changement d'environnement, stressant et graduel, représentant les changements climatiques globaux (Pease *et al.* 1989; Lynch *et al.* 1991; Lynch and Lande 1993). Puis la littérature s'est séparée en deux tendances autour des changements abrupts (Gomulkiewicz and Holt 1995) ou graduels (Burger and Lynch 1995) permettant de considérer des situations biologiques très différentes comme l'apparition de résistance à un traitement antibiotique ou l'adaptation aux changements climatiques.

Les modèles de sauvetage évolutif peuvent également être séparés sur la base des différences de leurs hypothèses quant à la base génétique à l'origine du sauvetage évolutif. Deux traditions existent dans la modélisation de la base génétique de l'adaptation à l'origine des sauvetages évolutifs, résumée par Alexander et al. (2014) : les modèles de génétique quantitative et les modèles génétiques discrets. Les modèles génétiques discrets supposent une base génétique de l'adaptation restreinte, pour laquelle une unique mutation bénéfique peut sauver une population isogénique (Gomulkiewicz and Holt 1995; Orr and Unckless 2008; Martin *et al.* 2013; Uecker *et al.* 2014; Orr and Unckless 2014; Uecker and Hermisson 2016; Uecker 2017). Ces modèles ont permis l'introduction de processus stochastiques dans les modèles de sauvetage évolutif (Holt and Gomulkiewicz 1997; Iwasa *et al.* 2003; Orr and Unckless 2008). Le gain dans la capacité prédictive associé à l'introduction des stochasticités démographiques et évolutives dans les modèles s'intéressant à la persistance des populations a été mis en évidence analytiquement (Lande 1993; Otto and Whitlock 1997) et numériquement (Burger and Lynch 1995; Boulding and Hay 2001; Holt *et al.* 2003). A l'opposé des modèles génétiques discrets, les modèles de génétique quantitative considèrent que l'adaptation est causée par l'évolution d'un trait quantitatif dont l'optimum varie selon l'environnement (Lynch *et al.* 1991; Burger and Lynch 1995; Gomulkiewicz and Holt 1995). Ces modèles font souvent l'hypothèse d'une large base génétique polygénique, permettant de considérer l'effet de multiples variants, mais négligent souvent la variabilité au cours du temps de la variance génétique. Les modèles supposant un changement évolutif abrupt intègrent pour la plupart des modèles génétiques discrets tandis que les modèles supposant un changement environnemental graduel intègrent souvent des modèles de génétique quantitative (même si des exceptions existent Gomulkiewicz and Holt (1995) ou Uecker *et al.* (2014)). La pertinence de ce choix de modélisation de la base génétique en fonction du taux de changement environnemental a été démontrée récemment de manière empirique (Lindsey *et al.*

2013; Gorter *et al.* 2017). Les changements environnementaux graduels autoriseraient des sauvetages évolutifs à partir d'une base génétique plus large que les changements environnementaux abrupts.

La littérature théorique a, dans un premier temps, été développée sur des modèles de sauvetage évolutif à une échelle locale pour des populations isolées, puis les modèles se sont spatialisés, ajoutant la migration aux forces évolutives déjà prises en compte. La migration est une force éco-évolutive interagissant fortement avec le potentiel évolutif d'une population en faisant varier la démographie et éventuellement la variance génétique disponible. Elle a été introduite dans les modèles de sauvetage évolutif par Holt and Gomulkiewicz (1997) via un modèle île-continent basé sur le modèle de MacArthur and Wilson (1967). La force de la migration et les variants génétiques associés dépendent alors de la connectivité entre les populations et de l'hétérogénéité des conditions environnementales. Cette spatialisation des modèles de sauvetage évolutif est également à l'origine de l'introduction de changements environnementaux spatiaux (Holt *et al.* 2003, 2004) en plus des changements temporels déjà considérés. Le destin démographique local d'une population est alors lié à la métapopulation (Uecker *et al.* 2014) voire même à la communauté d'espèce (Osmond and Mazancourt 2013; Osmond *et al.* 2017) avec laquelle elle interagit. La spatialisation des modèles étend également le sauvetage évolutif à l'étude des phénomènes d'invasion et de changement d'aire de répartition (Holt and Gomulkiewicz 1997; Holt *et al.* 2003, 2004; Odling-Smee *et al.* 2013). En associant les modèles de sauvetage évolutif au concept de niche écologique (ensembles de conditions environnementales nécessaires, caractérisant un espace où une population peut persister sans immigration (Holt *et al.* 2004), les aires de répartitions des espèces sont façonnées par l'équilibre entre les dynamiques de persistance des populations locales dans un environnement hétérogène, la connectivité entre les populations et les capacités de dispersion (Pease *et al.* 1989; Kubisch *et al.* 2014; Aguilée *et al.* 2016).

Tous ces modèles ont en commun, outre l'aspect central de la force et du taux auquel change l'environnement, l'importance de la taille de la population initiale et de sa variance génétique sur la probabilité de persistance des populations. La variance génétique disponible ou nouvellement créée va en effet impacter la vitesse d'adaptation (Fisher 1930). Son rôle central dans la réponse aux changements environnementaux et la persistance des populations, a été à de nombreuses reprises mis en avant dans la littérature (Hoffmann and Parsons 1997; Hoffmann and Merilä 1999; Willi and Hoffmann 2009).

II.3. Variance génétique, potentiel évolutif et sauvetage évolutif

La variance génétique peut être générée par de la migration, comme vu précédemment, mais dépend également, à un niveau plus local, d'autres forces évolutives. La création de variance génétique, en population isolée, dépend de la mutation et de la recombinaison. Dans de nombreux modèles de sauvetage évolutif (entre autres), la recombinaison est considérée dans le cadre d'équilibres (recombinaison-sélection) où la variance génétique disponible est maintenue constante au cours du processus d'adaptation. Cette hypothèse simplifie ainsi les développements analytiques de nombreux modèles basés sur des traits quantitatifs sous sélection stabilisante. La recombinaison est en effet une force importante de création de nouvelles combinaisons d'allèles chez des espèces sexuées. Elle accélère la dynamique adaptative, ce qui se révèle essentiel dans un cadre de risque d'extinction à court terme. Un modèle de sauvetage évolutif intégrant un modèle de recombinaison explicite a été développé par Uecker and Hermisson (2016) mais celui-ci reste inféodé à des cas à deux loci bi-alléliques. La mutation est également un processus de création de variance génétique historiquement utilisé dans les modèles de sauvetage évolutif, principalement dans les modèles génétiques discrets, avec des espèces asexuées. Les modèles de mutation utilisés considèrent qu'une mutation avec un certain effet sélectif est présente dans la population ou apparaît au cours de la dynamique. Cette mutation ségrége ensuite dans la population jusqu'à sa fixation ou sa disparition (stochastique ou sélective) (Gomulkiewicz and Holt 1995; Orr and Unckless 2008; Uecker *et al.* 2014; Orr and Unckless 2014).

Dans les modèles génétiques discrets évoqués précédemment, la valeur sélective des variants considérés dépend de l'environnement de manière arbitraire : un allèle a un coût donné dans l'environnement initial et un avantage donné dans l'environnement stressant. Ils permettent de modéliser la probabilité que ces variants soient à l'origine d'un sauvetage évolutif mais n'intègrent pas l'effet des conditions environnementales sur la probabilité que ces variants apparaissent ou sur la distribution de leurs valeurs sélectives (avant ou après le changement environnemental). Cependant, un stress environnemental n'affecte pas uniquement la démographie de la population, mais également son taux d'adaptation (Hoffmann and Parsons 1997; De Visser and Rozen 2005; Agrawal and Whitlock 2010). En prenant le cas de la mutation, il a été montré que le taux d'apparition des mutations et la distribution de leurs effets change entre environnements, particulièrement en fonction du 'stress' imposé par ceux-ci (Martin and Lenormand 2006a; Wang *et al.* 2009; Agrawal and Whitlock 2010; Wang *et al.* 2014). De même, la distribution des effets sur la valeur sélective des

variants préexistants au changement d'environnement peut dépendre du stress environnemental. On pourrait par exemple s'attendre à ce qu'une mutation de résistance à un stress fort, soit aussi plus coûteuse et plus rare, qu'une résistance à un stress faible. Ces interactions, entre contextes génétiques et environnementaux (GxE), largement développées en génétique quantitative, peuvent jouer un rôle essentiel dans le lien entre un changement environnemental et la variance génétique et phénotypique disponible pour y répondre.

L'introduction d'une dépendance entre le potentiel évolutif et le contexte génétique et environnemental reste une lacune dans les modèles de sauvetage évolutif et plus généralement dans les dynamiques éco-évolutives. On peut parfois modéliser la dépendance entre génotype, phénotype, valeur sélective et environnement de manière précise pour certaines espèces modèles, dans des environnements bien contrôlés/caractérisés. Ces prédictions reposent sur une connaissance détaillée des variations des phénotypes, et leur impact sélectif, au niveau morphologique (Salazar-Ciudad and Jernvall 2010) ou métabolique (pour revue voir Papp *et al.* (2011)). Cependant, généraliser ces interactions à un ensemble d'environnements (potentiellement un gradient) ou d'espèces non modèles devient alors quasi-impossible. Alternativement, on peut perdre en précision et gagner en généralité en utilisant un modèle plus abstrait de ces relations génotype-environnement : un paysage adaptatif simple, dont les paramètres dépendent de l'environnement (voir la discussion dans Martin (2014)). Ces paysages 'classiques' (Fisher 1930; Lande 1976, 1980) ont été largement utilisés en évolution. Ils présentent une conceptualisation et un traitement analytiques, tout en ayant démontré un certain réalisme empirique (pour revue voir Tenaillon (2014)). La prise en compte de l'effet des changements environnementaux sur le taux d'apparition de mutants et la distribution des effets des mutations sur la valeur sélective, dans les modèles de sauvetage évolutif, est un des objectifs principaux de cette thèse. Nous l'abordons au moyen de ces paysages adaptatifs.

III. Les paysages adaptatifs et la dépendance au contexte génétique et environnemental

La section précédente a permis de mettre en évidence les nombreux mécanismes ayant été intégrés récemment dans les modèles de sauvetage évolutif. Cependant, ces modèles n'intègrent pas de dépendance entre l'environnement et le potentiel adaptatif du ou des génotypes de la population considérée. Une telle dépendance émerge automatiquement dans les modèles de paysages adaptatifs, sous une forme qui semble décrire une part substantielle des patrons observés empiriquement, quant

à l'effet sélectif des mutations entre environnements (Martin and Lenormand 2006a; Hietpas *et al.* 2013; Harmand *et al.* 2016) ou entre fonds génétiques (Martin *et al.* 2007; MacLean *et al.* 2010; Trindade *et al.* 2012). La qualité des prédictions quantitatives des modèles de sauvetage évolutif basés sur le processus de mutation pourrait donc être améliorée par l'inclusion de cette dépendance. La section suivante détaille une version particulière de ces paysages adaptatifs, le modèle géométrique de Fisher, et la compare à d'autres modèles d'adaptation, dans le cadre de la modélisation de l'adaptation aux changements environnementaux.

III.1. Les paysages adaptatifs et le modèle géométrique de Fisher

Les modèles de paysages adaptatifs sont nés dans la première moitié du XXème siècle. Le concept de paysage adaptatif a été introduit par Wright (1932) en tant que métaphore topographique afin de faciliter la compréhension des modèles d'adaptation développés dans ses travaux (Svensson and Calsbeek 2012). Originellement, l'analogie représentait une carte topographique dont les deux dimensions horizontales correspondaient à un espace génétique et la dimension verticale représentait la valeur sélective des génotypes, dans un environnement donné. La topographie en collines et vallées représentait les combinaisons génétiques ayant respectivement une forte et une faible valeur sélective. Cette métaphore a depuis été largement utilisée en évolution autant pour son intérêt didactique, que pour la simplicité méthodologique de sa géométrie dans le cadre de dérivations analytiques (résumé dans Orr 2005).

Vers la même époque, Fisher a proposé en quelques lignes, dans son livre de 1930 (Fisher 1930), un modèle géométrique d'adaptation dont la structure se prête à une métaphore similaire de «paysage adaptatif ». Dans ces deux versions, des pics et vallées correspondent à des génotypes de plus ou moins forte valeur sélective, et des sauts dans le paysage correspondent à des changements génétiques (mutations, recombinaisons), d'où une certaine confusion, parfois encore aujourd'hui, entre ces deux formes de 'paysages'. Pourtant, elles diffèrent grandement dans leurs caractéristiques centrales comme dans leur utilisation (pour une description des différentes formes de 'paysages adaptatifs', voir Gavrilets 2010). Dans le modèle de Fisher, un organisme est caractérisé par un ensemble de traits phénotypiques (le paysage adaptatif est donc phénotypique et non génétique comme celui de Wright). Un génotype est alors associé à une certaine valeur de ces traits (il s'agit donc en fait d'une 'valeur génétique' pour les traits et non d'un phénotype multivarié *sensu stricto*). A cette position dans l'espace phénotypique correspond une certaine valeur sélective, qui décroît avec sa distance à un optimum phénotypique (de valeur sélective maximale), pour l'environnement considéré. Le paysage adaptatif de Fisher possède donc un unique pic de valeur sélective, dans un environnement donné. Cette faible "rugosité" du paysage adaptatif (pic unique) le démarque du paysage adaptatif de Wright qui comporte typiquement plusieurs optimums génétiques locaux, séparés par des vallées adaptatives, dès lors que les allèles considérés dans l'espace génétique ont des relations d'épistasie. De fait, il est possible de définir un paysage de Wright à partir de celui de Fisher, dans un environnement donné. Il faut pour cela définir un nombre fini de mutations possibles (sinon l'espace génétique est de dimension infinie), échantillonnées dans l'espace phénotypique

continu. Le paysage génétique résultant est alors relativement rugueux (Hwang *et al.* 2017), car l'épistasie entre paires d'allèles est une caractéristique omniprésente dans le modèle de Fisher (Martin *et al.* 2007).

Le modèle géométrique de Fisher a initialement été défini afin de modéliser l'adaptation par de multiples mutations de faibles effets sous sélection stabilisante (autour de l'optimum unique). Cette vision micro-mutationniste, ou « graduelle », de l'adaptation ne permet pas a priori de rendre compte de l'adaptation par sauts mutationnels ponctuels de fort effet sur la valeur sélective, phénomène qui a été mis en évidence empiriquement (Lenski and Travisano 1994). Certaines formes de paysage adaptatif génétique de Wright, tel que le modèle NK (Kauffman 1993), ont été étudiées avec un focus particulier sur la rugosité, les sauts mutationnels et l'existence de pics locaux, liés à l'épistasie. Toutefois, ces paysages présentent des propriétés statistiques difficiles à appréhender, ainsi qu'une capacité limitée en termes de nombre de locus modélisable (Tenaillon 2014). D'autres formes de paysages génétiques, appelés paysages mutationnels, ont été développés à partir du modèle en "Château de cartes" (Gillespie 1983). Ces modèles ont permis de dériver des propriétés générales, attendues et observables, pour la distribution des mutations bénéfiques au cours de l'adaptation (par ex. Beisel *et al.* 2007), mais ne décrivent pas les relations épistatiques entre mutations comme le modèle NK et le modèle de Fisher. La pertinence du modèle de Fisher a ensuite été redécouverte grâce à divers études théoriques et empiriques (Tenaillon 2014). Premièrement, des développements théoriques de Kimura (1983) puis Orr (1998) ont étudié la distribution des mutations fixées durant une phase d'adaptation, à partir du modèle de Fisher. Ils ont montré que celui-ci ne prédit pas une adaptation basée sur les seules mutations d'effets faibles, mais sur une distribution de facteurs fixés, de taille décroissante au fur et à mesure que la population s'approche de l'optimum. Ces résultats réconcilient ainsi qualitativement le modèle avec les observations empiriques sur la taille des mutations impliquées dans l'adaptation. Deuxièmement, des analyses de données empiriques issues de l'évolution expérimentale (microbienne surtout) ont montré que le modèle prédit divers patrons observés quant à la distribution de l'effet des mutations sur la valeur sélective (voir introduction Chapitre I).

III.2. Les particularités du modèle géométrique de Fisher en tant que modèle d'adaptation

Description du modèle

Le modèle géométrique de Fisher (synthétisé dans Orr 2005 et Tenaillon 2014) permet donc de modéliser un organisme par un ensemble de n traits phénotypiques continus soumis à sélection stabilisante pour un optimum phénotypique. Le nombre de ces traits donne la complexité phénotypique de l'organisme dans l'environnement considéré. Ces traits sont des traits d'adaptation dont la variation affecte nécessairement la valeur sélective. L'espace des traits d'adaptation est alors relié à la valeur sélective par une fonction caractérisée par un unique maximum à l'optimum phénotypique. La mutation correspond à un déplacement aléatoire dans l'espace phénotypique, souvent distribué de manière gaussienne, centrée sur le phénotype parental, depuis l'introduction de « l'infinite allele model » par Kimura (1965). Chaque mutation affecte tous les traits d'adaptation (hypothèse de pléiotropie universelle) et son effet dépend de la forme de la fonction de valeur sélective dans l'environnement considéré ainsi que de la position du génotype parent dans l'espace phénotypique par rapport à l'optimum. Dans une forme plus générale, les traits ne sont pas équivalents (anisotropie) pour la mutation ou la sélection (par ex. Lande 1980; Waxman and Welch 2005; Martin and Lenormand 2006b). Par la définition d'une distance entre le phénotype ancestral et un optimum adaptatif, ce modèle permet d'expliciter le stress imposé par un environnement donné sur un organisme donné par le biais d'une paramétrisation relativement simple. Le modèle de Fisher est défini par trois grandes caractéristiques, ou « méta-paramètres » : la fonction reliant les traits d'adaptation à la valeur sélective (forme, équivalence ou non entre traits), la complexité phénotypique (dimensionnalité n) et la distribution des effets des mutations sur les traits d'adaptation (forme, équivalence ou non entre traits, additivité ou non dans l'espace phénotypique). Malgré un nombre limité de paramètres, du moins dans le cas « isotrope » (où tous les traits sont équivalents), le modèle géométrique de Fisher intègre un riche modèle de distribution d'effet des mutations, d'interactions épistatiques et d'interactions génotype-environnement, dont les propriétés sont émergentes et non définies a priori. A cela s'ajoute, dans toute théorie d'adaptation basée sur ce modèle, des hypothèses quant à la génétique des populations, concernant le nombre et les paramètres mutationnels des différents loci ainsi que niveau de recombinaison entre eux. Lorsque plusieurs loci sont considérés (avec ou sans recombinaison), la question de la modularité se pose alors : les paramètres mutationnels peuvent varier d'un locus à l'autre, introduisant alors des 'modules'

mutationnels présentant différentes matrices de variance-covariance des effets des mutations (multivariés gaussiens) entre loci.

Nous parlerons ci-dessous du modèle que nous appellerons « standard », qui est isotrope (les traits sont équivalents quant à la force de la sélection et la variance mutationnelle) et sans modules (on ne considère qu'un seul locus, ou tous ont les mêmes paramètres mutationnels) Dans ce sous cas, il existe toujours un repaire de l'espace phénotypique (une définition des traits) où la matrice de variance-covariance sélective est l'identité, et la matrice de variance-covariance mutationnelle est proportionnelle à l'identité (Lande 1980; Martin and Lenormand 2006b; Martin 2014). Il y a donc à la fois équivalence et indépendance sélective et mutationnelle entre les traits. Ce modèle mutationnel « standard » a 3 paramètres, pour un génotype parental donné dans un environnement donné : la dimension n, la variance mutationnelle par trait λ (standardisée par la force de la sélection) et la distance entre l'optimum et le parent, dans l'espace phénotypique (la direction est sans influence dans le modèle isotrope).

Hypothèses et limites du modèle

La simplicité du modèle de Fisher isotrope est un atout en tant qu'outil analytique mais découle d'hypothèses fortes qu'il est nécessaire d'expliciter :

- Pléiotropie universelle : La pléiotropie définit la capacité d'une mutation à modifier plusieurs traits phénotypiques simultanément. Dans le modèle de Fisher 'standard', les mutations ont un effet pléiotrope universel, c'est à dire qu'elles affectent l'ensemble des traits d'adaptation considérés. Il est difficile de trancher sur la validité de cette hypothèse d'un point de vue empirique au vue des débats techniques existant autour de la mesure du niveau de pléiotropie (Paaby and Rockman 2013). La sensibilité des prédictions du modèle de Fisher au niveau de pléiotropie considéré est complexe et discutée dans Tenaillon (2014).

- Unicité de l'optimum: Le modèle de Fisher dans sa version la plus simple se focalise sur l'adaptation à court terme à un environnement particulier. Dans ce modèle, un unique optimum phénotypique est considéré. Ceci implique une sélection stabilisante lorsque les phénotypes sont proches de l'optimum ou une sélection directionnelle en s'éloignant ce cet optimum. Ces deux types de sélection ont été mis en évidence empiriquement et l'existence d'un unique optimum est également cohérente avec des exemples d'évolution convergente

dans des expériences d'adaptation à long terme. Cependant, le modèle de Fisher ne permet pas de modéliser des cas de sélection disruptive et d'évolution divergente pourtant également observés empiriquement, avec des cas de divergence stable entre des populations évoluant dans les mêmes conditions (par ex. Schoustra *et al.* 2009). Pour les mêmes raisons, par construction, le modèle ne peut décrire des relations de fréquence–dépendance entre génotypes : dans le modèle de Fisher un génotype a une valeur sélective donnée, indépendamment des autres génotypes qu'il côtoie.

- Isotropie : Le modèle originel développé par Fisher (et le « standard » utilisé dans cette thèse) suppose l'isotropie (équivalence mutationnelle et sélective entre traits). L'existence d'évolution parallèle au niveau des gènes voire des allèles, suggère une forme d'anisotropie associée à une modularité (certaines directions sont favorisées parmi les mutations dans certains gènes, Chevin *et al.* 2010). Cette hypothèse peut être relâchée en définissant un modèle anisotrope, au prix d'un grand nombre potentiel de paramètres. On peut aussi voir le modèle isotrope comme une « heuristique » ou une limite décrivant l'adaptation à de nombreux modules favorisant diverses directions, le tout résultant en un paysage globalement isotrope sur l'ensemble des modules (Martin 2014). L'adaptation sur une large base génétique (nombreux allèles) pourrait alors être suffisamment approchée par le modèle isotrope.

- Complexité phénotypique : Du nombre de traits résulte le principe de coût de la complexité, traité par Orr (2000), traduisant un ralentissement du processus d'adaptation avec le nombre de dimensions. En considérant les traits d'adaptation comme des traits synthétisant les effets sur la valeur sélective de nombreux traits sous-jacents (Martin 2014) on peut supposer que le nombre de dimensions phénotypiques reste faible.

Avantage par rapport à d'autres modèles et validation expérimentale

L'influence du modèle de Fisher en tant que paysage adaptatif a grandi durant la dernière décennie grâce au compromis qu'il offre entre simplicité analytique, intuition conceptuelle et réalisme de certaines de ses propriétés émergentes que d'autres modèles simples ne semblent pas générer. Notamment, l'effet du contexte environnemental ou génétique sur la distribution des effets des mutations et la dynamique de l'adaptation (résumé dans Tenaillon 2014 et Sousa *et al.* 2016) est une de ces propriétés émergentes intéressantes dans le cas de changements environnementaux. Les

prédictions faites à partir de ce modèle, sur le niveau d'épistasie ou la distribution des effets des mutations, sont compatibles avec plusieurs observations issues d'expériences d'évolution expérimentale réalisées principalement sur des micro-organismes (Martin and Lenormand 2006a; Martin *et al.* 2007; MacLean *et al.* 2010; Manna *et al.* 2011; Trindade *et al.* 2012; Sousa *et al.* 2012; Gordo and Campos 2012; Hietpas *et al.* 2013; Weinreich and Knies 2013; Perfeito *et al.* 2014; Couce and Tenaillon 2015; Stearns and Fenster 2016; Harmand *et al.* 2016). De plus, malgré la simplicité de l'espace phénotypique considéré, Martin (2014) a montré que le modèle standard de Fisher peut être vu comme une approximation limite de modèles beaucoup plus complexes, mais résultant de l'intégration phénotypique d'un grand nombre de traits affectés par les mutations vers une nombre limité de traits déterminant directement la valeur sélective. Par ailleurs, de par la facilité à traiter d'environnements changeants, ce modèle est aussi la base conceptuelle de la plupart des études théoriques de l'adaptation dans ce contexte.

Le changement d'environnement dans le modèle de Fisher et les difficultés de modélisation dans le contexte du sauvetage évolutif

Le modèle de Fisher a également été utilisé depuis plusieurs dizaines d'années dans le cadre de l'étude de la réponse à des changements d'environnement dans l'espace et dans le temps (même s'il n'est pas toujours fait référence explicitement au terme « Modèle de Fisher », dans ce contexte). Un tel paysage peut être étendu à un contexte dynamique et/ou spatial, avec l'environnement (biotique ou abiotique) qui détermine la position de l'optimum dans l'espace et/ou le temps. Une telle approche a été utilisée pour aborder théoriquement des problèmes aussi diverses que l'évolution de la plasticité (par ex. Via and Lande 1985; Chevin *et al.* 2010), des aires de répartition des espèces (pour revue voir Kubisch *et al.* 2014), l'adaptation à un environnement changeant continuellement dans le temps (pour revue voir Kopp and Hermisson 2007; Matuszewski *et al.* 2014), les conflits entre sexes (Connallon and Clark 2014) ou l'évolution de la sénescence (Moorad and Promislow 2008). La plupart de ces résultats ont été obtenus via des modèles déterministes, et sans couplage explicite à une dynamique démographique, ou par des simulations (notamment dans le cas des dynamiques source-puit, Bazin *et al.* 2014).

Ainsi, alors que le modèle de Fisher est un outil très utilisé pour appréhender la réponse aux changements environnementaux et l'effet des mutations, il n'existe pas de modèle de sauvetage évolutif basé sur ce paysage, même dans le cas assez simple, et bien étudié empiriquement, d'une population isolée, asexuée, face à un changement environnemental abrupte. Cette lacune dans la

théorie du sauvetage évolutif tient peut-être au fait que l'implémentation des modèles classiques de sauvetage évolutif dans le contexte du modèle de Fisher nécessite de combiner des outils diverses aux hypothèses parfois difficilement conciliables. D'un côté, l'existence d'épistasie et d'interactions GxE omniprésentes impose de modifier les outils de génétique des populations et de démographie utilisés pour les modèles de sauvetage évolutif « discrets », qui négligent ces effets. D'un autre côté, les méthodes classiques d'étude du modèle de Fisher dans le cadre d'un changement environnemental reposent sur une approximation déterministe et à variance génétique additive constante qui ne s'applique donc pas non plus pour une population passant par de faibles tailles, et asexuée.

Les travaux de cette thèse se sont développés autour du projet de combiner des modèles de démographie et de génétique des populations, dans un cadre théorique où la sélection et la mutation sont décrites par un paysage adaptatif simple : le modèle géométrique de Fisher. Cette démarche a pour objectif d'intégrer les capacités de modélisation de changement d'environnement du modèle de Fisher dans la théorie du sauvetage évolutif. La section suivante résume les différents résultats obtenus dans le cadre de ce projet.

IV. Résumé des thèmes abordés au sein des différents chapitres de la thèse

Au cours de cette thèse, nous nous sommes intéressés à la modélisation de dynamiques éco-évolutives de populations en environnements changeants. Au sein de ce vaste sujet d'étude, nous avons cherché à atteindre trois objectifs principaux : (i) modéliser le processus de sauvetage évolutif dans des populations asexuées, (ii) intégrer le modèle de paysage adaptatif de Fisher aux modèles de sauvetage évolutif et (iii) dériver, pour ces modèles, des prédictions analytiques aussi simples que possible et testables empiriquement.

Pour atteindre les deux premiers objectifs, il est nécessaire de modéliser la trajectoire adaptative d'une population de taille variable dans un paysage adaptatif dont la topographie dépend des conditions environnementales. Dans le cadre du modèle géométrique de Fisher, on peut décrire analytiquement :

- la distribution des effets des mutations aléatoires sur le taux de croissance, dans le nouvel environnement, de mutants apparaissant *de novo* d'un génotype donné (c.a.d. pour une population initialement isogénique)

- la distribution des taux de croissance, dans le nouvel environnement, des différents génotypes présents initialement au sein d'une population à l'équilibre dans l'environnement précédent.

Connaissant ces distributions de paramètres démographiques des variants dans la population, selon les conditions environnementales et leur origine (de novo ou préexistant), il est alors possible de déterminer la probabilité de sauvetage évolutif d'une population face à un changement environnemental stressant, en combinant à ces distributions deux processus stochastiques : un processus de mutation (processus de Poisson, dans notre cas) et un processus démographique de survie/reproduction (processus de Feller (1951), dans notre cas).

Les modèles développés dans les chapitres I et II de cette thèse utilisent cette stratégie afin de modéliser la probabilité de sauvetage évolutif (versions des manuscrits datées de novembre 2017). Chaque chapitre considère un parmi deux régimes de mutation alternatifs et complémentaires, dont la prépondérance relative, en nature, a longtemps été débattue dans la littérature (pour une revue, voir Orr 2005).

- Dans le premier régime en taux de mutation faible (dénommé dans la suite « Strong Selection Weak Mutation », SSWM), l'adaptation est due à l'établissement de quelques mutations d'effets forts (étudié par notamment par Turelli (1984), pour une revue voir McCandlish and Stoltzfus (2014).

- Alors que dans le second, en taux de mutation fort (dénommé dans la suite « Weak Selection Strong Mutation », WSSM), de nombreuses mutations d'effets faibles contribuent à l'adaptation de la population (étudié notamment par Lande 1980).

La modélisation de la trajectoire adaptative d'une population sous chacun de ses deux régimes repose sur des outils analytiques différents, développés dans les chapitres I et II. Dans le premier chapitre, le sauvetage évolutif est provoqué par l'établissement d'une mutation d'effet fort dont les dynamiques évolutives et démographiques sont stochastiques. Dans le chapitre II le sauvetage évolutif est provoqué par l'augmentation conjointe de la fréquence de multiples génotypes accumulant potentiellement de multiples mutations d'effets faibles. Les dynamiques de ces multiples génotypes sont modélisées par le même processus démographique stochastique que dans le chapitre I, mais en intégrant dans les paramètres démographiques l'effet cumulé de multiples mutations au cours du temps. En revanche, l'adaptation est modélisée par une dynamique évolutive déterministe

permettant de suivre les dynamiques transitoires évolutives et démographiques, dans ce contexte plus complexe.

Les modèles dérivés dans les chapitres I et II sont exprimés sous forme de solutions analytiques explicites. Ces formules ont pour but de donner une relation de dépendance relativement intuitive et simple entre les paramètres du modèle et la probabilité de sauvetage évolutif (ainsi que les temps d'extinctions dans le chapitre II). Ces solutions ont également été dérivées dans le but d'être comparées et/ou ajustées à des données que nous aurions produit ou qui seraient issues de la littérature, afin d'atteindre le troisième objectif fixé précédemment. Les paramètres du modèle sont issus du modèle de Fisher « standard » isotrope et peuvent être mesurés expérimentalement dans le but de fournir des prédictions quantitativement testables sur la probabilité de sauvetage évolutif d'une population asexuée face à un stress. Cependant, les expérimentations sur le sauvetage évolutif ou les analyses de données de traitements antibiotiques n'ont pas pu être développées au cours de cette thèse, par manque de temps. Les travaux préliminaires, sur l'analyse de données de la littérature, sont réunis dans le chapitre III de cette thèse. Les solutions analytiques dérivées dans les chapitres I et II ont également été dérivées en restreignant au minimum la généralité des hypothèses afin de pouvoir étendre ces modèles à d'autres contextes que le sauvetage évolutif d'une population isolée, lors d'un changement abrupt simple de l'environnement. Le chapitre III propose des perspectives de développement de modèles en environnement hétérogène (en temps ou en espace) autour des solutions analytiques développées dans les chapitres I et II.

Bibliography

Agashe D., Falk J. J., Bolnick D. I., 2011 Effects of Founding Genetic Variation on Adaptation to a Novel Resource. Evolution 65: 2481–2491.

Agrawal A. F., Whitlock M. C., 2010 Environmental duress and epistasis: how does stress affect the strength of selection on new mutations? Trends Ecol. Evol. 25: 450–458.

Aguilée R., Raoul G., Rousset F., Ronce O., 2016 Pollen dispersal slows geographical range shift and accelerates ecological niche shift under climate change. Proc. Natl. Acad. Sci. 113: E5741–E5748.

Alexander H. K., Martin G., Martin O. Y., Bonhoeffer S., 2014 Evolutionary rescue: linking theory for conservation and medicine. Evol. Appl. 7: 1161–1179.

Bay R. A., Rose N., Barrett R., Bernatchez L., Ghalambor C. K., *et al.*, 2017 Predicting Responses to Contemporary Environmental Change Using Evolutionary Response Architectures. Am. Nat.: 000–000.

Bazin É., Mathé-Hubert H., Facon B., Carlier J., Ravigné V., 2014 The effect of mating system on invasiveness: some genetic load may be advantageous when invading new environments. Biol. Invasions 16: 875–886.

Beisel C. J., Rokyta D. R., Wichman H. A., Joyce P., 2007 Testing the Extreme Value Domain of Attraction for Distributions of Beneficial Fitness Effects. Genetics 176: 2441–2449.

Bell G., Collins S., 2008 Adaptation, extinction and global change. Evol. Appl. 1: 3–16.

Bell G., Gonzalez A., 2009 Evolutionary rescue can prevent extinction following environmental change. Ecol. Lett. 12: 942–948.
Bell G., 2012 Evolutionary rescue of a green alga kept in the dark. Biol. Lett.: rsbl20120823.
Bell G., 2013 Evolutionary rescue and the limits of adaptation. Phil Trans R Soc B 368: 20120080.
Boulding E. G., Hay T., 2001 Genetic and demographic parameters determining population persistence after a discrete change in the environment. Heredity 86: 313–324.
Burger R., Lynch M., 1995 Evolution and Extinction in a Changing Environment: A Quantitative-Genetic Analysis. Evolution 49: 151.
Charmantier A., Garant D., 2005 Environmental quality and evolutionary potential: lessons from wild populations. Proc. R. Soc. B Biol. Sci. 272: 1415–1425.
Chevin L.-M., Lande R., Mace G. M., 2010 Adaptation, Plasticity, and Extinction in a Changing Environment: Towards a Predictive Theory. PLOS Biol. 8: e1000357.
Colautti R. I., Alexander J. M., Dlugosch K. M., Keller S. R., Sultan S. E., 2017 Invasions and extinctions through the looking glass of evolutionary ecology. Philos. Trans. R. Soc. B Biol. Sci. 372: 20160031.
Connallon T., Clark A. G., 2014 Balancing Selection in Species with Separate Sexes: Insights from Fisher's Geometric Model. Genetics 197: 991–1006.
Couce A., Tenaillon O. A., 2015 The rule of declining adaptability in microbial evolution experiments. Front. Genet. 6.
De Visser J. a. G. M., Rozen D. E., 2005 Limits to adaptation in asexual populations. J. Evol. Biol. 18: 779–788.
Delord J., 2009 Écologie et évolution: Vers une articulation multi-hierarchisée. T Heams P Huneman G Lecointre M Silberstein Éd Mondes Darwiniens L'évolution L'évolution Paris Éd Syllepse: 607–628.
Feller W., others, 1951 *Diffusion processes in genetics*. University of California Press Berkeley, Calif.
Ferrière R., Dieckmann U., Couvet D., 2004 *Evolutionary conservation biology*. Cambridge University Press, Cambridge, UK; New York.
Ferriere R., Legendre S., 2013 Eco-evolutionary feedbacks, adaptive dynamics and evolutionary rescue theory. Phil Trans R Soc B 368: 20120081.
Fisher R. A., 1930 *The Genetical Theory of Natural Selection*. Oxford University Press.
Gandon S., Hochberg M. E., Holt R. D., Day T., 2013 What limits the evolutionary emergence of pathogens? Philos. Trans. R. Soc. Lond. B Biol. Sci. 368: 20120086.
Gillespie J. H., 1983 Some Properties of Finite Populations Experiencing Strong Selection and Weak Mutation. Am. Nat. 121: 691–708.
Gomulkiewicz R., Holt R. D., 1995 When does Evolution by Natural Selection Prevent Extinction? Evolution 49: 201.
Gomulkiewicz R., Holt R. D., Barfield M., Nuismer S. L., 2010 Genetics, adaptation, and invasion in harsh environments. Evol. Appl. 3: 97–108.
Gomulkiewicz R., Shaw R. G., 2013 Evolutionary rescue beyond the models. Philos. Trans. R. Soc. Lond. B Biol. Sci. 368: 20120093.
Gonzalez A., Ronce O., Ferriere R., Hochberg M. E., 2013 Evolutionary rescue: an emerging focus at the intersection between ecology and evolution. Philos. Trans. R. Soc. B Biol. Sci. 368: 20120404–20120404.
Gordo I., Campos P. R. A., 2012 Evolution of clonal populations approaching a fitness peak. Biol. Lett. 9: 20120239–20120239.
Gorter F. A., Derks M. F., Heuvel J. van den, Aarts M. G., Zwaan B. J., *et al.*, 2017 Genomics of adaptation depends on the rate of environmental change in experimental yeast populations. Mol. Biol. Evol.
Harmand N., Gallet R., Jabbour-Zahab R., Martin G., Lenormand T., 2016 Fisher's geometrical model and the mutational patterns of antibiotic resistance across dose gradients. Evolution: n/a-n/a.
Hendry A. P., Kinnison M. T., 1999 Perspective: the pace of modern life: measuring rates of contemporary microevolution. Evolution 53: 1637–1653.
Hendry A. P., 2016 *Eco-evolutionary Dynamics*. Princeton University Press.
Hietpas R. T., Bank C., Jensen J. D., Bolon D. N. A., 2013 Shifting Fitness Landscapes in Response to Altered Environments. Evolution 67: 3512–3522.
Hiltunen T., Virta M., Laine A.-L., 2017 Antibiotic resistance in the wild: an eco-evolutionary perspective. Phil Trans R Soc B 372: 20160039.
Hoffmann A. A., Parsons P. A., 1997 *Extreme environmental change and evolution*. Cambridge University Press, Cambridge; New York.

Hoffmann A. A., Merilä J., 1999 Heritable variation and evolution under favourable and unfavourable conditions. Trends Ecol. Evol. 14: 96–101.
Hoffmann A. A., Sgrò C. M., 2011 Climate change and evolutionary adaptation. Nature 470: 479–485.
Holt R. D., Gomulkiewicz R., 1997 The evolution of species' niches: a population dynamic perspective. Case Stud. Math. Model. Ecol. Physiol. Cell Biol.: 25–50.
Holt R. D., Gomulkiewicz R., Barfield M., 2003 The phenomenology of niche evolution via quantitative traits in a "black-hole" sink. Proc. R. Soc. B Biol. Sci. 270: 215–224.
Holt R., Barfield M., Gomulkiewicz R., 2004 Temporal Variation Can Facilitate Niche Evolution in Harsh Sink Environments. Am. Nat. 164: 187–200.
Hwang S., Park S.-C., Krug J., 2017 Genotypic complexity of Fisher's geometric model. Genetics 206: 1049–1079.
Iwasa Y., Michor F., Nowak M. A., 2003 Evolutionary dynamics of escape from biomedical intervention. Proc. R. Soc. B Biol. Sci. 270: 2573–2578.
Kauffman S. A., 1993 The origins of order: Self-organization and selection in evolution. Oxford University Press, USA.
Kimura M., 1965 A stochastic model concerning the maintenance of genetic variability in quantitative characters. Proc. Natl. Acad. Sci. 54: 731–736.
Kimura M., 1983 *The neutral theory of molecular evolution*. Cambridge University Press.
Kingsolver J. G., Diamond S. E., Siepielski A. M., Carlson S. M., 2012 Synthetic analyses of phenotypic selection in natural populations: lessons, limitations and future directions. Evol. Ecol. 26: 1101–1118.
Kopp M., Hermisson J., 2007 Adaptation of a Quantitative Trait to a Moving Optimum. Genetics 176: 715–719.
Kubisch A., Holt R. D., Poethke H.-J., Fronhofer E. A., 2014 Where am I and why? Synthesizing range biology and the eco-evolutionary dynamics of dispersal. Oikos 123: 5–22.
Lachapelle J., Bell G., 2012 Evolutionary Rescue of Sexual and Asexual Populations in a Deteriorating Environment. Evolution 66: 3508–3518.
Lande R., 1976 Natural Selection and Random Genetic Drift in Phenotypic Evolution. Evolution 30: 314.
Lande R., 1980 The Genetic Covariance Between Characters Maintained by Pleiotropic Mutations. Genetics 94: 203–215.
Lande R., 1993 Risks of population extinction from demographic and environmental stochasticity and random catastrophes. Am. Nat. 142: 911–927.
Lenski R. E., Travisano M., 1994 Dynamics of adaptation and diversification: a 10,000-generation experiment with bacterial populations. Proc. Natl. Acad. Sci. 91: 6808–6814.
Levins R., 1966 The strategy of model building in population biology. Am. Sci. 54: 421–431.
Levins R., 1968 Evolution in changing environments: some theoretical explorations. Princeton University Press.
Lindsey H. A., Gallie J., Taylor S., Kerr B., 2013 Evolutionary rescue from extinction is contingent on a lower rate of environmental change. Nature 494: 463–467.
Lowe W. H., Kovach R. P., Allendorf F. W., 2017 Population Genetics and Demography Unite Ecology and Evolution. Trends Ecol. Evol. 32: 141–152.
Lynch M., Gabriel W., Wood A. M., 1991 Adaptive and demographic responses of plankton populations to environmental change. Limnol. Oceanogr. 36: 1301–1312.
Lynch M., Lande R., 1993 Evolution and extinction in response to environmental change. Biot. Interact. Glob. Change: 234–250.
MacArthur R. H., Wilson E. O., 1967 *The Theory of Island Biogeography*. Princeton University Press.
MacLean R. C., Perron G. G., Gardner A., 2010 Diminishing Returns From Beneficial Mutations and Pervasive Epistasis Shape the Fitness Landscape for Rifampicin Resistance in Pseudomonas aeruginosa. Genetics 186: 1345–1354.
Manna F., Martin G., Lenormand T., 2011 Fitness Landscapes: An Alternative Theory for the Dominance of Mutation. Genetics 189: 923–937.
Martin G., Lenormand T., 2006a The Fitness Effect of Mutations Across Environments: A Survey in Light of Fitness Landscape Models. Evolution 60: 2413–2427.
Martin G., Lenormand T., 2006b A General Multivariate Extension of Fisher's Geometrical Model and the Distribution of Mutation Fitness Effects Across Species. Evolution 60: 893–907.
Martin G., Elena S. F., Lenormand T., 2007 Distributions of epistasis in microbes fit predictions from a fitness landscape model. Nat. Genet. 39: 555–560.

Martin G., Aguilée R., Ramsayer J., Kaltz O., Ronce O., 2013 The probability of evolutionary rescue: towards a quantitative comparison between theory and evolution experiments. Phil Trans R Soc B 368: 20120088.
Martin G., 2014 Fisher's Geometrical Model Emerges as a Property of Complex Integrated Phenotypic Networks. Genetics 197: 237–255.
Matuszewski S., Hermisson J., Kopp M., 2014 Fisher's Geometric Model with a Moving Optimum. Evolution 68: 2571–2588.
Mayhew P. J., 2006 Discovering evolutionary ecology: bringing together ecology and evolution. Oxford University Press, Oxford ; New York.
Mayr E., 1982 The growth of biological thought: diversity, evolution, and inheritance. Belknap Press, Cambridge, Mass.
McCandlish D. M., Stoltzfus A., 2014 Modeling Evolution Using the Probability of Fixation: History and Implications. Q. Rev. Biol. 89: 225–252.
Moorad J. A., Promislow D. E. L., 2008 A Theory of Age-Dependent Mutation and Senescence. Genetics 179: 2061–2073.
Moreno-Fenoll C., Cavaliere M., Martínez-García E., Poyatos J. F., 2017 Eco-evolutionary feedbacks can rescue cooperation in microbial populations. Sci. Rep. 7.
Odling-Smee J., Erwin D. H., Palkovacs E. P., Feldman M. W., Laland K. N., 2013 Niche Construction Theory: A Practical Guide for Ecologists. Q. Rev. Biol. 88: 3–28.
Orr H. A., 1998 The Population Genetics of Adaptation: The Distribution of Factors Fixed during Adaptive Evolution. Evolution 52: 935.
Orr H. A., 2000 Adaptation and the Cost of Complexity. Evolution 54: 13–20.
Orr H. A., 2005 The genetic theory of adaptation: a brief history. Nat. Rev. Genet. 6: 119–127.
Orr H. A., Unckless R. L., 2008 Population Extinction and the Genetics of Adaptation. Am. Nat. 172: 160–169.
Orr H. A., Unckless R. L., 2014 The Population Genetics of Evolutionary Rescue. PLOS Genet. 10: e1004551.
Osmond M. M., Mazancourt C. de, 2013 How competition affects evolutionary rescue. Philos. Trans. R. Soc. Lond. B Biol. Sci. 368: 20120085.
Osmond M. M., Otto S. P., Klausmeier C. A., Goodnight C. J., Michalakis Y., 2017 When Predators Help Prey Adapt and Persist in a Changing Environment. Am. Nat.: 000–000.
Otto S. P., Whitlock M. C., 1997 The Probability of Fixation in Populations of Changing Size. Genetics 146: 723–733.
Paaby A. B., Rockman M. V., 2013 The many faces of pleiotropy. Trends Genet. TIG 29: 66–73.
Papp B., Notebaart R. A., Pál C., 2011 Systems-biology approaches for predicting genomic evolution. Nat. Rev. Genet. 12: 591–602.
Pease C. M., Lande R., Bull J. J., 1989 A Model of Population Growth, Dispersal and Evolution in a Changing Environment. Ecology 70: 1657–1664.
Pelletier F., Garant D., Hendry A. P., 2009 Eco-evolutionary dynamics. Philos. Trans. R. Soc. Lond. B Biol. Sci. 364: 1483–1489.
Perfeito L., Sousa A., Bataillon T., Gordo I., 2014 Rates of Fitness Decline and Rebound Suggest Pervasive Epistasis. Evolution 68: 150–162.
Pianka E. R., 2011 *Evolutionary ecology*. Eric R. Pianka.
Popper K., 1959 The logic of scientific discovery. Routledge.
Roughgarden J., 1979 Theory of population genetics and evolutionary ecology: an introduction.
Salazar-Ciudad I., Jernvall J., 2010 A computational model of teeth and the developmental origins of morphological variation. Nature 464: 583–586.
Samani P., Bell G., 2010 Adaptation of experimental yeast populations to stressful conditions in relation to population size. J. Evol. Biol. 23: 791–796.
Samani P., Bell G., 2016 The ghosts of selection past reduces the probability of plastic rescue but increases the likelihood of evolutionary rescue to novel stressors in experimental populations of wild yeast. Ecol. Lett. 19: 289–298.
Schoener T. W., 2011 The Newest Synthesis: Understanding the Interplay of Evolutionary and Ecological Dynamics. Science 331: 426–429.
Schoustra S. E., Bataillon T., Gifford D. R., Kassen R., 2009 The Properties of Adaptive Walks in Evolving Populations of Fungus (NH Barton, Ed.). PLoS Biol. 7: e1000250.
Slobodkin L. B. L. B., 1961 *Growth and regulation of animal populations*. Holt, Rinehart and Winston,.

Sousa A., Magalhães S., Gordo I., 2012 Cost of Antibiotic Resistance and the Geometry of Adaptation. Mol. Biol. Evol. 29: 1417–1428.
Sousa J. A. M. de, Alpedrinha J., Campos P. R. A., Gordo I., 2016 Competition and fixation of cohorts of adaptive mutations under Fisher geometrical model. PeerJ 4: e2256.
Stearns F. W., Fenster C. B., 2016 Fisher's geometric model predicts the effects of random mutations when tested in the wild. Evolution 70: 495–501.
Stockwell C. A., Hendry A. P., Kinnison M. T., 2003 Contemporary evolution meets conservation biology. Trends Ecol. Evol. 18: 94–101.
Sutherland W. J., Freckleton R. P., Godfray H. C. J., Beissinger S. R., Benton T., *et al.*, 2013 Identification of 100 fundamental ecological questions (D Gibson, Ed.). J. Ecol. 101: 58–67.
Svensson E. I., Calsbeek R. (Eds.), 2012 *The adaptive landscape in evolutionary biology*. Oxford University Press, Oxford ; [New York].
Tenaillon O., 2014 The Utility of Fisher's Geometric Model in Evolutionary Genetics. Annu. Rev. Ecol. Evol. Syst. 45: 179–201.
Trindade S., Sousa A., Gordo I., 2012 Antibiotic Resistance and Stress in the Light of Fisher's Model. Evolution 66: 3815–3824.
Turelli M., 1984 Heritable genetic variation via mutation-selection balance: Lerch's zeta meets the abdominal bristle. Theor. Popul. Biol. 25: 138–193.
Uecker H., Otto S. P., Hermisson J., 2014 Evolutionary Rescue in Structured Populations. Am. Nat. 183: E17–E35.
Uecker H., Hermisson J., 2016 The Role of Recombination in Evolutionary Rescue. Genetics 202: 721–732.
Uecker H., 2017 Evolutionary rescue in randomly mating, selfing, and clonal populations. Evolution 71: 845–858.
Via S., Lande R., 1985 Genotype-Environment Interaction and the Evolution of Phenotypic Plasticity. Evolution 39: 505.
Wal E. V., Garant D., Festa-Bianchet M., Pelletier F., 2013 Evolutionary rescue in vertebrates: evidence, applications and uncertainty. Phil Trans R Soc B 368: 20120090.
Wang A. D., Sharp N. P., Spencer C. C., Tedman-Aucoin K., Agrawal A. F., 2009 Selection, Epistasis, and Parent-of-Origin Effects on Deleterious Mutations across Environments in *Drosophila melanogaster*. Am. Nat. 174: 863–874.
Wang A. D., Sharp N. P., Agrawal A. F., 2014 Sensitivity of the Distribution of Mutational Fitness Effects to Environment, Genetic Background, and Adaptedness: A Case Study with Drosophila. Evolution 68: 840–853.
Waxman D., Welch J. J., 2005 Fisher's microscope and Haldane's ellipse. Am. Nat. 166: 447–457.
Weinreich D. M., Knies J. L., 2013 FISHER'S GEOMETRIC MODEL OF ADAPTATION MEETS THE FUNCTIONAL SYNTHESIS: DATA ON PAIRWISE EPISTASIS FOR FITNESS YIELDS INSIGHTS INTO THE SHAPE AND SIZE OF PHENOTYPE SPACE: THE FGM AND THE FUNCTIONAL SYNTHESIS. Evolution: n/a-n/a.
Willi Y., Hoffmann A. A., 2009 Demographic factors and genetic variation influence population persistence under environmental change. J. Evol. Biol. 22: 124–133.
Wright S., 1932 The roles of mutation, inbreeding, crossbreeding, and selection in evolution. na.

CHAPTER I
Evolutionary rescue over a fitness landscape

Yoann Anciaux[1]; Luis-Miguel Chevin[2] ; Ophélie Ronce[1]; Guillaume Martin[1]

[1] Institut des Sciences de l'Evolution de Montpellier (UMR 5554 ISE-M), CNRS – Université Montpellier 2, Place Eugène Bataillon, 34095 Montpellier Cedex 05, France

[2] Centre d'Ecologie Fonctionnelle et Evolutive (UMR 5175), 1919 route de Mende, 34293 Montpellier Cedex 5, France

Contact : yoann.anciaux@umontpellier.fr

Keywords : Antibiotic resistance; Evolutionary rescue; Fisher's Geometric Model; Fitness landscape; Mutation

Abstract

Evolutionary rescue describes a situation where adaptive evolution prevents the extinction of a population facing a stressing environment. Models of evolutionary rescue could in principle be used to predict the treatment levels most likely to limit the emergence of resistance in pests or pathogens. Stress levels are known to affect both the rate of decline of the population (demographic effect) and the speed of adaptation to the stressing environment (evolutionary effect), but the latter aspect has received less attention. Here, we derive a model of evolutionary rescue that includes both effects, using Fisher's Geometric Model of adaptation. In this model, the fitness effects of mutations depend both on the genotype and environment in which they arise. In particular, the model introduces a dependence between the proportion of rescue mutants, their cost, and the level of stress. Analytic results were obtained under a strong selection weak mutation regime, and their accuracy was tested by simulations. Stress can affect different parameters of the fitness landscape in our model, which are amenable to empirical measurements. These effects can be summarized into a single composite parameter, measuring stress intensity. Using this composite parameter, we describe a narrow 'characteristic stress window' of stress levels, over which the rescue probability drops from very likely to very unlikely. The rescue probability drops more sharply with increasing stress than in previous models without context-dependent mutation. We discuss how to test these predictions with rescue experiments across gradients of stress.

Introduction

Understanding the persistence or decline to extinction of populations is a crucial challenge both for the conservation of biodiversity and the eradication of pests or pathogens (Gonzalez *et al.* 2013; Alexander *et al.* 2014; Carlson *et al.* 2014). In evolutionary biology, 'environmental stress' broadly characterizes an environment that induces a reduction in fitness for organisms (Koehn and Bayne 1989; Bijlsma and Loeschcke 2005). Here, we will focus on the case where environmental stress causes a reduction of population mean fitness that is harsh enough to trigger a decline in abundance (Hoffmann and Parsons 1997). In such a stressful environment, if heritable variation in fitness is available or arises by mutation, then adaptive evolution may allow the population to escape extinction. This phenomenon has been called 'evolutionary rescue' (ER) (Gomulkiewicz and Holt 1995). Evolutionary rescue is of particular importance for understanding the emergence of genetic resistance to drugs or treatments in medicine and agronomy (Davies and Davies 2010).

Empirical evidence supports the idea that stress levels critically determine ER probabilities (Samani and Bell 2010; Moser and Bell 2011; Lindsey *et al.* 2013). For example, the probability of antibiotic resistance emergence in bacteria (that is, the probability to avoid antibiotic-induced extinction through ER) typically declines sharply, in a strongly non-linear way, with increasing drug concentration (Drlica 2003). Evolutionary rescue thus shifts from being highly likely to highly unlikely over a narrow window of stress levels. This critical range of stress depends on the strain, especially on its evolutionary history with respect to exposure to the stress (Gonzalez and Bell 2013). Stress level, as controlled by drug concentration, has also been shown to affect the genetic basis of resistance (Harmand *et al.* 2016), with a wider diversity of genes and alleles conferring resistance at low than at high doses. However, the underlying causes for this relationship between stress level and the probability/genetic basis of ER is still poorly understood, challenging our ability to predict these eco-evolutionary dynamics. Our aim here is to derive new analytical predictions for the relationship between ER and stress level, predicting in particular the critical window of stress levels above which ER is very unlikely, and allowing direct comparison with experimental data.

In the theoretical literature (Alexander *et al.* 2014), most ER models indeed predict a dependence of ER probability on stress levels, as measured by the decay rate of the stressed population. Indeed, higher stress levels directly impose a faster decay to extinction. This leaves less time for the population to adapt before extinction, be it by rare *de novo* mutations (e.g. (Orr and Unckless 2008)) or through standing genetic variance (e.g. (Gomulkiewicz and Holt 1995)). Some models however predict that, when adaptation stems from rare pre-existing mutants (e.g. standing variance model in (Orr and Unckless 2008, 2014)), the initial decay rate of the population does not impact rescue probabilities.

Stress level may also have indirect effects on ER. Indeed, a stressful environment may not only affect the demographic properties of the population, but also its rate of adaptation (Hoffmann and Parsons 1997; De Visser and Rozen 2005; Agrawal and Whitlock 2010). The rate of mutations and the distribution of their effects on fitness change across environments (Martin and Lenormand 2006a; Wang *et al.* 2009; Agrawal and Whitlock 2010; Wang *et al.* 2014). In particular, the fraction of beneficial mutations was found to increase in stressful environments (Remold and Lenski 2001, 2004). Standing variation for quantitative traits, and in particular fitness components, also frequently depends on the environment where it is measured (Hoffmann and Merilä 1999; Sgrò and Hoffmann 2004; Charmantier and Garant 2005). Finally, the initial frequency of preexisting variants able to rescue the population from extinction in a stressful environment depends on their selective cost in the past environment. Variations in this cost across stress levels (i.e. between mutations conferring resistance to different levels), could induce corresponding variations in ER probability. In light of this empirical evidence, it seems clear that progress towards understanding and predicting ER across stress levels requires addressing, in a quantitative way, the joint effect of stress on the demography and genetic variation of a population exposed to stressful conditions. This is our goal in the present article.

To do so, we develop a model that is a hybrid between two modeling traditions in ER theory, summarized by Alexander et al. (Alexander *et al.* 2014): discrete genetic models, and quantitative genetics models. Discrete genetic models assume a narrow genetic basis for adaptation (and ER), whereby a single beneficial mutation can rescue an otherwise monomorphic population (Orr and Unckless 2008, 2014; Martin *et al.* 2013; Uecker *et al.* 2014; Uecker and Hermisson 2016). This approach was initially proposed for ER by Gomulkiewicz and Holt (1995), and later extended to account for (i) evolutionary and demographic stochasticity (Orr and Unckless 2008),

and (ii) variation in the selection coefficients of mutations that may cause rescue, with an arbitrary distribution of fitness effects (Martin *et al.* 2013). However, such models do not predict how the fitness effects of mutations vary with stress level, i.e. how the genetic and/or environmental context determine these effects. For this reason, they make it difficult to jointly address the two fundamental components of stress mentioned above. On the contrary, quantitative genetics models inherently address the influence of stress on the rate of adaptation by assuming that adaptation (and ER) is caused by evolution of a quantitative trait whose optimum changes with the environment (Lynch *et al.* 1991; Burger and Lynch 1995; Gomulkiewicz and Holt 1995). In these models, both the rate of decline and the rate of adaptation in the stressful environment depend on the distance between the phenotypic optima in the past and present environments. However, analytical predictions were derived assuming a broad, polygenic basis for adaptation with a stable genetic variance of the quantitative trait. The population genetic processes underlying adaptation were not explicitly modelled, and the stochasticity involved in fixation and establishment neglected. These complications were only explored by simulations (Gomulkiewicz *et al.* 2010).

In order to take the best of both approaches, we rely on Fisher's (1930) Geometrical Model (hereafter "FGM"), which predicts how the selective coefficients of mutations change across environments (and stress levels). Variation in fitness in the FGM is assumed to emerge from variation on multiple putative traits, undergoing stabilizing selection that depends on the environment. This model allows analytical tractability, while retaining various aspects of realism (Tenaillon 2014). In particular, it predicts accurately how fitness effects of mutations change across environments (Martin and Lenormand 2006a; Hietpas *et al.* 2013; Harmand *et al.* 2016) or genetic backgrounds (Martin *et al.* 2007; MacLean *et al.* 2010; Trindade *et al.* 2012). Here, we combine this FGM with population genetic approaches that account for demographic and evolutionary stochasticity (Martin *et al.* 2013). The distribution of the demographic parameters of mutant genotypes then depends on both the genotype in which they arise, and on the environment in which they are expressed. Importantly, the FGM also predicts the covariation of selection coefficients across environments (Martin and Lenormand 2015). This creates a tractable connection, across stress levels, between (i) the decay rate, (ii) the rate and effect of rescue mutants, and (iii) their potential costs in the original environment, before the onset of stress.

We here use the FGM to analyze how the demographic and evolutionary effects of stress level affect evolutionary rescue caused by individual mutations. We consider either rescue from de novo mutations, or from standing variance at mutation-selection balance. We model evolutionary rescue in large asexual populations, similar to bacterial populations exposed to antibiotics, or populations of cancerous cells exposed to chemotherapy. Following (Martin *et al.* 2013), we use diffusion approximations, which can accommodate various demographic models. Explicit analytical approximations are obtained for an initially large asexual population undergoing relatively harsh stress, and checked against stochastic simulations. Our approximations assume that selection is strong and mutations rare (Gillespie 1983). In all cases, we predict a narrow window of stress levels over which evolutionary rescue shifts from being highly likely to highly unlikely. This window can be computed from experimentally measurable quantities. Our model integrates the different effects of stress on the demography and genetic variation for fitness and interestingly shows that these effects can be approximately summarized into a single composite measure that captures the 'effective stress level'. When measured on this scale, the critical stress window depends only on the initial population size and the mutation rate.

Methods

In this section, we detail the assumptions of the model and the approximations used for its mathematical analysis, in terms of environmental change, eco-evolutionary dynamics and the mutational model.

Abrupt environmental shift:

We define two environments: (1) a non-stressful one, denoted as "previous environment", in which the population has a positive mean growth rate, and a large enough population size that demographic stochasticity can be ignored; and (2) a stressful one, denoted "new environment", in which the population initially has a negative mean growth rate, and the population size is subject to demographic stochasticity. Conditions shift abruptly from the previous to the new environment at $t = 0$, at which time the population size is N_0.

Eco-evolutionary dynamics:

Extinction or rescue ultimately depends on details of the stochastic population dynamics of each genotype, which are here assumed to be mutually independent (no density or frequency-dependence, see Chevin (Chevin 2011)). As in (Martin *et al.* 2013), we approximate these dynamics by a Feller diffusion (Feller 1951). This approximation reduces all the complexity of the life cycle into two key parameters for each genotype i: the expected growth rate r_i (our 'fitness' here), and the variance in reproductive output σ_i. As an illustration, our simulations below assume discrete generations and Poisson offspring distributions, wherein $\sigma_i = 1 + r_i \approx 1$ for any genotype, as long as their growth rate is not too large ($r_i \ll 1$, in per-generation time units, see Appendix 1 and (Martin *et al.* 2013). As detailed in (Martin *et al.* 2013), this diffusion approximation requires density-independent and 'smooth' demographic processes (moderate growth or decay).

To cause a rescue, a resistant mutant ($r_i > 0$) must 'establish', by avoiding extinction when rare. The probability that this happens, for a lineage with growth rate $r_i > 0$, starting in single copy (i.e., ignoring later mutations) is $\pi_F(r_i) = 1 - e^{-2\,r_i} \approx 2\,r_i$ (still assuming $r_i \ll \sigma_i$, with $\sigma_i \approx 1$ in the example used in simulations). We ignore stochasticity in the decay dynamics of the subpopulation of all non-resistant genotypes ($r_i < 0$). This is accurate as long as this subpopulation has large initial size, of order $N_0 \gg 1$ (Martin *et al.* 2013).

Finally, we assume that mutation rates per capita per unit time are constant over time. This is exact in models with discrete generations, but is only approximate in continuous-time models, where mutations occur during birth events, leading to higher mutation rates per unit time for genotypes with larger birth rates. The approximation then applies if birth and death rates are large relative to growth rates (birth minus death), which is also required to approximate birth death processes by a Feller diffusion (Martin *et al.* 2013).

ER from standing variance versus *de novo* mutation:

At the onset of stress ($t = 0$), the population either consists of a single 'ancestral' clone, or is polymorphic at mutation-selection equilibrium in the previous environment. In the first case, we must derive the distribution of fitness effects, in the new environment, of mutants arising in the ancestral clone. In the second case, we must describe the potential rescue variants already

present in the previous environment, plus the range of mutants that they may generate *de novo* after the onset of stress.

House-of-Cards approximation:

We are interested in modeling the context-dependence of mutation-fitness effects, in order to capture the different effects of stress described above. However, this context dependence implies epistasis, which makes the problem highly intractable in general. To make analytical progress, we assume a regime of strong selection and weak mutation rate (SSWM, (Gillespie 1983), which allows substantial simplification. This regime arises when mutation rates are small relative to their typical effect (as detailed below). In our context, this assumption implies that most rescue variants are only one mutational step away from the (non-rescue) background in which they arise, such that we can ignore the accumulation of multiple mutations causing ER.

When considering a population initially at mutation-selection balance, the SSWM regime allows for further key simplifications. At mutation-selection balance, the equilibrium phenotype and fitness distributions both depend on a complex interplay between deleterious and compensatory mutations. However, in the SSWM regime, most segregating phenotypes remain within a narrow neighborhood of the phenotype that is optimal in the previous environment (the fittest genotype). We can thus derive the mutation-selection balance distribution of phenotypes and fitness by assuming that all mutations in each generation originate from the optimum phenotype in the previous environment. This is essentially the House-of-Cards approximation (Turelli 1984; Martin and Roques 2016) extended to the FGM in arbitrarily many dimensions (Martin and Roques 2016).

Under this assumption, ER from standing variance depends on the fitness distribution of variants, at mutation-selection balance in the previous environment. ER from *de novo* mutations depends on the distribution of fitness effects among mutants arising from the previous optimum phenotype as the only wild-type. We can thus directly borrow the results from Martin et al. (Martin *et al.* 2013), which are based on an arbitrary joint distribution of fitness effects in the new and the previous environment. The problem thus reduces to computing this joint distribution of

fitness effects in the FGM, for random mutations arising in a single 'ancestral clone' that is optimal in the previous environment.

Context dependent mutations under Fisher's geometrical model (FGM):

In any environment, growth rate (Malthusian fitness, or log fitness in discrete-time models) is assumed to be a quadratic function of n quantitative (continuous) phenotypic traits. The breeding values (heritable components) for these traits are concatenated in a vector $\mathbf{z} \in \mathbb{R}^n$, with optimum multivariate phenotype $\mathbf{z}_*$, at which the maximal growth rate is r_{max}. All genotypes are assumed to have the same stochastic variance in reproductive success (see above), leading to

$$\begin{array}{c} r(\boldsymbol{z}) = r_{max} - \|\boldsymbol{z} - \boldsymbol{z}_*\|^2/2 \\ \sigma(\mathbf{z}) \approx \sigma \gg r(\mathbf{z}), \text{for all } \mathbf{z} \end{array} . \qquad [1]$$

Assuming a single peak in the phenotype-fitness landscape in each environment, the optimum in the new environment is set at $\mathbf{z}_* = \mathbf{0}$ without loss of generality. The optimum in the previous environment is set equal to the phenotype of the ancestral ('A') mean phenotype $\mathbf{z}_* = \mathbf{z}_A$. When starting from a clone, the previous environment is irrelevant, only the maladaptation of this clone counts. When starting from a population initially at mutation-selection balance, following the House-of-Cards approximation above, we also consider that all mutations emerge from the optimal phenotype in the previous environment, $\mathbf{z}_* = \mathbf{z}_{\boldsymbol{A}}$. The fitness of the ancestral clone in the new environment is $r(\mathbf{z}_A) = r_{max} - \|\boldsymbol{z}_{\boldsymbol{A}}\|^2/2 = -r_D$, where r_D is its rate of decay. This means that stress involves a shift of the optimum (from $\mathbf{z}_* = \mathbf{z}_A$ to $\mathbf{z}_* = \mathbf{0}$) by an amount $\left|\left|\mathbf{z}_A\right|\right| = \sqrt{2(r_D + r_{max})}$ in phenotype space.

Mutations occur as a Poisson process with rate U per unit time per capita, constant over time and across genotypes but potentially variable across environments. Each mutation creates a random perturbation $\mathbf{dz}$ the on phenotype, which is unbiased and follows an isotropic multivariate Gaussian distribution, $\mathbf{dz} \sim N(\mathbf{0}, \lambda\, \mathbf{I}_{\boldsymbol{n}})$, where $\mathbf{I}_n$ is the identity matrix in n dimensions and λ is a scale parameter. This parameter regroups both variances of selective and mutational effects on each trait, in the following we will refer to λ only as the mutational variance on each trait but it still integrates the variance of the selective effect on each trait. Mutation effects add up on *phenotype* (no epistasis), but not on *fitness* because $r(\mathbf{z})$ is nonlinear.

Figure 1 illustrates the rescue process in the FGM. At the onset of stress ($t = 0$), the optimum shifts abruptly to a new position, such that the mean growth rate becomes negative with $-r_D < 0$ (**fig 1.C**). Meanwhile, the population size starts to drop from an initial value N_0 (**fig 1.C**), facing extinction in the absence of evolution. In this context, one or several mutants or pre-existing variants may be close enough to the new optimum to have a positive growth rate ('resistant genotypes', **fig.1A,B**). These may then establish and ultimately "rescue" the population ('rescue genotypes' **fig 1.A,B**).

Within the context of the FGM, increasing stress level may have different effects. First, increasing stress may involve a larger shift in the position of the optimum phenotype, resulting in a larger drop in fitness (to $-r_D$) of the formerly optimal phenotype, as assumed in most models of adaptation to a changing environment (Kopp and Matuszewski 2014). However, increasing stress may further involve a reduction in the quality of the environment, such that the maximum fitness r_{max} for the best possible phenotype is lower than in the non-stressful environment, and the absolute fitness is reduced for of all genotypes under stress. Finally, increasing stress may imply a change in the mutational parameters (U and λ), inducing shifts in evolvability. For instance, higher stress may release cryptic genetic variance on underlying phenotypic traits (Scharloo 1991; Hermisson and Wagner 2004), or cause increased mutation rates via SOS responses in bacteria (Foster 2007).

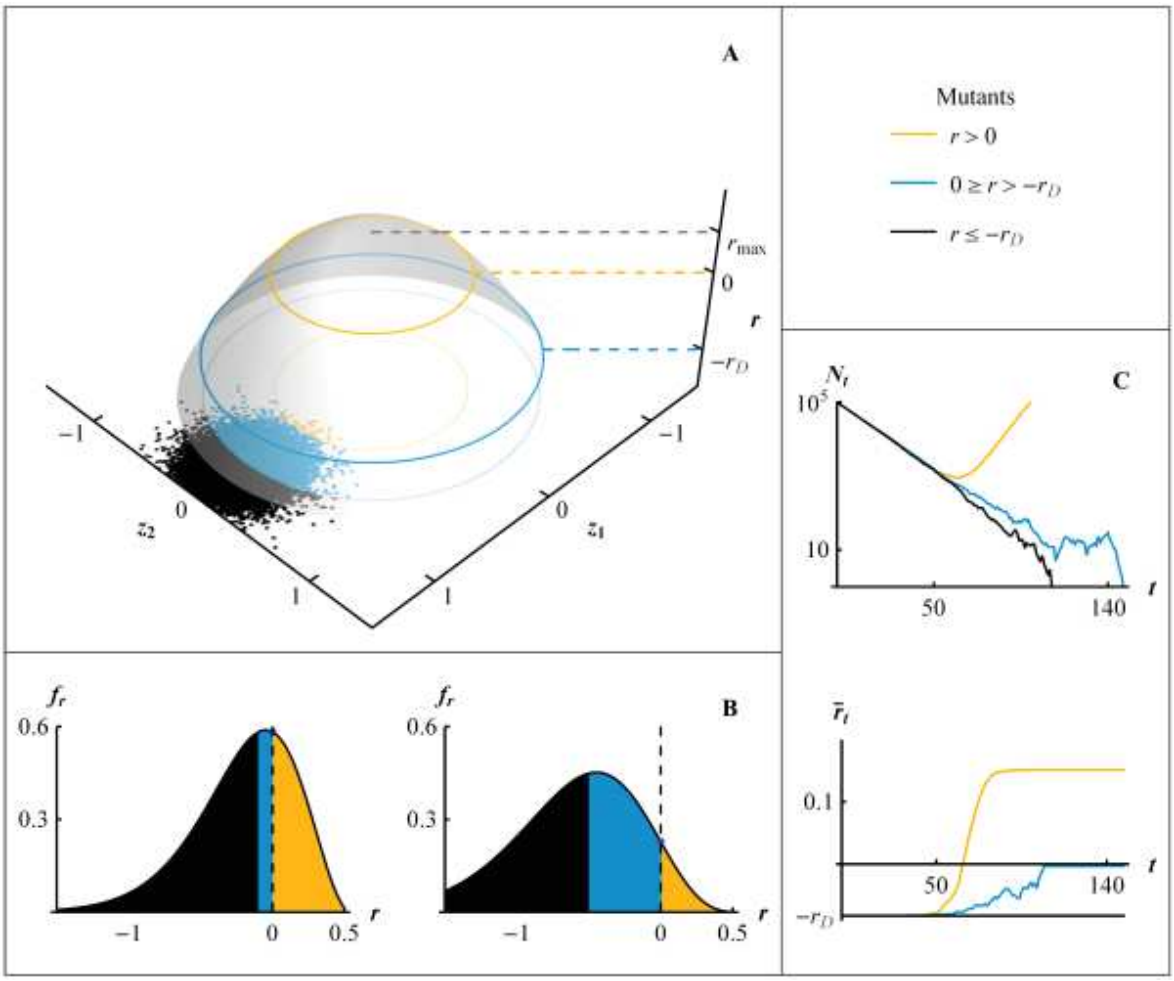

Figure 1: Evolutionary rescue in Fisher's geometric model (SSWM regime). *In all panels, black refers to deleterious mutations and neutral mutations ($-r_D \geq r$), blue to beneficial but not resistant mutations ($-r_D < r < 0$) and orange to resistant mutations ($r \geq 0$).* ***(A)*** *Fitness landscape (FGM) with growth rate r (z-axis) determined by two phenotypic traits z_1 and z_2 . The growth rate of the wild-type clone in the stressful environment is $-r_D$, and r_{max} is the maximal fitness at the phenotypic optimum.* ***(B)*** *Distribution of mutation effects on growth rate (distribution of fitness effects) for the wild type with two decay rates $r_D = 0.1$ (left) and $r_D = 0.5$ (right). The colored areas give the proportions of each corresponding type of mutation.* ***(C)*** *Dynamics of the population size N_t and mean fitness $\bar{r}_t$ of a population starting from a clone at $-r_D = -0.083$ at size $N_0 = 10^5$. The black line represents the case without fixation of a beneficial mutation, the blue line the case with extinction in spite of the fixation of a beneficial non-resistant mutation, and the orange line the case of a rescue. Parameters for the simulations are $r_{max} = 1.5$, $U = 2 * 10^{-5}$, $n = 4$ and $\lambda = 5 * 10^{-3}$.*

Scaled and compound parameters:

It proves simpler and sufficient (see Appendix) to study the scaled (and unitless) growth rate $y = r/r_{max} \in [-\infty, 1]$, so that $y_D = r_D/r_{max} \in [0, +\infty]$ is the decay rate of the ancestor scaled to the maximum possible growth rate in the new environment which we denote the stress intensity.

It will also prove useful to introduce another scaling by the mutational step size λ, thus introducing $\rho_D = r_D/\lambda$ and $\rho_{max} = r_{max}/\lambda$ (note that $y_D = \rho_D/\rho_{max}$). The dimensionality n of the phenotypic fitness landscape naturally arises in the formulae as $\theta = n/2$ (Martin and Lenormand 2006b). As we will see, all our results can in fact be expressed in terms of five parameters (N_0U , r_D , r_{max} , λ, θ). **Table 1** (at the end of the document) summarizes all notations in the article.

Maximal mutation rate for the SSWM regime:

As we have seen, our whole approach relies on the SSWM assumption. We conjecture that this assumption should hold below some threshold mutation rate U_c, i.e. whenever $U < U_C = \theta^2 \lambda$. Indeed, (Martin and Roques 2016) found that below U_C, the full fitness distribution at mutation-selection balance is exactly that expected from a single wild-type genotype at the optimum, while above U_C there is no dominant genotype in the equilibrium population. Whether this same condition is sufficient for most rescue events to stem from single step mutations is not justified theoretically, and was simply tested by extensive stochastic simulations. **Supplementary figure 1** further explores the range of validity of this approximation. It shows, in a rescued population, the proportion of wild-type, simple mutant, double mutant, and so on, as a function of the mutation rate.

Distribution of fitness effects in the new environment:

Let s be the selection coefficient (difference in growth rate), in the new environment, of a random mutant (with phenotype $\mathbf{z}$) relative to its ancestor (with phenotype $\mathbf{z}_A$). The distribution of $s = r(\mathbf{z}) - r(\mathbf{z}_A) = r + r_D$ among random mutants has a known exact form in the isotropic FGM (Martin 2014; Martin and Lenormand 2015). From it, the distribution of growth rates ($r = s - r_D$), in the new environment, is readily obtained. The scaled growth rates $y = r/r_{max}$ have the following probability density function:

$$f_y(y) = e^{-\rho_{max}(2+y_D-y)}(\rho_{max})^{\theta}(1-y)^{\theta-1}\frac{{}_0F_1\left(\theta, (\rho_{max})^2(1+y_D)(1-y)\right)}{\Gamma(\theta)}, \quad [2]$$

$$y \in]-\infty, 1]$$

where ${}_0F_1(.,.)$ is the confluent hypergeometric function and $\Gamma(z)$ the gamma function. In the SSWM regime, this probability density function approximately describes *de novo* mutations

produced after the onset of stress by the whole population, be it initially clonal or at mutation-selection balance.

Fitness distribution in the previous environment:

Consider the subset of random mutations, among those that arise from the ancestral clone, that have a scaled growth rate within the infinitesimal class of scaled growth rates $[y, y + dy]$, in the new environment. Let us introduce the conditional random variable $c|y$, which is the cost (equal to the negative of the selection coefficient relative to the ancestral clone), in the previous environment, of a random mutant within this subset (thus, conditional on y). Note that, because the mutation-selection balance is fully characterized by relative fitnesses, the maximal growth rate in the previous environment may differ from r_{max}, without impacting the distribution of the costs $c|y$. Importing results from (Martin *et al.* 2013) for the SSWM regime, the total number of pre-existing variants within the class $[y, y + dy]$ is Poisson distributed with mean $N_0\ U\ f_y(y)/c_H(y)dy$, where $c_H(y) = 1/\mathbb{E}_c(c^{-1}|y)$ is the harmonic mean of the cost $c|y$ among de novo resistant mutations. This conditional harmonic mean depends on the joint distribution of fitness effects (c, y) across two environments in the FGM (given in (Martin and Lenormand 2015). In our context, the ancestral clone is optimal in the previous environment and the preexistent mutants are close to this ancestral clone. In this case, using results in (Martin and Lenormand 2015), the resulting conditional harmonic mean $c_H(y)$ takes a tractable form (see Eq.(A6) in **Appendix**):

$$c_H(y) = 1/\mathbb{E}_c\left(\frac{1}{c}\middle|y\right) = \frac{\lambda}{e^{v(y)}E_{\theta-1/2}\big(v(y)\big)} \quad \text{with } v(y) = \rho_{max}\left(2 + y_D - 2\sqrt{(1+y_D)(1-y)} - y\right), \qquad [3]$$

where $E_k(z) = \int_1^\infty e^{-z\,t}/t^k\ dt$ is the exponential integral function.

Stochastic simulations of a discrete-time model:

We checked the robustness of our assumptions and approximations using stochastic simulations, where we tracked the population size and genetic composition of a population across discrete, non-overlapping generations. The size N_{t+1} of population at generation $t + 1$ was drawn as a Poisson number $N_{t+1} \sim Poisson(N_t\ \overline{W})$, with $\overline{W} = \overline{e^r}$ the mean multiplicative

fitness ($W = e^r$) and N_t the population size, in the previous generation. The genotypes forming this new generation were then sampled with replacement in the previous one with weight $W_i = e^{r_i}$. This is faster and exactly equivalent to drawing independent Poisson reproductive outputs for each individual, or genotype. Because of the underlying assumptions of the simulations, the corresponding analytical approximation for the stochastic reproductive variance in Eq.**[1]** is $\sigma_i = \sigma \approx 1$ (assuming small growth rates $r_i \ll 1$). Mutations occurred according to a Poisson process, with a constant rate U per capita per generation. Mutation phenotypic effects were drawn from a multivariate normal distribution $N(\mathbf{0}, \lambda\, \mathbf{I_n})$, with multiple mutants having additive effects on phenotype, and their fitness computed according to the FGM (Eq.**[1]**).

Rescue probability was estimated by running 1000 replicate simulations until either extinction or 'rescue' occurred. A population was considered 'rescued' when it reached a population size N_t and mean growth rate $\bar{r}_t$ such that its extinction probability, if it were monomorphic, would lie bellow 10^{-6} ($\exp(-N_t\bar{r}_t) < 10^{-6}$). For rescue from populations at mutation-selection balance, 8 replicate initial equilibrium populations were generated, each by starting from an optimal clone and running the same algorithm with fixed population size ($N_t = 10^6$) until the mean Malthusian fitness stabilized to its theoretical equilibrium value $\bar{r}_{eq} = r_{max} - U$ (for $U < U_c$). Then 1000 replicate rescue simulations were performed from these initial populations as previously. All simulations and mathematical derivations were performed in *MATHEMATICA v. 9.0* (Wolfram Research 2012).

Results

General form of the rescue probability:

Extinction occurs when no resistant mutation manages to establish (i.e. to avoid stochastic loss). For compactness, we define a "rate of rescue" ω_R per individual mutant (independent of N_0 and U), such that, following (Martin *et al.* 2013), ER probabilities take the general form: $P_R = 1 - e^{-N_0 U\, \omega_R}$. The rate of rescue from *de novo* mutations alone is ω_R^{DN} ('DN' for *de novo*), while that from pre-existing variance alone is ω_R^{SV} (for 'standing variants'). For a purely clonal population, $\omega_R = \omega_R^{DN}$, while $\omega_R = \omega_R^{DN} + \omega_R^{SV}$ when the population is initially at mutation-

selection balance. Applied in the context of the FGM, the rates ω_R^{DN} and ω_R^{SV} depend on the distributions of fitness effects described in methods as follows (see **Appendix**):

$$\begin{aligned} &\omega_R^{DN} = 2/y_D \int_0^1 y\, f_y(y) dy \\ &\omega_R^{SV} = \omega_R^{DN}\, \beta \\ &\text{with } \beta = \rho_D \int_0^1 y\, f_y(y) dy \Big/ \int_0^1 y/c_H(y)\, f_y(y) dy \end{aligned} \quad . \qquad [4]$$

ω_R^{DN} in Eq.[4] is basically the average establishment probability among de novo resistant mutants divided by the rate of decay. ω_R^{SV} is proportional to ω_R^{DN} but depends on the costs of the pre-existing mutations in the previous environment. The factor by which pre-existing variance alone may achieve more or less effectiveness in rescuing the population than de novo mutations, is summarized by β. Because both $f_y(y)$ (Eq.[2]) and $c_H(y)$ (Eq.[3]) depend only on r_{max}, r_D, λ and θ, so do the two rates of rescue in Eq.[4]. Moreover, the growth rates of the optimal genotype (r_{max}) and the ancestral genotype ($-r_D$) only affect ER probabilities in a way that is scaled by the variance in phenotypic effects (λ) or through the stress intensity $y_D = r_D/r_{max}$. This result is reminiscent of results regarding the proportion of beneficial mutations in the FGM which greatly depend on the mutational variance (Fisher 1930; Orr 2000).

The log-linearity of rescue probability with N_0 ($P_R = 1 - e^{-N_0 U\, \omega_R}$) has received empirical support (Martin et al. 2013). It holds whenever each individual lineage present at the onset of stress contributes independently to the rescue process (whether by being itself a rescuer, or by generating *de novo* mutants), that is, when density or frequency-dependence in selection is negligible. Log-linearity with the mutation rate U however arises here because of the SSWM regime, where multiple mutations are ignored: it might not hold at higher mutation rates (when $U > U_c$). As such, Eq.[4] makes no further assumption than the SSWM regime ($U < U_c$); it can easily be evaluated numerically to provide a general testable theory for rescue probabilities across stress levels, in the FGM. Yet, in order to gain more quantitative/intuitive insight into the effects of stress, we now study an approximate closed form for the rates in Eq.[4], focusing on *de novo* rescue first.

Weak mutation effects approximation:

We now assume that mutation effects are weak relative to the maximal growth rate under stress. More precisely, we introduce $\epsilon = 1/\sqrt{\rho_{max}}$ and assume that $\epsilon \ll 1$, while retaining the SSWM regime ($U < U_c = \theta^2\lambda$). Overall mutation effects are thus assumed to fall within the range: $U/\theta^2 < \lambda \ll r_{max}$. We further require for analytical simplifications that $y_D \geq 2\epsilon$ in the new environment, but this only excludes situations where rescue is *de facto* certain. The weak effect assumption $\lambda \ll r_{max}$ can alternatively be interpreted as follows (see **Appendix**): we require that the new optimum lies several mutational steps away from the subset of 'critical' phenotypes (i.e. those with growth rate $r = 0$). We assume (i) a sufficiently stressful environment (inducing non-vanishing decay), (ii) but one that leaves room for substantial later adaptation, when starting from a barely resisting genotype. It means that resistant variants typically do not overshoot the optimum. This assumption is only problematic when analyzing rescue in very low quality environments where r_{max} is very low (See **Supplementary figure 6B**).

This weak effect assumption (see **Appendix**) allows substantial simplification of the probability density function $f_y(y)$ in Eq.[2] and the harmonic mean of the scaled cost $\tilde{c}_H$ in Eq.[4]. Let us first define the following variables, which depend on r_D, r_{max} and λ:

$$\begin{aligned} \psi_D &= 2\left(\sqrt{1+y_D}-1\right) \\ \alpha &= \frac{\psi_D^2\,\rho_{\max}}{4} + 1/2 \end{aligned} \quad , \qquad [5]$$

where ψ_D is a transformed variable of the scaled fitness distance to the optimum and α is "the effective stress level". Both increases with r_D and decreases with an increasing r_{max}. α also increases with the scaled maximal growth rate $\rho_{\max}$, for which λ can only variate with r_{max} to respect the weak mutation effects assumption. The non-linear dependence between α and ψ_D on the parameters r_D, r_{max} and $\rho_{\max}$ summarizes the effects of the stress in our model.

Under the weak effect assumption ($U/\theta^2 < \lambda \ll r_{max}$) the rate of de novo rescue (Eq.[4]), using the variables describes above, is approximately :

$$\begin{aligned} \omega_R^{DN} &\approx \left(\frac{1-\psi_D/(4\alpha)}{1+\psi_D/2}\right)^{\theta\,-\,1/2} g(\alpha) \\ \text{with } g(\alpha) &= \frac{\mathrm{e}^{-\,\alpha\,-\,1/2}}{\sqrt{2}\,\alpha\,\sqrt{1+\alpha}} \end{aligned} \quad . \qquad [6]$$

Differentiating ω_R^{DN} in Eq.[6] with respect to the model parameters allows evaluating the sensitivity of ER probability to them (**Supplementary file S1**). ER probability always increases with increasing per-trait mutational variance λ, decreasing decay rate r_D, increasing height of the fitness peak r_{max} and decreasing dimensionality ($\theta = n/2$). The effects of λ and r_{max} are expected as it is easier to 'send' mutants in the phenotype subspace corresponding to resistance ($r > 0$) when mutation effects are large (larger λ), and when this subspace is wider (higher peak r_{max}). The effect of n is reminiscent of the "cost of complexity", which already arises in the FGM in the absence of demographic decay (Orr 2000). ER decreases with r_D due to the fast demographic decay, as in previous models, but also due to its negative impact on the proportion of resistant mutants. This latter effect of r_D might at first sight seem inconsistent with classic results on the FGM, where the proportion of beneficial mutations typically increases with maladaptation. Resistance mutations however form a typically small subset of mutations, sufficiently beneficial to grow while their ancestor decays ($s > r_D > 0$). This subset gets smaller as the decay rate increases. ψ_D and the effective stress level α affects the probability of ER in a more complex way than the parameters r_{max}, r_D and λ that is difficult to show from Eq.[6] and will be investigated in detail in the next section using simpler approximated form.

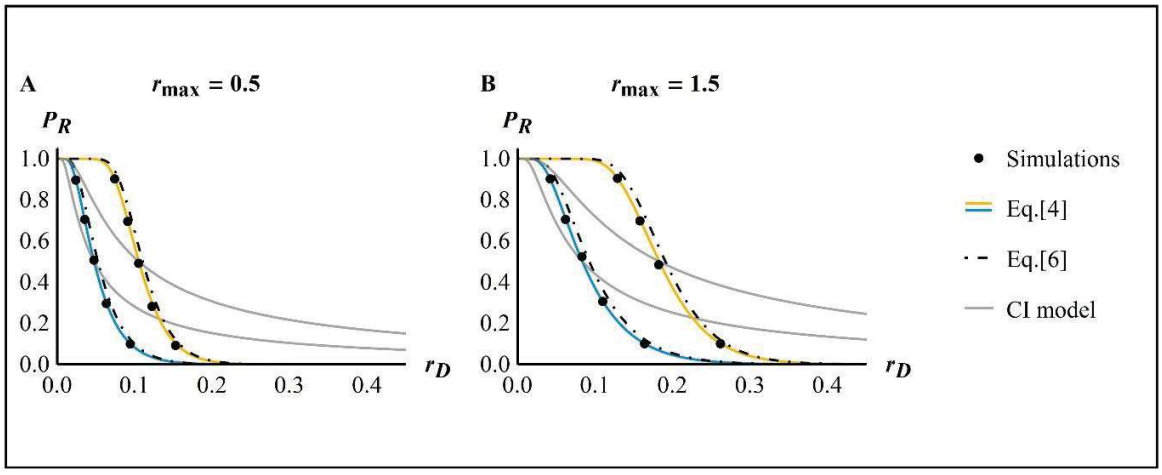

Figure 2: Rescue probability from de novo mutations*. The ER probability as a function of stress levels, expressed as the initial mean decay rate of the population, is given for various values of the mutations rate $U = 10^{-3}\,U_c$ (blue) or $U = 10^{-2}\,U_c$ (orange) and the maximal fitness reachable in new the environment $r_{max} = 0.5$ (A) or 1.5 (B). Dots give the results from simulations, solid lines (blue and orange) show the corresponding theory computed numerically (Eq.[4]). The dashed lines give the corresponding analytical approximations (Eq.[6]). The gray lines correspond to an equivalent theory without context-dependence (modified from (Orr and Unckless 2008). This model was computed using a fixed proportion of resistant*

mutation equal to the one in Eq.[4] for a rescue probability of 0.5 *(which explain why the two curves cross exactly at* $P_R = 0.5$*). Other parameters are* $n = 4$, $N_0 = 10^5$, $\lambda = 0.005$.

Figure 2 shows the agreement between simulations (stochastic discrete time demographic model) and the analytical expressions in Eq. [6], over the full range of stress (quantified as r_D) for two values of r_{max} and U (**Supplementary figure 3** further explores the range of validity of this approximation). Interestingly, ER probability drops sharply with stress levels (i.e. with decay rate r_D here), much more so than predicted by a context-independent model (gray lines on **Figure 2**), in which stress do not affect the evolutionary potential of mutants and the rate of rescue is $\omega_R \propto 1/r_D$. This stems from the fact that in the FGM, increased stress means faster decay (as in context-independent models), but also fewer and weaker resistance mutations. This second effect is a driving factor in the pattern of ER probabilities across stress levels in the FGM, and is dominated by the term $g(\alpha)$ in Eq. [6] as we detail below.

Low dimensionality/mild stress:

The interplay of all parameters $(\lambda, \theta, r_D, r_{max})$ determines the stress-dependent drop in ER probability, but in a way not directly obvious from Eq.[6]. For example, the key variable ψ_D (itself roughly proportional to the stress intensity $y_D = r_D/r_{max}$) enters the rate of rescue in a highly nonlinear fashion. However, the pattern simplifies substantially if dimensionality is small and/or stress is mild (y_D small). Indeed, whenever the factor $(1 - \psi_D/(4\alpha))/(1 + \psi_D/2)$ in Eq.[6] approaches 1 (the condition being less stringent as $\theta \to ½$), Eq. [6] becomes $\omega_R^{DN} \approx g(\alpha)$ (see **Appendix III.2** for the detailed analysis). Stress may in general impact all landscape parameters $(\lambda, \theta, r_D, r_{max})$, but its resulting impact on ER probabilities is then fully captured (via the function $g(.)$) by the effective stress level α in Eq.[5]. More precisely, this simplification holds approximately when the two following conditions are jointly verified:

$$\left.\begin{array}{l} \text{(a)}\ \ \theta - 1/2 \ll \sqrt{2\,\rho_{max}} = \sqrt{2}/\,\epsilon \\ \text{(b)}\ \ If\ \theta > 1/2,\ \ r_D \ll 2\,r_{max}/(\theta - 1/2) \end{array}\right\} \Rightarrow\ \omega_R^{DN} \approx\ g(\alpha)\,. \qquad [7]$$

The conditions are always met in $n = 1$ dimension ($\theta - 1/2 = 0$), when $\epsilon \gg 1$ as we have assumed all along. The conditions extend to higher dimensions, as long as n remains limited (condition (a)) and the decay rate is small relative to the maximal growth rate (condition (b)). The conditions in Eq. [7] show that the complex parametrization due to the FGM can be simplified

when stress and complexity are relatively low, the effect of stress is entirely mediated by α and is approximately independent of dimensionality (of θ).

This simplification is illustrated in **Figure 3**, where we explore different possible effects of stress (as captured by Eq.[6]): on the maladaptation of the wild type through r_D, on the maladaptation of the wild type and the quality of the environment through r_D and r_{max} jointly, or on the maladaptation of the wild type and its evolvability through r_D and λ jointly (**Figure 3A**, blue, orange and red, resp.). These various effects are accurately summarized by a single effect of stress on α (**Figure 3B**), which is approximately independent of dimensionality (compare circles $n = 1$ and squares $n = 6$ on **Figure 3B**) and is captured by Eq.[7]. Using numerical computations from Eq.[4], instead of Eq.[6], over this wide range of parameters, leads to similar results. The range of validity of the approximation from Eq.[7] is tested more extensively in **Supplementary figure 5**. We also note that Eq.[7] always overestimates the 'exact' ER probability from Eq.[4], so it provides a conservative bound when considering control of emerging pathogens.

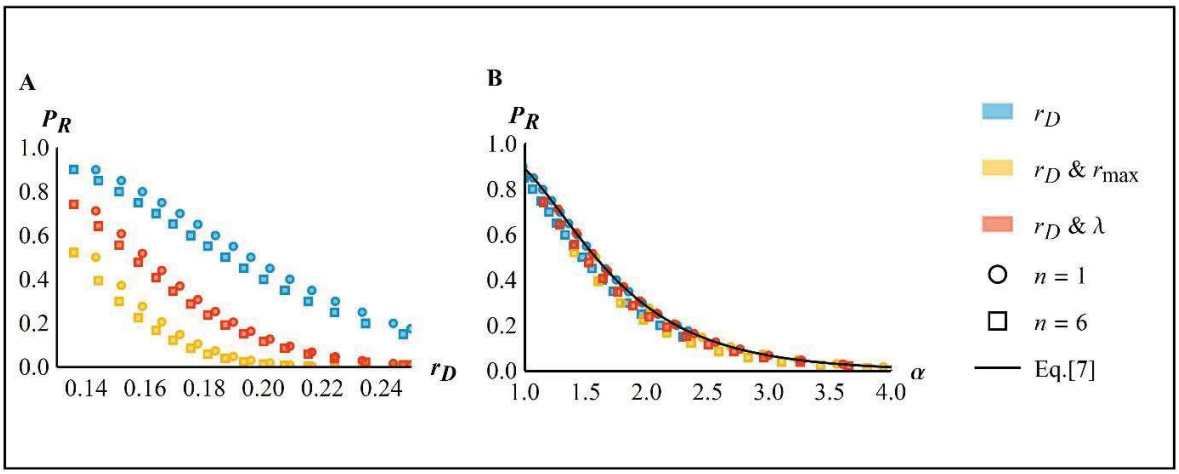

Figure 3: Composite stress measure. *Rescue probability for clonal populations versus initial decay rate* r_D ***(A)*** *or* the effective stress level α ***(B)****. In both panels symbols show Eq.[6] and colors refer to different effects of increased stress level: blue symbols show only* r_D *increasing, orange symbols* r_D *increasing and* r_{max} *decreasing linearly with* r_D *(according to* $r_{max} = 1.5 - 5\, r_D$*) and red symbols* r_D *increasing and* λ *decreasing linearly with* r_D *(according to* $\lambda = 0.005 - 10^{-2}\, r_D$*). In each case, the results for both* $n = 1$ *(circles) and* $n = 6$ *(squares) are shown. The black plain line on the right panel gives the result from Eq.[7]: a single composite measure of stress* (α) *approximately captures the impact of stress-induced variations in the various parameters* $(r_D, r_{max}, \lambda, n)$*. Other parameters are* $N_0 = 10^6$ *and* $U = 2 * 10^{-5}$*.*

'Characteristic stress window':

From Eqs. [6]-[7], the function $g(.)$ provides a quantification of the 'window' of stress levels over which ER drops from highly likely to highly unlikely. As this drop is important in characterizing the typical range of environments in which a given population may persist, it is important to obtain analytical insight on its bounds. This is detailed in section IV of the **Appendix**, and we summarize the main results below.

We define an 'isorescue' line of a given level $p \in [0,1]$ as the set of values of parameters $(N_0, U, r_{max}, r_D, \lambda, n)$ for which the rescue probability is p. At low dimensionality, from Eq.[7] we can show this isocline (for given N_0U) may be characterized approximately by the set (r_{max}, r_D, λ) that corresponds to a given value of α, i.e. to $\alpha = \alpha_p = g^{-1}(-\log(1-p)/N_0U)$. Using the simplification $g(\alpha) \approx \alpha^{-3/2}e^{-\alpha}/\sqrt{2e}$ (from Eq.[6] whenever $\alpha \gg 1$) this isocline can be derived explicitly (Eq. A25). Of particular relevance is the isocline of level $p = 1/2$, which defines the 'characteristic stress' $\alpha_{0.5}$ where the ER probability is $1/2$. From Eq.(A25) in section V of the **Appendix**, we obtain

$$\alpha_{0.5} \underset{N_0U \gg 1}{\approx} 0.9 \log(N_0U) - 2.33 , \qquad [8]$$

where Eq.[8] applies for large $N_0U \gg 1$ (see Appendix for a more general expression). The characteristic stress levels $\alpha_{0.5}$ that a population can typically withstand increases only log-linearly with population size and mutation rate. Predicting how sharply the ER probability drops around the characteristic stress is also important. This drop can be characterized by a 'characteristic stress window', which we define as the range of α over which the ER probability drops from 75% to 25%. The width $\Delta\alpha$ of this window can be scaled by the value of the characteristic stress $\alpha_{0.5}$, to get a scale-free measurement of its steepness. This simply gives:

$$\frac{\Delta\alpha}{\alpha_{0.5}} \approx \frac{1}{1 + 0.7\alpha_{0.5}} , \qquad [9]$$

The width $\Delta\alpha$ (in absolute value) increases with increasing N_0U. However, when scaled by the intermediate value $\alpha_{0.5}$ the width of the scaled "characteristic stress window" (in relative value) is less than 1, and becomes small for large $\alpha_{0.5}$ (hence for large N_0U (see Eq.[8])), indicating a sharp

drop in ER probability, relative to the stress level around which it occurs (as illustrated in **Figure 4**).

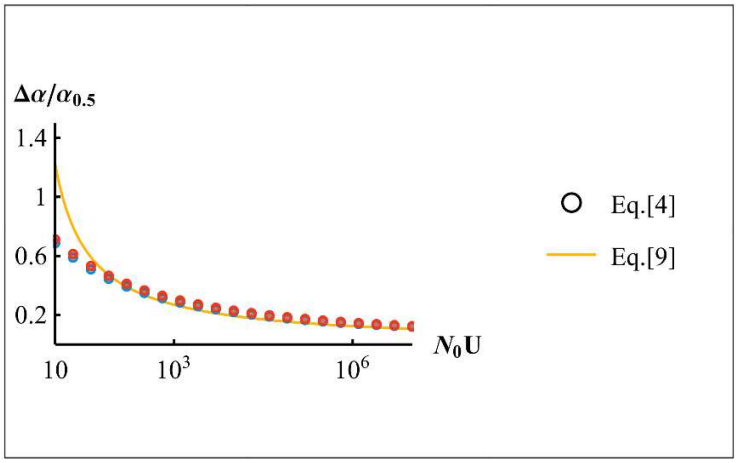

Figure 4: Scaled width of the characteristic stress window $\Delta\alpha/\alpha_{0.5}$ versus the population-scale mutation rate N_0U. *The dots are obtained by numerical inversion of the 'exact' Eq. [4] with two values of $r_{max} = 2$ (blue) and $r_{max} = 0.1$ (red). The orange line shows the approximate characteristic scale derived in Eq.[9]. Other parameters $n = 4$, $\lambda = 0.005$.*

This simple behavior described in Eq.[9] is indeed consistent with the less approximated ratio from Eq.[4] in the low dimensionality/mild stress conditions detailed in Eq.[7] (**Figure 4**). The accuracy of the approximate form of Eq.[9] breaks down for low N_0U with $\Delta\alpha/\alpha_{0.5}$>1 as shown in **Figure 4**. Interestingly, Eq.[9] provides a scale-free measure that may be compared across experiments, as it only depends on the genomic mutational input N_0U (via $\alpha_{0.5}$), as seen in **Figure 4**. However, like all results so far, eq. [9] only considers ER from *de novo* mutation. We now turn to ER from standing genetic variation.

Rate of rescue from a population at mutation-selection balance:

In the SSWM regime, and for a population at mutation-selection balance in the previous environment, each rescue event can be tracked back to either a pre-existing variant, or a *de novo* mutation (Orr and Unckless 2008, 2014; Martin *et al.* 2013). The proportion ϕ_R^{SV} of rescue events caused by standing variance thus provides a natural characterization of its relative contribution to ER, and is simply given by (see **Appendix**):

$$\phi_R^{SV} = \frac{\omega_R^{SV}}{\omega_R^{DN} + \omega_R^{SV}} = \frac{\beta}{1+\beta} \underset{\substack{r_{max} \gg \lambda \\ \alpha \geq 1}}{\approx} \frac{\rho_D}{(\alpha+\theta)+\rho_D}. \qquad [10]$$

The right-hand side expression corresponds to the weak effect approximation ($\rho_{max} \gg 1$) with substantial stress ($\alpha \geq 1$), in which case $\beta^* \underset{\rho_{max} \to \infty}{\approx} \rho_D / (\alpha+\theta)$ · (see Eq.(A18) in Appendix III.I). The ER probability is $P_R = 1 - e^{-N_0 U \omega_R}$ where $\omega_R = \omega_R^{DN} + \omega_R^{SV} = \omega_R^{DN}/(1-\phi_R^{SV})$. **Figure 5A** shows how P_R varies with stress (here, increasing r_D), in the presence of standing variance, and the agreement between simulations, Eq.[4] and the a closed form expressions described in the following. It is apparent from eq. [10] and **Figure 5B** that the contribution from standing variance is dominant ($\lim_{r_D \to \infty} \phi_R^{SV} = 0.5$ from Eq.(A22) in **Appendix IV**) when r_D is large (low ER probability from *de* novo mutations), but decreases ($\lim_{r_D \to 0} \phi_R^{SV} = 0$ from Eq.[10]) for very low stress (ER probability from *de* novo mutations is highly likely).

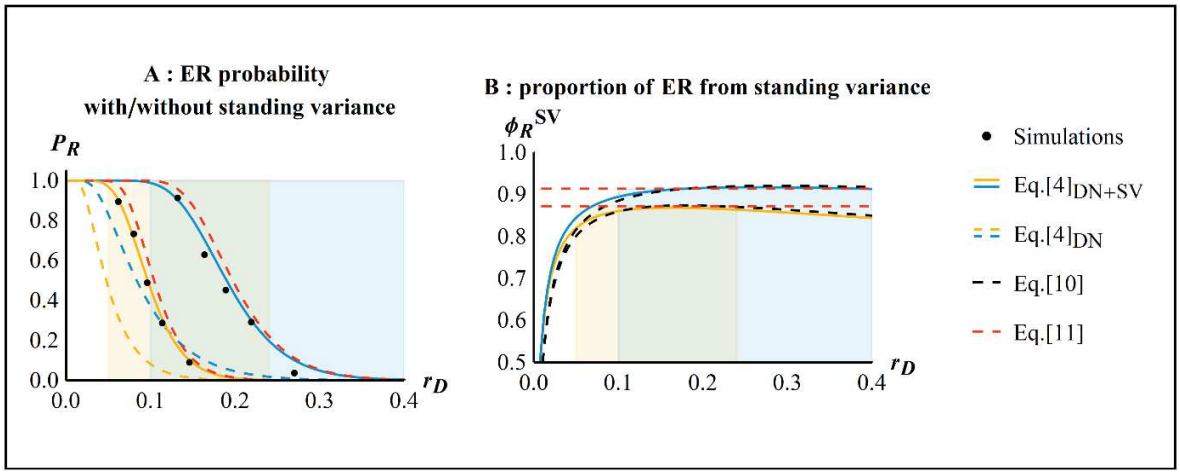

***Figure 5**: **ER probability in the presence of standing genetic variation.** In each panel, orange and blue correspond to two values of the maximal fitness in the new environment: $r_{max} = 0.5$ or 1.5 (respectively). Stress only affects the decay rate r_D (shifting optimum). **(A)** ER probability in the presence of standing genetic variation as a function of stress level r_D: simulations (dots) versus corresponding theory (dashed and plain lines, see legend) for either de novo rescue alone ('DN') or de novo plus standing variance ('DN'+'SV'). The dotted black line gives the simpler expression for the overall rescue rate: $\omega_R \approx \omega_R^{DN}/(1-\phi_R^*)$, from ϕ_R^* in Eq.[11]. **(B)** Proportion of rescue from standing variance as a function of r_D: the lines give the corresponding theory, based on $\tilde{c}_H$ in Eq. [4] or on $\tilde{c}_H \approx \theta + \alpha$ (approximation in Eq. [10]). Each colored shaded area (orange or blue, and green when overlapping) shows, for the corresponding value of r_{max} (0.5 or 1.5 respectively), the range of r_D for which ER probability drops from 0.99 to 10^{-3}. Other parameters: $n = 4, N_0 = 10^5, \lambda = 0.005$.*

We observe a very similar drop in ER probability with stress as with *de novo* mutation (**Figure 5A**), but at higher 'characteristic stress'. **Figure 5B** shows that ϕ_R^{SV} is maximal at intermediate stress levels, as captured both by the approximation $\phi_R^{SV} \approx \rho_D/((\alpha+\theta)+\rho_D)$ (dashed lines) and the more exact expression based on ω_R^{DN} and ω_R^{SV} in Eq.[4] (plain lines). This

stems from the nonlinearity of the effectiveness of standing variance β with the scaled stress ρ_D in Eq. [10]. At very mild stress, rescue stems from mild effect mutations, the cost of which is roughly independent of ρ_D (Martin and Lenormand 2015). Thus, their contribution is roughly stable across mild stress levels, while that from *de novo* mutations decreases with stress (as $1/\rho_D$). Overall, rescue stems more from standing variants as ρ_D increases, in this range. At very large stress levels, rescue stems from strong effect mutations: these pay a substantial 'incompressible cost' (Martin and Lenormand 2015), that increases faster than ρ_D. Therefore, the contribution from standing variants decreases again with stress, in this range (remaining dominant: $\phi_R^{SV} \geq 1/2$).

However, the variation of ϕ_R^{SV} may be negligible in practice. Assume a large $N_0\ U$ and that stress only affects ρ_D (rather than ρ_{max} or θ). Then over a wide range of stress levels (shaded area), ϕ_R^{SV} is close to maximal and roughly constant (**Figure 5B**). In our illustration, this range covers $P_R{\sim}0.99$ to $P_R{\sim}10^{-3}$. Mathematically, the curvature of ϕ_R^{SV} with r_D is large (of order $\sqrt{\frac{\rho_{max}}{\theta+1/2}}$, see **Appendix IV.**) as long as $\rho_{max} \gg (\theta + 1/2)$, when P_R only varies with ρ_D. Overall, over a large range of stress levels in which ER probability falls from highly likely to highly unlikely, ϕ_R^{SV} hardly deviates from its maximal value ϕ_R^*, which is given below (dotted line in **Figure 5B**). This means that the rate of rescue with standing variance is approximately proportional to that with only *de novo* mutation, with constant proportionality largely independent of the stress level:

$$\begin{aligned} &\phi_R^{SV} \approx \phi_R^* = \max_{\rho_D \in \mathbb{R}^+} \phi_R^{SV} \approx \frac{1}{1 + 0.7\ (\theta/\rho_{max})^{0.4}}\ . \\ &\omega_R = \omega_R^{DN} + \omega_R^{SV} \approx\ \omega_R^{DN}/(1 - \phi_R^*) \end{aligned} \qquad [11]$$

This constant contribution from standing variance decreases with increasing dimensionality (θ) and with a lower fitness peak (ρ_{max}). The rough constancy of ϕ_R^{SV} also means that all the results obtained previously for *de novo* ER apply in the presence of standing variance, when stress only shifts the optima. The characteristic stress is higher ($\alpha_{0.5} \underset{N_0U \gg 1}{\approx} 0.9 \log(X) - 2.33$ from Eq.[8] with $X = N_0U/(1 - \phi_R^{SV})$ in this context), with the same profile (stress window), as captured by the approximation $\omega_R \approx \omega_R^{DN}/(1 - \phi_R^*)$ (Eq. [11], dotted black line in **Figure 5A**).

Finally, note that U may also change across environments, from U_P (for previous) to U_N (for new). In the SSWM regime, this would simply amount to multiplying β by U_P/U_N (in Eq. [10]) to account for the different mutation rate in the rate of ER from standing genetic variance. For example, a stress-induced increase in DNA copy error would yield $U_N > U_P$ and a larger contribution from

de novo mutation (lower ϕ_R^{SV} in Eq.[10]). On the contrary, a decrease in birth rate under stress, combined with birth-dependent mutation (as is typical in microbes) would imply $U_N < U_P$ and a larger contribution from standing variance (higher ϕ_R^{SV} in Eq.[10]).

Discussion

Main results:

We investigated the persistence of a population of asexual organisms under an abrupt environmental alteration. This 'stress' affects a multidimensional fitness landscape with a single peak (FGM), which the population must 'climb' to avoid extinction. From this landscape emerges a quantitative constraint, linking the initial decay rate of the population, the proportion and growth rate of resistance alleles among random mutants, and their selective cost before stress. In the model, a continuum of stress levels may modify the landscape in various ways: shifting the optimum, changing the peak height or the phenotypic scale of mutations. Under a SSWM regime and assuming weak mutations effects, all these effects are approximately captured by the variation, across stress levels, of a single composite parameter α (Eq. **[6], Figure 3, Figure 4, Supplementary figure 4**) , which we denote the "effective stress level". The probability of ER drops sharply with the measure of the effective stress α (Eq.[9], **Figure 4**), more so than in previous context-independent models (**Figure 2**). The 'characteristic stress window', over which this drop occurs, approximately only depends on N_0U: as N_0U gets larger, the window gets narrower (**Figure 4**) and shifts towards higher stress levels, approximately as $\log(N_0U)$ (Eq.[8]). when standing variance is available (population at equilibrium before stress), its contribution to ER is dominant and approximately constant across a wide range of stress levels (Eqs.[10]-[11], **Figure 5**), in this same regime (SSWM and weak mutation effects). The model thus integrates multiple environmental and mutational factor potentially empowering or hindering ER through the effective stress level and predict that a narrow increase of stress tremendously increases the probability to eradicate a pathogen population. Moreover the intensity of stress needed to creates such a drop in ER probability increases with the population size and the mutation rate, but log-linearly with stress. This means for antibiotic treatments against pathogens, under the approximation that the concentration of the stressor is linear with stress, that an accurate range of concentration of effective treatment can be predicted from the model (assuming its predictive

ability validated on data) and adapted to the level of infection and the mutation capacity of the organism.

Empirical validation of the model for treatments against pathogens:

For treatments against pathogens, stress level is the main factor under our control (dose regimes etc.). Empirically, it is also perhaps the best-studied factor in this context (Gunderson et al. 2001; Drusano 2004). Therefore, it seems important to provide a predictive model of ER probabilities over a range of stress levels comparable to experimental data in order to give insights into the complex trade-off between curing infections and managing resistance (Day and Read 2016; Levin-Reisman et al. 2017). In general, to test our predictions and any ER model, it is critical to empirically relate physical measures of stress level (e.g. concentrations, temperatures, salinities etc.) with demographic measures (decay rates). Here we consider, for example, the concentration υ of an antibiotic. With such data our model could be tested in several ways. First, assuming that increased υ only implies larger shifts in the optimum, then only r_D depends on υ. This parameter ($r_D(\upsilon)$) can be measured over a range of concentrations via classic kill-curve studies (Regoes *et al.* 2004). The probability of resistance emergence ($P_R(\upsilon)$), from a purely clonal population, can also be measured across the same range of υ. We then expect a predictable relationship between $P_R(\upsilon)$ and $r_D(\upsilon)$, which could depend on other parameters as r_{max}, λ or even U according to the model considered (Eqs.[6][7][10]).

For a more powerful test of the model, the full set of parameters may be inferred from additional measures. The FGM parameters (λ, θ, assumed constant across υ) and mutation rate U may be estimated from random mutation data in the model species considered (Martin and Lenormand 2006a; Perfeito *et al.* 2014). The maximal growth rate under stress would ideally have to be measured on lines well-adapted to each particular concentration υ (e.g. Harmand et al. *submitted*). If too challenging, this last parameter could be assumed constant and estimated from the P_R versus r_D relationship. An alternative use of our results is to infer the parameter $\alpha(\upsilon)$ across concentrations υ, from the observed relationship $P_R(\upsilon)$, given a known value of N_0U, by inverting $g(\alpha)$ (assuming limited dimensionality, Eq.[7]). Finally, the simple scale free characterization of the characteristic stress window (Eqs.[9]) could be tested across various inoculum sizes (i.e. across N_0U).

Density-dependence and competitive release:

Our model ignores density dependence but it could be introduced easily. *A minima*, one could consider a single density dependence coefficient (common to all genotypes) and use logistic diffusion approximations (Lambert 2005). This would potentially allow for 'competitive release' effects (Read *et al.* 2011). Such effects are expected in density-dependent models when resistant variants are present before stress. Then higher stresses may actually favor the emergence of resistance by rapidly depleting the sensitive wild-type population, thus releasing limiting resources for resistant genotypes. Previous models that showed competitive-release effects assumed context-independent mutation (Read *et al.* 2011; Day and Read 2016), where the number of standing resistant mutants is independent of stress level. Thus, increased stress mostly limits *de novo* rescue mutation with more limited impact on the contribution from standing variance. On the contrary, the FGM imposes a similar drop, with stress, in the rate of rescue from *de novo* and preexisting mutants (Eq.[11]).The positive effects of competitive release on ER probability may thus be less important, in the FGM, than predicted from these previous models.

Small peak limit:

In the "weak mutation effect limit" (Eqs. [6]-[7]), resistant mutants are typically much less fit that the optimal phenotype under stress ($r \ll r_{max}$). They belong to the *tail* of the mutant phenotypic distribution and are packed in the portion of the subspace of all resistant phenotypes closest to the ancestor (see **Supplementary figure 6A**). An alternative situation (still described by Eq.[4] but not Eqs. [6]-[7]) is in a poor environment when resistant mutants typically cover the whole subspace of resistance phenotypes, but this subspace is very small relatively to mutation effects on phenotype (so that ER remains unlikely). This situation (illustrated in **Supplementary figure 6A**) corresponds to a case where mutation effects are similar or larger than the maximal growth rate ($\lambda = O(r_{max})$). The fitness peak under stress is then not very high (r_{max} is small), and mutations can easily overshoot the optimum in the new environment. In this situation, at least for mild decay rates, resistant phenotypes are a small subset from the *bulk* of the mutant phenotypic distribution. The volume (in phenotype space) occupied by this subset is roughly constant across stress and determines the ER probability, together with decay rate (by a direct demographic effect). The cost of complexity is more important in this regime, as it strongly determines the volume of the resistance subspace (see **Supplementary figure 6B**).

Anisotropy and parallel evolution in drug resistance:

The present model is isotropic, in that all directions in phenotype space are equivalent (in terms of mutation and selection). Yet, in general, module-dependent anisotropy (where particular genes mutate along favored directions) is the key requirement for the FGM to generate substantial parallel evolution (Chevin 2013). Parallel evolution, whereby some (portions or sets of) genes contribute most of the resistance mutations, is often observed among drug resistance alleles, and can further increase with stress (Harmand *et al.* 2016). Although not explored here, we conjecture that our model may accommodate some anisotropic extensions. First, mild anisotropy (even environment-dependent) might have limited impact. If mutational covariances between traits merely "turn", "shrink" or "expand" the phenotypic mutant cloud, this would approximately amount to a mere change in λ in an equivalent isotropic landscape (Martin and Lenormand 2006b; Martin 2014). Second, a particular form of strong anisotropy may arise when mutant phenotypes (in a given module) spread along a single favored direction (Martin 2014). It may then be sufficient to reduce the n dimensional model to a single dimension version of the present isotropic model ($n = 1$: Eq.[7] is then exact). This conjecture would require further investigation.

Robustness of the limiting assumptions:

Several limiting assumptions of the evolutionary model used here can be justified by the short timescale and rarity of rescue events. Assuming a single optimum seems reasonable in a harsh environment: most rescue trajectories will *a priori* stem from the few mutants reaching the closest local optimum in the landscape. The use of the SSWM approximation also seems reasonable in the context of rescue. Indeed, mutants that show substantial decay rates do not persist long enough in the population to contribute much secondary mutations (Martin *et al.* 2013). This argument applies if the genomic mutation rate is low enough (roughly $U < U_c = \theta^2\lambda$, **Supplementary figure 1**). In contexts where the mutation rate is higher (e.g. viruses or mutator bacterial strains), multiple mutants must be accounted for as a source of ER. These can in principle be introduced in the framework used here (Martin *et al.* 2013), but, especially when applied to the FGM, the results quickly become intractable. Alternative population genetics assumptions would have to be used, which is beyond the scope of this work.

Conclusion:

Recently, the FGM has received renewed interest by its ability to provide testable, quantitative and often accurate predictions regarding patterns of mutation effects on fitness, across various species and contexts (Tenaillon 2014). The present model is an attempt to extend its scope to model the evolution of resistance to stress. We hope that future experimental tests will evaluate its accuracy and potential to tackle pressing applied issues, in particular regarding resistance management.

Bibliography

Agrawal A. F., Whitlock M. C., 2010 Environmental duress and epistasis: how does stress affect the strength of selection on new mutations? Trends Ecol. Evol. 25: 450–458.

Alexander H. K., Martin G., Martin O. Y., Bonhoeffer S., 2014 Evolutionary rescue: linking theory for conservation and medicine. Evol. Appl. 7: 1161–1179.

Bijlsma R., Loeschcke V., 2005 Environmental stress, adaptation and evolution: an overview. J. Evol. Biol. 18: 744–749.

Burger R., Lynch M., 1995 Evolution and Extinction in a Changing Environment: A Quantitative-Genetic Analysis. Evolution 49: 151.

Carlson S. M., Cunningham C. J., Westley P. A. H., 2014 Evolutionary rescue in a changing world. Trends Ecol. Evol. 29: 521–530.

Charmantier A., Garant D., 2005 Environmental quality and evolutionary potential: lessons from wild populations. Proc. R. Soc. B Biol. Sci. 272: 1415–1425.

Chevin L.-M., 2011 On measuring selection in experimental evolution. Biol. Lett. 7: 210–213.

Chevin L.-M., 2013 GENETIC CONSTRAINTS ON ADAPTATION TO A CHANGING ENVIRONMENT. Evolution 67: 708–721.

Davies J., Davies D., 2010 Origins and Evolution of Antibiotic Resistance. Microbiol. Mol. Biol. Rev. 74: 417–433.

Day T., Read A. F., 2016 Does High-Dose Antimicrobial Chemotherapy Prevent the Evolution of Resistance? PLoS Comput. Biol. 12: e1004689.

De Visser J. a. G. M., Rozen D. E., 2005 Limits to adaptation in asexual populations. J. Evol. Biol. 18: 779–788.

Drlica K., 2003 The mutant selection window and antimicrobial resistance. J. Antimicrob. Chemother. 52: 11–17.

Drusano G. L., 2004 Antimicrobial pharmacodynamics: critical interactions of "bug and drug." Nat. Rev. Microbiol. 2: 289–300.

Feller W., 1951 Diffusion processes in genetics. In: Proceedings of the Second Berkeley Symposium on Mathematical Statistics and Probability,

Fisher R. A., 1930 *The Genetical Theory of Natural Selection*. Oxford University Press.

Foster P. L., 2007 Stress-Induced Mutagenesis in Bacteria. Crit. Rev. Biochem. Mol. Biol. 42: 373–397.

Gillespie J. H., 1983 Some Properties of Finite Populations Experiencing Strong Selection and Weak Mutation. Am. Nat. 121: 691–708.

Gomulkiewicz R., Holt R. D., 1995 When does Evolution by Natural Selection Prevent Extinction? Evolution 49: 201.

Gomulkiewicz R., Holt R. D., Barfield M., Nuismer S. L., 2010 Genetics, adaptation, and invasion in harsh environments. Evol. Appl. 3: 97–108.

Gonzalez A., Bell G., 2013 Evolutionary rescue and adaptation to abrupt environmental change depends upon the history of stress. Philos. Trans. R. Soc. Lond. B Biol. Sci. 368: 20120079.

Gonzalez A., Ronce O., Ferriere R., Hochberg M. E., 2013 Evolutionary rescue: an emerging focus at the intersection between ecology and evolution. Philos. Trans. R. Soc. B Biol. Sci. 368: 20120404–20120404.

Gunderson B. W., Ross G. H., Ibrahim K. H., Rotschafer J. C., 2001 What Do We Really Know About Antibiotic Pharmacodynamics? Pharmacother. J. Hum. Pharmacol. Drug Ther. 21: 302S–318S.

Harmand N., Gallet R., Jabbour-Zahab R., Martin G., Lenormand T., 2016 Fisher's geometrical model and the mutational patterns of antibiotic resistance across dose gradients. Evolution: 1–32.

Hermisson J., Wagner G. P., 2004 The Population Genetic Theory of Hidden Variation and Genetic Robustness. Genetics 168: 2271–2284.

Hietpas R. T., Bank C., Jensen J. D., Bolon D. N. A., 2013 Shifting Fitness Landscapes in Response to Altered Environments. Evolution 67: 3512–3522.

Hoffmann A. A., Parsons P. A., 1997 *Extreme environmental change and evolution*. Cambridge University Press, Cambridge; New York.

Hoffmann A. A., Merilä J., 1999 Heritable variation and evolution under favourable and unfavourable conditions. Trends Ecol. Evol. 14: 96–101.

Koehn R. K., Bayne B. L., 1989 Towards a physiological and genetical understanding of the energetics of the stress response. Biol. J. Linn. Soc. 37: 157–171.

Kopp M., Matuszewski S., 2014 Rapid evolution of quantitative traits: theoretical perspectives. Evol. Appl. 7: 169–191.

Lambert A., 2005 The branching process with logistic growth. Ann. Appl. Probab. 15: 1506–1535.

Levin-Reisman I., Ronin I., Gefen O., Braniss I., Shoresh N., *et al.*, 2017 Antibiotic tolerance facilitates the evolution of resistance. Science: eaaj2191.

Lindsey H. A., Gallie J., Taylor S., Kerr B., 2013 Evolutionary rescue from extinction is contingent on a lower rate of environmental change. Nature 494: 463–467.

Lynch M., Gabriel W., Wood A. M., 1991 Adaptive and demographic responses of plankton populations to environmental change. Limnol. Oceanogr. 36: 1301–1312.

MacLean R. C., Perron G. G., Gardner A., 2010 Diminishing Returns From Beneficial Mutations and Pervasive Epistasis Shape the Fitness Landscape for Rifampicin Resistance in Pseudomonas aeruginosa. Genetics 186: 1345–1354.

Martin G., Lenormand T., 2006a The Fitness Effect of Mutations Across Environments: A Survey in Light of Fitness Landscape Models. Evolution 60: 2413–2427.

Martin G., Lenormand T., 2006b A General Multivariate Extension of Fisher's Geometrical Model and the Distribution of Mutation Fitness Effects Across Species. Evolution 60: 893–907.

Martin G., Elena S. F., Lenormand T., 2007 Distributions of epistasis in microbes fit predictions from a fitness landscape model. Nat. Genet. 39: 555–560.

Martin G., Aguilée R., Ramsayer J., Kaltz O., Ronce O., 2013 The probability of evolutionary rescue: towards a quantitative comparison between theory and evolution experiments. Philos. Trans. R. Soc. Lond. B. Biol. Sci. 368: 20120088.

Martin G., 2014 Fisher's geometrical model emerges as a property of complex integrated phenotypic networks. Genetics 197: 237–255.

Martin G., Lenormand T., 2015 The fitness effect of mutations across environments: Fisher's geometrical model with multiple optima. Evolution 69: 1433–1447.

Martin G., Roques L., 2016 The Non-stationary Dynamics of Fitness Distributions: Asexual Model with Epistasis and Standing Variation. Genetics: genetics.116.187385.

Moser C., Bell G., 2011 Genetic correlation in relation to differences in dosage of a stressor. J. Evol. Biol. 24: 219–223.

Orr H. A., 2000 Adaptation and the Cost of Complexity. Evolution 54: 13–20.

Orr H. A., Unckless R. L., 2008 Population extinction and the genetics of adaptation. Am. Nat. 172: 160–9.

Orr H. A., Unckless R. L., 2014 The Population Genetics of Evolutionary Rescue. PLOS Genet. 10: e1004551.

Perfeito L., Sousa A., Bataillon T., Gordo I., 2014 Rates of Fitness Decline and Rebound Suggest Pervasive Epistasis. Evolution 68: 150–162.

Read A. F., Day T., Huijben S., 2011 The evolution of drug resistance and the curious orthodoxy of aggressive chemotherapy. Proc. Natl. Acad. Sci. 108: 10871–10877.

Regoes R. R., Wiuff C., Zappala R. M., Garner K. N., Baquero F., *et al.*, 2004 Pharmacodynamic Functions: a Multiparameter Approach to the Design of Antibiotic Treatment Regimens. Antimicrob. Agents Chemother. 48: 3670–3676.

Remold S. K., Lenski R. E., 2001 Contribution of individual random mutations to genotype-by-environment interactions in Escherichia coli. Proc. Natl. Acad. Sci. U. S. A. 98: 11388–11393.

Remold S. K., Lenski R. E., 2004 Pervasive joint influence of epistasis and plasticity on mutational effects in Escherichia coli. Nat. Genet. 36: 423–426.

Samani P., Bell G., 2010 Adaptation of experimental yeast populations to stressful conditions in relation to population size. J. Evol. Biol. 23: 791–796.

Scharloo W., 1991 Canalization: genetic and developmental aspects. Annu. Rev. Ecol. Syst. 22: 65–93.

Sgrò C. M., Hoffmann A. A., 2004 Genetic correlations, tradeoffs and environmental variation. Heredity 93: 241–248.

Tenaillon O., 2014 The Utility of Fisher's Geometric Model in Evolutionary Genetics. Annu. Rev. Ecol. Evol. Syst. 45: 179–201.

Trindade S., Sousa A., Gordo I., 2012 Antibiotic Resistance and Stress in the Light of Fisher's Model. Evolution 66: 3815–3824.

Turelli M., 1984 Heritable genetic variation via mutation-selection balance: Lerch's zeta meets the abdominal bristle. Theor. Popul. Biol. 25: 138–193.

Uecker H., Otto S. P., Hermisson J., 2014 Evolutionary Rescue in Structured Populations. Am. Nat. 183: E17–E35.

Uecker H., Hermisson J., 2016 The Role of Recombination in Evolutionary Rescue. Genetics 202: 721–732.

Wang A. D., Sharp N. P., Spencer C. C., Tedman-Aucoin K., Agrawal A. F., 2009 Selection, Epistasis, and Parent-of-Origin Effects on Deleterious Mutations across Environments in *Drosophila melanogaster*. Am. Nat. 174: 863–874.

Wang A. D., Sharp N. P., Agrawal A. F., 2014 Sensitivity of the Distribution of Mutational Fitness Effects to Environment, Genetic Background, and Adaptedness: A Case Study with Drosophila. Evolution 68: 840–853.

Wolfram Research I., 2012 *Mathematica*. Wolfram Research, Inc, Champaign, Illinois.

Notation	Description	Formula
t	Time elapsed since onset of stress	
N_t, N_0	Population size at time t after the onset of the stress, N_0: initial population size at the onset.	
U	Mutation rate *per* individual *per* unit time.	
n, θ	n: number of traits under stabilizing selection (θ: dimensionality)	$\theta = n/2$
λ	Variance of mutational effects on each trait traits	$\mathbf{dz} \sim N(\mathbf{0}, \lambda\, \mathbf{I}_n)$
U_c	Maximal mutation rate under which the WMSS regime is valid.	$U_C = \theta^2\, \lambda$
$\mathbf{z}$	n-dimensional vector $\mathbf{z} \in \mathbb{R}^n$ of (breeding values for) phenotype	
$\mathbf{z}_A, \mathbf{z}_*$	$\mathbf{z}_*$: optimal phenotype in a given environment $\mathbf{z}_A$: average phenotype of the ancestral population (before the onset of stress)	$\mathbf{z}_* = \mathbf{0}$: new environment $\mathbf{z}_* = \mathbf{z}_A$: previous environment
r, σ	Growth rate (r) and reproductive variance (σ) of a given genotype, in the new environment.	$r(\mathbf{z}) = r_{max} - \lVert \mathbf{z} - \mathbf{z}_* \rVert^2/2\,, \mathbf{z} \in \mathbb{R}^n$(Eq.[1]) $\sigma \approx 1$
r_{max}	Maximum possible growth rate in the new environment.	$r(\mathbf{z}_*) = r_{max}$
r_D	Rate of decay of the ancestral phenotype $\mathbf{z}_A$ in the new environment.	$r(\mathbf{z}_A) = r_{max} - \lVert \mathbf{z}_A \rVert^2/2 = -r_D$
c	Cost of a mutation: selective disadvantage of the mutant, relative to the optimal phenotype, in the previous environment.	
$c_H(y)$	Harmonic mean of the cost $c\|y$ among de novo resistant mutations.	Eq.[3]
β	Effectiveness of the standing variance relatively to *de novo* mutations for ER.	Eq. [10]
y	Growth rate of a genotype, in the new environment, scaled by r_{max}.	$y = r/r_{max} \in [-\infty, 1]$

$f_y(y)$	PDF of y among random single step mutations	Eq.[1]
y_D	Stress intensity: Rate of decay scaled by r_{max}.	$y_D = r_D/r_{max}$
ρ_D	Scaled decay rate	$\rho_D = r_D/\lambda$
ρ_{max}	Scaled maximal growth rate	$\rho_{max} = r_{max}/\lambda$
ψ_D	Alternative measure of y_D	$\psi_D = 2\left(\sqrt{1+y_D}-1\right)$ (Eq.[5])
α	Composite measure of stress level.	Eq.[5]
$g(\alpha)$	Function driving the dependence of rescue probabilities on stress levels.	Eq.[6]
ω_R^{DN}	Rate of rescue from *de novo* mutations scaled by $N_0\ U$	Eqs. [4],[5],[6]
ω_R^{SV}	Rate of rescue from standing variants scaled by $N_0\ U$, in an equilibrium population.	Eqs.[4],[10]
P_R	Probability of rescue.	$P_R = 1 - e^{-N_0 U\ \omega_R}$
ϕ_R^{SV}	% of rescue events caused by standing variants	Eq. [11]

Table 1: *Notations*

CHAPTER I
Appendix: Analytical derivation

In this appendix, we detail the analytical derivations leading to the equations given in the main text, in three parts. First, in section I. "Settings and general results", we give more detailed insight about the methods section and briefly recall the derivations from Martin et al. (2013) leading to the evolutionary rescue (ER) probability. Then, in section II. "Application to Fisher's Geometric Model (FGM)", we detail the derivations of the distribution of fitness effects (Martin and Lenormand 2015) that is included in the model, leading to the so-called 'exact' form of the ER probability in the SSWM regime (Eq.[4]). In section III. "Simplified closed form expressions", we derive simplified approximations based on two levels of assumptions:

- First (III.1), we assume non-vanishing stress and weak mutation effects relative to the maximal fitness. This simply means that the edge of the resistant phenotype subspace (genotypes with $r_i = 0$) lies at many mutational steps from the optimum in the stress. This allows using (i) a simplified analytical form for the DFE and (ii) Laplace approximations for the integrals involved in the ER probabilities, ultimately yielding general explicit expressions for ER from both *de novo* and preexisting mutants.

- Second (III.2), we further assume small dimensionality and mild stress (within a known range of decay rates) and focus on *de novo* ER. The general explicit formula for ER probability then simplifies to an expression that depends on a single composite parameter α.

- Then, in section "IV. Proportion of rescue from standing variance" we use the analytic expressions in section III.1 to study the probability that an ER event stems from a pre-existing mutant or a *de novo* mutation when both are available. Finally, in the last section "V. Characteristic stress and stress window", we use the simpler results from section III.2 to study the characteristic stress window over which *de novo* ER drops from very likely to very unlikely.

I. Settings and general results

We follow the general model and approximations described in Martin *et al.* (2013), the results of which we recall briefly below. We then apply it to the case where the genotype-phenotype-fitness map follows Fisher's Geometrical Model (FGM). We denote as 'new environment' the environment imposed at the onset of stress ($t = 0$): it is characterized by the fact that the initial population under study decays in it. The environment in which the population was before the onset of stress (important when considering standing variance) is denoted as 'previous environment'.

General stochastic demography:

Each genotype present at $t = 0$ or later produced by mutation (via a Poisson process) is characterized by the parameters (r_i, σ_i) of a Feller diffusion approximating its stochastic demography. Let $N_i(t)$ be the size of the genotypic class at time t. The growth rate r_i is defined as the expected relative change of that class size ($r_i = E(\Delta N_i|N_i)/N_i$) over some time interval (infinitesimal in the diffusion limit), conditional on current size N_i at time t. The demographic variance parameter σ_i is the corresponding scaled stochastic variance of this conditional change: $\sigma_i = V(\Delta N_i|N_i)/N_i$. In the diffusion limit, the population size of the genotypic class is then characterized by the stochastic differential equation $dN_i(t) = r_i N_i(t)dt + \sqrt{\sigma_i\, N_i(t)}dB_t$ where B_t is a standard Brownian motion.

Application to a discrete time model with Poisson offspring distribution:

In our case, we consider, as an example, discrete non-overlapping generations where the subclass consisting of individuals of genotype i produces $N_i(t+1) \sim Poisson(W_i N_i(t))$ offspring over one generation, where W_i is the absolute Darwinian (i.e., multiplicative) fitness of this genotype. In this case $r_i = E(N_i(t+1))/N_i(t) = W_i - 1$, while $\sigma_i = V(N_i(t+1))/N_i(t) = W_i$ are two constant coefficients for any genotype. The diffusion limit applies when the demographic changes per generation are small, which requires $W_i \to 1$. In this case we retrieve a Feller diffusion where $r_i = W_i - 1 \to \log(W_i)$ is the absolute Malthusian fitness of genotype i, while $\sigma_i = W_i \to 1$ is constant across genotypes (Martin *et al.* 2013).

Establishment probability:

Extinction of the population occurs if none of the genotypes present or produced over the course to extinction avoids extinction: following classic notation, non-extinction (over infinite time) is denoted "establishment". The probability of establishment, for a lineage started in single copy and with growth rate r and stochastic variance σ in the new environment is $\pi_F(r) = 1 - e^{-2\,r/\sigma}$ for $r > 0$ and 0 otherwise. With Poisson reproduction ($\sigma \approx 1$) as in our simulation examples, and assuming weak growth ($r \ll \sigma \approx 1$) this can be written in compact form as $\pi_F(r) \approx 2\,r\,\Theta(r)$ where $\Theta(.)$ is the Heaviside theta function ($\Theta(x) = 1$ over $\mathbb{R}^+$ and $\Theta(x) = 0$ over $\mathbb{R}^-$). This fairly classic linear approximation is *a priori* justified here, particularly when stress is strong, because rescue is mostly achieved by barely growing mutants ($r \ll 1$).

Strong selection weak mutation (SSWM):

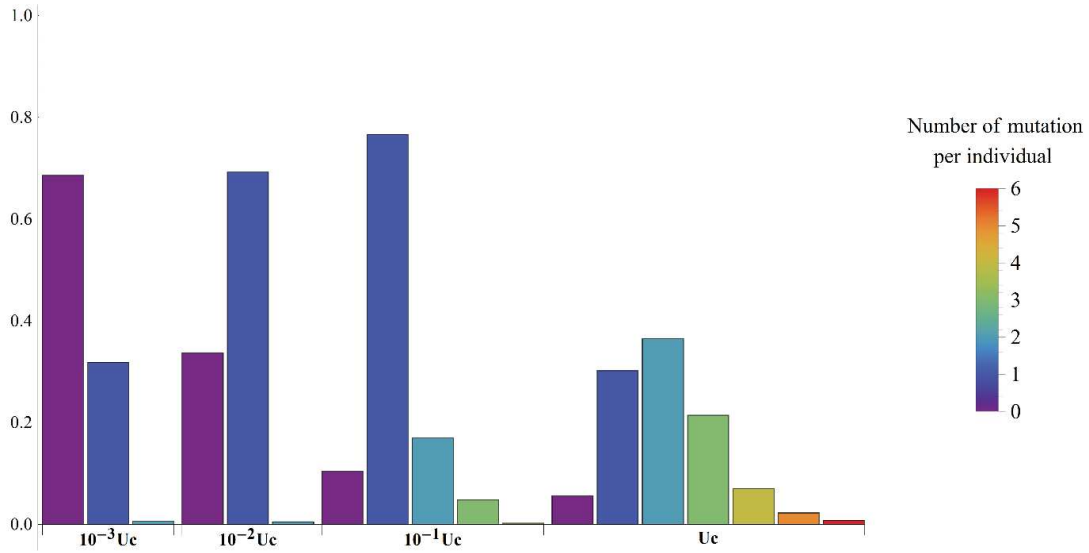

Supplementary Figure 1: proportion of individuals carrying different numbers of mutations in rescued populations*, from exact simulations. This proportion was evaluated in those populations having been rescued, at the time where they reach our stop criterion, which is when their current mean growth rate and population size imply a very low probability of future extinction, even in the absence of future adaptation (see simulation methods in main text). The distributions are given for different mutation rates (x-axis), given relative to the critical mutation rate ($U_c = 0.1$ here) below which the SSWM assumption should hold. Populations were initially composed of a single clone, with $N_0 = 10^5$, $n = 4$, $\bar{s} = 0.01$, $r_{max} = 1.5$, $r_D = 0.042$. Whenever $U \ll U_c$, rescued populations mostly consist of the wild type (0 mutation, purple bars) and single mutants (blue bars). As U approaches U_C, a substantial proportion of multiple mutants starts to be found in late rescued populations. Note however that this illustration does not ascertain whether these multiple mutants are the cause of the rescue or not.*

In this work we use a SSWM approximation (Gillespie 1983; McCandlish and Stoltzfus 2014). We consider that the mutation rate is low relative to the strength of selection, so that rescue typically stems from only one mutation (which is sampled from the pool of possible mutants), be it present before the onset of stress (from standing variance, hereafter 'SV') or arising after it (*de novo* hereafter 'DN'). We thus only consider rescue from a single allele, which is randomly drawn among all possible alleles, weighted by their probability to produce a rescue (illustrated in **Supplementary figure 1**). Under the SSWM approximation, all possible rescue events (SV or DN, from any given allele) arise as alternative Poisson events (Martin *et al.* 2013). The overall probability of extinction is thus simply the zero class of the Poisson distribution with rate equal to the sum of all rates. The probability of evolutionary rescue (ER) is that of the complementary event ('no extinction'). For similar reasons, the probability of each alternative event is just the relative contribution of its Poisson rate over the total rate of rescue. The key to describe the process is therefore to derive these various rates. All along, expectations of a given quantity, taken over some random variable X are denoted $\mathbb{E}_X(.)$.

Rescue from *de novo* mutation:

We first consider rescue starting from a clonal population (of inoculum size N_0), so that any rescue event is caused by *de novo* mutations ('DN'). Starting from a large inoculum size, stochasticity in the initial clone's decay dynamics can be neglected. We define the rate of 'DN' rescue events ω_R^{DN} per individual per mutation present at the onset of stress, such that $N_0\ U\ \omega_R^{DN}$ is the parameter of the Poisson number of 'DN' rescue events. Ignoring stochasticity in the decay dynamics of the wild-type (large $N_0 r_D$), this rate is approximately (Martin *et al.* 2013)

$$\omega_R^{DN} = \frac{\mathbb{E}_r(\pi_F(r))}{r_D} = \frac{1}{r_D}\int_{r>0}(1-e^{-2\,r})\,f(r)dr\ , \qquad \text{(A1)}$$

where $\mathbb{E}_r(.)$ is an expectation over the distribution of mutant growth rates r (in the new environment) and $f(r)$ is the pdf of this distribution. The corresponding probability of extinction is then $P_{ext} = e^{-N_0\ U\ \omega_R^{DN}}$ (Martin *et al.* 2013).

Rescue from standing variance:

In an alternative scenario, the initial population (of size N_0) is previously at equilibrium in the non-stressful 'previous environment'. In the SSWM regime, the rescue process results from

the contribution from two independent processes: rescue caused by a mutant appearing after the onset of stress and rescue caused by a mutant already present at the onset of stress. The number of each such event overall is approximately Poisson distributed, with rates ω_R^{DN} (given in Eq.(A1)) and ω_R^{SV}, respectively. The latter depend on the joint distribution of the cost $\mathcal{C}$ of resistance mutations in the previous environment, and of their growth rate in the new environment. The cost is equal to the negative of the selection coefficient of the mutation relative to the ancestor background in which it arises (Martin *et al.* 2013): we have

$$\omega_R^{SV} = \mathbb{E}_{\mathcal{C},r}\left(\frac{\pi_F(r)}{\mathcal{C}}\right) = \mathbb{E}_r\left(\pi_F(r)\,\mathbb{E}_{\mathcal{C}}\left(\frac{1}{\mathcal{C}}\middle|r\right)\right) = \int_{r>0}\frac{(1-e^{-2r})}{\mathcal{C}}\,f(\mathcal{C},r)dr\,, \quad \text{(A2)}$$

where the expectation $\mathbb{E}_{\mathcal{C},r}(.)$ is taken over the joint distribution (pdf $f(\mathcal{C},r)$) of costs $\mathcal{C}$ and growth rates r, among random mutations. This Poisson approximation applies under the SSWM regime (Martin *et al.* 2013), regardless of whether the population is initially at stochastic mutation-selection-drift balance at constant size N_0, or at quasi-deterministic mutation-selection balance (at some size $N \gg N_0$) followed by a bottleneck at the onset of stress (to reach size N_0). The extinction probability in the presence of both initial standing variance and *de novo* mutations is $P_{ext} = e^{-N_0\,U\,(\omega_R^{DN}+\omega_R^{SV})}$ and, because these are Poisson distributed events, the proportion p_R^{SV} of rescues from standing variants (over all rescue events) is

$$\phi_R^{SV} = \frac{\omega_R^{SV}}{\omega_R^{DN}+\omega_R^{SV}}\,. \quad \text{(A3)}$$

II. Application to Fisher's Geometric Model (FGM)

In our case, the joint distribution of c and r emerges from the FGM: growth rates (both in the previous and new environment) are quadratic functions of phenotype, around an environment – dependent optimum. Let us derive the above quantities in this context. Define n (and $\theta = n/2$) the dimension of the fitness landscape (number of traits under stabilizing selection) and λ, the variance of mutational effects on each trait (constant across traits in this isotropic version). In our model both the strength of the selection and the effect of the mutation are handled by λ. In an isotropic model, we can define the fitness of a phenotype $\boldsymbol{z}$ as $m(\boldsymbol{z}) = \frac{\boldsymbol{z}^t\,\boldsymbol{S}\,\boldsymbol{z}}{2}$ with S the matrix of the selective effect of all traits which is $\boldsymbol{S} = \lambda_s\,\boldsymbol{I}_n$ and λ_s the variance of selective effect

on each trait. Each mutation creates a random perturbation $\mathbf{dz} \sim N(\mathbf{0}, \mathbf{M})$ with $\boldsymbol{M} = \lambda_M \boldsymbol{I}_n$ and λ_M the variance of mutation effect on each trait. As we focus only on fitness here we can find a unique transformation $z \to y$ of the phenotypic space, which gives $m(y) = -\left|\left|y\right|\right|^2/2$ and $dy \sim N(\mathbf{0}, \lambda\, \mathbf{I_n})$ with $\lambda = \lambda_s\, \lambda_M$. Thus if we consider that phenotypic traits are in unit of the variance of selective effect, $\lambda_s = 1$ and $\lambda = \lambda_M$ the variance of mutation effect on each trait. The alternative phenotypic change of unit can be done with λ_M, which will change mutation and selective effects on traits but not on fitness. Thus a change in λ, can change both selective and mutation effects. Mutation effects on phenotype follow an unbiased isotropic multivariate normal distribution $\mathbf{dz} \sim \mathcal{N}(\mathbf{0}, \lambda\, \mathbf{I}_n)$. The mean fitness effect of random mutations is then $|E(s)| = \lambda\, \theta$, in absolute value (Martin and Lenormand 2015), in the absence of phenotypic plasticity.

Define the scaled parameters $\rho_D = r_D/\lambda$ and $\rho_{max} = r_{max}/\lambda$ and the ratio $y_D = \rho_D/\rho_{max} = r_D/r_{max}$. In the SSWM approximation, we can consider that the dominant phenotype (with growth rate $-\,r_D$) is the background on which all mutations arise. For de novo rescue this simply requires that double mutants be ignored, otherwise a secondary mutation would arise on a background that is not the initial clone, hence with a different distribution of effects. For rescue from standing variance this implies that we consider that the equilibrium population is dominated by a phenotype lying at the center of the standing phenotypic distribution, which coincides with the optimum in the previous environment. Other backgrounds are present and may contribute to the rescue process, but the effect of such variation in backgrounds on the mutant effect distributions can simply be neglected in the SSWM regime. Indeed, phenotypic distributions are then narrow at mutation – selection balance, with a spike of optimal genotypes and most other backgrounds lying nearby in phenotype space (Martin and Roques 2016).

Rescue from *de novo* mutation:

The initial clone lies at fitness distance $s_0 = r_D + r_{max}$ from the optimum in the new environment, which, together with n and λ, fully determines the distribution of mutant selection coefficients (and hence growth rates r). The distribution of selection coefficients $s = r + r_D$ of random mutants relative to the ancestor has known exact form for the isotropic FGM (eq.(3) in Martin and Lenormand 2015). From it, the distribution of growth rates r among random mutants, within the new environment, is readily obtained. It has stochastic representation:

$$r = r_{max} - \frac{\lambda}{2}\,\chi_n^2\big(2\rho_{max}(1+y_D)\big)$$

where $\chi_n^2(\nu)$ is a non-central chisquare with n d.f. and non-centrality parameter ν. It proves simpler to study the scaled variable $y = r/r_{max} \in [0,1]$, which has stochastic representation $y = 1 - 2/\rho_{max}\,\chi_n^2\left(2\rho_{max}\big(1+y_D\big)\right)$ and pdf

$$f_y(y) = e^{-\rho_{max}(2+y_D-y)}\rho_{max}^{\theta}(1-y)^{\theta-1}\frac{{}_0F_1\big(\theta,\rho_{max}^2(1+y_D)(1-y)\big)}{\Gamma(\theta)}\,, y \in]-\infty,1] \quad \text{(A4)}$$

where ${}_0F_1(.,.)$ is the confluent hypergeometric function. Plugging Eq.(A4) into Eq.(A1) directly yields the rate of rescue from *de novo* mutations. A simplification arises by considering a linearized probability of non-extinction $\pi_F(r) = (1-e^{-2\,r})\Theta(r) \approx 2\,r\,\Theta(r)$ (recall that $\Theta(.)$ is the Heaviside theta function ($\Theta(x) = 1$ over $\mathbb{R}^+$ and $\Theta(x) = 0$ over $\mathbb{R}^-$). Recalling that $r = y\,r_{max} = y\,\lambda\,\rho_{max}$, while $r_D = \lambda\,y_D\,\rho_D$ we get:

$$\omega_R^{DN} = \frac{1}{r_D}\mathbb{E}_y(\pi_F(y\,r_{max})) \approx \frac{1}{r_D}\int_0^{r_{max}} 2\,r_{max}\,y\,f_y(y)dr = \frac{2}{y_D}\int_0^1 y\,f_y(y)dy, \quad \text{(A5)}$$

where $f_y(y)$ is given by Eq.(A4). This integral must be computed numerically; yet, we already note that the 'DN' rescue probability only depends on three composite parameters: $(\theta, \rho_{max}, y_D)$.

Distribution of the cost of rescue mutations:

For rescue from standing variants ('SV'), the distribution of the cost, in the previous environment, of mutations with growth rate r in the new environment must also be known (see Eq.(A2)). As we have seen, we neglect the effect of background variation on the distribution of mutant genotypes present in the population before the onset of stress. Instead, we consider that the joint distribution of (c, r) is the one generated by mutations arising from the dominant genotype in the previous environment, which has the optimal phenotype in this environment (same as the initial clone in the DN rescue problem). Recall that the cost $\mathcal{C}$ in the previous environment is the negative of the selection coefficient, relative to the dominant background, of random mutations arising in this very background. The distribution of $\mathcal{C}$ has a known form, conditional on its effect ($s = r + r_D$) in the new environment. For a background optimal in the previous environment, it has a simple stochastic representation (from eq. (9) in Martin and Lenormand 2015): $c|s \sim\ c_{min}(s) + \gamma$, where $\gamma \sim \Gamma(\theta - 1/2, \lambda)$ is a gamma deviate and $c_{min}(s) = 2s_0 - s - 2s_0\sqrt{1 - s/s_0}$, with $s_0 = r_{max} + r_D$, is a deterministic function of s. Expressed in terms of scaled growth rates y ($s = y\,r_{max} + r_D$), we have: $c_{min}|y = \big(2 + y_D - 2\sqrt{(1+y_D)(1-y)} -$

y) r_{max} and $c|y \sim c_{min}(y) + \gamma.\, c_{min}(y)$ can be simply interpreted as an incompressible cost that all mutants within the class $[y, y+dy]$ must pay because they cannot get close to the new optimum without moving away from the former one. The stochastic component γ reflects the distance, to the former optimum, of the mutants within the class $[y, y+dy]$ that lie on the subspace of phenotypes equally distant to the new optimum (an n - dimensional tore in this case). This component happens to be independent of y, which simplifies our derivations.

It proves handy to scale the incompressible cost scaled by the phenotypic variance of mutation effects on each trait λ, which we denote $v(y) = c_{min}(y)/\lambda$. The corresponding scaled incompressible cost, which we denote $v(y)$, is $v(y) = c_{min}(y)/\lambda = \left(2 + y_D - 2\sqrt{(1+y_D)(1-y)} - y\right)\rho_{max}$. We also introduce $c_H(y)$, the harmonic mean cost of mutations within the infinitesimal class $[y, y+dy]$, as defined above Eq. (3) in the main text: $c_H(y) = 1/\mathbb{E}_c(\mathcal{C}^{-1}|y)$. Again, we use the linear approximation for non-extinction probability: $\pi_F(r) \approx 2\, r\, \Theta(r)$ with $r = \rho_{max} y\, \lambda$. Applying Eq.(A2) to the FGM then yields $\omega_R^{SV} = \mathbb{E}_{\mathcal{C},r}(\pi_F(r)/\mathcal{C}) \approx 2\, \rho_{max}\, \mathbb{E}_y(y\, \Theta(y)\, /\, c_H(y))$. From the stochastic representation of c given above, we then retrieve the explicit expression for this harmonic mean cost given in the main text (Eq. (3)):

$$c_H(y) = 1/\mathbb{E}_\gamma\left(\frac{1}{\mathcal{C}}\middle|y\right) = 1/\mathbb{E}_\gamma\left(\frac{1}{\gamma + \mathrm{c}_{min}(y)}\right) = \frac{\lambda\, e^{-\,v(y)}}{E_{\theta-1/2}\big(v(y)\big)}$$
$$\text{with } v(y) = \mathrm{c}_{min}(y)/\lambda = \rho_{max}\left(2 + y_D - 2\sqrt{(1+y_D)(1-y)} - y\right), \quad \text{(A6)}$$

where $\mathbb{E}_\gamma(.)$ is an expectation taken over the distribution of $\gamma \sim \Gamma(\theta - 1/2, \lambda)$ and $E_k(z) = \int_1^\infty e^{-z\,t}/t^k\, dt$ is the exponential integral function.

Rate of rescue from standing variance:

Using Eq. (A6), Eq.(A2) yields

$$\omega_R^{SV} \approx 2\, r_{max} \int_0^1 \frac{y}{c_H(y)}\, f_y(y)dr = 2\, \rho_{max} \int_0^1 y\, e^{v(y)}\, E_{\theta-1/2}(v(y))\, f_y(y)dr. \quad \text{(A7)}$$

The result is entirely determined by the four parameters $(r_{max}, y_D, \lambda, \theta)$. Recalling that $y_D = r_D/r_{max}$, the result can be related to the rate of rescue from de novo mutations in Eq.(A5) as

$$\omega_R^{SV} \approx \omega_R^{DN}\, \beta$$
$$\beta = \rho_D * \frac{\int_0^1 y\, /c_H(y)\, f_y(y)dy}{\int_0^1 y\, f_y(y)dy} \quad \text{(A8)}$$

The constant β is the effectiveness of standing variance relatively to de novo mutations in ER.

III. Simplified closed form expressions

Approximation for weak effect mutations:

Eqs. (A5) and (A7) provide a mathematical framework to predict rescue from both *de novo* mutants and standing variants, in the SSWM regime. However, they do not provide simple closed form expressions (the integrals must be computed numerically). To gain more analytical insight, we rely on some further approximations. These can be summarized as follows. We assume that

(i) decay is not too weak: $r_D \geq 2\sqrt{\lambda\, r_{max}}$, so that $y_D \geq 2/\sqrt{\rho_{max}}$

(ii) mutation effects are small: $r_{max} \gg \lambda$.

As we will see below, these assumptions mean that critical mutants with zero growth rate $r = 0$ in the new environment (at the edge of resistance) lie many mutational steps away from the optimum in this environment. These assumptions are relatively weak in our biological scenario. We assume (i) a sufficiently stressful environment (inducing non-vanishing decay), (ii) but one that leaves room for substantial later adaptation, when starting from a barely resisting genotype. All derivations below are provided in **Supplementary Mathematica Notebook file S1**, where further illustrative figures are also given to check several steps of the derivations. The main approximations are illustrated in the Supplementary figures below (generated in **Supplementary Mathematica Notebook file S1**).

Large $\boldsymbol{\rho_{max}}$ small $\boldsymbol{y}$ approximation:

The assumptions (i-ii) imply that most mutants grow much more slowly than the optimal genotype, hence $r \ll r_{max}$: $y \ll 1$. On the contrary, (ii) also implies that $\rho_{max} \gg 1$ This means that the second argument in the hypergeometric function in Eq. (A4) is large: $z = \rho_{max}^2(1 + y_D)(1 - y) = O\big(\rho_{max}^2(1 + y_D)\big) \gg 1$. We can thus use an asymptotic expansion for the regularized hypergeometric function: ${}_0F_1(\theta, z)/\Gamma(\theta) \approx z^{1/4-\theta/2}\, e^{2\sqrt{z}}/(2\sqrt{\pi})$, when $z \to \infty$ (Wolfram Research 2001). Plugging this into Eq.(A4) yields a simplified expression for the pdf of the mutant growth rate distribution:

$$f_y(y) \approx \mathrm{e}^{-v(y)}\,(1-y)^{\theta/2\,-\,3/4}\;\frac{(1+y_D)^{1/4\,-\,\theta/2}\sqrt{\rho_{max}}}{2\sqrt{\pi}}\,, \qquad y \in [0,1]\,, \quad \text{(A9)}$$

where $v(y) = \rho_{max}\left(2 + y_D - 2\sqrt{(1+y_D)(1-y)} - y\right)$ was defined in Eq.(A6).

Change of variables $\boldsymbol{y \to \psi}$:

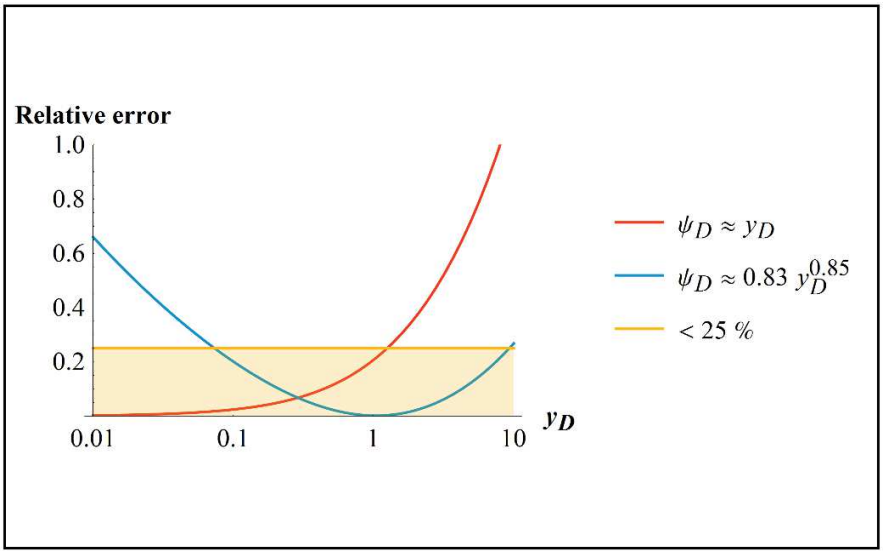

Supplementary Figure 2: Relative error implied by alternative approximations to $\boldsymbol{\psi_D}$.

This distribution takes a more compact form by using a bijective change of variable, which corresponds to an alternative measure of the mutant growth rate y. More precisely, we consider $\psi(y) = 2\left(1 - \sqrt{1-y}\right)$ as a measure of growth rate ($y = \psi(y)\,(1 - \psi(y)/4)$). The growth rate of the initial clone is $-y_D$ which yields a corresponding decay rate $\psi_D = |\psi(-y_D)| = 2\left(\sqrt{1+y_D} - 1\right)$. The transformation is bijective and strictly increasing ($\psi'(y) = 1/\sqrt{1-y} > 0$), from $y \in [0,1]$ to $\psi \in [0,2]$. For small y, $\psi(y) = y + o(y)$ so that the distributions of y and ψ are similar in this case. Similarly ψ_D is a bijective strictly increasing function of y_D. A linear approximation $\psi_D \approx y_D$ about $y_D \ll 1$ yields a relative error $\leq 25\%$ for all $y_D \in [0,1]$. A log-log approximation about $y_D = 1$ gives $\psi_D \approx 0.83\ y_D^{0.85}$, which yields a relative error $\leq 25\%$ for all $y_D \in [0.1,10]$. The latter therefore covers a wide range of y_D. These relative errors are shown in **Supplementary Figure 2** below.

PDF of $\boldsymbol{\psi}$:

The pdf $f_\psi(.)$ of the transformed variable ψ, based on the approximate pdf of y in Eq. (A9), is $y'(\psi)f_y(y(\psi))$ yielding:

$$f_\psi(\psi) \approx \frac{\sqrt{\rho_{max}}}{2\sqrt{\pi}}\, \mathrm{e}^{-\frac{1}{4}\rho_{max}(\psi+\psi_D)^2} \left(\frac{2-\psi}{2+\psi_D}\right)^{\theta-\frac{1}{2}}, \psi \in [0,2]. \qquad \text{(A10)}$$

Consistency check and range of validity:

Let us now look for the range of validity of this large ρ_{max} small y approximation. Consistency requires that $\psi \approx y \ll 1$ over the distribution of possible rescue mutants. Assuming $\psi \ll 1$, we can ignore the factor $2-\psi$ in eq.(A10), and the pdf is approximately exponential: $f_\psi(\psi) \propto e^{-\frac{1}{4}\rho_{max}(\psi+\psi_D)^2} \approx e^{-a\,\psi}$ where $a = \rho_{max}\,\psi_D/2$. This means that the distribution of ψ conditional on $\psi > 0$ is approximately exponential: $\psi \sim Exp(a)$. The approximation $0 < y \ll 1$ is thus consistent when $\mathbb{E}(y|y>0) \approx \mathbb{E}(\psi|\psi>0) = 1/a \leq \epsilon$ with some $\epsilon \ll 1$. Set $\epsilon = 1/\sqrt{\rho_{max}}$: we have $\epsilon \ll 1$ by assumption (ii) above and $1/a = 2\epsilon^2/\psi_D$, which is less than ϵ whenever $\psi_D \geq 2\epsilon$. Overall, we see that a sufficient condition (though not necessary) for the approximation to be consistent and hence accurate is $\psi_D \geq 2\epsilon = 2/\sqrt{\rho_{max}}$. As this lower bound is small ($\psi_D \approx y_D$), it is equivalent to a lower bound on $y_D \geq 2\epsilon$, namely to $r_D \geq 2\sqrt{\lambda\, r_{max}}$, which is thus our quantitative condition (i).

Geometric interpretation of the assumptions (i-ii):

A geometric interpretation can also be given to these conditions. The standard deviation of mutational changes, on phenotype, along any given dimension is $\sqrt{\lambda}$. The phenotypic distance to the optimum, from a 'critical' mutant with exactly zero growth rate, is $z_c = \sqrt{2\, r_{max}}$ while that from the ancestral clone to the optimum is $z_0 = \sqrt{2(r_D + r_{max})}$. Our condition (ii) $r_{max}/\lambda = \epsilon^{-2}$ with $\epsilon \ll 1$ implies that $z_c = \sqrt{2\lambda}/\epsilon$, namely that the 'critical' mutants lie many ($\sqrt{2}\,\epsilon^{-1} \gg 1$) mutational standard deviations ($\sqrt{\lambda}$) away from the optimum, in phenotype space. Similarly, the variable ψ_D can be expressed as $\psi_D = 2\,(z_0 - z_c)/z_c$, so that our condition (i) $\psi_D \geq 2\,\epsilon$ can be written $z_0 - z_c \geq \sqrt{2\,\lambda}$. This means that the ancestral clone must lie at least at $\sqrt{2}$ mutational standard deviations ($\sqrt{\lambda}$) from its closest critical mutant (the one on the line connecting the ancestral clone and the optimum **Supplementary figure 6**).

Corresponding approximate integrals over $\boldsymbol{\psi}$:

The integrals from section II can be approximated by the corresponding integrals (indicated by a $*$) over the distribution of ψ, as our conditions guarantee that $\psi \approx y \ll 1$. The rate of *de novo* rescue is approximately (Eq. (A5)):

$$\omega_R^{DN} \approx \omega_R^{DN*} = \frac{2}{y_D}\int_0^2 \psi\, f_\psi(\psi)d\psi \approx \frac{2}{\psi_D}\int_0^2 \psi\, f_\psi(\psi)d\psi. \qquad \text{(A11)}$$

Note that the right-hand side expression further approximates $\psi_D/y_D \approx 1$. The discrepancy between ω_R^{DN*} and its right-hand side approximate expression involves a factor $\psi_D/y_D \approx 0.83\, y_D^{-0.15}$ which is fairly negligible unless y_D is substantially large.

The effectiveness of the standing genetic variance relatively to *de novo* mutations (Eq. (A8)) also simplifies when expressed in terms of ψ. From the original expression in Eq.(A6), in terms of y, we define the corresponding quantity expressed in terms of ψ: $v(y) = (\psi+\psi_D)^2\rho_{max}/4 \equiv v_*(\psi)$. We then have

$$\beta \approx \beta^* = \rho_D * \frac{\int_0^2 \psi\, e^{v_*(\psi)}\, E_{\theta-1/2}\big(v_*(\psi)\big)\, f_\psi(\psi)d\psi}{\int_0^2 \psi\, f_\psi(\psi)d\psi}. \qquad \text{(A12)}$$

Qualitative effect of the landscape parameters on the rate of rescue de novo:

We can use (A5) to analyze how each parameter ($\rho_{max}, \rho_D, \theta$) qualitatively affects the rate of rescue $\omega_R^{DN} \approx \omega_R^{DN*}$ using the sign of the derivative of the integrand $I = \psi\, f_\psi(\psi)/\psi_D$ in Eq.(A11) with respect to each parameter. We note that (i), because ψ_D is an increasing function of y_D, they have similar qualitative effects, and that (ii) as $I > 0$, we can perform the analysis directly on the derivatives of $\log I$, which are of similar sign as those of I. The analysis (see computations in **Supplementary Notebook file S1**) yields the following general conclusions: the rate ω_R^{DN*} decreases with the phenotypic dimensionality θ and with scaled decay rate ρ_D. The effect of ρ_{max} is not directly available but the derivative is driven by its leading order for small $\epsilon \ll 1$: $\partial_{\rho_{max}} \log I = \psi_D^2(1+\psi_D/4)^2(\psi+\psi_D)/(\rho_D(2+\psi_D))\ \epsilon^{-2} + O(1)$ which is of positive sign. Therefore, the rate ω_R^{DN*} increases with ρ_{max} in the range of validity of our simplification.

Laplace Approximations:

The integrals in Eqs. (A11)-(A12) are substantially simpler but still do not easily yield a closed form. Fortunately, assumption (ii) ($\rho_{max} = \epsilon^{-2} \gg 1$) also implies that we can use the classic Laplace method (Breitung 1994) to approximate these integrals around the maximum of their integrand. Define the following functions:

$$\begin{aligned} q(\psi) &= (\psi + \psi_D)^2/4 - \log(\psi)\,/\rho_{max} \\ h(\psi) &= \sqrt{\frac{\rho_{max}}{4\pi}}\left(\frac{2-\psi}{2+\psi_D}\right)^{\theta-\frac{1}{2}} \\ \eta(\psi) &= e^{v_*(\psi)}\, E_{\theta-1/2}\big(v_*(\psi)\big) \end{aligned} \quad , \qquad \text{(A13)}$$

recalling from Eq. (A12) that $v_*(\psi) = \rho_{max}(\psi + \psi_D)^2/4$. The integrals in Eqs. (A11)-(A12) can be written in terms of these functions: we have $\int_0^2 \psi\, f_\psi(\psi) d\psi = \int_0^2 h(\psi)\, e^{-\rho_{max}\, q(\psi)} d\psi$ and $\int_0^2 \psi\, e^{v_*(\psi)}\, E_{\theta-1/2}\big(v_*(\psi)\big)\, f_\psi(\psi) d\psi = \int_0^2 \eta(\psi)\, h(\psi)\, e^{-\rho_{max}\, q(\psi)} d\psi$. The Laplace method then provides a closed form approximation for these integrals, accurate when ρ_{max} is large, by computing the integral on a Taylor series of $q(\psi)$ around its minimum value ψ_* (i.e. around the maximum of $e^{-\rho_{max}\, q(\psi)}$). As long as $\rho_{max} > (2+\psi_D)^{-1}$, i.e. as long as $\rho_{max} > 1/2$ for any ψ_D, the function $q(.)$ has a unique minimum over $\psi \in [0,2]$ at $\psi = \psi_* = \psi_D/(2\alpha)$ where we define

$$\alpha = \left(\sqrt{1 + \frac{8}{\psi_D^2 \rho_{\max}}} - 1\right)^{-1} \underset{\alpha \to \infty}{\approx} \frac{\psi_D^2\, \rho_{max}}{4} + \frac{1}{2}. \qquad \text{(A14)}$$

The approximation on the right-hand side of eq. (A14) is an asymptotic series when $\psi_D^2\, \rho_{max} \gg 1$. In the range of validity of our assumptions (i-ii), $\psi_D \geq 2/\sqrt{\rho_{max}}$ so that $\psi_D^2\, \rho_{max} \geq 4$, and the relative error implied by the approximation is always $\leq 10\%$ and decays rapidly as ψ_D increases beyond its lower bound $2/\sqrt{\rho_{max}}$ (illustrated in **Supplementary Notebook file S1**). Therefore, we use this simplified expression all along, and directly report this approximate value in the main text (Eq. (5)). By the Laplace method as $\rho_{max} \to \infty$, the integrals in Eqs. (A11)-(A12) are approximately

$$\int_0^2 h(\psi)\, e^{-\rho_{max}\, q(\psi)} d\psi \underset{\rho_{max} \to \infty}{\approx} \sqrt{\frac{2\pi}{\rho_{max}\, |q''(\psi_*)|}}\, h(\psi_*)\, e^{-\rho_{max}\, q(\psi_*)} \quad , \qquad \text{(A15)}$$

where $q(.)$ and $h(.)$ are given in Eq. (A13). Plugging this approximation into Eq. (A11) and simplifying, we obtain the expression in Eq. [6] of the main text:

$$\omega_R^{DN} \underset{\rho_{max}\to\infty}{\approx} \omega_R^{DN*} \approx g(\alpha)\left(\frac{1-\psi_D/4\alpha}{1+\psi_D/2}\right)^{\theta-1/2} \quad . \qquad \text{(A16)}$$
$$g(\alpha) = \frac{\mathrm{e}^{-\alpha}}{\sqrt{2\,e}\,\alpha\sqrt{1+\alpha}} \underset{\alpha\to\infty}{\approx} \frac{\alpha^{-3/2}\,e^{-\alpha}}{\sqrt{2\,e}}$$

The approximation for $g(\alpha)$ on the right-hand side of Eq. (A16) entails a relative error $\leq 30\%$ over the range $\alpha \geq 1.36$ compatible with our assumptions (i-ii) ($\psi_D^2\,\rho_{max} \geq 4$) and decays relatively slowly with α (see **Supplementary file S1**). Therefore, while it always gives a correct order of magnitude, we use the exact expression (left-hand side) as much as possible. **Supplementary Figure 3** bellow illustrates the accuracy of (A16) (right-hand side) corresponding to Eq.[6], compared to the numerical integration of (A5) corresponding to Eq.[4].

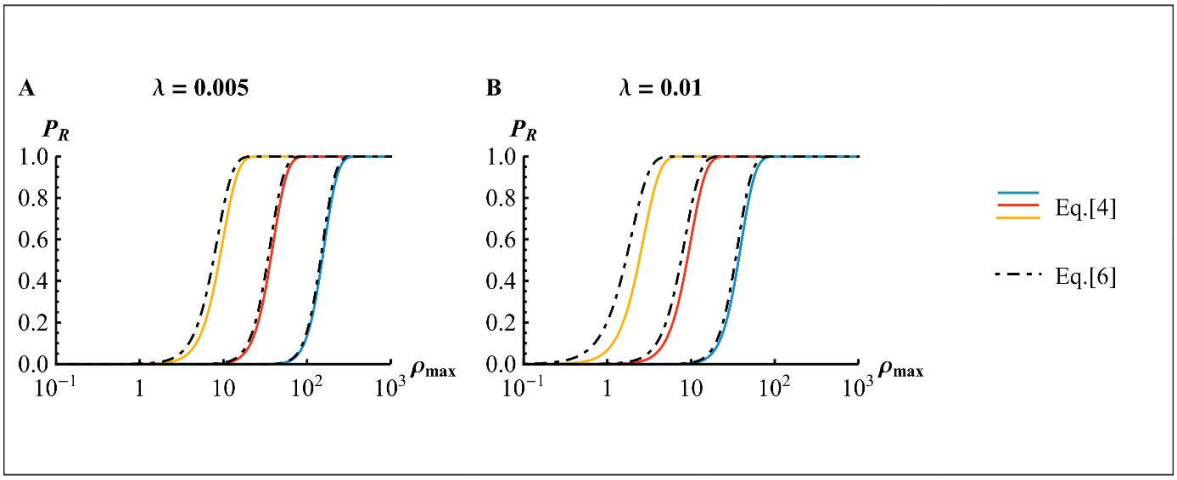

Supplementary Figure 3. Accuracy of the Laplace approximation across ρ_{max} values*. ER probability from de novo mutations is plotted against ρ_{max} for three decay rates $r_D = 0.05$ (orange), $r_D = 0.1$ (red) and $r_D = 0.2$ (red). The mutational variance is $\lambda = 0.005$* ***(A)*** *and $\lambda = 0.01$* ***(B)****. Plain lines show the result of the numerical integration of Eq.[4](A5) and dot-dashed lines show the result of Eq.[6](A16). Eq. (A16) proves fairly accurate when ρ_{max} is large enough. Other parameters were $N_0 = 10^7$, $U = 2 * 10^{-5}$and $\theta = 2$ ($n = 4$). All else equal, the accuracy improves with weaker mutation effects (smaller λ, compare A and B) as expected.*

The effectiveness of the standing genetic variance β is approximated by the same Laplace method as Eq.(A15): Eq. (A12) then becomes:

$$\beta^* = \rho_D * \frac{\int_0^2 \eta(\psi)\, h(\psi)\, e^{-\rho_{max}\, q(\psi)} d\psi}{\int_0^2 h(\psi)\, e^{-\rho_{max}\, q(\psi)} d\psi}$$
$$\beta^* \underset{\rho_{max} \to \infty}{\approx} \rho_D * \frac{\eta(\psi_*)h(\psi_*)}{h(\psi_*)} = \rho_D * \eta(\psi_*) = \rho_D * \frac{E_{\theta\,-\,1/2}(\alpha + 1/2)}{\mathrm{e}^{-\,1/2\,-\,\alpha}}, \qquad \text{(A17)}$$

with the same α as in Eqs.(A14) and [5] and $\eta(.)$ given in Eq. (A13). In fact, the exponential integral function in Eq. (A17) further simplifies when α gets large (see **Supplementary Notebook file S1**). It is defined by $E_k(v) = \int_1^\infty e^{-v\,t} t^{-k} dt$ and a Laplace approximation can be used when $v \gg 1$ (in our context $v = \alpha + 1/2 = \rho_{max}(\psi_D/2)^2 + 1$). This time, the maximum of the integrand is at the left boundary $t = 1$ about which $t^{-k} \approx e^{-k(t-1)}$ and we obtain $e^v E_k(v) \approx e^v \int_1^\infty e^{-v\,t} e^{-k(t-1)} dt = 1/(k+v)$. Plugged into Eq. (A17), this approximately yields

$$\beta^* \underset{\rho_{max} \to \infty}{\approx} \frac{\rho_D}{\alpha + \theta}\,. \qquad \text{(A18)}$$

This approximation proves very robust and accurate: for any $\alpha \geq 1.36$ (large ρ_{max}) compatible with our assumptions (i-ii), and for all $\theta \geq 1/2$, the relative error is less than 15% (it is exact for $\theta = 1/2$), see **Supplementary Notebook file S1** and **Supplementary Figure 4** below. Therefore, we directly provide this approximation in the main text (Eq. [10]).

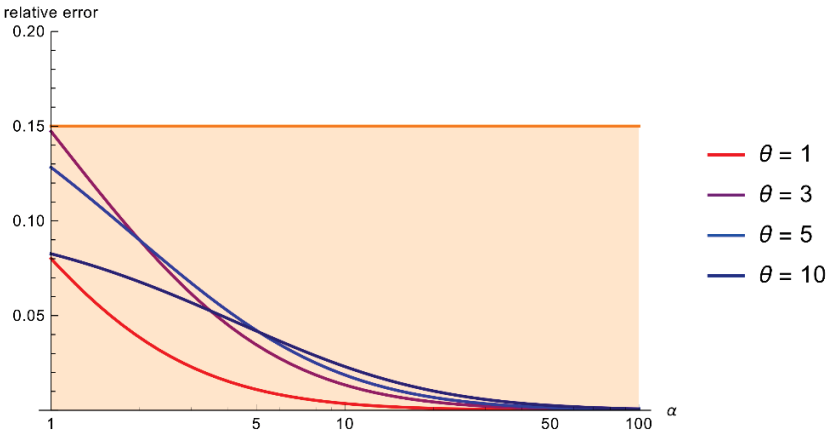

Supplementary Figure 4. *Relative error of the approximation* $e^{-\,1/2\,-\,\alpha}/E_{\theta\,-\,1/2}(\alpha + 1/2) \approx \alpha + \theta$ *: as a function of* α *(*≥ 1.36 *under assumptions (i) – (ii)), for different values of* θ *(indicated in legend).*

Overall, Eqs.(A16) and (A18) provide simple yet accurate and robust closed form expressions for the rate of rescue, from either purely *de novo* mutations (A16) or standing variance (A18). From these results, the overall rate of rescue in the presence of standing variance is $\omega_R \approx \omega_R^{DN*} + \omega_R^{SV_*} \approx \omega_R^{DN*}(1 + \rho_D/(\alpha + \theta))$. For both scenarios, a critical quantity determining the process is the composite parameter α.

Further simplifications for small dimensionality and mild decay rates

Eq.(A16) simplifies greatly in $n = 1$ dimension: setting $\theta = 1/2$, the right-hand factor in Eq.(A16) vanishes:

$$\omega_R^{DN} \underset{\rho_{max} \to \infty}{\approx} \omega_R^{DN*} \underset{\theta=1/2}{=} g(\alpha) \quad . \tag{A19}$$

In this situation, *all* the various effects of stress (on r_D, r_{max}, λ) on ω_R^{DN} are mediated by their composite impact on α in Eq.(A14). In fact, this simplification extends approximately to higher dimensions, with mild decay rates. To show this, let us see when the right-hand factor $((1 - \psi_D/4\alpha)/(1 + \psi_D/2))^{\theta - 1/2}$ in Eq.(A16) converges to 1. Define $\phi(\psi_D) = 1 - \psi_D/(4\alpha)$ where α is given by Eq.(A14). We have $\phi'(\psi_D) \propto 1 - \rho_{max}\,\psi_D/\sqrt{\rho_{max}\,(8 + \rho_{max}\,\psi_D^2)} > 0$ so that $\phi(.)$ is strictly increasing over $\psi_D \in \mathbb{R}^+$, and $\lim_{\psi_D \to 0} \phi(\psi_D) = 1 - 1/\sqrt{2\rho_{max}}$ and $\lim_{\psi_D \to \infty} \phi(\psi_D) = 1$. Therefore, we get the following bounds: $1 - 1/\sqrt{2\rho_{max}} \leq 1 - \psi_D/4\alpha \leq 1$. Furthermore, under the weak mutation effect assumption (ii) of the whole section II, we have $\sqrt{\rho_{max}} = \epsilon^{-1}$ so that the numerator in the right-hand factor in Eq.(A16) is bounded by:

$$1 - \frac{\epsilon}{\sqrt{2}}\left(\theta - \frac{1}{2}\right) \approx \left(1 - \frac{1}{\sqrt{2\rho_{max}}}\right)^{\theta - 1/2} \leq \left(1 - \frac{\psi_D}{4\alpha}\right)^{\theta - 1/2} \leq 1\,. \tag{A20}$$

Therefore, this factor has limited impact on the rate of rescue in the parameter range assumed for the whole section, as long as $\theta - 1/2 \ll \epsilon^{-1}\sqrt{2}$. The remaining factor is $(1 + \psi_D/2)^{1/2-\theta} = (1 - \psi_D/(2 + \psi_D))^{\theta - 1/2}$, which remains close to 1 as long as $\theta - 1/2 \ll (2 + \psi_D)/\psi_D$. In summary, two jointly sufficient conditions to approximate $\omega_R^{DN*} \approx g(\alpha)$ are

$$\begin{array}{l} a)\ \theta - 1/2 \ll \sqrt{2\rho_{max}} \\ b)\ If\ \theta > 1/2\,,\ \psi_D/(2 + \psi_D) \ll 1/(\theta - 1/2) \end{array}\,. \tag{A21}$$

This implies that dimensionality must not be too large and the decay rate must be small enough relative to the maximal growth rate: roughly $r_D \ll 2\,r_{max}/(\theta - 1/2)$ (using $\psi_D \approx y_D$ and small). In these conditions, the rate of rescue is entirely driven by the effect of α alone, and we have $\omega_R^{DN} \approx g(\alpha)$ as in the one dimension case.

Sup. Figure 5 explores the accuracy of the approximation $\omega_R^{DN} \approx g(\alpha)$, across a range of $y_D = r_D/r_{max}$ and of dimensionalities θ. As λ gets small, all else equal, the ER probability becomes independent of dimensionality, as predicted by Eq.[7]: compare dashed lines ($\lambda = 0.025, \rho_{max} = 40$) vs. plain lines ($\lambda = 0.001, \rho_{max} = 1000$). Even with ρ_{max} less large (dashed lines), Eq.[7] still

qualitatively captures the shape of the drop in ER probability with decay rates r_D, but it does not capture the exact stress 'window' over which it occurs.

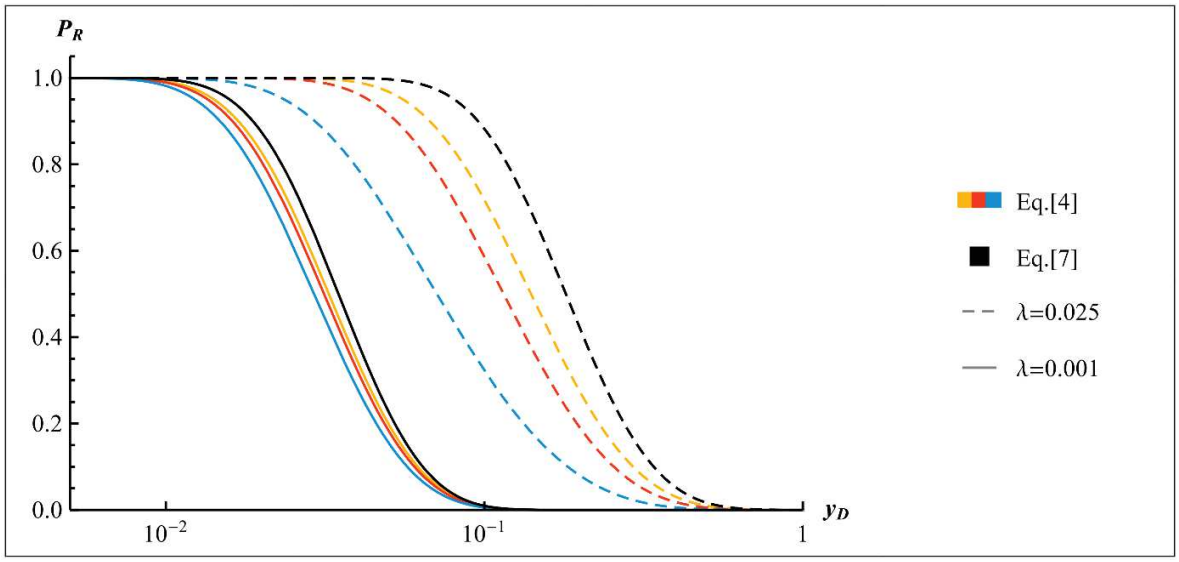

Supplementary Figure 5. Accuracy of Eq.[7](A19) compared to Eq.[4](A5) against y_D. *ER probability from de novo mutations against y_D. Colored lines show the results from the numerical integration of the 'exact' Eq.[4](A5), for three values of dimensionality $n = 3$ (orange), $n = 7$ (red) and $n = 15$ (blue). Black lines show the corresponding result from the simplified approximation ($\omega_R^{DN} \approx g(\alpha)$, Eq.[7](A19)), independent of n. The mutational variance is either $\lambda = 0.025$ (dashed lines) or $\lambda = 0.001$ (plain lines). Other parameters were $N_0 = 10^5$, $U = 2 * 10^{-5}$ and $r_{max} = 1$.*

Low vs. high peak limits:

The Laplace approximation scheme used in this section is based on the assumption that $\rho_{max} \gg 1$, which implies that resistance mutants typically lie far from the fitness peak in the stress ($y \ll 1$). In **Supplementary Figure 6** below, we illustrate this case (high peak limit, $\rho_{max} \gg 1$, panel B) together with the opposite case (low peak limit, $\rho_{max} \ll 1$, panel B). In the high peak limit, most resistant mutants are packed in the portion of the 'resistance zone' closest to the ancestor. This is at the intersection of the line connecting the ancestor and the optimum in the stress (dashed black line), and the edge of the resistance zone (dashed gray line). In the low peak limit, mutants are spread over the whole resistance zone, but this subspace is much smaller (even smaller than appears on graph, see the scale of each phenotypic space).

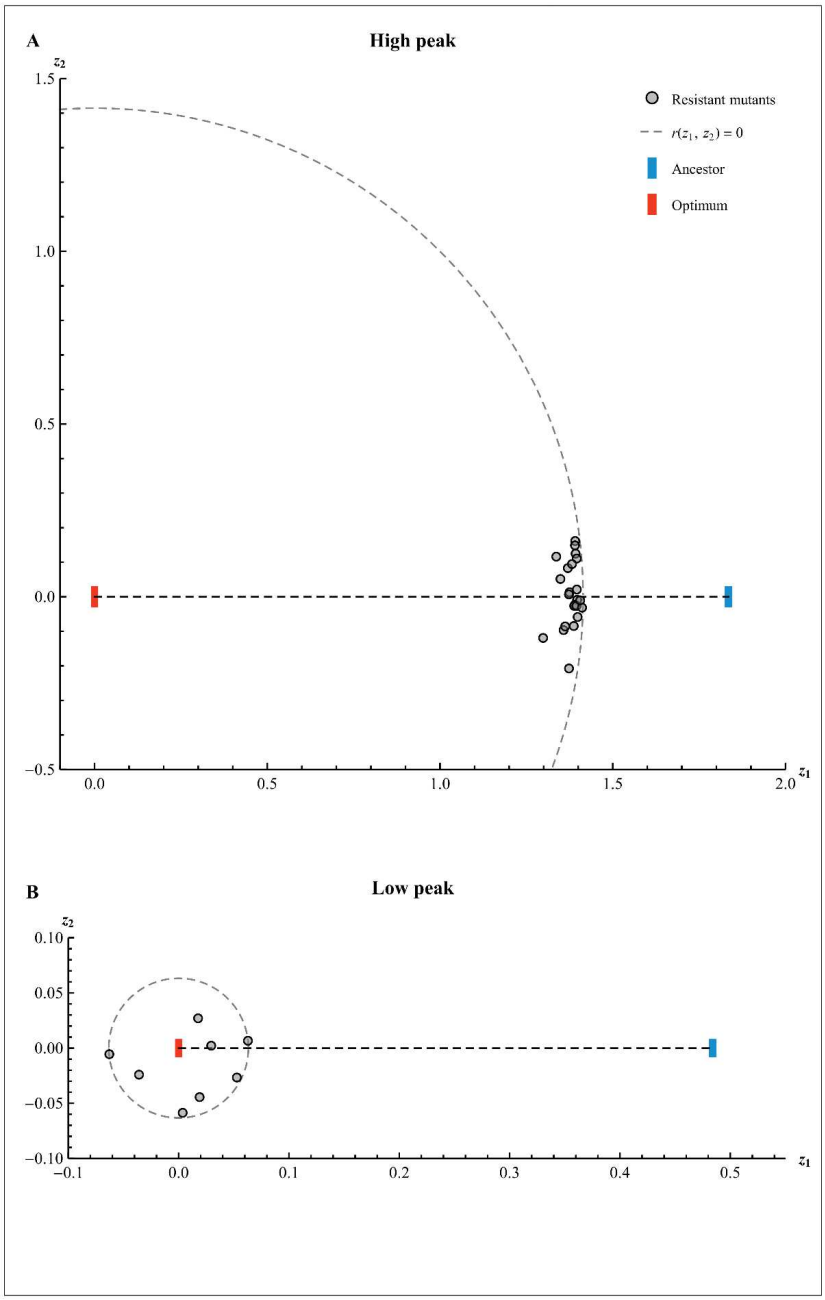

Supplementary Figure 6. Alternative limits for ρ_{max}. *The mutants (gray points), from a total of 9664 mutants simulated in A and 8674 mutants simulated in B, that lie within the resistance zone (delimited by the gray dashed line) are shown in an $n = 2$ dimensional phenotypic space (z_1, z_2). Two extreme limits are shown with the parameters chosen to yield the same ER probability: A. high peak ($\rho_{max} = 50, r_D = 0.68$) and B. low peak ($\rho_{max} = 0.1, r_D = 0.12$). In each case, ancestor (blue rectangle) and optimum (red rectangle), respectively, show the position of the ancestor phenotype in which mutants arise and of the optimum in the stress. Parameters were $N_0 = 10^5$, $U = 2 * 10^{-5}$ and $\lambda = 0.02$.*

Proportion of rescue from standing variance

The result in Eq.(A18) provides a simple formula for the proportion of rescue events that are caused by pre-existing variants. Define $\xi = (\theta + 1/2)/\rho_{max}$, we use the approximations $\alpha \approx \psi_D^2\, \rho_{max}/4 \; + 1/2$ (Eq.(A14)) to obtain a simple expression in terms of ψ_D (see **Supplementary Notebook file S1**):

$$\phi_R^{SV} \approx \frac{\beta^*}{1+\beta^*} \approx \frac{\psi_D(1+\psi_D/4)}{\left(\xi + \psi_D(1+\psi_D/2)\right)} \;, \qquad \text{(A22)}$$

where we recall that $\psi_D = 2(\sqrt{1+y_D} - 1)$ and $y_D = \rho_D/\rho_{max} = \psi_{\mathrm{D}}(1+\psi_{\mathrm{D}}/4)$. ϕ_R^{SV} shows qualitatively the same dependence on ψ_D and on y_D as they are in strictly increasing bijection so the maxima with respect to ψ_D and y_D are the same. A sign analysis of $\partial_{\psi_D}\phi_R^{SV} \propto 2\,\xi + \psi_D(\xi - \psi_D/2)$ shows that it increases with ψ_D from 0 then plateaus at some maximum and decays again, ultimately reaching $1/2$ as $\psi_D \to \infty$. The maximum is reached at $\psi_D = \xi + \sqrt{4\xi + \xi^2}$ and is given by

$$\max \phi_R^{SV} \approx \frac{1 - \xi/2 - \sqrt{\xi\,(1+\xi/4)}}{1 - 2\,\xi} \underset{\xi \leq 1}{\approx} \frac{1}{1 + \; e^{-\sqrt{\xi}/2}\,\sqrt{\xi}} \,. \qquad \text{(A23)}$$

This maximum decreases from 1 as $\xi \to 0$ ($\theta - 1/2 \ll \rho_{max}$) to $1/2$ as $\xi \to \infty$ (i.e. with effectively infinite dimensionality ($\theta \gg \rho_{max} = \epsilon^{-2}$). It remains fairly high unless dimensionality gets huge: for example, as long as $\rho_{max} \geq 6\;(\theta + 1/2)$ ($\xi > 1/6$) it lies above 75%. The curvature of ϕ_R^{SV} around this maximum (about $\psi_D = \xi + \sqrt{4\xi + \xi^2}$) is typically large as long as $\rho_{max} \gg \theta$: $|\partial_{\psi_D}^2 \phi_R^{SV}| = O(1/(4\sqrt{\xi}))$ for small ξ. This means that the proportion remains close to its maximum over a large range of values of ψ_D: the proportion of rescue form standing variance remains roughly constant across stress levels, over a wide range of stress levels around $\psi_D = \xi + \sqrt{4\xi + \xi^2}$, where $\alpha \approx 1 + \theta + O\left(\sqrt{\xi}\right)$ for small ξ.

IV. Characteristic stress and stress window

The relationship between the parameters characterizing the stress (ρ_{max}, y_D) and the rate of rescue shows a sharp drop from no extinction to nearly certain extinction. We try here to derive a heuristic characterization of this behavior. We do so by starting from the heuristic behavior suggested by Eq.(A20) for mild decay: $\omega_R^{DN} \approx g(\alpha)$. We use the mild

approximation $g(\alpha) \approx e^{-\alpha}\alpha^{-3/2}/\sqrt{2e}$ (Eq. (A16), valid for substantial α values). Here too, all derivations below are provided in **Supplementary Mathematica Notebook file S1.**

Rescue isocline:

We define a 'rescue isocline' of level p by the set of parameter values where $P_R = p$. Under the approximate heuristic derived above, such an isocline is characterized by $p = P_R \approx 1 - \exp(-N_0 U\, g(\alpha(p)))$, with $g(\alpha) \approx e^{-\alpha}\alpha^{-3/2}/\sqrt{2e}$. This implies $g\big(\alpha(p)\big) = -\log(1-p)\,/N_0 U$, and inversion of $g(.)$ then yields:

$$\begin{aligned}\alpha_p &\approx \frac{3}{2}\mathcal{W}\left(0.38\left(\frac{N_0 U}{\log(1/(1-p))}\right)^{2/3}\right) \\ &\approx -2.66 + 0.9\left(\log(N_0 U) - \log\left(\log\left(\frac{1}{1-p}\right)\right)\right)\end{aligned}, \qquad \text{(A24)}$$

where $\mathcal{W}(.)$ is Lambert's ('productlog') function. The second expression stems from a linear regression of $\mathcal{W}(x)\ vs.\log(x) - 1$ (checked by visual inspection, see **Supplementary Notebook file S1**) which suggests that, over a biologically relevant range $x \in [10, 10^{12}]$: $\mathcal{W}(x) \approx 0.9(\log(x) - 1)$.

Characteristic stress and characteristic stress window:

A characteristic stress can be defined as the value of the stress $\alpha_{0.5}$ where the ER probability is 50%. It characterizes the level of stress about which rescue drops from highly likely to highly unlikely. From Eq.(A24), it is given by

$$\alpha_{0.5} \approx \frac{3}{2}\mathcal{W}\big(0.484\,(N_0 U)^{2/3}\big) \approx 0.9\log(N_0 U) - 2.33\ . \qquad \text{(A25)}$$

Around this characteristic stress, the ER probability falls off more or less sharply. We define a characteristic stress window of level q over which P_R drops from $1/2 + q$ to $1/2 - q$. As an illustration, we use $q = 0.25$ so that the window characterizes the drop from 75% to 25% ER. This window can be directly computed from Eq.(A24) as $\Delta\alpha = \alpha_{0.25} - \alpha_{0.75}$. It is also approximately given by the inverse of the slope of the ER probability with α, at $\alpha = \alpha_{0.5}$, namely: $\Delta\alpha \approx 0.5/|P_R'(\alpha_{0.5})|$. The width of the window can be scaled by the value of the characteristic stress $\alpha_{0.5}$ around which the drop occurs, in order to characterize how sharp the drop is. We note that, in the exact form of $g(\alpha)$ in Eq.(A16), $g'(\alpha) = -g(\alpha)\,(2+\alpha)(1+2\alpha)/(2\alpha(1+\alpha))$. In fact, for any $\alpha \geq 1$ we can accurately approximate,

through a first-order Taylor approximation in large , $g'(\alpha) \approx -g(\alpha)(1 + 3/(2\alpha))$, and we obtain a simple expression:

$$\frac{\Delta\alpha}{\alpha_{0.5}} \approx \frac{0.5}{\alpha_{0.5}|P_R'(\alpha_{0.5})|} \approx \frac{2}{\log 8 + \log 4\ \alpha_{0.5}} \approx \frac{1}{1 + 0.7\ \alpha_{0.5}}\ . \qquad \text{(A26)}$$

This provides a good approximation to the exact value based on $\Delta\alpha = \alpha_{0.25} - \alpha_{0.75}$, as illustrated in **Figure 4** of main text. Obviously, this simple heuristic, based on a linear approximation for P_R, gets more accurate over narrower windows, e.g. it is very accurate to describe the decay from 70% to 30%, and less accurate to describe the decay from 95% to 5%.

Bibliography

Breitung K. W., 1994 *Asymptotic approximations for probability integrals*. Springer-Verlag, Berlin ; New York.

Gillespie J. H., 1983 Some Properties of Finite Populations Experiencing Strong Selection and Weak Mutation. Am. Nat. 121: 691–708.

Martin G., Aguilée R., Ramsayer J., Kaltz O., Ronce O., 2013 The probability of evolutionary rescue: towards a quantitative comparison between theory and evolution experiments. Phil Trans R Soc B 368: 20120088.

Martin G., Lenormand T., 2015 The fitness effect of mutations across environments: Fisher's geometrical model with multiple optima. Evolution 69: 1433–1447.

Martin G., Roques L., 2016 The Non-stationary Dynamics of Fitness Distributions: Asexual Model with Epistasis and Standing Variation. Genetics: genetics.116.187385.

McCandlish D. M., Stoltzfus A., 2014 Modeling Evolution Using the Probability of Fixation: History and Implications. Q. Rev. Biol. 89: 225–252.

Wolfram Research, 2001 Confluent hypergeometric function 0F1: Series representations.

CHAPTER II
Population persistence under high mutation rate: from evolutionary rescue to lethal mutagenesis

Yoann Anciaux[1]; Amaury Lambert[2], Ophélie Ronce[1]; Lionel Roques[3]; Guillaume Martin[1]

[1] Institut des Sciences de l'Evolution de Montpellier (UMR 5554 ISE-M), CNRS – Université de Montpellier, Place Eugène Bataillon, 34095 Montpellier Cedex 05, France

[2] LPMA, UPMC Paris 06, 75252, Paris, France

[3] BioSP, INRA, 84914, Avignon, France

Contact : yoann.anciaux@umontpellier.fr

Introduction

Understanding how environmental changes might ease or hinder the spread of populations (including in particular invasive species or pathogens) is essential in the fields of medicine or conservation. Extreme environmental changes may entail demographic threats on populations and lead them to extinction. Populations can be rescued by plastic responses, by immigration from another population or by dispersing to a more suitable environment. However, when none of these processes are sufficient to avoid extinction, only adaptation from de novo or standing genetic variation can rescue the population. This process has been called evolutionary rescue (hereafter ER). In isolated asexual populations, the probability of ER is largely determined by the rate of appearance and fitness effects of new (adaptive) mutations (Anciaux et al. in rev.). The population genetics of adaptation behind the rescue process sketchily fall into two alternative regimes: rescue may stem (i) from few mutations of large effects (strong selection weak mutation 'SSWM' regime) or (ii) from multiple mutations of small effects (weak selection strong mutation 'WSSM' regime) (reviewed in Gomulkiewicz et al. 2010; Alexander et al. 2014). The SSWM regime of adaptation has been extensively investigated via "origin-fixation" models describing the average behavior of stochastic evolutionary dynamics (McCandlish and Stoltzfus 2014) whereas the WSSM regime has been widely analyzed via deterministic models of quantitative genetics (Lande 1976, 1980). Corresponding ER models further include a coupling of adaptation and demographic dynamics, and naturally fall into the same two regimes (discussed in Anciaux et al. in rev.). Up to now, these ER models have addressed the impact of the origin and level of adaptive genetic variance available for ER in a given environment. However, very few

have explicitly investigated the role, in ER, of complex mutation effects distributions or their interactions with the environment. Martin et al. (2013) described general mutation kernels in the SSWM regime for a single given shift in conditions. Anciaux et al.(in rev.) studied the interaction of such complex kernel with a gradient of environmental stress levels, in the same SSWM regime, using a single peak fitness landscape. However, the alternative WSSM regime of ER is more challenging, as ER may then stem from the cumulative effect of multiple mutations arising over time in a given lineage. Consequently, no analytical result exists coupling both evolutionary and demographic dynamics on the probability of ER (in a given environment) in such more polymorphic regimes. Yet, this regime may be relevant to some 'real-world' situations, at least in highly mutable viruses, or mutator strains of bacteria (e.g. Springman et al. 2010). Here, we investigate ER over a single peak fitness landscape (as in Anciaux et al. in rev.), but in the more polymorphic WSSM regime.

In ER, genetic variance in fitness (either pre-existing or de novo) plays a major role by feeding the adaptive dynamics via selection. However, increased mutation rates, which yield higher genetic variance, may come at the cost of an increased load, because mutations tend to be deleterious on average. Consequently, such higher mutability may not always lead to increased population mean fitness and hence to increased ER probability. In classic single peak phenotype-fitness landscapes, this double-edged sword of increased phenotypic variation has been well investigated. For example, in some regimes of (periodically or randomly) changing environments, an increase in genetic variance can increase the so-called 'variance load' caused by stabilizing selection, to a point where it reduces the population's mean fitness overall, in spite of ongoing adaptation (Bürger and Krall 2004). Even in the abrupt environmental change investigated here, mutation may have transient favorable effects and lasting detrimental effects: it produces genetic variation that may favor the transient adaptive response but also builds-up a mutational load that may lower the ultimate mean fitness of the population. This second effect may be important at high mutation rates and has even be proposed as a means to weaken or even eliminate pathogen populations (i.e. avoid ER), by a process denoted lethal mutagenesis (Loeb et al. 1999). Lethal mutagenesis has been investigated empirically for treatment against viruses (Springman et al. 2010), bacteria (Bull and Wilke 2008) or cancer cells (Liu et al. 2015). Models of lethal mutagenesis have so far focused on large populations with deterministic evolution (Bull et al. 2007) and have recently integrated epistasis and distribution of mutation effects on fitness in

lethal mutagenesis (reviewed in Matuszewski et al. 2017). Under the Fisher's Geometric Model (hereafter "FGM"), this issue can be addressed analytically as in Martin and Gandon (2010). This study modelled the ultimate mutational load in the presence of epidemiological feedbacks, but ignored stochastic effects or the transient action of adaptation to new conditions. Here we focus on a simpler demographic context, but explicitly track stochastic eco-evolutionary dynamics, over time, in the context of an environmental change of given magnitude. We derive the probability and time dynamics of rescue events, using Fisher's Geometric Model (hereafter "FGM") to describe distributions of mutation fitness effects. This landscape entails pervasive epistasis between mutations at different sites and interactions between genotypes and alternative stress environments (Martin and Lenormand 2006; Tenaillon 2014). Because it focuses both on the transient and ultimate state of populations and considers the WSSM regime, the proposed approach aims to capture the continuum from evolutionary rescue to lethal mutagenesis, as mutation rate increases.

The dichotomy between SSWM and WSSM entails a somewhat simplistic view of adaptation regimes, at the two extremes of all possible mutation rates. However, these approximations reflect different views of population genetics, which both have received empirical support. The SSWM regime of ER is characterized by the fact that the first resistant lineage to establish (and thus cause rescue) is only at one mutational step from the dominant sensitive 'wild-type' lineage (e.g. Feder et al. 2016). However, Wilson et al. (2017) have shown that ER is often driven by soft selective sweeps, where multiple adaptive mutations spread through the population simultaneously. When these multiple mutations cause rescue by their cumulative effect, then the SSWM assumption no longer applies. Models that describe such highly polymorphic dynamics (WSSM regime) exist, but they then rely on classic deterministic quantitative genetics, under the infinitesimal model assumptions (many unlinked polymorphic loci), which does not apply to asexuals. In the WSSM regime, the exact stochastic evolutionary dynamics become quickly intractable, and have only been studied by simulation so far (Holt et al. 2003, 2004). Here, we take advantage of the fact that, while the evolutionary dynamics are more complex at high mutation rates, they are also more predictable and less prone to stochastic fluctuations, even in relatively small populations (Martin and Roques 2016). We thus use a combination of tractable deterministic evolutionary dynamics and stochastic demographic dynamics: the population's mean growth rate evolves deterministically, while its population size

follows (time-inhomogeneous) stochastic dynamics. Beyond a derivation of the probability of ultimate rescue or extinction, this approach further allows tracking the rescue process over time. As stated in Gomulkiewicz et al. (2017) transient dynamics (population size dynamics, distributions of extinction times) may hold the most important information on the rescue process, which are not readily available from previous theory, as it focused mainly on ultimate outcomes. Gomulkiewicz et al. (2017) treated these dynamics analytically by focusing on the distribution of extinction times for populations doomed to extinction. The present work seeks to extend this analysis to include multiple mutations, whose effect is further distributed, and depends on the genotypic and environmental context. These are key features of classical phenotype-fitness landscapes and are also generally observed empirically (e.g. Remold and Lenski 2001, 2004).

The analytical model described here shows how increased mutation rates allow populations to withstand higher levels of stress. However, it also shows a continuum from ER to lethal mutagenesis, in which ER probabilities increase with mutation rate at low mutation rate and decreases at high mutation rate because of lethal mutagenesis effects, ultimately leading to certain extinction beyond a threshold. Interestingly, some parameter ranges prove to greatly limit evolutionary rescue at all mutation rates, i.e. in spite of the possible apparition of mutators. Moreover, we show that, even if extinction never occurs in purely deterministic models (deterministic evolutionary and demographic dynamics), the minimum expected population size that is reached by these models can be a good predictor of ER probability. This provides a mathematical ground for the heuristic argument in (Gomulkiewicz and Holt 1995), which related ER to this minimal population size from deterministic models.

Methods

This section first describes the evolutionary and demographic assumptions of the model. Then the evolutionary models are detailed for an initially isogenic population or an initially polymorphic population, previously at equilibrium. Then the probability of ER is expressed by coupling these models with the stochastic demographic model detailed in the first section. Finally, the stochastic simulations are used to evaluate analytical approximations are briefly summarized.

I. General framework

The population is initially adapted to a non-stressful environment where its mean growth rate is positive. At the onset of stress, the population size is N_0 and the mean growth rate of the population shifts to a negative value due to the new stressful environment. Without evolution, the population is doomed to extinction. Evolutionary rescue occurs, if at least one resistant lineage (with a positive growth rate in the new environment) establishes, in spite of demographic stochasticity. These resistant lineages can be either already present in the population or arise *de novo* after the onset of stress. To investigate ER, it is crucial to determine the number of mutations that can arise and their growth rates. Both may be affected by the new environmental conditions and the parent genotypes already present in the population. To implement this complex dependence while keeping mathematical tractability and *a priori* empirical realism, we assume a single peak phenotype-to-fitness landscape: the FGM (for a review of the FGM model see Tenaillon 2014).

Fitness landscape

In the FGM, a given phenotype is a vector in a phenotypic space of n dimensions that determine fitness (here the growth rate r). The phenotype of an individual with genotype i, is characterized by a vector $\mathbf{z}_i \in \mathbb{R}^n$ of the breeding values (heritable components) for the n traits, its growth rate is r_i. Note that we do not consider any phenotypic plasticity or epigenetic effect from genotypes to phenotypes. In a given environment, fitness decays as a quadratic function of the phenotypic distance to a single phenotypic optimum, where the growth rate r_{max} is maximal at a given absolute level ('height of the peak'). In the scenario investigated here, in the non-stressful environment, the population is close to the 'ancestral' optimum $\mathbf{z}_A$. When the environment changes, it is assumed to determine a new optimum $\mathbf{z}_\star$. Without loss of generality, the height of the peak may also differ between the ancestral and new environments. However we do require that the n dimensions that determine fitness remain the same (in nature and number) across environments. In the new environment, the growth rate of an individual with genotype i is given by:

$$r(\mathbf{z}_i, \mathbf{z}_\star) = r_{max} - \frac{\left|\left|\mathbf{z}_i - \mathbf{z}_\star\right|\right|^2}{2}. \quad [1]$$

Demographic dynamics

We restrain our analysis to finite haploid asexual populations. Individuals have independent evolutionary and demographic fate so that frequency or density dependence is ignored. Each genotype i has a growth rate r_i and a reproductive variance σ_i ($r_i = r(\mathbf{z_i}, \mathbf{z}_*)$ in a given environment with optimum $\mathbf{z}_*$), which define its stochastic demographic parameters in the context of a Feller diffusion approximation (Feller 1951), as in e.g. (Martin et al 2013) or (Gomulkiewicz 2017). As an illustration, our simulations assume discrete generations and Poisson offspring distributions, as detailed in Anciaux et al. (*in rev.*) where $\sigma_i = 1 + r_i \approx 1$ for any genotype, assuming small growth rates $r_i << 1$, in per-generation time units. However, the analytical derivations rely on a Feller diffusion (1951) approximation, which approximately covers other demographic models (e.g. birth death models, see Martin et al. 2013; Gomulkiewicz et al. 2017).

II. Evolutionary dynamics.

In this section, we describe the model of evolutionary dynamics over the fitness landscape (FGM of the previous section), which is embedded into the ER model. In the following, *de novo* mutations (appearing after the onset of stress) are denoted "DN" and mutations from standing genetic variance (mutants already present before the onset of stress) are denoted "SV". Correspondingly, evolutionary rescue dynamics from an isogenic population, adapting only from *de novo* mutations, are labelled "DN" and dynamics from a polymorphic population, adapting from both *de novo* mutations and standing genetic variance, are labelled "DN + SV".

Evolutionary dynamics from an isogenic population.

The population is maladapted in the new stressful environment and its growth rate is $-r_D$, corresponding to a decay rate $r_D > 0$. Mutations arise every generation following a Poisson process with rate U per unit time per capita. For a given parent phenotype, each mutation creates

a random perturbation $\boldsymbol{dz}$ on phenotype, which is unbiased and follows an isotropic multivariate Gaussian distribution, $\boldsymbol{dz} \sim \mathcal{N}(0, \lambda\, \mathbf{I}_n)$ where $\mathbf{I}_n$ is the identity matrix in n dimensions and λ combines the selective intensity and the mutational variance per trait. Mutation effects add-up on phenotype, but not on fitness because $r(.)$ is nonlinear (epistasis on fitness and not on phenotype).

In the WSSM regime, the mean growth rate of the population shows limited stochastic variation among replicates, even in reasonably small populations. We thus approximate the evolutionary process by a deterministic fitness trajectory, derived in the WSSM regime under the FGM (Martin and Roques 2016) to gain analytical insight on the dynamics of multiple mutations, while keeping mathematical tractability. This seemingly rough approximation can be justified *a priori* as most of the ER process is decided over a short timescale, where fitness trajectories are driven by selection and mutation in the bulk of the fitness distribution (more deterministic than the stochastic events in the tails) . Simulations in the same discrete generation model as used here (Martin and Roques 2016) showed that mean fitness trajectories are indeed close to the deterministic prediction (with limited variation among replicates), in the WSSM regime, as long as $NU \gg 1$. While this condition is obviously not met during the whole ER trajectory (as population sizes become smaller), the approach proves sufficient to capture the ER process approximately, in this regime. Provided that $U \gg U_c = n^2\lambda/4$, the expected trajectory of the population's mean growth rate (expectation over replicates denoted by $\langle . \rangle$) is approximately (Martin and Roques 2016):

$$\left\langle \overline{r}_t^{\mathrm{DN}} \right\rangle = r_{max} - (r_D + r_{max})\, sech(\mu\, t)^2 - \theta\, \mu \tanh(\mu\, t), \qquad [2]$$

where $\mu = \sqrt{U\lambda}$ is a composite parameter of the mutational parameters and $\theta = n/2$ relates to the number of phenotypic dimensions n. Recall that r_D is the decay rate of the isogenic population and r_{max} is the maximum fitness that can be reached in the new environment (with $r_D + r_{max}$ the fitness distance between the parent genotype's fitness and the top of the fitness peak).

Evolutionary dynamics from an initially polymorphic population (at mutation-selection balance)

The evolutionary dynamics of rescue from a polymorphic population is obtained by a similar approximation. We assume that the population is initially at mutation-selection balance in the non-stressful environment, with an arbitrary positive mean growth rate. The phenotypic distribution at the onset of stress is centered on a mean phenotype $\bar{\mathbf{z}}$, which growth rate in the new environment is used to characterize the harshness of the stress imposed. We again denote this growth rate $-r_D = r(\bar{\mathbf{z}}, \mathbf{z}_*)$, where $r_D > 0$ is the decay rate of the central genotype as in the previous section. Resistant mutants may already be present in the population at the onset of stress ("SV" mutants) or appear by *de novo* mutation ("DN"mutants), or arise as combinations of these (multiple step rescue mutants). Using the same assumptions as in the previous subsection, provided that $U \gg U_c = \theta^2\lambda$, the expected trajectory of the population's mean growth rate is approximately (Martin and Roques 2016):

$$\left\langle \overline{r}_t^{DN+SV} \right\rangle = r_{max} - e^{-2\mu t}(r_D + r_{max}) - \theta\mu. \qquad [3]$$

In a polymorphic population at mutation-selection balance, the presence of a mutational load implies that the mean growth rate of the population in Eq.[3] is lower than the mean growth rate of an isogenic population in the same environmental conditions, with the same central genotype. In the following section, the deterministic fitness trajectories from Eq. [2] and [3] are fed into the stochastic demographic model presented in the first section, to compute ER probabilities.

III. Evolutionary rescue probability

The demographic dynamics of the population can be modeled by an inhomogeneous Feller diffusion of parameters $\overline{r}_t$ and $\overline{\sigma}_t$, which vary stochastically under the effects of drift, selection and mutation. However, as described in the previous subsection, the variation in $\overline{r}_t$ is limited among replicates. Therefore, we approximate each replicate's fitness trajectory by its deterministic expectation $\overline{r}_t \approx \langle \overline{r}_t \rangle$, using the relevant cases from Eq.[2] or [3]. Furthermore, it is assumed that the reproductive variance σ is approximately constant across genotypes: for example, in the discrete generation model with Poisson offspring number that is used for our simulations, $\overline{\sigma}_t \approx \sigma \approx 1$. Therefore, the model approximately reduces to a Feller diffusion with constant σ and time-inhomogeneous deterministic growth rate $\langle \overline{r}_t \rangle$. We then use the results from

Bansaye and Simatos (2015) on inhomogeneous Feller diffusions to derive the probability that the population is extinct before time t:

$$P_{\text{ext}}(t) = Exp(-\frac{2\,N_0}{\int_0^t \overline{\sigma}_u\ e^{-\rho_u} du}),$$
$$\rho_u = \int_0^u \overline{r}_v\ dv\ , \qquad \overline{\sigma}_u \approx 1, \qquad [4]$$

where $\bar{r}_t$ is given by Eq.[2] or [3]. This expression can be evaluated numerically at any time $t > 0$. ER depends on the establishment of resistant mutations, if none of them establishes, then the population goes extinct. Hence, the general form of the rescue probability is readily obtained as the complementary probability of the infinite time limit of Eq.[4], namely the probability of never getting extinct: $P_R = 1 - P_E$ with $P_E = P_{\text{ext}}(\infty)$, the extinction probability after infinite time.

IV. Invidual-based stochastic simulations

The analytical predictions are tested against exact stochastic simulations of the population size and genetic composition of populations across discrete, non-overlapping generations. The simulation algorithm is described in Anciaux et al. (*in rev.*). Briefly, reproduction is Poisson distributed every generations with parameter e^{r_i} for genotype i, mutations occur according to a Poisson process with constant rate U per capita per generation. The phenotypic effects of the mutations are drawn from a multivariate normal distribution, with multiple mutations having additive effects on phenotype. Fitnesses are computed according to the FGM using Eq. [1].

Results

In the following sections, we further provide the analytic expression for the ER probability in the presence or absence of initial standing variance. We quickly state the main differences and similarities with some existing ER models. We then compare our WSSM results to those for the SSWM regime in Anciaux et al. (*in rev.*) and to exact stochastic simulations. We then focus on how ER probability varies across a gradient of stress levels or of mutation rates. We then study the relative contribution of standing genetic variance on the ER process. Finally,

we investigate the transient time dynamics of the ER process: population size dynamics, distribution of times to extinction and the link between minimum population size and ER probability.

Rescue probability: general form

Define the rate of rescue per lineage present at the onset of stress as $R = -\log(P_{ext}(\infty))/N_0$, so that the ER probability takes the general form

$$P_R = 1 - e^{-N_0 R}$$

Before providing the results, it proves useful to define two scaled parameters: $\epsilon = \theta\,\mu/r_{max}$ and $x = r_D/r_{max}$. Recall that $\theta = n/2$ measures dimensionality and $\mu = \sqrt{U\lambda}$ depends on both mutation rates and effect. Consistently with (Anciaux et al. *in rev.*), the parameter $x = r_D/r_{max}$ describes how fast the initial clone decays, compared to how fast the optimal genotype grows, it gives a scaled measure of the harshness of the stress imposed. The parameter $\epsilon = \theta\,\mu/r_{max}$ is the ratio of the mutation load (at mutation-selection balance) and the maximal absolute growth rate that can be reached in the stress. It measures how far, in parameter range, we are from the regime of lethal mutagenesis. Certain extinction by lethal mutagenesis occurs whenever the load is equal or larger than the maximal growth rate (i.e. $\epsilon \geq 1$), so that even after reaching mutation-selection balance in the stress, the population would show no absolute growth. A small value of ϵ means that we are far from this certain extinction regime.

In spite of their difference in the population genetics underlying ER, the two scenarios (with or without standing variance) yield qualitatively similar expressions for the rate of ER. Under the WSSM regime $\rho_t = \int_0^t \overline{r}_v\, dv$ in Eq.[4] can always be written explicitly, form simple functions $f(.)$ and $h(.)$ given below. The rate of ER can thus can be expressed in the same general form for both scenarios (Eqs. (A5) and (A11-A12) in Appendix):

$$R = 2\,/\int_0^\infty e^{-\rho_u}\,du = 2\,\mu\,/\int_0^\infty h(y)^\theta \exp\left(-\frac{\theta}{\epsilon}\,f(y)\right)\,dy \quad , \quad \begin{matrix} DN: \ f(y) = y - (1+x)\tanh(y) \ , h(y) = \cosh(y) \\ DN+SV: \ f(y) = y - (1+x)\,(1-\mathrm{e}^{-2\,y})/2 \ , h(y) = e^y \end{matrix} \qquad [5]$$

The two scenarios differ only in the particular form of the functions $f(.)$ and $h(.)$. In the scenario with standing variance ($DN + SV$), the rate R in Eq.[5] takes an explicit form (Eq. (A12) in

Appendix), but the dependences on the parameters are not simple. In the scenario without standing variance (DN), no exact explicit expression could be found for the integral.

Weak selection, intermediate mutation approximation

To get a more direct insight into the impact of each parameter, we sought an approximate expression for the rate of rescue per lineage, as ϵ gets small (i.e. a mutation regime far from lethal mutagenesis). In the parameters range of weak selection and intermediate mutation rate, lethal mutagenesis has negligible influence on the demography, which depends mainly on the short term adaptation of the population to the stress. The strategy of approximation relies on the fact that as ϵ gets small, the exponent θ/ϵ in the integral in Eq. [5] becomes large, allowing the use of a so-called Laplace approximation for integrals (see **Appendix**). This approximation requires that the WSSM approximation be accurate, while ϵ remains small. More precisely, we require that (i) $U \gg U_c = \theta^2\,\lambda$, while (ii) $r_{max} \gg \theta\,\mu = \theta\sqrt{U\,\lambda}$, i.e. that $\lambda \ll U/\theta^2$ and $\lambda \ll r_{max}^2/(\theta^2 U)$. This is why we call this approximation a 'weak selection, intermediate mutation' approximation: λ must be weak enough and U must be substantial yet not too extreme (depending on r_{max} and θ). Obviously, the approximation is all the more accurate as the fitness peak r_{max} is high, selection intensity or mutational phenotypic variance is low (small λ) and dimensionality θ is limited.

Under this approximation, the ER probability can always be computed explicitly via the Laplace approximation, with yields accurate albeit somewhat complicated expression (Eqs.(A8) and (A13) in Appendix). These expressions further simplify (albeit becoming slightly less accurate) as ϵ gets small (dropping terms in ϵ): these simpler forms are given below. As for the exact result in Eq.[5], the *per capita* rate of rescue R takes roughly similar form for both scenarios (with or without standing variance), as ϵ gets small (detailed in Eqs. (A9) and (A14) in Appendix):

$$R \underset{\epsilon \ll 1}{\approx} 2\sqrt{\frac{r_{max}\,\mu}{\pi}}\exp\left(-\frac{r_{max}}{\mu}\,g(x)\right)$$
$$DN:\ g(x) = g_{DN}(x) = \sqrt{x(1+x)} - \cosh^{-1}\left(\sqrt{1+x}\right)\ . \qquad [6]$$
$$SV + DN:\ g(x) = g_{DN+SV}(x) = (x - \log(1+x))/2$$

In both cases, the function $g(.)$ is positive and increasing (roughly log-log linearly) with $x = r_D/r_{max}$. It is relatively straightforward from these expressions to show that R (and hence the ER probability) decreases with the stress r_D (for any increasing $g(.)$) and increases with the composite mutational parameter μ (for any positive $g(.)$). It also increases with r_{max} (provided

that $g(x) < x\, g'(x)$, which is the case for both $g_{DN}(.)$ and $g_{DN+SV}(.)$). The accuracy of this approximation is illustrated in **Supplementary figures 1** and **3** and **Figures 1** and **2**. Interestingly, in this range of parameters where the approximation applies ($\epsilon \ll 1$), the ER probability is independent of dimensionality (θ).

Comparison to existing ER models

Let us first detail the differences and similarities between these results and previous models of ER probability. The exponential dependence to N_0 ($P_R = 1 - e^{-N_0 R}$) is similar to that, e.g. in Orr and Unckless (2008,2014), Martin et al. (2013), or Anciaux et al.(*in rev.*), although none of these models allow for a contributions from multiple mutants. This stems from the same assumption of independence of the lineages that we consider in our model, i.e. all these results are obtained in the absence of any form of interactions between individual lineages (whether these change through time by the accumulation of mutations or not). Indeed, frequency or density dependence are ignored and there is no evolutionary interaction between lineages under pure asexuality. Therefore, each of the N_0 lineages initially present contributes independently to ER, yielding the exponential relationship to initial size. On the contrary, the dependence to mutation rates differs from these previous models of single step rescue. In the WSSM regime, R is no longer proportional to the mutation rate U, which reflects the fact that mutation is a double-edged sword, both enhancing adaptation via beneficial mutations and hindering it via the build-up of a mutation load. The latter process cannot be captured by single step mutation theory.

As in the SSWM regime (Anciaux et al. *in rev.*), the ER probability seems fairly independent of dimensionality (Eq.[6] is independent of θ) over a range of dimensions for which other quantities in the FGM could vary significantly (e.g. the proportion of beneficial mutations). Otherwise, the other parameters affect the ER probability in a different way in the SSWM and WSSM regimes. In particular, what we denote 'mutational parameters', namely the mutation rate (U) and mutational variance per trait (λ) only affect ER probabilities as a product here, via $\mu = \sqrt{U\,\lambda}$. We do indeed expect key differences between the WSSM and SSWM regimes, for the same landscape. First, multiple mutants should produce resistant genotypes across a wider phenotypic distance, allowing the populations to withstand higher stress levels than anticipated by the SSWM approximation. Second, as we have seen, the build-up of the mutational load should yield a non-monotonous relationship between ER and mutation rate, which is also not captured by SSWM

regimes (or by the approximate Eq.[6]). Obviously, these three effects are indeed negligible at low mutation rates where previous SSWM approximations apply, but they become substantial at higher mutation rates. On the other hand, neglecting evolutionary stochasticity, as was done here, should generate inaccuracies at lower mutation rates, where mean fitness dynamics introduce extra noise, in addition to demographic dynamics. Overall, we expect the SSWM and WSSM approximations to roughly capture complementary domains of the mutation rate spectrum.

Sharp decay in ER probability with increasing stress levels.

A possible measure of stress in ER is the rate of decay r_D of a population after the environmental change (see also Anciaux et al. in rev.). While the stress can affect different parameters of the FGM, in this section, we focus on the effect of stress mediated by r_D alone, hence when the stress gradient imposes increasingly shifted optima. We also consider the interaction with the fitness peak height r_{max}, which may change with the environment and the interaction with dimensionality n, which we consider constant across environments. As in Anciaux et al. (*in rev.*), increased r_D means both a faster decay (purely demographic effect of stress) and a larger shift in optimum (which affects the whole distribution of fitness effect of mutations), which both decrease the ER probability. On the contrary, increasing r_{max} increases the ER probability through two effects. First, the size of the phenotypic space of resistance increases with r_{max} (as in the SSWM regime, see Anciaux et al *in rev.*). Second a large r_{max} counterbalances a high mutational load $L = \theta\ \mu$ as can be seen in Eq.[2] (this latter effect is only captured in the WSSM approximation). At last, increased dimensionality, both in the previous and the new environment, induces lower ER probabilities.

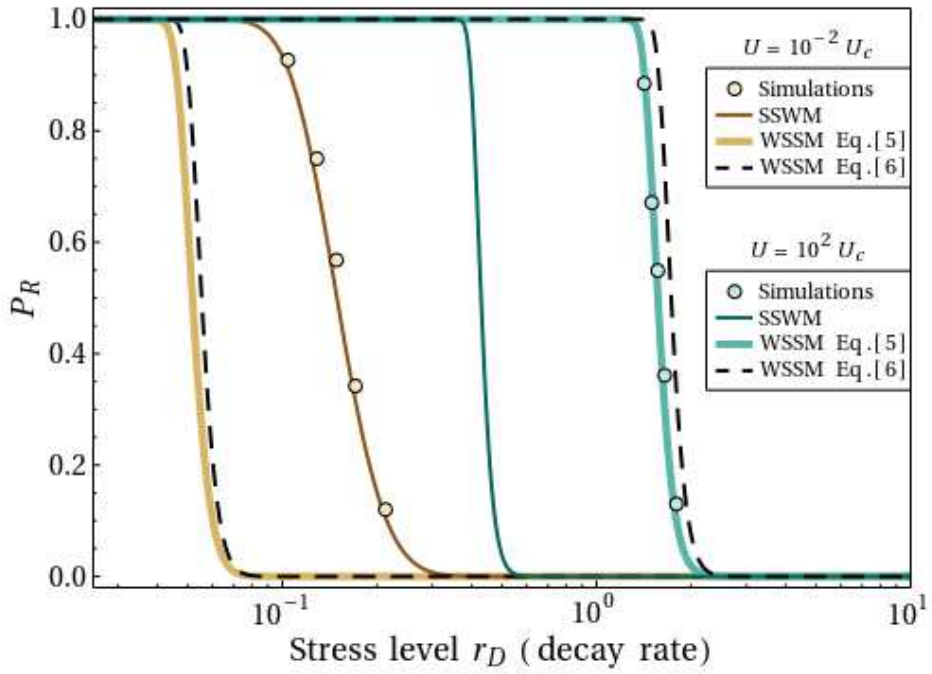

Figure 1*: ER probability against decay rate r_D. Dots show the results of* 10^3 *simulations, thin plain lines the SSWM approximation Eq.[6] from Anciaux et al. (in rev.), thick plain lines the WSSM approximation in Eq.[5] and dashed lines the corresponding closed form expression in Eq.[6]. All models and simulations are shown for a high mutation rate (blue) or a low mutation rate (brown), indicated in legend. Other parameters are* $N_0 = 10^5$, $n = 4$, $r_{max} = 1$ *and* $\lambda = 5.10^{-3}$

Figure 1 illustrates how the ER probability drops sharply with decay rate, both in the SSWM regime (brown curves) and in the WSSM regime (blue curves). Despite this qualitatively similar behavior, due to common constraints imposed by the FGM, the key differences anticipated earlier between the two approximations are also observed. We can see, as expected, that the alternative approximations (SSWM vs. WSSM) capture a different and complementary portion of the range of possible mutation rates and stress levels. With a milder stress, the transition in ER probability (from certain to impossible) occurs at relatively low mutation rates. In this context, the SSWM approximation is accurate while the WSSM is not. Indeed, the evolutionary stochasticity cannot be ignored in the dynamics of the few mutants that arise, invalidating the deterministic approximation used in the present model. With harsher stress, the same transition occurs at higher mutation rates, where the SSWM approximation becomes inaccurate,

underestimating the level of stress that the population can withstand. Indeed, multiple mutant rescue are then key to the ER process, while evolutionary stochasticity is negligible (compared to demographic stochasticity), so that Eqs.[5] and [6] become accurate.

Non monotonous relationship between ER probability and mutational parameters

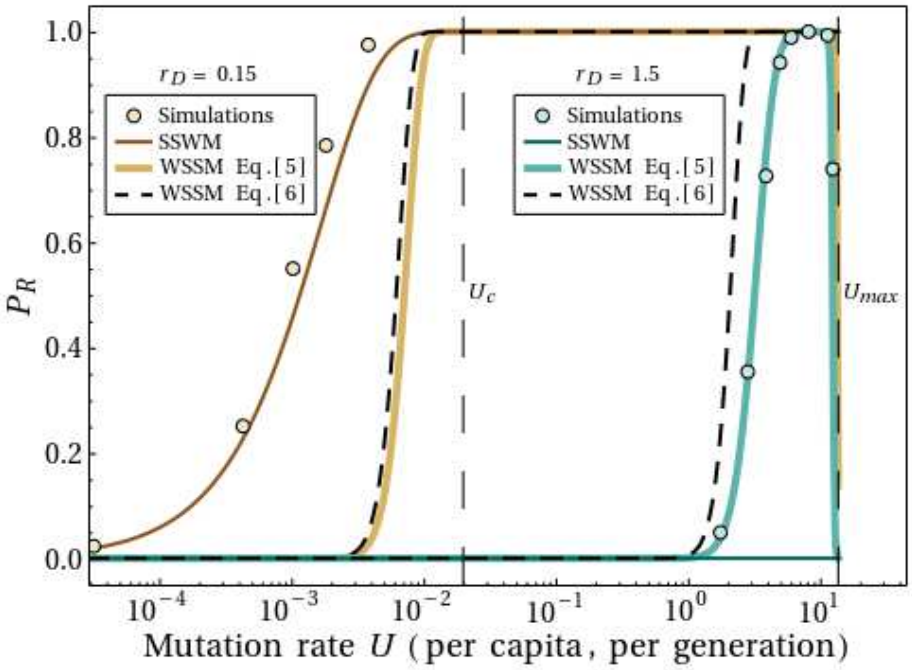

Figure 2*: ER probability against mutation rate U. Dots show the results of* 10^3 *simulations, thin plain lines show the SSWM approximation in Eq.[6] from Anciaux et al.(in rev.), thick plain lines show the WSSM approximation in Eq.[5] and dashed lines the corresponding closed form expression in Eq.[6]. All models and simulations have been tested in low stress (blue) and high stress (brown). Other parameters are* $N_0 = 10^5$, $n = 4$, $r_{max} = 1$ *and* $\lambda = 5.10^{-3}$

In the following section we now investigate the effect of mutational parameters. Both the rate U and effect variance λ of mutations affect the system in a similar fashion through the composite parameter $\mu = \sqrt{U\lambda}$. At small t (in Eq.[4]), an increase in μ speeds the early adaptive process, thus favoring rescue. However, over large times, the detrimental effect of the mutational load build-up becomes apparent. These two effects of μ are antagonistic and create a non-monotonic relationship between the rescue probability and mutational parameters. **Figure 2**

shows that this behavior is indeed observed in simulations and captured by Eq.[5] through the parameter $\epsilon = \theta\ \mu/r_{max}$ (and not by Eq.[6], which is only valid for intermediate μ). The range of mutation rate in **Figure 2** reach very high values, but the absolute values in this mutation rate window depends on other parameters (especially on λ through $\mu = \sqrt{U\ \lambda}$), which have been chosen arbitrarily. The rescue probability increases with the mutation rate and reaches a maximal value for which the mutation rate could be deemed "optimal". For low stress r_D the rescue probability approximately reaches 1 while increasing with mutation rate, forming a plateau as in **Figure 2** (see **Supplementary Figure X** for higher stress values). Beyond this optimal mutation rate, the rescue probability drops back to 0 at $U = U_{max} = (4\, r_{max}^2)/(n^2\ \lambda)$ (i.e. when the mutation load $n/2\ \sqrt{U\ \lambda}$ is equal to the maximal growth rate r_{max}), which is the mutation rate beyond which certain extinction is enforced by lethal mutagenesis. Indeed, beyond this threshold, the mutation load, at mutation-selection balance, is larger than the maximal growth rate that can be reached in the stress. Hence, even if ER allowed the population to invade the new environment, it could not generate a stable population once at mutation-selection balance. The population is thus doomed to ultimate extinction (Bull *et al.* 2007). Indeed, the integral in Eq.[5] becomes infinite as soon as $\epsilon \geq 1$ (or equivalently $U \geq U_{max}$), leading to $R = 0$.

Mutation window for ER :

In the previous subsections, we have shown that the ER probability drops sharply with increasing stress and is maximal over a finite range of mutation rates, that we denote the "mutation window" for ER. The "width" (range of mutation rates) and the "height" (maximum of ER probability over the range) of this window strongly depends on stress. In the following we detail the dependence of these characteristics of the mutation window on the parameters of the model.

To characterize the mutation window, its upper and lower bounds must be defined. The lower bound of the window (denoted $U^\star$) corresponds to the mutation rate at which the rescue probability rises above $1/2$. Thus, this lower bound is only defined if the height of the window lies above $1/2$ ($\max(P_R) \geq 1/2$). The upper bound of the window should correspond to the highest mutation for which the rescue probability is equal to $1/2$. However, this bound is more difficult to derive, so we set it to the mutation rate U_{max} beyond which certain extinction is enforced by lethal mutagenesis. This simplification is justified as the ER probability drops off very

sharply close to U_{max}, so that, approximatively, ER is only likely within the mutation window $U_* \leq U \leq U_{max}$. These two bounds are derived in Appendix Eq. (A17):

$$U_{max} = \frac{r_{max}^2}{\theta^2 \lambda}$$
$$U_* \approx \frac{g(x)^2\, r_{max}^2}{\lambda\, \mathcal{W}(N_0)^2} \qquad [7]$$

where $\mathcal{W}(u) \approx \log(u/\log(u))$ is Lambert's productlog function and $g(x)$ is the function of stress intensity given in Eq.[6], which describes how stress intensity ($x = r_D/r_{max}$) affects ER rates. Depending on the scenario, one uses $g(x) = g_{DN+SV}(x)$ or $g(x) = g_{DN}(x)$ in the presence or absence of standing variance, respectively. **Figure 3** illustrates the accuracy of the approximation for U_* in Eq.[7], compared to its numerical estimation from Eq.[5]. **Figure 3** also shows that this bound increases roughly log-log linearly with stress (as log (U_*)~8/3 log(x) + constant).

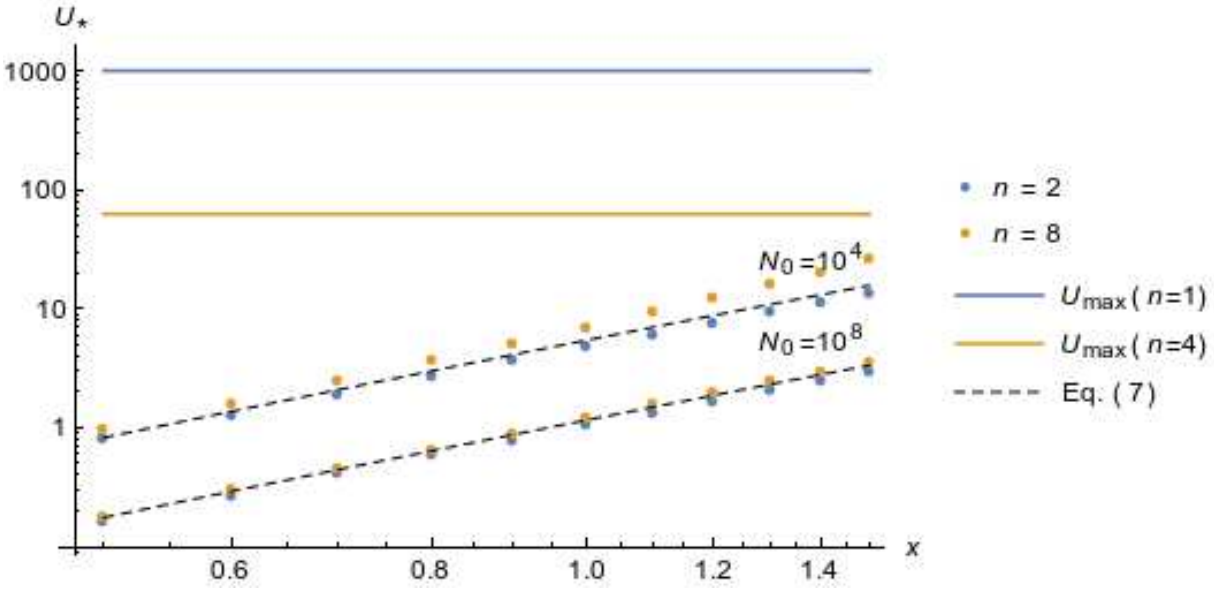

Figure 3: *Variation of the critical mutation rate U_* with increasing stress level ($x = r_D/r_{max}$ with constant $r_{max} = 1$). Dots show the numerical estimations of U_* from Eq.[5] for two dimensionalities (n given in legend) and population size (indicated on the graph). Colored solid lines show the value of the upper bound of the window U_{max} for the same two dimensionalities, independent of N_0. Dashed lines show the result of Eq.[7], independent of n. Other parameters are $r_{max} = 1$, and $\lambda = 10^{-3}$.*

The upper bound U_{max} is independent of initial conditions or stochasticity, as lethal mutagenesis depends on the deterministic equilibrium state of the population, once adapted to the stress. Therefore, U_{max} does not depend on the presence or absence of initial standing variance, the decay rate imposed by the environmental change (x) or the initial population size N_0. On the contrary, the lower bound U_* depends on these factors as it is determined by the

capacity of the population to transiently adapt to the new conditions. It shows, however, little dependence on dimensionality (θ), as is also apparent in **Figure 3** (compare $n = 2$ and $n = 8$). Overall, the width of the mutation window where ER is likely decreases with increasing stress r_D (**Figure 3**) and increases with initial population size N_0, it decreases with dimensionality θ and increases with the maximum fitness in the new environment r_{max}, because the upper bound of the window U_{max} decreases with these parameters.

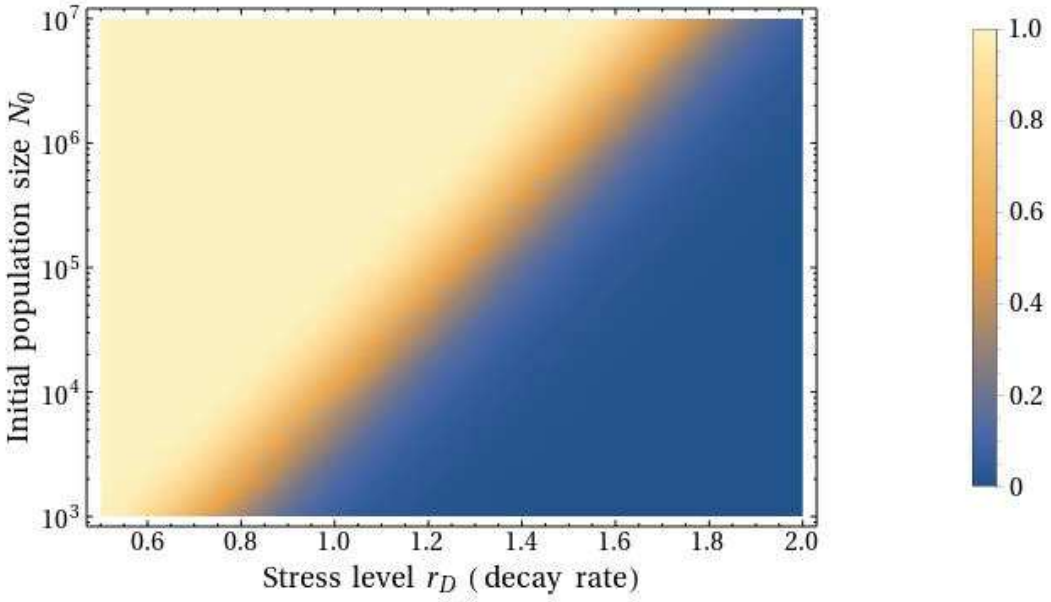

***Figure 4**: Maximum ER probability reached as U is varied, for different values of r_D and N_0. The maximal possible ER probability is found by varying U over the range $[U_*, U_{max}]$, and evaluating Eq.[5] numerically. High values are in light colors and low value in dark colors (see legend). The maximum of the ER probability drops over a short range of increasing r_D for a given N_0, or over a short range of decreasing N_0 for a given r_D. Other parameters are $r_{max} = 0.5$, $n = 4$, and $\lambda = 5.10^{-3}$*

The height $\max(P_R)$ of the mutation window is more challenging to derive analytically. However, it can be computed numerically by evaluating Eq.[5] over the range of mutation rate $[U_c, U_{max}]$ (similar results would be obtained over a range of λ). The results are shown on **Figure 4**, across a range of initial population size N_0 and stress intensity (as measured by the decay rate r_D). **Figure 4** shows that the height of the mutation window $\max(P_R)$ drops sharply with increasing stress (sharp transition from yellow to blue areas, details ER probabilities against mutation rate for scenarios DN and $DN + SV$ are in **Supplementary Figure 3**). In the example

shown, a large part of the combinations of the two parameters N_0 and r_D correspond to max(P_R) lower than 10%. For a given inoculum size N_0, there is always a threshold of stress level beyond which ER is nearly impossible, whatever the mutation rates or mutation effect variances in the population. It thus provides a threshold stress level that is *a priori* robust to resistance evolution, even in the face of mutation rate evolution.

Contribution from standing genetic variance

The results presented in the previous figures illustrate rescue from *de novo* mutations. In the presence of additional standing genetic variance, rescue mutants can arise from *de novo* mutants, from pre-existing mutants or from a combination of both. Eqs.[5]-[6] show the qualitative similarity between the case with and without standing genetic variance, in their dependence to each parameter (x, μ, r_{max}). **Figure 5** (top panels) confirms that the addition of standing genetic variance does not qualitatively modify the relationship between the rescue probability and stress intensity (r_D, **Figure 5a**) or mutational parameters (here U, **Figure 5b**). The same window of mutation rate exists where ER is likely ($U \in [U_*, U_{max}]$ similarly given by Eq.[7]). However, it is always wider in the presence of standing genetic variance (**Figure 5b**). Indeed U_* is lower ($g_{DN}(x)^2 > g_{DN+SV}(x)^2$ for all x in Eq.[7], see **Supplementary Figure 4**) while U_{max} is independent of initial conditions (hence on the presence of standing variance). Furthermore, the maximal ER probability and the level of stress that the population can withstand are higher in the presence of standing variance (**Figure 5a**).

Beyond this observation, we may be interested in the quantitative contribution of standing variance, relative to *de novo* rescue, in the polymorphic WSSM regime. Typically, this contribution is quantified, in single mutation ER theory, by the ratio of the rate of ER from standing variant lineages only, to the rate of ER from both *de novo* and standing variant lineages. Indeed, under a single step ER assumption, this ratio gives the probability that a given rescue event arises from a preexisting variant, as opposed to *de novo* (e.g. Anciaux et al. *in rev.*, Orr and Unckless 2008, 2014). However, in the WSSM regime, this simple interpretation is no longer valid: ER does not necessarily stem from single mutants of given origin. The lineage establishing for the first time in a given population (an ER event) might be a pre-existing variant that later accumulated *de novo* mutations to ultimately become resistant. Yet, the relative contribution from standing variance can still be quantified by this ratio, even if its stochastic interpretation no

longer holds. We thus define the same relative contribution ϕ_R^{SV} as in these single step ER theories (e.g. Anciaux et al. *in rev.*). Here, the rates of ER from each type do not simply add-up but ϕ_R^{SV} still measures how much more ER events result from the addition of initial standing variance.

$$\phi_R^{\mathrm{SV}} = 1 - \frac{R^{DN}}{R^{DN+SV}} \underset{\epsilon \ll 1}{\approx} 1 - \exp\left(-\frac{r_{max}}{\mu}\Delta g(x)\right) \quad . \qquad [8]$$
$$\Delta g(x) = g_{DN}(x) - g_{DN+SV}(x) \approx 0.38\, x^{1.2}$$

The explicit formula in the second line of Eq. [8] is derived from Eq.[6] and is thus valid over intermediate mutation rates (far below the lethal mutagenesis threshold U_{max}). The approximation $\Delta g(x) \approx 0.38\, x^{1.2}$ stems from a Taylor series around $x = 1$, but remains fairly accurate over the range $(0.1 \leq x \leq 10)$.

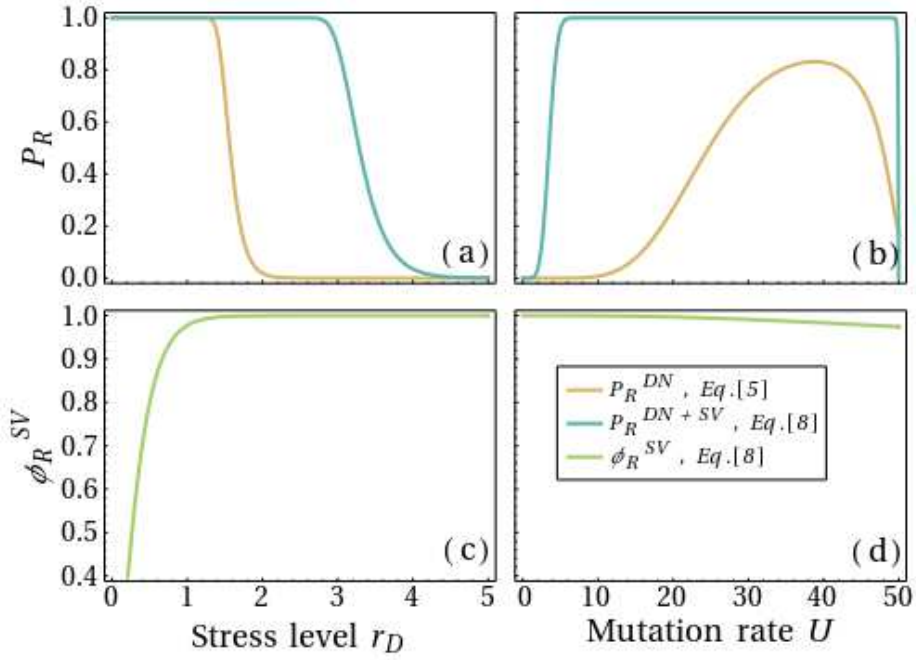

Figure 5: *Contribution of standing genetic variance ϕ_R^{SV} in the ER probability against r_D (panels (a) and (c)) and U (panels (b) and (d)). Panels (a) and (b) give the ER probabilities from de novo mutants only (orange; Eq.[5]) or both from de novo and pre-existent mutants (blue; Eq.[5]). Panels (c) and (d) give the proportion of ER from standing genetic variance ϕ_R^{SV} in the ER probability (green). Other parameters are $N_0 = 10^5$, $r_{max} = 1$, and $\lambda = 5.10^{-3}$. In panels (a) and (c) $U = 2$ and in panels (b) and (d) $r_D = 4$*

The contribution of the standing genetic variance to the rescue rises rapidly towards 1 as the harshness of stress (x) increases (r_{max} and μ remaining constant). This rise is faster with larger r_{max}/μ. For strong stress ($\Delta g(x)$ becomes large) the ER process is fully dominated by standing variance, when available, whatever the mutation rate (within $U_c \leq U \leq U_{max}$). This behavior is illustrated in **Figure 5** (bottom panels).

Generalization: dynamics of the ER process in the WSSM regime

The previous results focused on the probability of non-extinction after infinite time. Let us now focus on the transient dynamics of the ER process in the WSSM regime. ER has been commonly characterized by a U-shaped population size dynamics, obtained under a purely deterministic model (Gomulkiewicz and Holt (1995)). These dynamics are given by $N_t = N_0\, e^{\rho_t}$, for a given deterministic model of mean fitness $\bar{r}_t$ trajectory (with $\rho_t = \int_0^t \bar{r}_v\, dv$) and demographic dynamics. In our case, the fitness trajectory stems from the FGM and $\rho_t = \theta/\epsilon\ f(\mu\, t)$ is given by Eq.[5]. **Supplementary Figure 6** shows this U-shaped deterministic dynamics and how it captures, reasonably well, the average population size dynamics of exact stochastic simulations, in the WSSM regime. Note however that variation around this expectation is expected and indeed observed, even in this regime.

In fact, these fully deterministic dynamics prove more informative on the ER process than one may anticipate. The deterministic population size trajectory has a given minimum N_*, which is reached at some time t_* where $\partial_t \rho_t = \bar{r}_t = 0$. This minimum size has been proposed heuristically in Gomulkiewicz and Holt (1995) as a crucial predictor of extinction: ER being highly unlikely in parameter ranges where N_* is below some threshold. In fact, a more quantitative relationship exists between the minimum population size under the deterministic ER model, and the probability of ER, accounting for demographic stochasticity. This relationship goes beyond a particular model for the adaptive dynamics underlying rescue (in our case, the climbing of a fitness peak in the FGM). A general result arises, assuming a general regime where (i) evolutionary stochasticity can be ignored relative to demographic stochasticity and (ii) the stochastic reproductive variance σ is roughly constant, across lineages and thus over time (e.g. $\sigma \approx 1$ in our discrete time simulations) and (iii) density-dependence can be ignored (Feller diffusion applies). In that case, the following general rule (Eq. (A18)-(A19) in Appendix) applies for the probability of ER:

$$P_R = 1 - \exp(-2\,N_H/\sigma) \approx 1 - \exp\left(-\sqrt{2\,\Delta\bar{r}_*/\pi}\;N_*/\sigma\right) \\ N_* = N_0 e^{\rho t_*} \text{ and } \Delta\bar{r}_* = \partial_t \bar{r}_t \text{ at } t = t_* \; where\; \bar{r}_{t_*} = 0 \quad [9]$$

Here, N_H is the harmonic mean of the trajectory of population size in the purely deterministic model, taken over infinite time, N_* is minimum size reached by this deterministic model and $\Delta\bar{r}_*$ is the rate of adaptation of the deterministic evolutionary model, at the time when this minimum size is reached. Note that the right hand side approximation in Eq.[9] arises from a Laplace approximation (as used to obtain Eq.[6]).

Eq.[9] shows how purely deterministic dynamics predict the stochastic outcome of the ER process, in the WSSM regime. It also stresses the wisdom in Gomulkiewicz and Holt's (1995) early insight: the lower the minimum size, the lower the likelihood of ER, all else equal (and indeed harmonic means are notoriously driven by their minimum). Getting back to our particular model (FGM in the WSSM regime), **Figure 6a** (P_R vs. N_*) illustrates this pattern and the accuracy of Eq.[9] in capturing it. However, Eq.[9] also shows that N_* is not the only predictor of ER, the adaptation rate $\Delta\bar{r}_*$ (taken at the point where the population size is minimal) is equally important. In our particular model (see Eqs.(A20-21) in Appendix), it so happens that this factor is roughly $\Delta r_* \approx 2\,r_{max}\,\mu$, which is independent of (i) the scenario considered (with or without standing variance), (ii) the dimensionality θ or (iii) the stress level r_D. This means that when comparing across peak heights r_{max} or mutational parameters μ, minimal size is not sufficient to predict ER. However, it is sufficient when comparing across stress levels, or between scenarios concerning initial genetic variance. This is indeed confirmed in **Figure 6b)** (P_R vs. x for each scenario), where the dashed line shows the theory in Eq.[9] assuming $\Delta r_* \approx 2\,r_{max}\,\mu$. Differences between scenarios (DN or DN+SV) and environments (x) are indeed well captured. **Figure 6a** however reminds us that this simplification is not absolutely accurate, at least for the DN scenario (blue curve and dots slightly deviate from the dashed black line $\Delta r_* \approx 2\,r_{max}\,\mu$).

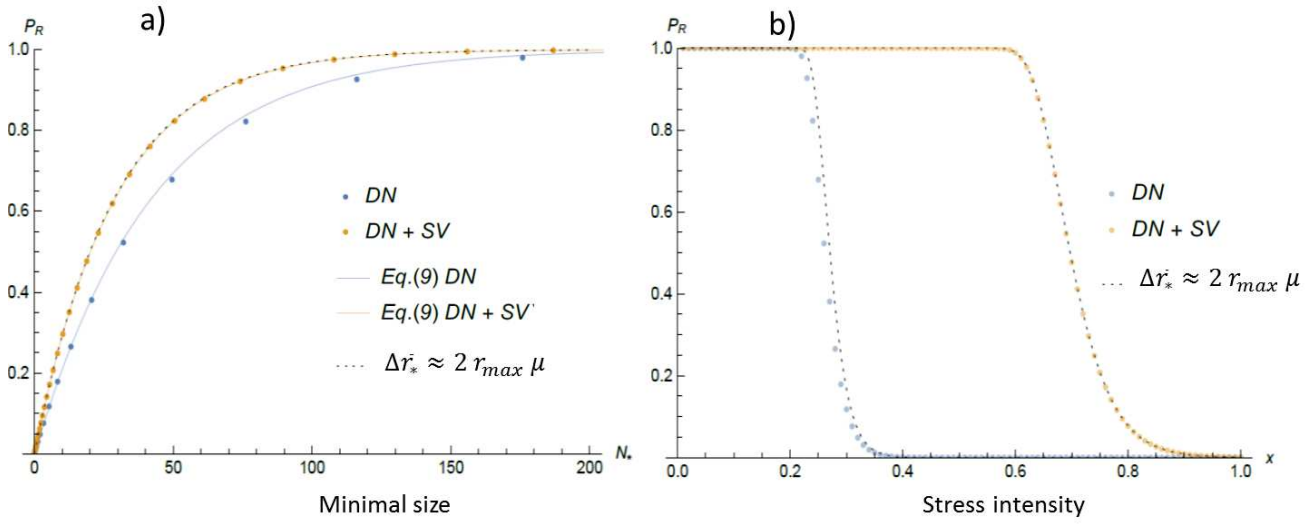

Figure 6: ***a)*** *Probability of ER vs. minimum population size. Dots show numerical computations from Eq.[5], when x is varied from 0 to 1, in the presence or absence of standing variance (DN+SV or DN, respectively, in legend). Plain lines show the corresponding approximation in Eq.[9] and the dashed black line shows Eq.[9] with $\Delta\bar{r}_* \approx 2\, r_{max}\, \mu$ for both scenarios.* ***b)*** *Same as* ***a)*** *but plotted against x, and with only the simpler result. $N_0 = 10^5, n = 4, \lambda = 5.10^{-4}, r_{max} = 0.3, U = 20\, U_c$.*

Distribution of extinction times

It has been proposed (Gomulkiewicz *et al.* 2017) that the full distribution of extinction times may hold important information on the ER process. In the context of treatment against pathogens and resistance, this distribution is also a key quantity to know how long a pathogen population must be 'treated' for example, such that it is almost certain to be extinct by the end of the treatment. From Eq.[4] we can derive the probability density $\varphi(t)$ of this distribution, in either of the two scenarios considered (purely clonal population DN or population at mutation-selection balance $DN + SV$). We get

$$\varphi(t) = \frac{\partial_t\, P_{ext}(t)}{P_{ext}(\infty)} = 2\, N_0\, \frac{P_{ext}(t)}{P_{ext}(\infty)}\, \frac{\Psi'(t)}{\Psi(t)^2}$$
$$\Psi(t) = \int_0^t \mathrm{e}^{-\rho_v}\, \mathrm{d}v = \int_0^t \mathrm{e}^{-\frac{\theta}{\epsilon} f(\mu\, v)}\, \mathrm{d}v \qquad , \qquad [10]$$

where the function $f(.)$ depends on the scenario considered and is given explicitly in Eq.[5]. **Figure 8** illustrates the accuracy of this result and how the distribution of extinction times varies with stress intensity r_D and mutation rate U. In spite of neglecting evolutionary stochasticity, Eq.[10] still captures the shape and scale of extinction time distributions, in the WSSM regime.

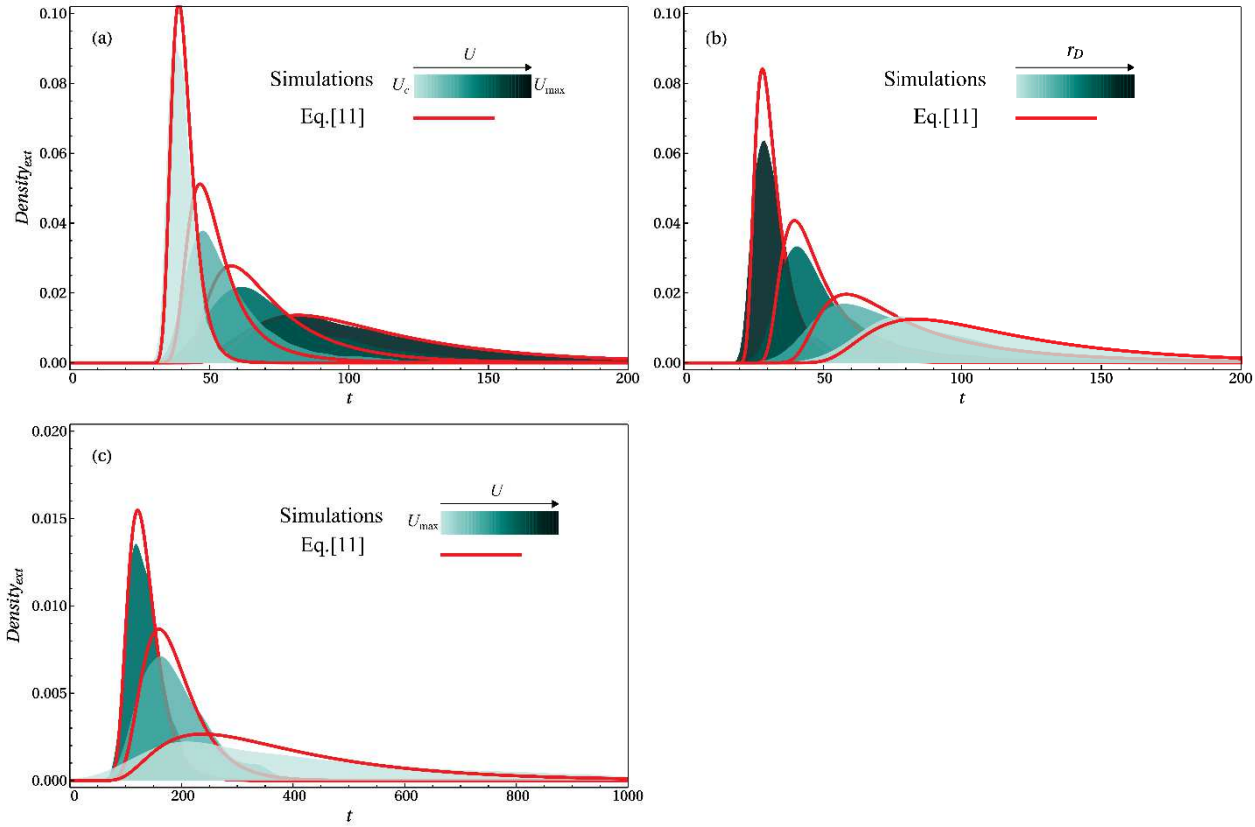

Figure 7*: Density of the extinction probability dynamic against U (panel **a** and c) and r_D (panel **b**). The distributions of extinction times from simulations started with an isogenic population are shown by shaded histograms, with the corresponding theory (Eq.[10]) given by the plain red lines. The color gradient corresponds to increasing levels r_D panel **b**) or U (lower range in panel **a** and higher range in panel **c**, as indicated on the legend). Each simulated distributions is drawn from 1000 extinct populations among a varying number of replicates depending on the ER probability.*

Figure 7b shows that decreasing the stress of an environmental change (via r_D) increases the mean duration of persistence of the population and also increases the variance on this duration. This behavior is expected, as decreasing the stress via r_D decreases the deterministic rate at which the population decays. The opposite behavior is observed when considering changes in mutation rates. Increasing mutation rate, as long as the mutation rate is below the lethal mutagenesis threshold ($U_c \leq U \leq U_{max}$, **Figure 7a**), increases the mean and the variance of the duration of persistence of the population. This likely stems from transient subcritical mutations ($0 > r > r_D$, beneficial but not resistant) that can transiently invade the population, thus delaying its extinction. However, beyond the lethal mutagenesis threshold ($U > U_{max}$, **Figure 7c**), the trend is reversed: extinctions (which is always certain then) occurs faster at high mutation rates (panel c). Therefore, even in these cases where ER probabilities are uninformative ($P_R = 0$), the

distribution of extinction times conveys important information on the underlying adaptive or maladaptive dynamics.

Discussion

We investigated the effect of an abrupt environmental change on the persistence of asexual populations with a large mutational input of genetic variance (WSSM regime), adapting either from *de novo* mutations arising after the environmental change (DN scenario) or from both de novo and pre-existing mutations ($DN + SV$ scenario). The key contributions of the model are to (i) allow for multiple step mutations to cause rescue and (ii) to consider adaptation over a phenotype-fitness landscape (Fisher's geometrical model FGM). The latter point implies the existence of pervasive epistasis between multiple mutations and imposes a relationship between the initial decay rate of the population, the proportion and growth rate of resistance alleles among random mutants, and their selective cost before stress (see also Anciaux et al. (in rev.)).

The weak selection strong mutation (WSSM) regime in ER:

In spite of its complexity, the ER process in this context can readily be captured by simple analytic approximations (Eqs.[5] and [6]) that neglect evolutionary stochasticity compared to demographic stochasticity. In this context, a general rule holds approximately (Eq. [9]), which should be valid beyond the particular adaptive dynamics implied by the FGM. The rate of ER (minus the logarithm of the extinction probability) is proportional to the minimal population size reached in the purely deterministic model of ER and to the square root of the adaptation rate at the time when this minimum is reached. Gomulkiewicz and Holt (1995) posited that extinction would be almost certain in those conditions where the deterministic demographic trajectory reaches a very low minimum. Our result provides a mathematical support to this early insight, and extends its potential applicability to any model where these two key factors can be derived. In the particular case where adaptation stems from the FGM, the proportionality coefficient between the rate of ER and the minimal size is simply $\sqrt{r_{max}\mu}$, whatever the level of stress or the presence/absence of standing genetic variance.

As with previous models of ER, we show an increase in ER probability with decreasing stress (**Figure 1**). We also show increasing ER probability with increasing mutation rates but only for intermediate mutation rates (high enough that the WSSM regime applies). When the mutation rate increases, two differences emerges when accounting for multiple mutations (e.g. as opposed to the results in Anciaux et al (*in rev.*), for single step ER in the same landscape). Quantitatively, multiple steps mutations allow withstanding higher stress than what the single step approximation anticipates. In our model, the FGM allows for a wide variety of allelic combinations (distributed effects and epistasis) that can lead to these multiple steps rescue. However the same qualitative decrease of ER probability with stress would still be expected in simpler models that ignore epistasis or multiple alleles (e.g. Orr and Unckless 2008, 2014). A second key difference with previous single-step ER models is that the dependence between the ER probability and the mutation rate is not monotonic. The model shows an optimal mutation rate for the ER probability, at which the maximal ER probability may be less than 1 (depending on the stress) and beyond which the ER probability drops down. This non-monotonic dependence reflects the continuum between ER and lethal mutagenesis along increasing mutation rates. This behavior is captured in the model by the dynamical build-up of the mutational load under the FGM, in which the proportion of deleterious (resp. beneficial) mutations increases (resp. decreases) as the population gets close to the optimum. This effect should also hold generally with other mutational models than the FGM.

Experimental test and parametrization:

To experimentally test the prediction, the assumptions of the WSSM regime a priori imply to use organisms with relatively high mutation rates, such as viruses, highly mutating strains of bacteria or possibly cancer cells. For a complete experimental test of the predictions, the parameters N_0, U, r_D, r_{max}, λ and θ must be measured. The methods and challenges in measuring these parameters are discussed in Anciaux et al. (*in rev*.). The full parametrization of the model will imply feasible but demanding measurements of the parameters with potential errors of measurement. However, if the model is valid, fitting an observed distribution of extinction times (**Figure 7**) might provide estimates of most parameters of the model. This would allow using not only the information from rescued populations but that from extinct ones. However such

empirical test will require fine-scale time series of the population size or at least the extinction status over time.

Finally, a simple empirical test of the relationship (Eq.[9], **Figure 6**) between the minimum size N_* and the probability of ER seems possible. To estimate N_*, one would start ER experiments at large initial size, so that the demographic dynamics might be expected to be deterministic. If density dependence effects can be ignored, then the observed N_* should be fairly repeatable, and should scale with N_0 (which can be checked empirically). The ER experiments would then be performed in the same conditions, but at lower initial size, where some probability of extinction could be estimated. Using the rate of rescue from these ER trajectories scaled by the N_* of the deterministic trajectories (both rate and N_* scaled by the appropriate N_0), the relationship between ER probability and N_* could be tested across a range of stress levels for example (e.g. antibiotic doses).

Treatment against pathogens, hyper-mutators and lethal mutagenesis

Our model as well as previous ones all suggest that the effectiveness of a given treatment depends on the mutation rate of the organism. Polymorphism for mutation rate and invasion of hyper-mutator genotypes is thus a potentially important issue for treatments against pathogens. However, our results show that a sufficiently strong stress could be effective in spite of hyper-mutator evolution. Indeed, because of the lethal mutagenesis effect (**Figure 2**) ER is only possible within a mutation rate window: a hyper-mutator would have to hit this window to be advantageous, and the width of the window narrows with increased stress (**Figure 3**). At sufficiently higher stress levels, ER is unlikely whatever the mutation rate (**Figure 4**), making these strong treatments robust to hyper-mutator evolution. Whether this pattern is confirmed empirically and whether the required treatment levels are then not too harmful for the treated subject remain open questions.

Our results cover the continuum from stress induced extinction to extinction induced by lethal mutagenesis. The latter might be an option, especially for organisms for which no "stress treatment" exists, or whose high mutation rates (above U_* in our model) allows them to withstand even strong stresses. Our results indeed confirm that increasing the mutation rate in this context (above U_{max}) will allow to fully remove the population. The addition of a stressor

might also help in the process, as has been suggested before (Pariente *et al.* 2001, 2003, 2005): indeed, the ER probability does drop faster with increasing U (as we approach U_{max}) in the presence of a strong stress (with high x), see **Supplementary Figure 4**.

Treatment duration issues.

However, one may also wonder how long a treatment must last (be it by stress effect or by lethal mutagenesis) for it to be efficient. From the distribution of extinction times (**Figure 7**), it is possible to predict the duration of the treatment needed to get rid of, say, 99% of the pathogen populations. Populations go extinct or rescue quite fast when treated by stressor (high x). Strong stresses (dark blue histogram in **Figure 7a**) both decrease the overall ER probability and the tails of extinction times. This means they are more efficient overall and require shorter treatment duration, with less risk of occasional treatment failure. However, when the mutation rate increases toward U_{max} (treatment by lethal mutagenesis), although extinction becomes highly likely ($P_R \to 0$, Figure 2), the times to extinction get more spread and the mode of the distribution increases (**Figure 7b**). If the mutation rate increases beyond U_{max}, the opposite pattern is observed (extinction times get shorter and less variable **Figure 7c**). Hence, a treatment by lethal mutagenesis, even if guaranteeing total extinction after infinite time, may need to be applied for a long time to significantly decrease ER probability (if the resulting U is close to U_{max}). Whether these behaviors are realistic remains a question of empirical test, and we see again how the distribution of extinction times holds valuable information, both for model testing and treatment optimization.

Limits of the model

The different results and applications described above are limited by the hypotheses of the model. First, the dynamics of the populations considered must not be density or frequency-dependent. Moreover the approximation of the demography by a Feller diffusion imposes that variations in population remain be smooth, which may exclude the modelling of some strong burst dynamics, in viruses for example. Besides, the model assumes a WSSM regime, which excludes its application to organisms with lower mutation rate (relative to selection intensity $U < U_c$). The latter could however be handled by complementary models under the SSWM regime such as Anciaux et al. (*in rev.*), under the same landscape assumptions. Finally, our

results assume a sharp change in the environment, which does not reflect all forms of stresses, including stresses that are imposed by a sudden treatment (e.g. antibiotics can have complex pharmacokinetic patterns over time). In that respect, extensions to more complex ecological scenarios might be useful: some are a priori possible using the same broad modelling framework as used here.

Bibliography

Alexander H. K., Martin G., Martin O. Y., Bonhoeffer S., 2014 Evolutionary rescue: linking theory for conservation and medicine. Evol. Appl. 7: 1161–1179.

Bansaye V., Simatos F., 2015 On the scaling limits of Galton-Watson processes in varying environments. Electron. J. Probab. 20.

Bull J. J., Sanjuán R., Wilke C. O., 2007 Theory of Lethal Mutagenesis for Viruses. J. Virol. 81: 2930–2939.

Bull J. J., Wilke C. O., 2008 Lethal Mutagenesis of Bacteria. Genetics 180: 1061–1070.

Bürger R., Krall C., 2004 Quantitative-genetic models and changing environments.

Feder A. F., Rhee S.-Y., Holmes S. P., Shafer R. W., Petrov D. A., *et al.*, 2016 More effective drugs lead to harder selective sweeps in the evolution of drug resistance in HIV-1. Elife 5: e10670.

Feller W., others, 1951 *Diffusion processes in genetics*. University of California Press Berkeley, Calif.

Gomulkiewicz R., Holt R. D., 1995 When does Evolution by Natural Selection Prevent Extinction? Evolution 49: 201.

Gomulkiewicz R., Holt R. D., Barfield M., Nuismer S. L., 2010 Genetics, adaptation, and invasion in harsh environments. Evol. Appl. 3: 97–108.

Gomulkiewicz R., Krone S. M., Remien C. H., 2017 Evolution and the duration of a doomed population. Evol. Appl.: n/a-n/a.

Holt R. D., Gomulkiewicz R., Barfield M., 2003 The phenomenology of niche evolution via quantitative traits in a "black-hole" sink. Proc. R. Soc. B Biol. Sci. 270: 215–224.

Holt R., Barfield M., Gomulkiewicz R., 2004 Temporal Variation Can Facilitate Niche Evolution in Harsh Sink Environments. Am. Nat. 164: 187–200.

Lande R., 1976 Natural Selection and Random Genetic Drift in Phenotypic Evolution. Evolution 30: 314.

Lande R., 1980 The Genetic Covariance Between Characters Maintained by Pleiotropic Mutations. Genetics 94: 203–215.

Liu L. L., Li F., Pao W., Michor F., 2015 Dose-Dependent Mutation Rates Determine Optimum Erlotinib Dosing Strategies for EGFR Mutant Non-Small Cell Lung Cancer Patients. PLoS ONE 10.

Loeb L. A., Essigmann J. M., Kazazi F., Zhang J., Rose K. D., *et al.*, 1999 Lethal mutagenesis of HIV with mutagenic nucleoside analogs. Proc. Natl. Acad. Sci. 96: 1492–1497.

Martin G., Lenormand T., 2006 A General Multivariate Extension of Fisher's Geometrical Model and the Distribution of Mutation Fitness Effects Across Species. Evolution 60: 893–907.

Martin G., Gandon S., 2010 Lethal mutagenesis and evolutionary epidemiology. Philos. Trans. R. Soc. Lond. B Biol. Sci. 365: 1953–1963.

Martin G., Aguilée R., Ramsayer J., Kaltz O., Ronce O., 2013 The probability of evolutionary rescue: towards a quantitative comparison between theory and evolution experiments. Phil Trans R Soc B 368: 20120088.

Martin G., Roques L., 2016 The Non-stationary Dynamics of Fitness Distributions: Asexual Model with Epistasis and Standing Variation. Genetics: genetics.116.187385.

Matuszewski S., Ormond L., Bank C., Jensen J. D., 2017 Two sides of the same coin: A population genetics perspective on lethal mutagenesis and mutational meltdown. Virus Evol. 3.

McCandlish D. M., Stoltzfus A., 2014 Modeling Evolution Using the Probability of Fixation: History and Implications. Q. Rev. Biol. 89: 225–252.

Orr H. A., Unckless R. L., 2008 Population Extinction and the Genetics of Adaptation. Am. Nat. 172: 160–169.
Orr H. A., Unckless R. L., 2014 The Population Genetics of Evolutionary Rescue. PLOS Genet. 10: e1004551.
Pariente N., Sierra S., Lowenstein P. R., Domingo E., 2001 Efficient Virus Extinction by Combinations of a Mutagen and Antiviral Inhibitors. J. Virol. 75: 9723–9730.
Pariente N., Airaksinen A., Domingo E., 2003 Mutagenesis versus Inhibition in the Efficiency of Extinction of Foot-and-Mouth Disease Virus. J. Virol. 77: 7131–7138.
Pariente N., Sierra S., Airaksinen A., 2005 Action of mutagenic agents and antiviral inhibitors on foot-and-mouth disease virus. Virus Res. 107: 183–193.
Remold S. K., Lenski R. E., 2001 Contribution of individual random mutations to genotype-by-environment interactions in Escherichia coli. Proc. Natl. Acad. Sci. U. S. A. 98: 11388–11393.
Remold S. K., Lenski R. E., 2004 Pervasive joint influence of epistasis and plasticity on mutational effects in Escherichia coli. Nat. Genet. 36: 423–426.
Springman R., Keller T., Molineux I. J., Bull J. J., 2010 Evolution at a High Imposed Mutation Rate: Adaptation Obscures the Load in Phage T7. Genetics 184: 221–232.
Tenaillon O., 2014 The Utility of Fisher's Geometric Model in Evolutionary Genetics. Annu. Rev. Ecol. Evol. Syst. 45: 179–201.
Wilson B. A., Pennings P. S., Petrov D. A., 2017 Soft Selective Sweeps in Evolutionary Rescue. Genetics 205: 1573–1586.

CHAPTER II

Appendix: Mathematical derivations and approximation

General WSSM approximation to ER.

In the present model, we approximate the stochastic dynamics of each lineage by a Feller diffusion (Feller 1951) or continuous branching CB-process (Lambert 2008), with parameters $\{r_i, \sigma_i\}$ for lineage i. We ignore any density or frequency dependence and assume that all lineages have similar stochastic reproductive variance ($\sigma_i \approx \sigma$). The resulting total population size N_t (cumulating all lineage that co-segregate) can then also be approximated by a CB process, which follows the Stochastic Differential Equation:

$$dN_t = \bar{r}_t \, N_t \, dt + \sqrt{\sigma \, N_t} \, dB_t \ , \qquad \text{(A1)}$$

where B_t is a Weiner process, $\bar{r}_t = 1/N_t \sum_{i=1}^{N_t} r_i$ is the mean growth rate of all lineages present at time t and σ is the common stochastic reproductive variance of all lineages. In the WSSM regime (i.e. when $U \gg U_c = \theta^2 \, \lambda$), we can ignore the evolutionary stochasticity introduced by mutation and drift as a first approximation. Then, the mean growth rate $\bar{r}_t \approx \langle \bar{r}_t \rangle$ (expectation over replicates denoted by $\langle . \rangle$) is approximately deterministic and given by the WSSM results in (Martin and Roques 2016) for the FGM. The probability of such a time inhomogeneous CB process to be extinct by time t is given by (Bansaye and Simatos 2015):

$$P_{\text{ext}}(t) = \exp\left(-\frac{2N_0}{\psi_t}\right) \ , \qquad \text{(A2)}$$

where $\psi_t = \int_0^t e^{-\rho(v)} dv$ and $\rho(u) = \int_0^u \langle \bar{r}_v \rangle \, dv$. The probability of ER is the complementary probability of not being extinct over infinite time, namely $P_R = 1 - P_{\text{ext}}(\infty)$.

Explicit expression for a population initially clonal

Define r_D the decay rate of the initial clone, and r_{max} the maximal attainable growth rate (that of a genotype optimal in the stressful environment). In this case, the mean fitness trajectory, relative to the optimal genotype ($\langle \bar{m}_t \rangle = \langle \bar{r}_t \rangle - r_{max}$), under the WSSM approximation, for an initially clonal population is (eq. (12) in Martin and Roques 2016)

$$\langle \bar{m}_t \rangle = m_0 \,\mathrm{sech}(\mu\, t)^2 - \theta\, \mu \tanh(\mu\, t)\,, \tag{A3}$$

where $\mu = \sqrt{U\,\lambda}$ and $\theta = n/2$, sech(.) and tanh(.) are the hyperbolic secant and tangent functions and m_0 is the fitness difference between the original clone and the optimal genotype. Now, we require the absolute mean fitness trajectory here (mean growth rate), which is obtained by noting that, by definition, $\langle \bar{m}_t \rangle = \langle \bar{r}_t \rangle - r_{max}$ and $m_0 = -r_D - r_{max}$. Denoting $x = r_D/r_{max}$, $\epsilon = \theta\,\mu/r_{max}$ we obtain

$$\langle \bar{r}_t \rangle = \frac{\theta\,\mu}{\epsilon}\,(1 - (x+1)\,\mathrm{sech}(\mu\, t)^2 - \epsilon \tanh(\mu\, t))\,, \tag{A4}$$

The integral $\rho_t = \int_0^t \langle \bar{r}_v \rangle\, dv$ of this growth rate over time can be expressed in compact form by using the change of variable $y = \mu\, t$, yielding

$$\begin{aligned} \rho_t &= \frac{\theta}{\epsilon} f(y) - \theta \log\big(h(y)\big) \\ h(y) &= \cosh(y) \\ f(y) &= y - (1+x)\tanh(y) \end{aligned}\,. \tag{A5}$$

Finally, the same change of variable ($dt = \mu\, dy$) can also be used to express the indefinite integral that determines extinction probabilities, yielding the rate of ER per lineage present at the onset of stress:

$$\begin{aligned} R^{DN} &= -\frac{\log P_{\mathrm{ext}}(\infty)}{N_0} = \frac{2}{\int_0^\infty e^{-\rho_u}\, du} \\ R^{DN} &= 2\,\mu \Big/ \int_0^\infty h(y)^\theta\, \mathrm{e}^{-\theta\, f(y)/\epsilon}\, \mathrm{d}y \end{aligned}\,. \tag{A6}$$

Laplace approximations for small ϵ

Eq.(A6) is fully analytic but yields no explicit expression, which would be useful to get a more intuitive grasp of how each parameter affects the ER probability. When the mutation rate and effects are small enough that the load $\theta\,\mu$ is small relative to the maximal growth rate r_{max} (so that we are well away from lethal mutagenesis), then $\epsilon \ll 1$. This means that $\theta/\epsilon \gg 1$ and the integral in Eq.(A6) is amenable to the Laplace Approximation (as $h(y)$ is monotonous over $y \in \mathbb{R}^+$). This approximation can be formulated as follows :

$$\int_0^\infty h(y)^\theta \, \mathrm{e}^{-\theta\, f(y)/\epsilon}\, \mathrm{d}y \underset{\epsilon \to 0}{\approx} \sqrt{\frac{2\,\pi\,\epsilon}{\theta\, f''(y_0)}}\, h(y_0)^\theta \, \mathrm{e}^{-\theta\, f(y_0)/\epsilon} \tag{A7}$$

where $y_0 = \cosh^{-1}(\sqrt{1+x})$ is the unique minimum of $f(.)$ over $y \in \mathbb{R}^+$. The Laplace approximation in Eq.(A7) then yields a fully explicit expression for the rate of ER per lineage present at the onset of stress defined in Eq.(A6). Rewriting in terms of the original parameters ($\theta/\epsilon = r_{max}/\mu$), we get

$$R^{DN} \underset{\epsilon \to 0}{\approx} 2\sqrt{\frac{r_{max}\,\mu}{\pi}} \exp\left(-\frac{r_{max}}{\mu}\,\gamma(x)\right)$$
$$\gamma(x) = \sqrt{x(1+x)} - \cosh^{-1}\left(\sqrt{1+x}\right) + \epsilon\left(\left(1+\frac{1}{2\,\theta}\right)\frac{\log(1+x)}{2} - \frac{1}{\theta}\frac{\log(x)}{4}\right). \tag{A8}$$

The accuracy of this expression is illustrated in **Supplementary Figure 1**.

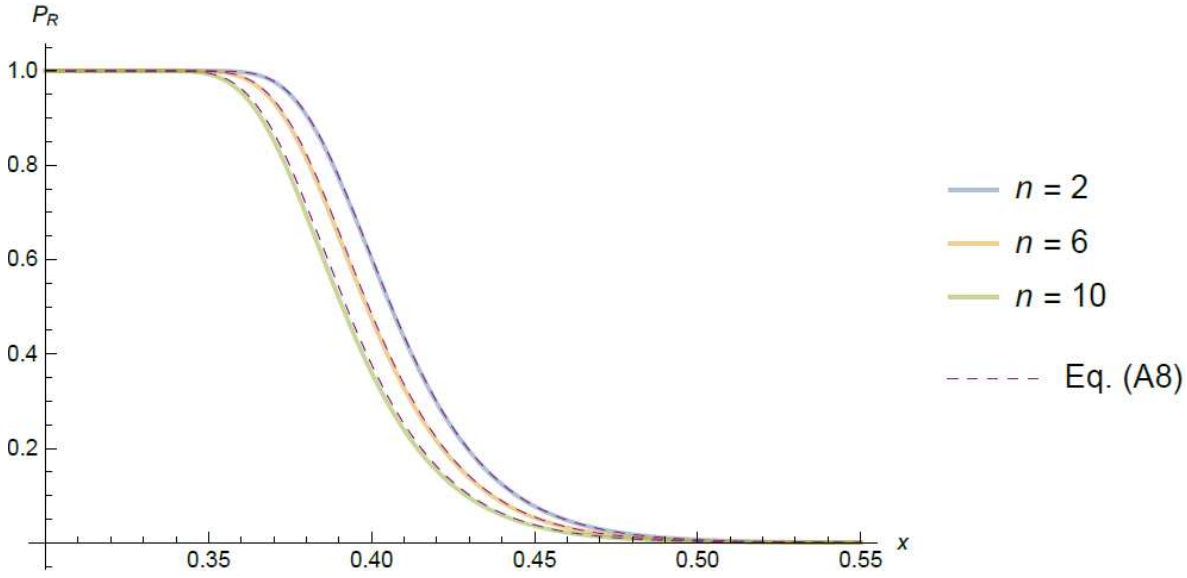

Supplementary Figure 1: *P_R as a function of x for three values of the dimensionality (given in legend), as computed from the 'exact' Eq.(A6) vs. Laplace Approximation Eq.(A8). Parameters are* $r_{max} = 1, \lambda = 5.10^{-4}, U = 0.5, N_0 = 10^7$.

In fact, unless we consider narrow range of stress variation, as in **Supplementary Figure 1**, it appears that, in the limit $\epsilon \to 0$, P_R shows limited dependency on dimensionality, provided that it remain limited (n varies by five-fold above). This is confirmed by further simplifying Eq. (A8) to produce a rough but reasonably accurate approximation, in a range that is a priori of most biological relevance, say for $x > 0.1$, i.e. not-too mild a stress. In this range both $\log(1+x)/2$ and $\log(x)/4$ or of similar or smaller order than $g(x) = \sqrt{x(1+x)} - \cosh^{-1}\left(\sqrt{1+x}\right)$. Therefore, as $\epsilon \to 0$ (as we assume here), the right hand factor in $\gamma(x)$, proportional to ϵ, becomes negligible,

relative to the left hand term, and $\gamma(x) \approx g(x)$. Eq. (A8) thus simplifies to the expression given in Eq.(6) for *de novo* rescue:

$$R^{DN} \underset{\substack{\epsilon \to 0 \\ x \geq 0.1}}{\approx} 2\sqrt{\frac{r_{max}\,\mu}{\pi}}\exp\left(-\frac{r_{max}}{\mu}\,g(x)\right). \qquad \text{(A9)}$$
$$g(x) = \sqrt{x(1+x)} - \cosh^{-1}\left(\sqrt{1+x}\right)$$

This simpler approximation is less precise but still provides a good order of magnitude, when ϵ is small enough. **Supplementary Figure 2** illustrates its accuracy and the fact that the ER rate is indeed roughly independent of dimensionality θ in this parameter range.

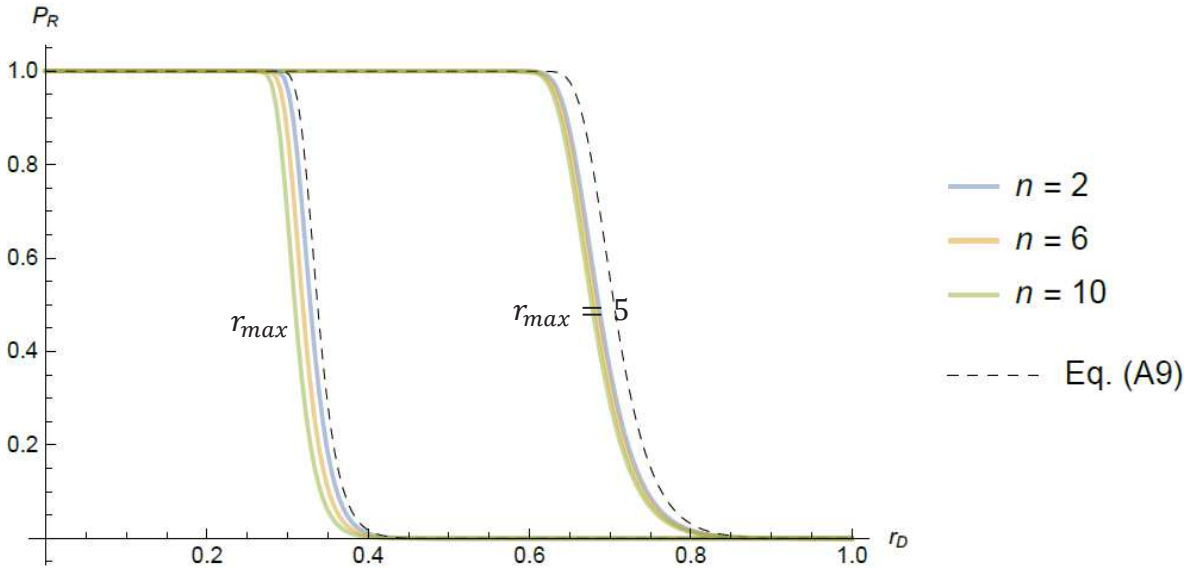

Supplementary Figure 2: *Same as* ***Supplementary Figure 1*** *(same parameters, except r_{max}, indicated on the graph), this time as a function of r_D and compared to Eq.(A9) (dashed lines).*

Explicit expression for a population initially at mutation-selection balance

This time we assume initially mutation-selection balance, then a shift in optimum occurs without any change in U or λ: adaptation is driven by both standing variance and de novo mutations. Based on the corresponding WSSM approximation (eq. (13) in Martin and Roques 2016) with the same approach and parameterization as for Eq.(A4) we get

$$\langle \bar{r}_t \rangle = r_{max}(1 - \mathrm{e}^{-2\,\mu\,t}(1+x) - \epsilon)\,, \qquad \text{(A10)}$$

which then yields the corresponding expression for ρ_t (same form as Eq.(A5)):

$$\begin{aligned}\rho_t &= \frac{\theta}{\epsilon} f\big(y(t)\big) - \theta \log(h(y)\\ f(y) &= y - (1+x)\,(1-\mathrm{e}^{-2y})/2\\ h(y) &= e^{y}\end{aligned}. \tag{A11}$$

The rate of ER takes a similar form as in the DN scenario (Eq.(A6)), but this time an explicit exact expression is found:

$$\begin{aligned}R^{DN+SV} &= -\log P_{\text{ext}}(\infty)/N_0 = \frac{2}{\int_0^\infty e^{-\rho_u}\,du} = 2\,\mu/\int_0^\infty h(y)^\theta e^{-\theta\, f(y)/\epsilon} dy\\ R^{DN+SV} &= 4\,\mu\frac{\mathrm{e}^{-\xi}\,\xi^\beta}{\Gamma(\beta)-\Gamma(\beta,\xi)}\end{aligned} \tag{A12}$$

Where $\xi = (1+x)\,\theta/(2\,\epsilon)$ and $\beta = (1-\epsilon)\,\theta/(2\,\epsilon)$ and $\Gamma(.)$ and $\Gamma(.,.)$ are Euler's gamma function and the incomplete gamma function, respectively.

Laplace approximations for small ϵ

Although this is already explicit, a Laplace approximation can be used to get a simpler result, again away from the lethal mutagenesis regime ($\epsilon \ll 1$). The function $f(.)$ has a unique minimum at $y_0 = \log\big(\sqrt{1+x}\big)$ and the resulting Laplace approximation for the rate of ER is of the same form as Eq.(A8):

$$\begin{aligned}R^{DN+SV} &\underset{\epsilon\to 0}{\approx} 2\sqrt{\frac{r_{max}\,\mu}{\pi}}\exp\left(-\frac{r_{max}}{\mu}\,\gamma(x)\right)\\ \gamma(x) &= \frac{x-(1-\epsilon)\log(1+x)}{2}\end{aligned}, \tag{A13}$$

From which, as $\epsilon \ll 1$, arises the same expression as Eq.(A9) with a different function $g(.)$:

$$\begin{aligned}R^{DN+SV} &\underset{\epsilon\to 0}{\approx} 2\sqrt{\frac{r_{max}\,\mu}{\pi}}\exp\left(-\frac{r_{max}}{\mu}\,g(x)\right)\\ g(x) &= \frac{x-\log(1+x)}{2}\end{aligned}. \tag{A14}$$

The accuracy of this approximation is illustrated in **Supplementary Figure 3** below. Note also how the drop in ER probability occurs at higher stress levels here than with purely *de novo* mutation (in **Supplementary Figure 2**).

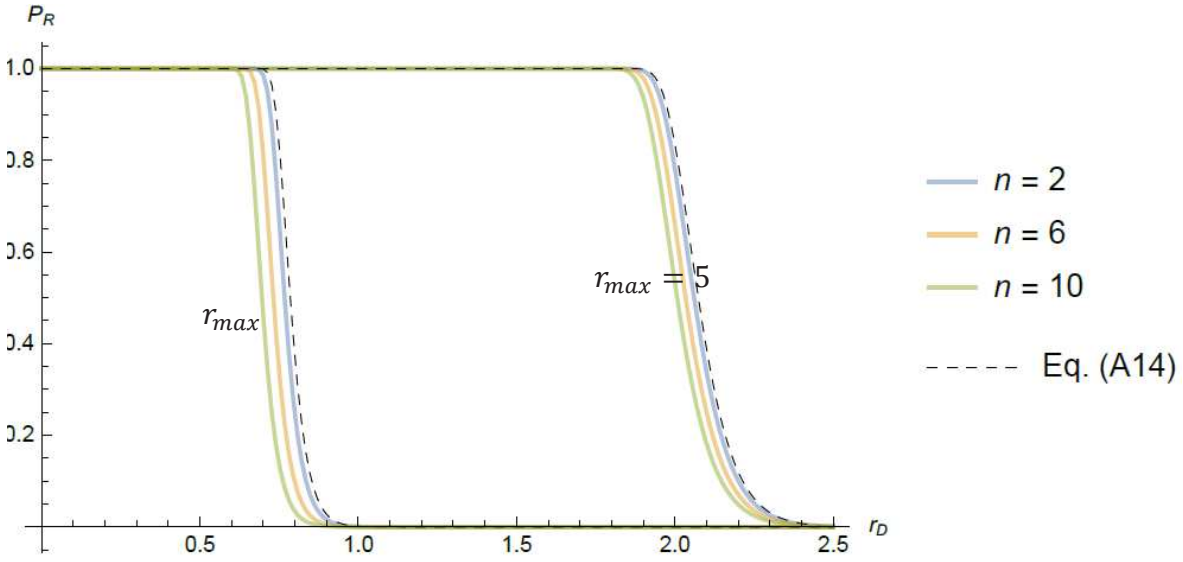

Supplementary Figure 3: *Same as* ***Supplementary Figure 2*** *(same parameters) with standing variance plus de novo mutation, and the corresponding approximation Eq.(A14).*

Critical mutation rates

We now wish to evaluate the mutation at which ER switches from very likely to very unlikely. We know that the rate of ER drops sharply at some upper threshold mutation rate, due to lethal mutagenesis effects, when $\mu\,\theta = r_{max}$. This implies a maximal mutation rate $U_{max} = r_{max}^2/(\theta^2\lambda)$, above which lethal mutagenesis leads to certain extinction of the population.

Here, we are interested in the parameter range, far below lethal mutagenesis, where the ER probability increases (sharply too) with the mutation rate. We thus first seek the value μ_* at which the ER occurs 50% of the time. This 'critical mutation rate', is the one above which ER becomes likely. The ER probability is $P_R(\mu_*) = 1/2$, so that the ER rate is $R_* = -\log(1 - P_R(\mu_*))/N_0 = \log(2)/N_0$. In this range, we can use the approximate expressions in Eqs (A9) and (A14): $R(\mu) \approx 2\,N_0\,\sqrt{r_{max}\,\mu/\pi}\,\exp(-r_{max}\,g(x)/\mu)$. Solving for this equation yields a unique solution:

$$\mu_* \approx \frac{2\, g(x)\, r_{\max}}{\mathcal{W}(5.3\, g(x)\, N_0^2 r_{\max}^2)} \quad , \tag{A15}$$

Where $\mathcal{W}(.)$ is Lambert's function. This rate is in fact of much simpler form, approximately, if we note that N_0^2 is typically very large compared to $g(x)$ and r_{max} which are of order 1. Therefore the productlog term is driven by the asympotitc limit of $\mathcal{W}(.)$ ($\mathcal{W}(v) \approx \log(v/\log(v))$, for large v) and by the terms in N_0. Overall, to a reasonably good approximation:

$$\mu_* \approx \frac{g(x)\, r_{\max}}{\mathcal{W}(N_0)} \approx \frac{g(x)\, r_{\max}}{\log\left(\frac{N_0}{\log(N_0)}\right)} \quad . \tag{A16}$$

Recalling that $\mu = \sqrt{U\,\lambda}$, the critical mutation rate where the ER probability is 50% is

$$U_* \approx \frac{g(x)^2\, r_{max}^2}{\lambda\, \mathcal{W}(N_0)^2} \approx \left(\frac{g(x)\,\theta}{\mathcal{W}(N_0)}\right)^2 U_{max}\,. \tag{A17}$$

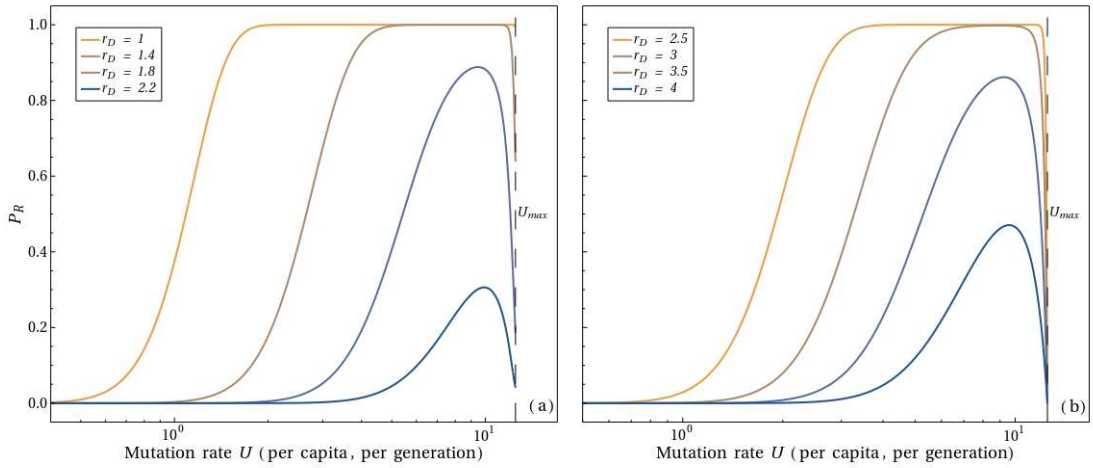

Supplementary Figure 4: *Decrease of the width and height of the mutation window with stress. Plain lines show Eq.[6] for ER from de novo mutations (**a**) or from pre-existing standing genetic variance and de novo mutations (**b**). The colors are the same as in **Figure 4** for increasing r_D.*

This means that ER is only likely within a window of mutation rate $U_* \leq U \leq U_{max}$. This window narrows down as stress increases (increased decay rate and hence $g(x)$) **Supplementary Figure 4**, or as N_0 gets smaller and its lower bound is roughly independent of dimensionality. The accuracy of this approximation is illustrated in **Figure 3** for the DN scenario

($g(x) = \sqrt{x(1+x)} - \cosh^{-1}(\sqrt{1+x})$) and in **Supplementary Figure 5** below for the SV+DN scenario in the presence of standing variance ($g(x) = (x - \log(1+x))/2$).

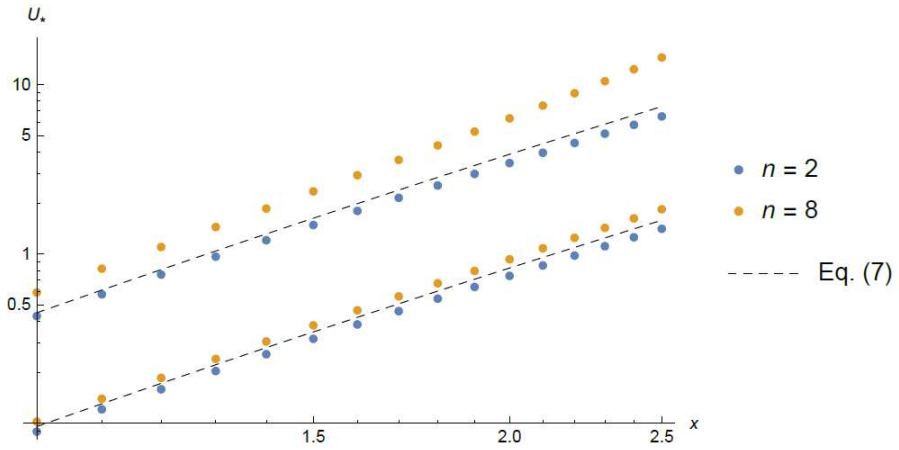

Supplementary Figure 5: *same as* ***Figure 3*** *with standing variance plus de novo mutation.*

ER probability vs. deterministic population size dynamics

A fully deterministic model of population size dynamics can be readily derived from the ER model, it yields a deterministic trajectory $\widetilde{N}_t$ that approximately predicts the average population size among replicate ER simulations: $E(N_t) \approx \widetilde{N}_t = N_0 e^{\rho(t)}$ (as seen in **Supplementary Figure 6** below).

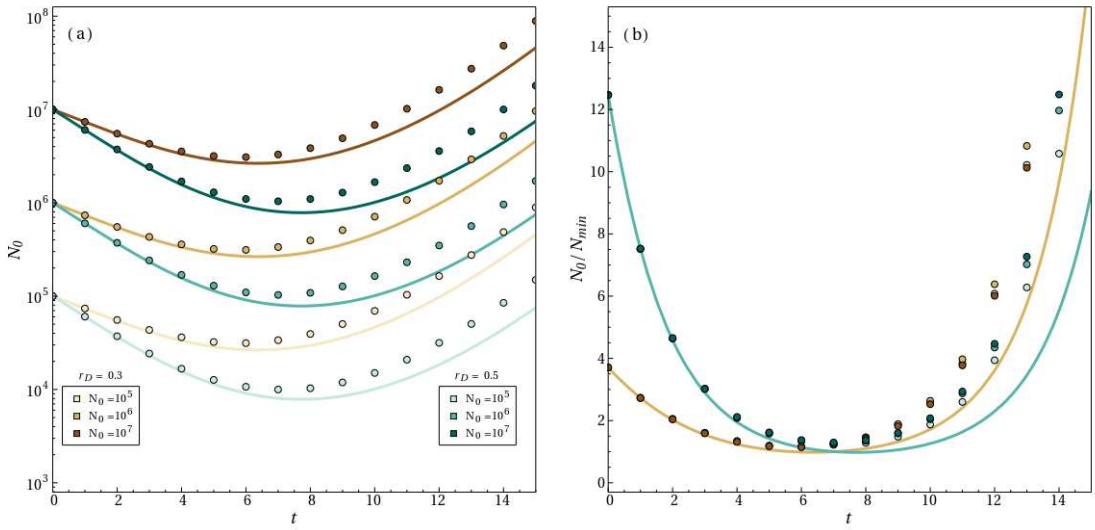

Supplementary Figure 6: *Population size dynamics. Panel (a) shows population dynamics for $r_D = 0.3$ in blue and $r_D = 0.5$ in brown. The population dynamics start from $N_0 = 10^5, 10^6, 10^7$ for each r_D (gradients of color gets darker with the increase of population size). Lines show the theory from $E(N_t) = N_0 e^{\rho(t)}$ and dots the according simulations. Panel (b) shows the same simulations and the same theoretical curves but with the population size rescaled by its minimum. The theoretical curves for the different N_0 are confounded in a unique curve for each r_D. Other parameters are $r_{max} = 1$, $U = 2$, $n = 4$ and $\lambda = 5.10^{-3}$*

This relationship between ρ_t and the deterministic population size implies an interesting interpretation of the general formula for the ER probability in Eq.(A2). We have $e^{-\rho(t)} = N_0/\widetilde{N}_t$, which implies that $\int_0^\infty e^{-\rho(v)}dv = N_0/\int_0^\infty \widetilde{N}_v^{-1}dv = N_0/\widetilde{N}_H$, where $\widetilde{N}_H$ is the harmonic mean of the deterministic population size trajectory, over infinite time. In the WSSM regime, the ER probability is readily predictable from the harmonic mean of the deterministic population dynamics:

$$P_R \approx 1 - \exp\left(-\frac{2N_0}{\sigma \int_0^\infty e^{-\rho(v)}dv}\right) = 1 - \exp\left(-2\,\widetilde{N}_H/\sigma\right) . \qquad \text{(A18)}$$

The result obviously extends to intermediate times: the extinction probability up to time t is $P_{\text{ext}}(t) = \exp(-2\,\widetilde{N}_H(t)/\sigma)$, where $\widetilde{N}_H(t)$ is the harmonic mean taken over the time interval $[0, t]$.

From there, properties of harmonic means suggest that the minimum size of the deterministic population size dynamics will be a key predictor of ER probability. The Laplace approximation further provides a more formal connection. The deterministic trajectory of population size $\widetilde{N}_t = N_0 e^{\rho(t)}$ reaches a minimum $N_* = N_0 e^{\rho(t_*)}$ at the time t_* where $\rho'(t_*) = \bar{r}(t_*) = 0$, namely the time where the mean fitness trajectory crosses zero. The Laplace Approximation to P_{ext} approximates $\int_0^\infty e^{-\rho(t)}\,dt$ around the minimum $\rho(t_*)$ of $\rho(t)$, which is at the same time point ($\rho'(t_*) = \bar{r}(t_*) = 0$). This implies a general approximation for the probability of rescue:

$$P_R \approx 1 - \exp\left(-2\frac{N_0\, e^{\rho(t_*)}}{\sqrt{2\,\pi/\rho''(t_*)}}\right) = 1 - \exp\left(-N_*\sqrt{\frac{2\,\Delta r_*}{\pi}}\right), \tag{A19}$$

Where N_* is the minimal population size of the deterministic trajectory and $\Delta r_* = \bar{r}'(t_*) = \rho''(t_*)$ is the rate of adaptation at the point where the fitness trajectory crosses zero. The rate of rescue is proportional to the minimum size N_* reached by the deterministic trajectory, proportionally to the square root of the deterministic adaptation rate Δr_* at this minimum size.

***DN* rescue:** in the DN scenario where the population is initially clonal, we have, when $\epsilon \to 0$, $\rho(t) \approx \theta/\epsilon\, f_*(\mu\, t)$ with $f_*(y) = y - (1 + x)\tanh(y)$. We thus get

$$\sqrt{\frac{2\,\Delta r_*}{\pi}} = \sqrt{\frac{2\,\rho''(t_*)}{\pi}} \underset{\epsilon \to 0}{\approx} 2N_*\sqrt{r_{max}\,\mu/\pi}\left(\frac{x}{1+x}\right)^{1/4} \underset{\substack{\epsilon \to 0 \\ 0.1 \le x}}{\approx} 2N_*\sqrt{r_{max}\,\mu/\pi}\,. \tag{A20}$$

***DN + SV* rescue:** in the scenario where the population is initially at mutation-selection balance, we have, when $\epsilon \to 0$, $\rho(t) \approx \theta/\epsilon\, f_*(\mu\, t)$ with $f_*(y) = y - (1 + x)\,(1 - e^{-2y})/2$. We thus get

$$\sqrt{\frac{2\,\Delta r_*}{\pi}} = \sqrt{\frac{2\,\rho''(t_*)}{\pi}} \underset{\epsilon \to 0}{\approx} 2N_*\sqrt{r_{max}\,\mu/\pi}\,. \tag{A21}$$

We see that the rate of ER is proportional to the minimal population size, across stress levels x, as the coefficient $\sqrt{2\,\Delta r_*/\pi}$ is independent of x. We further find that, surprisingly, this coefficient

is the same in the presence or absence of standing genetic variation. This means that all the difference in ER probability between these two scenarios is entirely due to differences in the minimal size reached by the population, in the deterministic trajectory.

Bibliography :

Bansaye V., Simatos F., 2015 On the scaling limits of Galton-Watson processes in varying environments. Electron. J. Probab. 20.

Feller W., others, 1951 *Diffusion processes in genetics*. University of California Press Berkeley, Calif.

Lambert A., 2008 Population Dynamics and Random Genealogies. Stoch. Models 24: 45–163.

Martin G., Roques L., 2016 The Non-stationary Dynamics of Fitness Distributions: Asexual Model with Epistasis and Standing Variation. Genetics: genetics.116.187385.

CHAPTER III

Theoretical and empirical perspectives

I. Evolutionary rescue in a spatially heterogeneous environment: SSWM regime

When a population faces a stressing environmental change in its current habitat, it can adapt to these new conditions, as has been addressed in chapters I and II, but it may also disperse to other potentially more suitable habitats. In the first two chapters, habitats were considered homogeneous in space and time. Here, we investigate the phenomenon of evolutionary rescue in a spatially heterogeneous habitat, where a population may be rescued in its local deme or disperse to another habitat. Multiple papers have considered dispersion within ER models (Pease *et al.* 1989; Duputié *et al.* 2012; Aguilée *et al.* 2016). However, none of them tackled the dependence between the distribution of mutations effects and the heterogeneity of the environment. The goal of this part I is to establish a 'proof of concept' that the results of the first chapter can be extended to a two deme system, connected by migration, with heterogeneous conditions in each deme..

Evolutionary rescue and dispersion in an heterogeneous environment with two demes

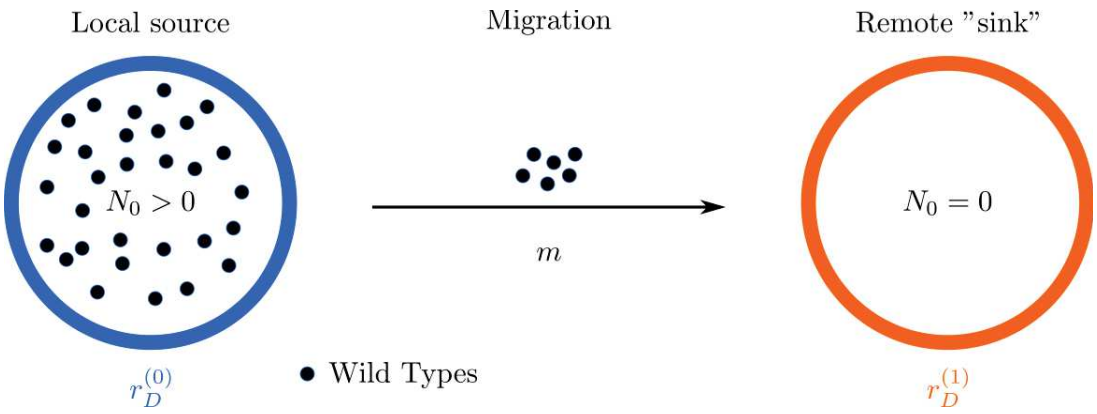

Figure 1: *Schematic illustration of the model of dispersion. Deme "0" denoted "local source" (blue circle) contains the isogenic population of size N_0 (black dots represent the individuals of the population) and migrants can disperse to deme "1" denoted "remote sink" (orange circle) at a rate m per capita per unit time.*

In the following, we only consider the scenario of an isogenic population from chapter I. However, the results from this chapter suggest a straightforward generalization to include

standing variance for a population at mutation-selection balance before the onset of stress. As in chapter I and II we use the FGM to link environmental conditions (level(s) of stress) and evolutionary potentiality of the population (rate and effects of resistance mutations). The basic assumptions of the model are the same as in chapters I and II (no density or frequency dependence), and we consider the SSWM regime (as in Chapter I) where ER is expected to stem from single-step mutations from the ancestral clone.

We consider a spatial configuration with two demes illustrated in **Figure 1**. In the classic source-sink framework, a 'source' (with positive growth rate) is connected to a 'sink' (with negative growth rate), which is initially empty. The problem is then no longer of the probability of ER but of the waiting time to it happening, which we will tackle briefly in a section below. Here on the contrary, we are interested in a 'sink-sink' system similar to the one developed in Débarre et al. (2013), extended to arbitrarily many dimensions, where ER is not certain. We consider the process of invasion of an initially empty deme ("1" or "remote sink") undergoing stressful conditions, by a neighboring deme ("0" or "local source") that is itself facing extinction risk and can send migrants to the "remote sink" (no reverse migration). At the onset of stress (time $t = 0$), the remote sink is empty and the local source population has size $N_0 > 0$, and the environments change to stressing conditions in both demes but with different levels of stress. Such scenario aims to capture a context where stress is heterogeneous in space. The approach proposed could a priori easily be extended to other initial conditions than the one chosen here, for the sake of illustration (empty remote sink, population initially clonal). The main goal here is to study the effect of "refuges", where stress is milder, on the likelihood and location of ER.

The change of environmental conditions shift the optimum, as explained in chapter I, leading to a fitness distance between the new optimum and the current genotype of the population in deme "0" of $r_{max} + r_D^{(0)}$, with r_{max} the maximal growth rate reachable under the new environmental conditions and $r_D^{(0)}$ the decay rate of the population in deme "0". The environmental change also affects deme "1", in which the fitness distance for a potential wild type migrant from the population of deme "0" is $r_{max} + r_D^{(1)}$. Otherwise, the two habitats impose the same fitness peak height r_{max}, and the same mutational parameters (U and λ) on the wild type genotype.

ER dynamics in deme "0"

The population is decaying in deme "0" and individuals may migrate from deme "0" to deme "1" at a rate m per individual per unit time. Emigration from the local source to the remote sink increases the decay rate in deme "0" to $r_D^{(0)} + m$. Hence, the decay rate of the population ($r_D^{(0)} + m$) and the evolutionary stress ($r_D^{(0)}$) are different in deme "0". Here we can directly import the model from chapter I (Eq.[7]) for the extinction probability in deme "0":

$$P_E^{(0)} = \exp\left(-\frac{N_0 r_D^{(0)}}{r_D^{(0)} + m}\, U\, g\left(\alpha\left(r_D^{(0)}\right)\right)\right)$$
$$g(\alpha) = \frac{e^{-1/2-\alpha}}{\sqrt{2(1+\alpha)\,\alpha}} \qquad . \qquad [1]$$
$$\alpha(r_D) = 1\Big/\sqrt{1 + \frac{8}{\Psi_D^2(r_D)\; r_{max}/\lambda}} \;\; where \;\; \Psi_D(r_D) = 2\left(\sqrt{1+\frac{r_D}{r_{max}}} - 1\right)$$

ER dynamics in deme "1"

We need only to compute the rate of ER in deme "1", conditional on extinction in deme "0". The number of migrants dispersing to deme "1" depends on the dynamics of the population size N_t^0 in deme "0", which then approximately follows a deterministic exponential decay at rate $r_D^{(0)} + m$. The total number of migrants dispersing to deme "1" over the course to extinction of deme "0" is Poisson with rate Λ (see the supplementary material of Martin *et al.* 2013 for the approximation), where

$$\Lambda = m \int_0^\infty N_t^{(0)}\, dt \underset{N_0>>1}{\approx} m \frac{N_0}{r_D^{(0)} + m}. \qquad [2]$$

We ignore polymorphism within the migrant pool from deme "0", assuming that all the migrants are wild-type genotypes from the initial isogenic population in deme "0" (with a growth rate $-r_D^{(1)}$ in deme "1"). Each individual migrant arrives in one copy and will produce a rescue with a given probability, which depends on the FGM and the stochastic demographic dynamics to extinction of this 'wild-type' migrant. Consider the probability that none of a total of K migrants, sent over the course to extinction of deme "0", mutates to a rescue mutant in deme "1". As lineages are evolutionarily and demographically independent, it is exactly the same as the probability of no ER from de novo mutations, in an isolated population, initially consisting of K wild-type genotypes. We may thus implement this probability directly from results in chapter I. The fully

stochastic treatment (accounting for stochasticity in the decay dynamics of the K lineages) can be derived explicitly from Eq.[S1.5] in (Martin et al. 2013). However, with $K = O(\Lambda)$ large enough and U small enough (which is required for the SSWM regime used here), we can ignore this stochasticity (Martin *et al.* 2013), just as we did in chapter I for large N_0 and small U. Overall, the probability of extinction in deme "1", given a total number of migrants K from deme "0", and given extinction in deme "0" is approximately:

$$P_{E|Ext(0)}^{(1)}|K \underset{\substack{u_* \ll 1 \\ K \gg 1}}{\approx} \exp(-K\, u_*), \qquad [3]$$

with $u_* = U\, g\left(\alpha\left(r_D^{(1)}\right)\right)$ the mutation rate to rescue in deme "1", per migrant arriving in the deme, for wild-type migrant genotypes with decay rate $r_D^{(1)}$. Integrating over the Poisson distribution of the total number of migrants $K \sim \mathcal{P}(\Lambda)$, we get the overall probability of extinction in deme "1", in the face of migration from "doomed" deme "0":

$$P_{E|Ext(0)}^{(1)} \underset{\substack{u_* \ll 1 \\ \Lambda \gg 1}}{\approx} \exp\left(-\Lambda(1 - e^{-u_*})\right) \approx \exp(-\Lambda\, u_*)\,. \qquad [4]$$

ER probability over the two demes

We can now derive the overall evolutionary rescue probability which is 1 minus the probability that the population goes extinct in both demes:

$$\begin{aligned} P_R &= 1 - P_E^{(0)} P_{E|Ext(0)}^{(1)} \\ &\approx 1 - \exp\left(-\frac{N_0 U}{r_D^{(0)} + m}\left(m\, g\left(\alpha\left(r_D^{(1)}\right)\right) + r_D^{(0)}\, g\left(\alpha\left(r_D^{(0)}\right)\right)\right)\right) \end{aligned} \qquad [5]$$

In this model, the ER probability strongly depends on the three parameters m, $r_D^{(0)}$ and $r_D^{(1)}$. It can be checked that the result is consistent in both extremes of the migration rate. When $m \ll r_D^{(0)}$ we retrieve the ER probability in deme "0", if it were isolated (ER rate $N_0\, U\, g(\alpha(r_D^{(0)}))$). As $m \gg r_D^{(0)}$ we retrieve the ER rate of an isolated deme "1" of initial size N_0 (ER rate $N_0\, U\, g(\alpha(r_D^{(1)}))$), as expected if all individuals instantaneously migrate to this deme. When $r_D^{(0)} = r_D^{(1)}$, there is no heterogeneity and migration has no effect (ER rate $N_0\, U\, g(\alpha(r_D^{(0)}))$), as expected too.

We tested the predictions of the analytical model against individual-based simulations using the same algorithm as in Chapter I (**Figure 2**), to which we added migration to a second deme, with different environmental conditions. Note that, as we use a discrete time algorithm, the migration process was simulated by drawing, each generation, a binomial sample of the current population of size $N_t^{(0)}$ in deme "0" with probability p_m per individual, to form the migrant pool, if any. The corresponding migration rate of the continuous time approximation is then set to $m = -\log(1 - p_m)$, to capture the resulting decay dynamics in deme "0". This continuous time approximation, for demography, was checked (see below).

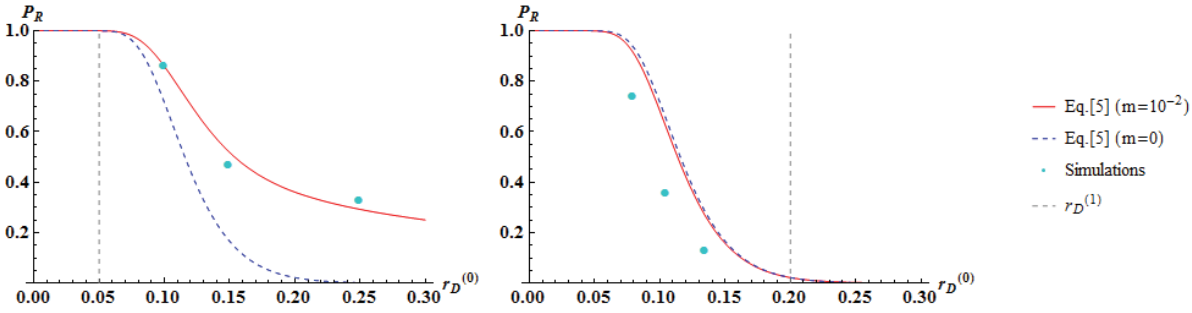

Figure 2: *Effect of stress on ER probability from Eq.[5] and results from 100 simulations with* $r_D^{(0)} > r_D^{(1)}$ *(a) and* $r_D^{(0)} < r_D^{(1)}$ *(b). The red solid lines correspond to Eq.[5], the blue dashed lines to Eq.[5] with no migration and the dots to simulations. In panel (a)* $r_D^{(1)} = 0.2$ *and in panel (b)* $r_D^{(1)} = 0.05$*. In both panel* $N_0 = 10^5$, $\lambda = 5.10^{-3}$, $U = 2.10^{-4}$ *and* $m = 0.01$.

When the stress is higher in deme "0" than in deme "1" ($r_D^{(0)} > r_D^{(1)}$), the model is fairly accurate (left panel), and captures the effect of migration on the ER process in the heterogeneous sink-sink system. However, when the stress is higher in deme "1" than in deme "0" ($r_D^{(0)} < r_D^{(1)}$), the model overestimates the ER probability (right panel). This seems to stem from the model underestimating the detrimental effect of migration in this case. The prediction with $m = 0$ (dashed blue line) is above that with migration (as indeed qualitatively expected), but too slightly so: simulations show a larger lowering of ER probabilities by migration. The discrepancies between the model and the simulations are discussed in the "limits and perspectives" section bellow.

The gain and cost of dispersion in ER

In these preliminary results, the dependence of ER probability on the parameters has only been checked numerically. The probability of ER decreases with increasing stress via $r_D^{(0)}$ or via $r_D^{(1)}$ as expected from Chapter I. On the contrary, the impact of dispersion on the ER probability is opposite in both demes (**Figure 3b**) and depends for deme "1", on the difference between $r_D^{(0)}$ and $r_D^{(1)}$ as shown in (**Figure 3**). As expected, the ER probability of the overall population (colored solid lines in **Figure 3**) is equal to the ER probability of the population in deme "0" (black dashed lines in **Figure 3**) for small migration rates ($m << 1$) and to the ER probability of the population in deme "1" (colored dashed lines in **Figure 3**) for large migration rates ($m >> 1$). For intermediate migration rates, when the migration rate increases, the gain or the cost of dispersion in ER depends on the sign of the difference between $r_D^{(0)}$ and $r_D^{(1)}$ (**Figure 3a**). When $r_D^{(0)} < r_D^{(1)}$, migrants arriving in deme "1" have a lower ER probability than in deme "0", therefore the ER probability of a dispersing population (red and purple solid lines **Figure 3a**) becomes larger than the ER probability of a non-dispersing one (horizontal dashed line **Figure 3a**). On the contrary, when $r_D^{(0)} > r_D^{(1)}$ the rescue probability is increased by the dispersion (blue and yellow solid lines **Figure 3a**) because migrants have higher ER probability in deme "1" than in deme "0". Finally, the same ER probability is retrieved for both dispersing (green solid line **Figure 3a**) and non-dispersing (black dashed line **Figure 3**) populations when the two demes are identical ($r_D^{(0)} = r_D^{(1)}$), as expected.

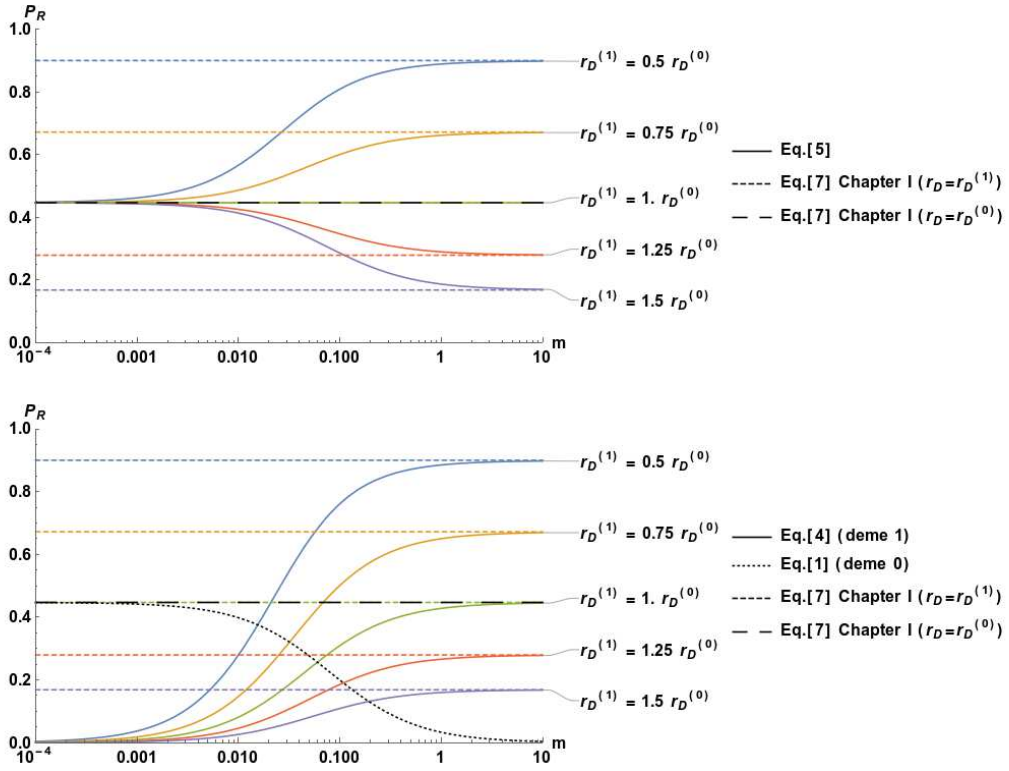

Figure 3: *Dependence of the ER probability on the migration rate over the two demes (a) or for each deme (b). In both panels the horizontal black dashed line correspond to Eq.[7] of Chapter I with* $r_D = r_D^{(0)}$ *(Eq.[5] without migration) and the colored dashed lines correspond to Eq.[7] of Chapter I with* $r_D = r_D^{(1)}$*, both are used as a reference for comparisons. In panel (a), the colored solid lines correspond to the ER probability of Eq.[5] for different stress levels in deme "1" (* $r_D^{(1)}$*). In panel (b), the colored solid lines correspond to the ER probability of Eq.[4] in deme "1" for different stress levels in deme "1" (* $r_D^{(1)}$*) and the dotted line to the ER probability of Eq.**[1]** in deme "0". The parameters in both panels are* $N_0 = 10^4$*,* $U = 2.10^{-4}$*,* $r_{max} = 0.5$*,* $\lambda = 5.10^{-3}$ *and* $r_D^{(0)} = 0.06$*.*

As a biological illustration, consider a treatment against a pathogen applied in the circulating system of the host. The concentration is assumed to be maintained constant over time by the treatment (a rough approximation arguably) and a difference in concentration may appear between the main circulating system (deme "0") and an organ ("deme 1"). Hence, the pathogen may invade and be sheltered in an organ with a lower concentration (case $r_D^{(0)} > r_D^{(1)}$), after invading its host via the circulating system initially.

Limits and perspectives

Our model has the same limitations as the model in chapter I for the mutation regime, the demography and the approximations used to derive the ER probability. It seems to be sufficient

to accurately predict the ER probability profile across stress levels, when deme "1" undergoes milder stress ($r_D^{(0)} > r_D^{(1)}$, left panel in **Figure 2**). It does capture the effect of migration, in increasing the ER profile compared to the no migration case (dashed blue line). This is encouraging but, as shown in right panel **Figure 2,** the model does not predict the observed ER probability when stress is harsher in deme "1" than in deme "0" ($r_D^{(0)} < r_D^{(1)}$). Initially, we thought that the model would fail in the opposite scenario (when $r_D^{(0)} > r_D^{(1)}$). Indeed, one strong hypothesis of our model is that all migrants are wild types from the isogenic population. This hypothesis is based on the low mutation rate regime, in which the few mutations that may appear and spread in the population will be rescuers in the deme "0", in which case the rescue in deme "1" is not of interest any more. However if the stress is too low in deme "1" in comparison to deme "0", numerous mutants that are sub-critical (i.e. have negative growth rate) or critical (i.e. have null growth rate) in deme "0" can be resistant (or super-critical, with positive growth rate) in deme "1". This would mean we are now neglecting the contribution from mutants that are only transiently subcritical, in the presence of migration. However, this approximation would lower the ER probability of the model compared to simulations, and the discrepancy should be visible only when stress is milder in deme "1", while neither effects are seen in **Figure 2**. That this heuristic approximation is accurate was also confirmed by forcing the migrant pool to consist only of wild types in the simulations. The results showed no discrepancy with the exact simulations where migrants are randomly sampled from the deme "0", whatever their genotype. To better understand the origin of the discrepancies, we tested the accuracy of the demographic model alone, namely the continuous time approximation for the discrete time simulation scheme. We compared simulations at $U = 0$ with the following predicted dynamics of population size in both demes:

$$N_t^{(0)} = \exp\left(-t\ \left(m + r_D^{(0)}\right)\right) N_0$$
$$N_t^{(1)} = \frac{\exp\left(-t\ r_D^{(1)}\right) m\, N_0}{m + r_D^{(0)} - r_D^{(1)}} \left(1 - \exp\left(-t\ \left(m + r_D^{(0)} + r_D^{(1)}\right)\right)\right) \quad [6]$$

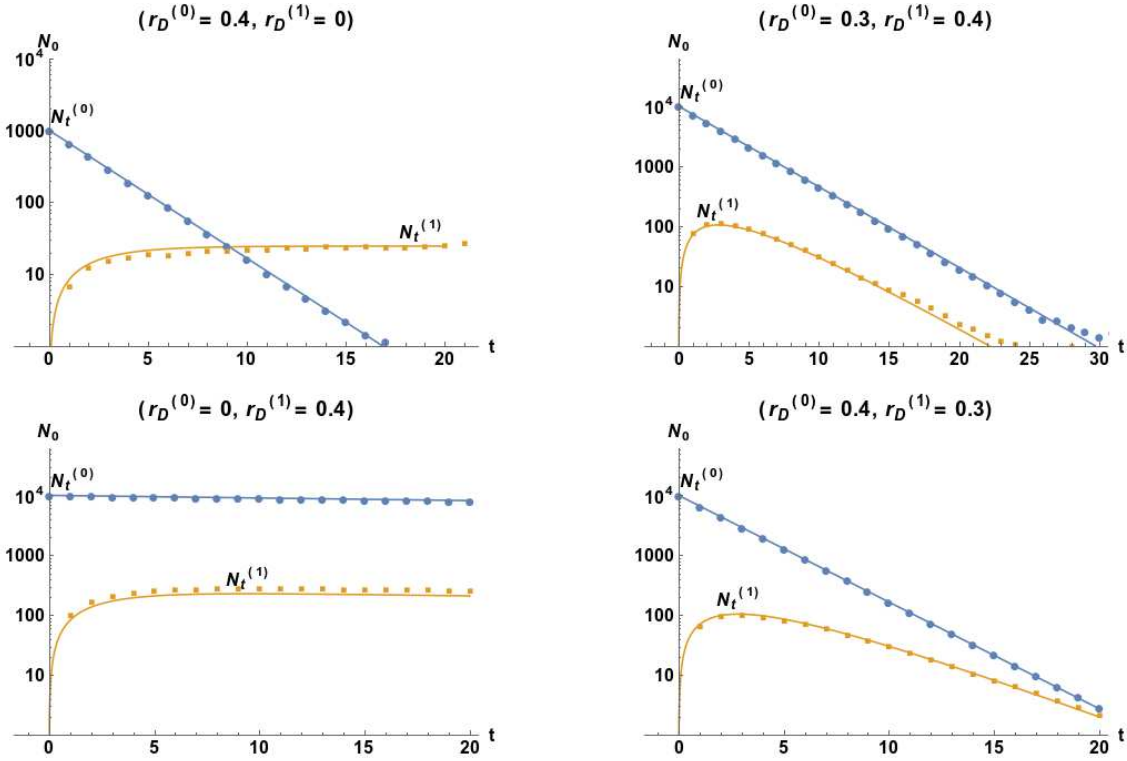

Figure 4: *Demographic dynamics in deme 0 (blue) and deme 1 (orange) from Eq.[6] (solid lines) and the simulations (dots and squares). The four panels represent different scenarios with stress higher or lower in deme 0 in comparison to deme 1. The dynamics are simulated with* $U = 0$.

The simulated demography are accurately predicted by the model in both demes as shown in **Figure 4**, whatever the sign of the difference between $r_D^{(0)}$ and $r_D^{(1)}$. Therefore, the problem does not stem from the difference between the continuous time model and discrete time simulations a priori. As to now, we did not find the reason for the discrepancies in **Figure 2** right panel, but these are preliminary results that will require further scrutiny.

II. Perspectives in the WSSM regime

General strategy for extensions of the model from chapter II

The model in chapter II considers a deterministic evolutionary model coupled with a stochastic demographic model. The demographic model uses the trajectory of the mean growth rate predicted from a deterministic evolutionary model. A priori, any evolutionary model providing a deterministic dynamic for the mean growth rate, can be used in the same framework, in the WSSM regime. A simple example for the application of this strategy, is to derive explicit ER probabilities in the model of Gomulkiewicz and Holt (1995), with polygenic autosomal inheritance in an FGM-like fitness landscape. The mean fitness dynamics provided in Eq.[5] can readily be inserted into our Eq.[6] chapter II or simpler expressions can be derived using the Laplace approximations (e.g. Eq. [9] chapter II). This would extend the results of this previous study, retrieving explicit ER probabilities and extinction time distributions for a population under polygenic autosomal inheritance (freely recombining genomes), provided a constant variance in phenotypes can be assumed over the timescale of ER (infinitesimal model assumed in this model). More generally, the strategy in chapter II can be applied to any scenario where deterministic evolutionary models provide explicit mean fitness dynamics. It is critical to have full trajectories and especially out of equilibrium, which greatly reduces the span of evolutionary models that can be implemented.

Evolutionary rescue in time varying environment: Successive antibiotic treatments

Using the time dynamics of the model from chapter II, we can treat scenarios where stress levels vary in time. For example, we can consider the following scenario: a first antibiotic is applied on the population at $t = 0$, then this antibiotic is abandoned and instantaneously shifted to another one, at some $t = t_1$, which is applied until the end of the process investigated. The population thus undergoes two successive abrupt shifts, and the phenotypic distribution at $t = t_1$ (initial standing variance for the second phase) depends on the evolutionary dynamics in the first environment up to this time t_1. In this scenario, we may consider any effect of the environmental changes on the landscape (optimum position, fitness peak height, mutation rate and effect), as we did in chapter II. The key insight lies in the fact that, in the WSSM regime, the distribution of phenotypes is Gaussian at all times, after a single abrupt change, and the dynamics

of its mean (position) and variance are given in Martin and Roques (2016), for the isotropic FGM. From the position of each of the two optima (each antibiotic) in the phenotypic space, the dynamics of mean fitness over the two successive phases should be readily obtained from Martin and Roques (2016). As the model can account for change in mutational parameters (rate and effect) and is independent of fitness peak height (relative fitness dynamics), changes in these factors should also be amenable to analytical treatment. From such model, it could be possible to optimize the timing of both treatments to maximize the extinction probability, depending on the relative positions of the optimums of each environment in the landscape.

This extension can only be applied in the WSSM regime, and in the case of successive treatments (e.g. Yen and Papin 2017). The analysis of simultaneous combinations of treatments would require further work, to properly characterize how combinations of stressors translate into landscape properties, and test the assumptions based on observed patterns of bivariate decay rate in the presence of two antibiotics (Chevereau and Bollenbach 2015).

Evolutionary rescue in a spatially heterogeneous environment: WSSM regime

Here we present collaborative and early results in the WSSM regime of the second chapter, on the ER process in spatially heterogeneous environments. First, we briefly present the results obtained in collaboration with Florian Lavigne (Master's project of spring 2017) on the scenario of immigration in a sink from a source with a constant population size. Then we give some preliminary approaches to extend the 'sink-sink' model described in the first part of this chapter, to the WSSM regime instead of the SSWM.

Source-sink scenario in a deterministic WSSMSM limit (Weak Selection Strong Mutation Strong Migration):

The scenario of immigration in a sink from a source is commonly considered to study the impact of migration on adaptation and rescue (e.g. Holt and Gomulkiewicz 1997; Holt *et al.* 2003). It considers migration from an unlimited source of migrants on adaptation in a stressful environment (sink). In the case described here, we started by considering a monomorphic source which sends maladapted migrants to the sink. This process has been implemented using the model from Martin and Roques (2016) with an input of migrants added from the source, which takes a simple form here as we ignore polymorphism within the source. In this case, the ER

probability is obviously 1 because the source population is stable and will always send migrants. However, the dynamic of the population in the sink is of interest, especially the time taken for the sink to become a source, i.e. for its mean growth rate to become positive. This issue was tackled in the context of a fully deterministic model. The main result is that the analytic, deterministic model captures the patterns observed in simulations when migration is sufficiently high, and in the parameter range where the WSSM is valid (see chapter II), a "WSSMSM" regime. With lower migration rates, the approach only qualitatively captures the average behavior of replicate stochastic simulations. The main conclusion from this study so far is that, for a harsh sink, the sink population size undergoes a two-step dynamics. First, the build-up of an equilibrium between migration and decay leads the population size to a transient plateau at $m\ N_0/r_D$ (with N_0 the source population size, m the migration rate and r_D the decay rate in the sink). Then, after a predictable waiting time, the sink shows a sudden burst in population size and becomes a 'source'. These results are based on a simple extension of the deterministic evolutionary model used in chapter II, to include migration. The same extension could be used to analyze the sink-sink ER process, in the WSSM regime. However, some complications will have to be accounted for, as explained in the following section.

"Sink-sink" scenario:

The sink-sink scenario treated in part 1 of this chapter, for the SSWM regime, is more complex to implement in the WSSM regime of chapter II. Indeed, the WSSM regime implies that we can no longer neglect the build-up of polymorphism in deme "0", on its course to extinction, as we did for the SSWM regime. The distribution of phenotypes and fitness have now to be modelled dynamically in two different environments. As shown in Débarre et al. (2013) the dynamics of this distribution is hard to follow analytically from pure moment equations, because these do not form a closed system (the dynamic of each moment depends on the moment of superior order). Two solutions are possible: (i) using moment closure approximation to close the system (e.g. in Débarre et al. (2013) for the closed forms) or (ii) extending the approach in Martin and Roques (2016) to model the full bivariate distribution of fitnesses, in each environment, dynamically. This latter option should a priori be feasible (and would be free of any Gaussian / moment closure approximation). Indeed, the main challenge will be to model the effect of mutation on the generating function of the joint fitness distribution in both environments, which is readily available from Martin and Lenormand (2015). This is necessary to model how migrants,

after their ancestors adapted for some time in deme “0” will fare in deme “1”. Moreover, another challenge is that the stochasticity of the demographic model has to be taken into account in both environments, with migration potentially creating mutual dependence (into a two-type inhomogeneous Feller process). Therefore, this approach is less straightforward than the scenario of source-sink described above.

III. Test of the models on experimental data

One of the aim of this thesis was to give quantitative and empirically testable predictions on the probability of ER and associated observable dynamics, across contexts (environments, genetic backgrounds etc.). The models of chapters I and II partially fulfill this goal. Indeed both models provide fairly accurate and analytically explicit predictions on the ER probability (thus enabling Maximum Likelihood analysis), under the FGM (an empirically 'sound' null model a priori), they cover complementary ranges of possible parameters, and are expressed in terms of a priori measurable quantities. However, empirical tests of these predictions will still be a challenging endeavor. Ideally, we may test them by directly comparing results of the models to ER data (e.g. observed extinction probabilities across stress levels), using estimated parameters from independent experiments. Alternatively, a less powerful but easier test is to simply evaluate whether observed patterns, in some relevant ER datasets, are consistent with (well fitted by) the proposed theory. In the following, we describe the available data in the literature, present different methods to estimate the missing parameters and then describe a method to fit the data with a limited number of necessary parameters.

Available data in the literature

In the literature, the main datasets available to test our models relate to antibiotic treatments on pathogens. In this context, the experiments which test the bactericidal potency of an antibiotic often use the method denoted "concentration-killing curves" (hereafter CKC) (Drlica 2003). In the method of CKC, bacterial populations are inoculated onto a series of agar medium containing a given concentration of drug and incubated. The number of viable bacteria from the initial inoculum that survive over a range of drug concentrations is then counted for each concentration and give a relation between the number of CFU per plate and the concentration of the drug (see Drlica (2003) and Liu *et al.* (2004) for more details). In our models, the number of recovered cells is a proxy for the rate of rescue and thus can be directly compared to the prediction. A full fluctuation test (Luria and Delbrück 1943) across doses would be preferable to avoid contingency of the results on the mutants randomly arising in the single preculture used for CKC, but such data are very scarce and heavy to produce (see Harmand *et al.* 2016). However, in most of these datasets, the initial population size is the only parameter available, thus yielding a direct test of our model on these data difficult. Moreover, the stress intensity is measured via the concentration

of the drug which has to be related to the biological parameters of the FGM to be used in the model. In the next section we detail some methods to estimate the missing parameters from these datasets.

Estimation of the basic parameters

The parameters of the models from both chapter I and II are N_0, U, λ, θ, r_D and r_{max}. The population size N_0 is the easiest parameter to obtain and is determined by each dataset. The other parameters are more challenging to get from the literature and can also potentially change between environments (i.e. between concentrations and between drugs). The mutation rate U, the selective intensity λ and the dimensionality of the phenotypic landscape θ can be estimated in a given environment using a combination of mutation accumulation experiments (reviewed in e.g. Bataillon 2000) (estimation of U and λ) and a fit on a distribution of single mutation effects on fitness (estimation of θ and λ, Martin and Lenormand 2006; Perfeito *et al.* 2014). U and θ may be less prone to vary between environments (Martin and Lenormand 2006 between stress), and our predictions do not depend on θ for small θ. However, λ has been observed to change between concentrations of an antibiotic, based on indirect measurements in strains evolved at different doses in Harmand et al. (2016). The maximal growth rate r_{max} is the most difficult parameter to estimate because a long-term adaptation experiment is needed for the population to reach an equilibrium state at the phenotypic optimum where r_{max} can be estimated. Thus, estimating this parameter in each concentrations represents a tremendous amount of experimental work.

The last parameter to estimate is the decay rate r_D. In the pharmacodynamic literature we can find measurements of decay rates against drug concentrations via "time-kill-curves" (hereafter TKC). However, unfortunately we didn't find any study with both CKC and TKC in the same strain and culture conditions. Several TKC studies, however, do point to a predictable form of the relationship between decay rates to concentrations of antibiotics, modeled by pharmacodynamic functions that gave good fit to observations. Regoes et al. (2004) derives and tests pharmacodynamic functions using Hill-functions which take the form :

$$r_D = r_{\max} - \frac{(r_{\max} - \psi_{\min})\left(\frac{c}{MIC}\right)^{\kappa}}{\left(\frac{c}{MIC}\right)^{\kappa} - \psi_{\min}/r_{\max}}, \qquad [12]$$

where c is the concentration of the drug, MIC is the minimum inhibitory concentration corresponding to the concentration where the growth rate is zero, $|\psi_{\min}|$ is the maximal decay rate that can be imposed by the drug and κ is the parameter corresponding to the "slope" of the Hill-function. Yet, implementing this function in our test adds a lot of parameters to fit, if they are not given for the species, strain, culture conditions in which the ER data is produced. However it is possible to simplify this relationship by considering the scaled decay rate $y_D = r_D/r_{max}$, the scaled concentration $x = c/MIC$ (commonly used in CKC where MIC is always measured) and the composite parameter $\epsilon = |\psi_{\min}|/r_{\max}$. Expressing Eq.[12] with y_D thus leads to:

$$y_D = \phi(x, \kappa, \epsilon) = \frac{1 - x^{\kappa}}{1 + \epsilon\, x^{\kappa}}. \qquad [13]$$

Under the approximation that U, λ, θ and r_{max} are constant across drug doses (namely that various concentrations only change the position of the optimum, see chapter I), we can implement the function from Eq.[13] in the model of chapter I in order to fit data from CKC experiment (ER rate across doses). An example of such a fit is detailed in the following section.

Example of fit of ER probability from concentration-killing-curves under the SSWM regime

In CKC data, the number of recovered cells is a proxy for the rate of ER, which is equal to $R = \log(1/(1 - P_R))$ in our models. The data considered here use bacteria with relatively low mutation rate that should be fitted by the model from chapter I in the low mutation rate regime. However we can neither directly apply the rate of rescue from *de* novo mutations nor de rate of rescue from both pre-existant mutant (at mutation-selection balance) and *de* novo mutation derived in chapter I. Indeed the population used in CKC experiments are grown from an isogenic population but mutants may appear during the exponential growth in the non-stressful environment before plating, and they may also appear during the decay of the inoculated population on the plate. To model standing genetic variance, we use classic and basic fluctuation test theory (which ignores the possibility of mutations or any birth event after plating). We ignore the cost c of resistance mutations before plating, which may be reasonable if $r_{max} \gg c$, as most mutants arise late during the growth phase and their cost has limited time to affect their relative

frequencies. We assume that the maximal growth rate in the non-stressful environment is the same as in the stressful environment and that the initial population size from which this pre-culture is started is negligible in comparison to its final size at plating, N_0 (the latter is typically true in these experiments). Using these assumptions, the average number of resistant mutants that will appear during the pre-culture's exponential growth and will not be stochastically lost after the onset of stress is $N_0\ U\ y_D\ g(\alpha)$. Similarly the average number of mutants that may appear de novo on the agar plate (during the decay under antibiotic pressure) is $N_0\ U\ g(\alpha)$. Thus, using the result from Eq.[7] in chapter I, the total rate of ER is:

$$\begin{aligned} R(y_D,\rho_{max}) &= N_0\ U\ g\big(\alpha(y_D,\rho_{max})\big)(1+y_D) \\ g(\alpha) &= \frac{e^{-1/2-\alpha}}{\sqrt{2(1+\alpha)}\,\alpha} \\ \alpha(y_D,\rho_{max}) &= \left(\sqrt{1+\frac{2}{\left(\sqrt{1+y_D}-1\right)^2\rho_{\max}}}-1\right)^{-1} \end{aligned} \quad . \qquad [14]$$

where $\rho_{max} = r_{max}/\lambda$ (see chapter I). This rate of rescue contains 3 different composite parameters (N_0U, y_D and ρ_{max}), the pharmacodynamic function in eq.[8] adds two parameters and some of these parameters cannot be distinguished in a fit. Thus, such a function cannot be readily fitted on the data. However, we can reduce the number of parameters by rescaling the rate of rescue and the concentration of antibiotics. The rate of rescue is scaled by the maximal rate of rescue from the experiment $R_{max} = R(y_{min},\rho_{max})$ observed at the lowest concentration analyzed (where $y_D = y_{min}$, the smallest scaled decay rate corresponding to the minimal concentration tested in the series). This smallest decay rate must be slightly above 0, which is the decay rate at the MIC ($y_D = 0$). Therefore, we know that the lowest scaled concentration analyzed, $x_{min} = c_{min}/MIC$, is slightly above 1 ($x_{min} = O(1)$). We then scale concentrations by this lowest concentration, thus defining $u = c/c_{min} = x/x_{min} = O(x)$. Overall we study the following relationship, which suppresses the parameter N_0U and provides a good guess for the parameter x_{min}:

$$Z(u) = \frac{R(y_D,\rho_{max})}{R(y_{min},\rho_{max})} = \frac{g(\alpha(y_D,\rho_{max}))\ (1+y_D)}{g(\alpha(y_{min},\rho_{max}))\ (1+y_{min})}\ , \qquad [15]$$

Where $y_D = \phi(u\ x_{min},\kappa,\epsilon)$ and $y_{min} = \phi(x_{min},\kappa,\epsilon)$, using the pharmacodynamic function $y_D = \phi(x,\kappa,\epsilon)$ of Eq.[13] to link y_D to the scaled concentration $u = c/c_{min} = x/x_{min}$. Both Z and u are

observables from experimental data, and are scaled which increases comparability between experiments. We then fit eq.[15] for $Z(u)$ to the scaled data, a function of $(\kappa, \epsilon, \rho_{max}, x_{min})$. With known values of ϵ and κ and x_{min} from a TKC for a given antibiotic, strain and culture medium, the relationship between Z and u can be fitted by a function of only one parameter: ρ_{max}.

We applied this method to data from Wetzstein (2005). In this assay, CKC gives the relationship between ER rate in *E.coli* strain ATCC 8739, incubated in 270ml flasks of casein-peptone soybean-peptone broth at 37°C, and various concentrations of the fluoroquinolone pradofloxacin (the scaled data correspond to blue points in **Figure 5**). The MIC is also reported in the study ($MIC = 0.015\ \mu g/ml$). No data is available for ciprofloxacin, apart from a MIC, which is very similar. The closest guess we found for the parameters of the pharmacodynamic function (κ, ϵ) for this antibiotic and strain, are given in Regoes et al. (2004) for the *E.coli* strain 08:K1:H7 against the fluoroquinolone ciprofloxacin, incubated in 50ml flasks of LB at 37°C. Therefore, the parameters for the pharmacodynamics function are those for a different strain, culture conditions and against a different fluoroquinolone drug. In spite of these clear limits, as shown by the **Figure 5A**, the fitting of the single parameter ρ_{max} allows to qualitatively capture the sharp log-log linear drop in ER rate Z with drug dose u, and even captures the overall shape of the relationship. The inferred value of $\hat{\rho}_{max} \approx 22$ seems consistent with the biological *a priori* that was used to derive the formula in chapter I ($\rho_{max} \gg 1$). **Figure 5B** shows a fit using arbitrary slightly different parameters for the pharmacodynamics function: a slightly larger ϵ and smaller κ. The resulting fit of eq.[15] is equally good, with a very different $\hat{\rho}_{max} \approx 64$. This shows that the fit itself may be insensitive to variations in the pharmacodynamic parameters. Therefore, it is critical to have access to reliable pharmacodynamic functions fitted on the same strain, conditions and antibiotics as the ones used to generate the CKC data. There is indeed a strong issue of identifiability of the parameters if we were to fit the pharmacodynamics parameters too.

Figure 5: *Scaled rate of rescue $Z = R/R_{max}$ of E.coli against the scaled concentration $u = c/c_{min}$ of pradofloxacin. Dots : rescaled data from Wetzstein (2005), lines:SSWM theory in eq.[15].*

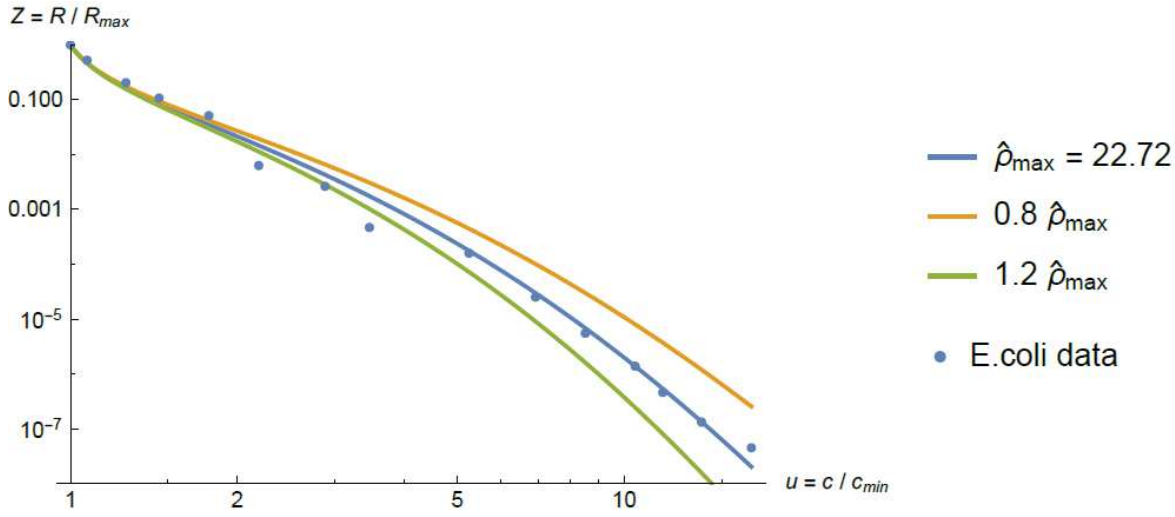

A) Fit of SSWM theory (blue line) using parameters from E.coli against ciprofloxacin in Regoes et al. (2005) ($\epsilon = 0.135, \kappa = 1.1, MIC = 0.015$) and $c_{min} = 0.0155$ (slightly above MIC). The orange and green lines show the same theory with 20% lower or higher ρ_{max}, respectively.

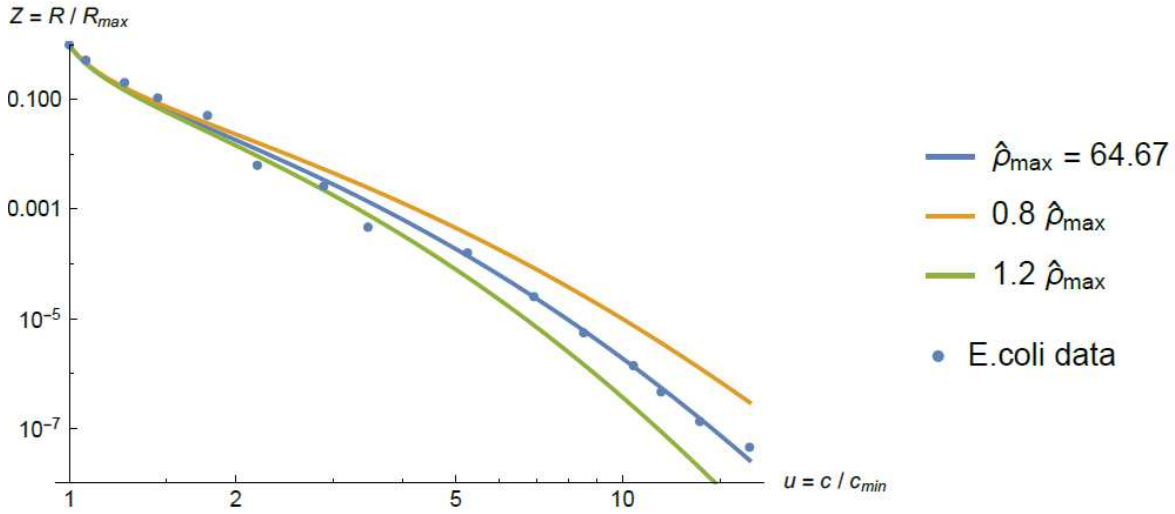

B) Same as **A)** with slightly different values of κ and ϵ assumed for the pharmacodynamics function ($\epsilon = 0.22, \kappa = 0.75$).

A similar approach can be used based on the WSSM theory of Chapter II. We expect the result to be less accurate, here, as *E.coli* is a priori not a highly mutating species, but this may be very dependent on the strain, mutator status etc. Here the theory is based on another simplified expression for the ER rate, obtained in the WSSM regime (eq.[6] in Chapter II):

$$\begin{aligned} R(y_D, \rho) &\propto \exp(-\rho\, g_{DN}(y_D)) \\ g_{DN}(y) &= \sqrt{y(1+y)} - \cosh^{-1}\left(\sqrt{1+y}\right) \end{aligned} \quad , \qquad [16]$$

where $\rho = r_{max}/\mu = r_{max}/\sqrt{U\,\lambda}$ is another parameter, that is similar but not equal to ρ_{max} in Eq.[15] and chapter I (scaled fitness peak height). As with the theory from chapter I, given known values of $(\kappa, \epsilon, x_{min})$ we can fit this theory to the same scaled dataset (R/R_{max} vs $u = c/c_{min}$), using the following theoretical relationship and a single unknown parameter ρ:

$$\begin{aligned} Z(u|\rho) &= \frac{R(y_D, \rho)}{R(y_{min}, \rho)} \\ &= \exp\left(-\rho\left(g_{DN}\left(\phi(u\, x_{min}, \kappa, \epsilon)\right) - g_{DN}\left(\phi(x_{min}, \kappa, \epsilon)\right)\right)\right) \end{aligned} \quad . \qquad [17]$$

The resulting fit of this theory, to the same dataset as in **Figure 5** and with the same assumed pharmacodynamic parameters, is given in **Figure 6**. Here too, a fit of the unique parameter ρ suffices to qualitatively capture the log-log decay of ER rate Z with antibtiotic concentration u, with values of $\hat{\rho} \gg 1$ consistent with the assumptions used to derive the simplified theory. However, as might have been expected for E.coli (at least for a non mutator strain), the fit is less good than that of the SSWM theory and does not capture the particular shape of the observed relationship as accurately.

Figure 6: *Scaled rate of rescue $Z = R/R_{max}$ of E.coli against the scaled concentration $u = c/c_{min}$ of pradofloxacin. Dots : rescaled data from Wetzstein (2005), lines: fit from eq.[17].*

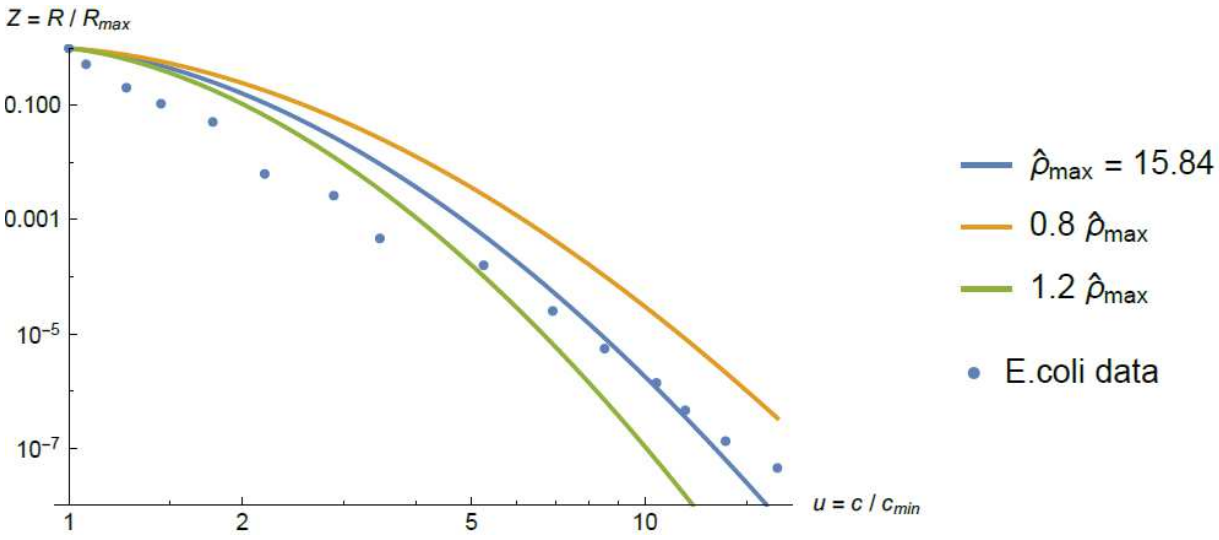

A) Same as **Figure 5A** with WSSM theory in eq.[17].

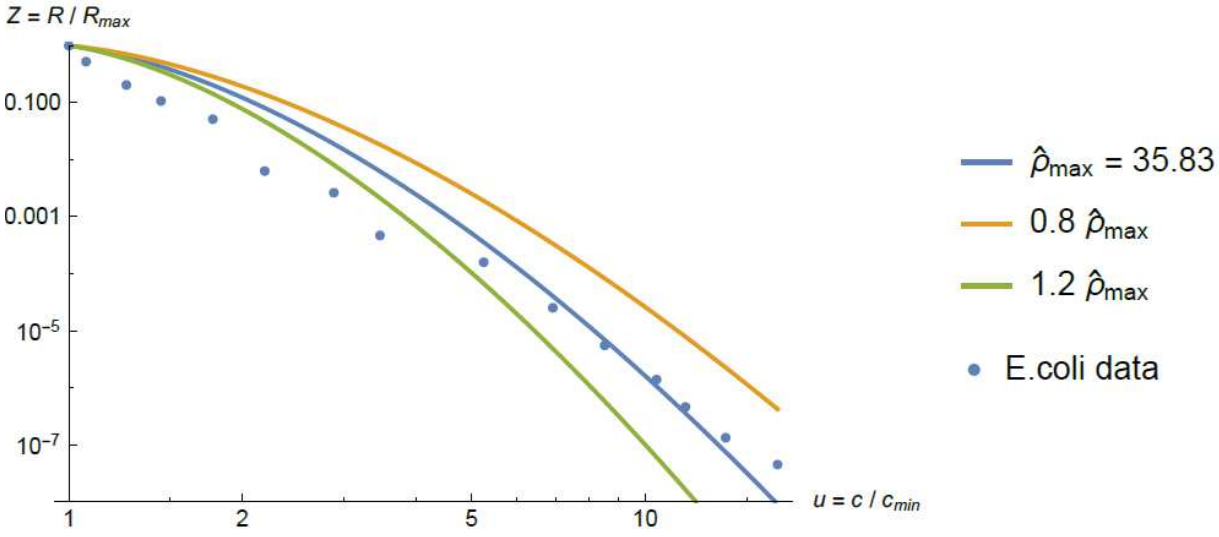

B) Same as **Figure 5B** with WSSM theory in eq.[17].

These results are obviously preliminary, and require further analysis, statistics etc. However, they do already give insights into the potential for the method and the theoretical ER models proposed here, when applied to CKC data. It also shows that statistical power is sufficient in this basic approach to compare and potentially reject alternative ER models (even between two regimes of the same landscape, SSWM vs WSSM). We also note that both models from chapter I and II capture the roughly log-log linear relationship observed between scaled ER rates Z and

drug concentrations u. Such log-log linearity is repeatably observed in CKC data, with even fairly stable log-log slopes in two pathogens with different fluoroquinolones (**Figure 7**).

The example given here considers that the parameters U, λ, θ and r_{max} are constant across drug doses which reduces the environmental changes to shifts of the position of the optimum in the phenotypic landscape. However, our model could also capture the effect on ER probability of changes in the height of the optimum or in selective intensity with the stress if we could find a relationship between the parameters λ and r_{max} and the changes in the drug concentrations.

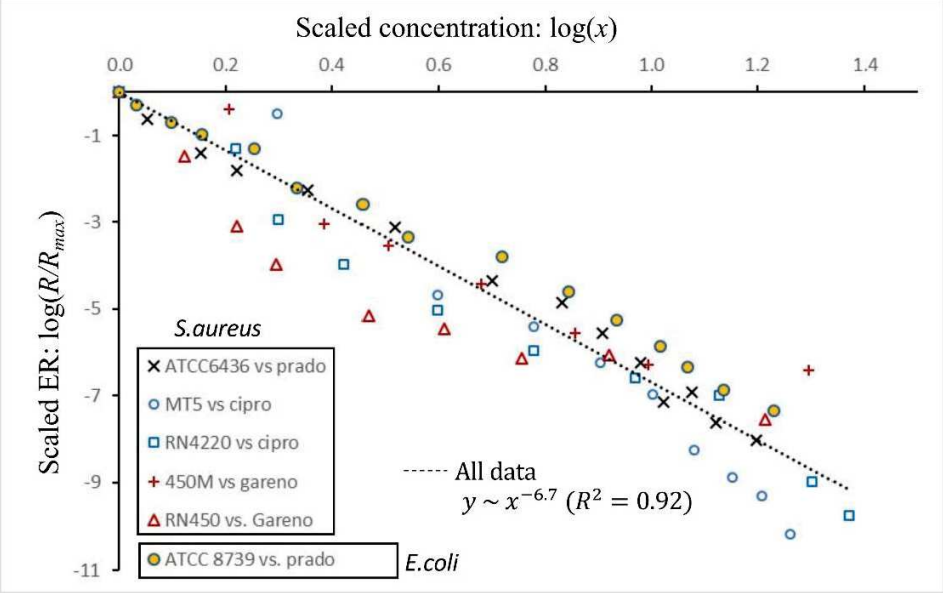

Figure 6: *Logarithm of the scaled rate of rescue R/R_{max} of E.coli and S.Aureus against the scaled concentration x of three fluoroquinolones (pradofloxacin, ciprofloxacin and garenofloxacin). All the symbols show the data from 4 publications (Dong et al. 1999; Xilin and Drlica 2002; Zhao et al. 2003; Wetzstein 2005) with the different combinations of pathogen strains and drugs. The dotted line give the linear fit on the whole points.*

Bibliography

Aguilée R., Raoul G., Rousset F., Ronce O., 2016 Pollen dispersal slows geographical range shift and accelerates ecological niche shift under climate change. Proc. Natl. Acad. Sci. 113: E5741–E5748.

Bataillon T., 2000 Estimation of spontaneous genome-wide mutation rate parameters: whither beneficial mutations? Heredity 84 (Pt 5): 497–501.

Chevereau G., Bollenbach T., 2015 Systematic discovery of drug interaction mechanisms. Mol. Syst. Biol. 11.

Débarre F., Ronce O., Gandon S., 2013 Quantifying the effects of migration and mutation on adaptation and demography in spatially heterogeneous environments. J. Evol. Biol. 26: 1185–1202.

Dong Y., Zhao X., Domagala J., Drlica K., 1999 Effect of Fluoroquinolone Concentration on Selection of Resistant Mutants of Mycobacterium bovis BCG andStaphylococcus aureus. Antimicrob. Agents Chemother. 43: 1756–1758.

Drlica K., 2003 The mutant selection window and antimicrobial resistance. J. Antimicrob. Chemother. 52: 11–17.

Duputié A., Massol F., Chuine I., Kirkpatrick M., Ronce O., 2012 How do genetic correlations affect species range shifts in a changing environment?: Multivariate adaptation and range shifts. Ecol. Lett. 15: 251–259.

Gomulkiewicz R., Holt R. D., 1995 When does Evolution by Natural Selection Prevent Extinction? Evolution 49: 201.

Harmand N., Gallet R., Jabbour-Zahab R., Martin G., Lenormand T., 2016 Fisher's geometrical model and the mutational patterns of antibiotic resistance across dose gradients. Evolution: n/a-n/a.

Holt R. D., Gomulkiewicz R., 1997 How Does Immigration Influence Local Adaptation? A Reexamination of a Familiar Paradigm. Am. Nat. 149: 563–572.

Holt R. D., Gomulkiewicz R., Barfield M., 2003 The phenomenology of niche evolution via quantitative traits in a "black-hole" sink. Proc. R. Soc. B Biol. Sci. 270: 215–224.

Liu Y. Q., Zhang Y. Z., Gao P. J., 2004 Novel Concentration-Killing Curve Method for Estimation of Bactericidal Potency of Antibiotics in an In Vitro Dynamic Model. Antimicrob. Agents Chemother. 48: 3884–3891.

Luria S. E., Delbrück M., 1943 Mutations of bacteria from virus sensitivity to virus resistance. Genetics 28: 491.

Martin G., Lenormand T., 2006 The Fitness Effect of Mutations Across Environments: A Survey in Light of Fitness Landscape Models. Evolution 60: 2413–2427.

Martin G., Aguilée R., Ramsayer J., Kaltz O., Ronce O., 2013 The probability of evolutionary rescue: towards a quantitative comparison between theory and evolution experiments. Phil Trans R Soc B 368: 20120088.

Martin G., Lenormand T., 2015 The fitness effect of mutations across environments: Fisher's geometrical model with multiple optima. Evolution 69: 1433–1447.

Martin G., Roques L., 2016 The Non-stationary Dynamics of Fitness Distributions: Asexual Model with Epistasis and Standing Variation. Genetics: genetics.116.187385.

Pease C. M., Lande R., Bull J. J., 1989 A Model of Population Growth, Dispersal and Evolution in a Changing Environment. Ecology 70: 1657–1664.

Perfeito L., Sousa A., Bataillon T., Gordo I., 2014 Rates of Fitness Decline and Rebound Suggest Pervasive Epistasis. Evolution 68: 150–162.

Regoes R. R., Wiuff C., Zappala R. M., Garner K. N., Baquero F., *et al.*, 2004 Pharmacodynamic Functions: a Multiparameter Approach to the Design of Antibiotic Treatment Regimens. Antimicrob. Agents Chemother. 48: 3670–3676.

Wetzstein H.-G., 2005 Comparative Mutant Prevention Concentrations of Pradofloxacin and Other Veterinary Fluoroquinolones Indicate Differing Potentials in Preventing Selection of Resistance. Antimicrob. Agents Chemother. 49: 4166–4173.

Xilin Z., Drlica K., 2002 Restricting the selection of antibiotic-resistant mutant bacteria: measurement and potential use of the mutant selection window. J. Infect. Dis. 185: 561–565.

Yen P., Papin J. A., 2017 History of antibiotic adaptation influences microbial evolutionary dynamics during subsequent treatment. PLOS Biol. 15: e2001586.

Zhao X., Eisner W., Perl-Rosenthal N., Kreiswirth B., Drlica K., 2003 Mutant Prevention Concentration of Garenoxacin (BMS-284756) for Ciprofloxacin-Susceptible or -Resistant Staphylococcus aureus. Antimicrob. Agents Chemother. 47: 1023–1027.

Discussion

Au cours de cette thèse, nous avons cherché à modéliser les dynamiques éco-évolutives de populations en environnement changeant. Les chapitres I et II de cette thèse donnent les clefs pour modéliser l'effet d'un changement environnemental abrupt sur la dynamique éco-évolutive de populations asexuées. L'intégration conjointe de l'adaptation, de la démographie et des effets des changements environnementaux au sein de ces modèles s'est révélée d'une complexité initialement sous-estimée et accrue par la recherche de réalisme et de précision dans les prédictions quantitatives. Cette thèse a aussi nécessité l'exploration extensive de l'espace des paramètres par simulations stochastiques, pour valider les approximations analytiques et caractériser leur domaine de validité. Le développement des modèles éco-évolutifs des chapitres I et II, autour du paysage adaptatif de Fisher, rejoint l'objectif de réalisme en intégrant un lien entre les différents environnements considérés et les capacités évolutives et démographiques des populations, dans le cadre d'un modèle ayant reçu un niveau substantiel de test expérimental. Plus particulièrement, le modèle de Fisher nous a permis d'intégrer un processus de mutation explicite, multi-allèles, épistatique et environnement-dépendant, dans les modèles de sauvetage évolutif, liant la distribution des effets des mutations et les conditions environnementales.

L'intégration de cette dépendance de la mutation aux contextes génétiques et environnementaux dans des modèles éco-évolutifs a été rendue possible par la dérivation de deux modèles de sauvetage évolutifs, considérant des régimes mutationnels opposés. Ces deux modèles sont basés sur les mêmes modèles de paysage adaptatif et de démographie, mais diffèrent par leurs modèles évolutifs, l'un représentant un régime « de mutation forte » et l'autre « de mutation faible ». Cela nous a permis de comparer les capacités de persistance de populations dans des régimes mutationnels différents, dans l'espoir de couvrir des contextes biologiques allant de l'eucaryote au virus à ARN.

Malgré la perte de généralité engendrée par la séparation des modèles sous deux régimes mutationnels, les deux théories développées s'appliquent potentiellement à des contextes évolutifs et démographiques assez généraux. Ces approches ne sont donc pas inféodées aux scenarios écologiques simples où nous les avons détaillés (population asexuée, isolée, face à un changement abrupt). Elles peuvent *a priori* être étendues à d'autre contextes de dynamiques éco-

évolutives requérant une gestion de l'interaction entre conditions environnementales et devenir éco-évolutif des populations. Ainsi, le chapitre III présente des exemples de perspectives d'utilisation de ces modèles dans d'autres contextes, axés autour de l'impact de l'hétérogénéité de l'environnement (dans l'espace ou le temps) sur la persistance des populations.

Outre les développements théoriques des chapitre I, II et III, l'application des modèles développés à des données expérimentales était initialement l'un des objectifs de cette thèse. Malheureusement, cet objectif n'a pu être atteint de par (i) le temps nécessaire aux développements théoriques des chapitres I et II, (ii) les difficultés techniques liées à la mise en place d'un test expérimental puissant, et (iii) l'absence de données directement exploitables dans la littérature que nous avons pu trouver. Cependant, certaines données existantes ont pu être en partie analysées et comparées aux modèles, comme nous l'avons détaillé dans le chapitre III, ouvrant la voie à un test plus complet, sur des données produites dans ce but. Les sections suivantes exposent les principaux résultats obtenus puis détaillent les hypothèses et limites des différents modèles ainsi que leurs extensions potentielles.

Stress, mutation et sauvetage évolutif en environnement changeants

Stress efficace et adaptation en régime de mutation faible (SSWM)

Le modèle dérivé dans le chapitre I sous un régime de mutation faible et de sélection forte permet de modéliser la dépendance de la probabilité de sauvetage évolutif d'une population au stress, en prenant en compte les stochasticités démographiques et évolutives essentielles sous ce régime. Un changement environnemental, dans le modèle de Fisher, impacte non seulement le taux de déclin de la population, comme dans d'autres modèles dérivés sous le même régime mutationnel (Orr 2008, 2014 Uecker 2014,2016), mais également la proportion de mutations résistantes à l'origine des sauvetages évolutifs, et leur coût (donc leur fréquence à l'équilibre) dans l'environnement passé. Cette proportion de mutations résistantes dépend alors de la qualité de l'environnement (taux de croissance maximale atteignable r_{max}), de la mal-adaptation initiale de la population (distance à l'optimum initiale et taux de déclin résultant r_D), de l'intensité sélective dans l'environnement stressant (force de la sélection mise à l'échelle de la variance phénotypique mutationnelle λ), et dans une moindre mesure de la dimension du paysage

(nombre de traits déterminant l'adaptation θ). Le modèle présenté dans le chapitre I permet de réunir ces différents effets liés à un changement d'environnement en un paramètre composite dénoté « stress efficace ». L'approximation ainsi obtenue semble pouvoir être ajustée aux données de résistance à différentes doses d'antibiotiques, d'après quelques tests préliminaires décrits dans le chapitre III, ceux-ci ne donnant qu'un appui qualitatif ('proof of concept') à notre approche pour le moment. Cela est notable car ces tests n'incluent que la variation la plus simple, parmi celles qui peuvent être décrite par le modèle, du paysage avec l'environnement : un déplacement d'optimum avec le stress, toutes choses égales par ailleurs. Le fait que ce modèle suffise à prédire la forme log-log linéaire typiquement observée entre probabilité de résistance et dose, est donc encourageant. Une telle relation n'est pas prédite par les modèles de sauvetage évolutif existants où le stress n'a qu'un effet démographique direct (sans affecter la probabilité de muter vers la résistance).

Du sauvetage évolutif à la mutagénèse létale (WMSM)

Le modèle du chapitre II est dérivé sous un régime de mutation forte et de sélection faible complémentaire du régime de mutation faible et sélection forte du chapitre I. Le stress y est modélisé à l'aide du paysage adaptatif de Fisher de la même manière que dans le chapitre I. En revanche, le modèle du chapitre II prend en compte l'apparition de mutations multiples en faisant l'hypothèse d'une évolution déterministe. Ceci nous a permis de modéliser un continuum, lorsque le taux de mutation augmente, allant du sauvetage évolutif par adaptation au stress (sous l'effet d'accumulations de mutations bénéfiques) à la mutagénèse létale, où l'extinction des populations est causée par l'accumulation de mutations délétères. Ce continuum, s'il semble assez intuitif, et s'applique probablement au-delà du modèle de Fisher, est toutefois plus complexe qu'il n'y parait. Un modèle arbitraire sans épistasie par exemple ne donne pas ce résultat, même si mutations délétères et bénéfiques ségrégent conjointement, car il n'inclut pas la possibilité d'un équilibre-mutation sélection dans l'environnement stressant (un fardeau créant la possibilité d'une extinction).

De par ce continuum, les résultats du chapitre II permettent de déterminer les conditions environnementales et de taille initiale de population pour lesquelles l'évolution de la résistance est très improbable, quel que soit le taux de mutation, donc robustes à la potentielle évolution de ce taux de mutation. Les modèles évolutifs et démographiques utilisés pour dériver le modèle du

chapitre II permettent également de suivre les dynamiques transitoires éco-évolutives d'une population subissant un changement d'environnement. Ces dynamiques transitoires sont très informatives sur le processus de sauvetage évolutif mais restent peu traitées dans la littérature. L'étude des dynamiques transitoires nous as permis de montrer une forte dépendance de la probabilité de sauvetage évolutif à la taille minimale de la population (comme prédit heuristiquement par Gomulkiewicz and Holt 1995). De plus, la distribution des temps d'extinction dérivée à partir de ces dynamiques permet de mettre en évidence des combinaisons de taux de mutation et de stress pour lesquels la probabilité d'extinction est certaine en temps infini, mais pour lesquels la durée avant extinction de 90% des populations se révèle très longue. Ce résultat montre ainsi une limite des modèles considérant uniquement le comportement en temps long lorsque les changements environnementaux ne sont pas permanents (comme les traitements anti-pathogènes).

Hétérogénéité de l'environnement

L'hétérogénéité temporelle, de même que l'hétérogénéité spatiale de l'environnement, sont des scénarios que nous n'avons pas traités dans les chapitres I et II. La complexité du processus démographique et évolutif dans ce contexte hétérogène a été soulignée dans des modèles couplant démographie et adaptation (Débarre *et al.* 2013) sous des hypothèses proches de celles décrite dans le chapitre III, et plus généralement dans les dynamiques éco-évolutives en environnements fragmentés (pour une revue voir Legrand *et al.* 2017). Le chapitre III dépeint brièvement certaines perspectives de modélisation en environnement hétérogène associées aux outils développés au cours de cette thèse. Les résultats préliminaires les plus aboutis, utilisant le modèle du chapitre I, montrent un effet positif ou négatif de la dispersion en fonction de l'hétérogénéité des stress présents dans l'environnement. D'autres résultats, moins aboutis, montrent qu'il est a priori possible, à l'aide des outils du chapitre II, de dériver des modèles analytiques d'invasions, de source-puit ou de changement temporel de l'environnement dans le cadre de paysages de Fisher, hétérogènes dans l'espace 'réel'.

Critiques et perspectives théoriques

L'ensemble des résultats évoqués ici ont été validés par le biais de simulations individus-centrées et présentent une bonne précision dans les deux régimes limites des chapitres I et II. Dans la section suivante, nous rappelons ces limites et proposons des moyens de relâcher les hypothèses de ces modèles, et de les étendre à d'autres contextes évolutifs et écologiques.

Régimes de mutation intermédiaires

Les régimes de mutations couverts par les chapitres I et II sont complémentaires et explorent les deux extrêmes d'un continuum allant de l'adaptation via une mutation d'effet fort à l'adaptation ou mal-adaptation par l'accumulation d'un grand nombre de mutations d'effets faibles. Nous avons pu montrer que les modèles dérivés dans les chapitres I et II donnent des résultats proches des résultats de simulations individus centrées pour la probabilité de sauvetage évolutif dans leurs régimes respectifs ($U \ll s$ ou $U \gg s$), mais s'écartent de ces résultats en dehors de ces régimes. Ainsi, pour des régimes intermédiaires où l'adaptation est causée par un certain nombre de mutations d'effets intermédiaires ($U \sim s$), les deux modèles donnent des résultats qualitatifs corrects mais s'écartent des simulations au niveau quantitatif. Afin d'améliorer les prédictions sur la probabilité de sauvetage évolutif dans ces régimes, deux options d'extensions des chapitre I et II sont possibles. Premièrement, il est possible d'étendre le modèle du chapitre I vers des régimes de taux de mutations plus forts, en considérant l'établissement de mutations en deux pas et non plus uniquement en un seul pas. Les résultats de génétique des populations nécessaires à cette extension ont été dérivés dans Martin et al. (2013), mais l'obtention de résultats explicites dans une application au modèle de Fisher est plus difficile. Deuxièmement, en partant du régime opposé, il est possible de considérer des régimes de taux de mutation plus faible dans le modèle du chapitre II en utilisant une dynamique évolutive stochastique et non plus déterministe. Toutefois, l'introduction de la stochasticité (introduite par la mutation et la dérive) dans les dynamiques évolutives seules requiert un changement qualitatif par rapport à l'approche de Martin et Roques (2016), basée sur des équations aux dérivées partielles, nécessairement déterministes. Par ailleurs les résultats utilisés dans ce chapitre sur les processus de Feller inhomogènes (Bansaye and Simatos 2015) requièrent que les coefficients de la diffusion varient de façon déterministe, a priori, ce qui ne serait plus le cas. Au final, la première option semble donc la plus facile à implémenter.

Variations du taux de mutation

Outres les limites de chacun des deux régimes mutationnels considérés, la variation du taux de mutation au cours d'une trajectoire peut également avoir un impact significatif sur la persistance de populations asexuées isolées, pour lesquelles la mutation est la seule source de variance génétique. Le taux de mutation peut varier de façon abrupte du fait du changement environnemental ou par l'apparition de génotypes mutateurs (voir discussion chapitre II). Le modèle du chapitre I autorise le changement du taux de mutation entre environnements mais n'autorise pas la modification du taux de mutation au cours de la trajectoire de sauvetage évolutif. Dans le chapitre II en revanche, il est possible de modifier le taux de mutation de l'ensemble des génotypes à n'importe quel temps au cours de la dynamique en utilisant des résultats issus de Martin et Roques (2016), tant que le taux reste commun à tous les génotypes. Ce changement de taux de mutation ne modélise donc pas l'évolution du taux de mutation mais plutôt l'effet d'un mutagène ou du stress environnemental impactant l'ensemble des individus.

Enfin, les paramètres démographiques peuvent déterminer le taux de mutation. Un modèle de naissance et mort, en temps continu, semble une description plus réaliste des dynamiques démographiques microbiennes que le modèle en temps discret utilisé pour illustrer nos résultats. Un tel modèle est également pris en compte par la diffusion de Feller, de sorte que les résultats s'appliquent aussi dans ce cadre *a priori* (voir par ex. Martin et al. (2013), et discussion du chapitre I). Toutefois, si le taux de naissance évolue (et non uniquement le taux de mort), alors le taux de mutation peut se trouver couplé à la dynamique d'adaptation, et un modèle évolutif spécifique (modifié de Martin et Roques 2016) sera alors requis, pour le régime WSSM. Pour le régime SSWM, le taux de naissance du génotype dominant détermine le taux de mutation du modèle et aucune modification n'est requise *a priori*.

Isotropie versus anisotropie

L'hypothèse d'isotropie dans le paysage adaptatif utilisé dans les chapitres I et II est une hypothèse relativement forte et discutable dans le contexte d'apparition de résistances contre des traitements anti-pathogènes (voir discussion chapitre I). En effet, des cas d'évolutions parallèles de la même résistance à un traitement antibiotique sont souvent mis en évidence expérimentalement, avec la réponse du même gène voire du même allèle dans plusieurs réplicats

expérimentaux, d'autant plus que la dose est forte (par ex. Harmand *et al.* 2016). Modéliser ces cas d'évolutions parallèles implique d'intégrer les covariances des effets sélectifs et mutationnels entre traits phénotypiques (anisotropie), qui changent d'un gène à l'autre (modularité) de sorte que certains ont plus de chance de produire une résistance (Chevin *et al.* 2010b; Harmand *et al.* 2016). L'introduction de l'anisotropie dans les modèles des chapitres I et II représente un certain défi méthodologique et introduit surtout de nombreux autres paramètres dans les prédictions. Cependant, il est possible de relâcher l'hypothèse d'isotropie dans le cas d'une faible dimensionnalité phénotypique (Martin and Lenormand 2006). Sous cette hypothèse Martin et Lenormand (2015) ont montré que le modèle de Fisher isotrope est également robuste à une faible anisotropie dans le cadre de changements d'environnements. Dans le cas d'une anisotropie très forte, il est également possible de se rapporter à un modèle à une seule dimension en projetant les phénotypes et les fonctions de valeur sélective sur l'axe phénotypique dominant. Comme les solutions approximatives obtenues dans cette thèse deviennent exactes (chapitre I) ou plus précises (chapitre II) en une seule dimension ($\theta = 1/2$), les prédictions devraient être facilitées. La variation entre gènes reposera alors sur les différentes projections associées à leurs différents axes dominants (variation de r_{max}), et sur les différents niveaux de variance phénotypique mutationnelles λ associées à chaque gène. Le problème anisotrope est toutefois « directionnel », en ce sens que la direction vers l'optimum, et plus seulement la distance à l'optimum, pour chaque dose, influence le résultat.

Plasticité phénotypique et effets maternels

La plasticité phénotypique peut impacter (négativement ou positivement) la persistance de populations face à un changement d'environnement (Ghalambor *et al.* 2007; Chevin *et al.* 2010a, 2013). Cependant, dans le cadre de traitements antibiotiques, une forme de plasticité phénotypique est à l'origine de la persistance, sur une durée limitée, de génotypes sensibles au stress, nommés « persisteurs », à partir desquels la population peut recroître une fois le traitement antibiotique terminé (Balaban *et al.* 2004) ou qui peuvent être un tremplin vers la mutation de résistances génétiques non-plastiques. Une implémentation de la plasticité (normes de réactions linéaires), dans le cadre de modèles de sauvetages évolutifs (dynamiques éco-évolutives déterministes, sous densité dépendance), et dans un paysage de type Fisher univarié, a été proposée dans Chevin et Lande (2010) et Chevin et al. (2010a). Les résultats reposent sur

le « modèle infinitésimal gaussien » (nombreux loci non liés, phénotypes gaussiens de variance constante). Les modèles des chapitre I et II considèrent un paysage adaptatif dont les dimensions phénotypiques représentent des valeurs génétiques (« breeding values ») et intègrent donc la variance phénotypique pour un génotype donné via le paramètre λ (c.f Chapitre I pour une définition complète de λ). Cependant cette variance est la même pour tous les traits du fait de l'isotropie du modèle, et il n'y a aucune tendance dans cette forme de plasticité (aucune norme de réaction) Il serait possible d'implémenter le même modèle que proposé dans Chevin et Lande (2010), avec des normes de réactions linéaires, pour obtenir les probabilités d'émergence de résistance pour des populations asexuées (où le modèle infinitésimal ne s'applique pas). Il est aussi possible, dans le cadre du régime WSSM (chapitre II) d'utiliser les résultats déterministes de Chevin et Lande (2010) pour dériver la probabilité de sauvetage dans un cadre stochastique, pour le même modèle infinitésimal sexué (voir méthode générale dans le chapitre III).

Les effets maternels peuvent également impacter la réponse à court terme à un changement environnemental, et donc le processus de sauvetage évolutif. Des expériences de sauvetage évolutif sur des insectes (Stewart *et al.* 2017) ont montré d'importants effets maternels nécessitant d'être standardisés pour évaluer la probabilité de sauvetage évolutif sur plusieurs réplicats. Ces effets maternels peuvent *a priori,* également être importants chez des organismes unicellulaires, héritant de l'ensemble du cytoplasme de leur cellule mère, issue d'un milieu non-stressé (voir discussion Orive *et al.* 2017). Ce mécanisme pourrait être à l'origine de retards dans l'effet d'antibiotiques, observés par exemple dans (Yourassowsky *et al.* 1985), ou sur des données non publiées générées par Guillaume Martin. Il semble alors important d'obtenir des données standardisées pour les effets maternels (comme dans Stewart *et al.* 2017) pour pouvoir les comparer aux modèles des chapitres I et II, voire d'implémenter ces effets dans les modèles.

Reproduction sexuée versus asexuée

Les modèles développés dans cette thèse ne considèrent que des populations asexuées. Le choix de ce contexte évolutif est motivé par l'application à des contextes de lutte contre des pathogènes se reproduisant de manière clonale, du moins sur les durées courtes associées au processus de sauvetage évolutif. Cependant dans ce même contexte, l'échange de résistances par reproduction « sexuée » (transferts horizontaux de plasmides) n'est pas à négliger. En effet, l'impact de la reproduction sexuée et de la recombinaison/ségrégation sur la persistance de

populations face à un changement d'environnement a récemment été mis en évidence par plusieurs modèles. Dans le cadre classique des modèles de sauvetage de type SSWM, dans lesquels la résistance est encodée par un ou deux locus bi alléliques (Uecker and Hermisson 2016; Uecker 2017) ou dans un modèle déterministe supposant de nombreux loci non liés (modèle infinitésimal gaussien), avec une clonalité partielle (Orive *et al.* 2017). Les avantages et inconvénients de la reproduction sexuée dépendent du mode de reproduction sexuée (autogamie *versus* allogamie) ainsi que du taux de recombinaison (Uecker and Hermisson 2016; Uecker 2017).

Il est a priori aisé d'implémenter, comme dans le chapitre II, des dynamiques stochastiques de sauvetage évolutif dans le cadre du modèle infinitésimal, donc pour des populations sexuées (nombreux loci non liés). Pour cela il est nécessaire d'implémenter une trajectoire du taux de croissance moyen de la population qui soit déterministe et hors-équilibre tel que décrit dans le chapitre III. On peut par exemple utiliser directement la trajectoire de la valeur sélective moyenne dérivée dans Gomulkiewicz et Holt (1995) (voir chapitre III) ou exploiter les dynamiques déterministes dérivées dans l'eq. 6 de (Orive 2017) en présence d'une clonalité partielle. On étendrait alors ces résultats existants à un cadre stochastique, et on obtiendrait les distributions des temps d'extinction dans ces scenarios.

Rétroactions entre écologie et évolution

Les approches décrites dans cette thèse ne considèrent que l'influence de l'évolution sur la démographie et non l'inverse. Les boucles de rétroactions entre écologie et évolution sont d'importants processus à prendre en compte dans la modélisation de certaines dynamiques éco-évolutives (voir Introduction ; Pelletier *et al.* 2009; Lowe *et al.* 2017). Ces boucles de rétroactions ont un impact significatif sur la persistance des populations, lorsque diverses formes de densité-dépendance ou fréquence dépendance sont en jeu. Elles peuvent engendrer des cas de « suicide évolutif » (ou l'évolution n'empêche plus mais cause l'extinction) tel que modélisé dans Ferrière et Legendre (2013). La modélisation de ces rétroactions nécessite donc la prise en compte de ces processus de densité-dépendance ou de fréquence-dépendance, souvent modélisés dans le cadre de la théorie de la dynamique adaptative (« adaptive dynamics ») (Ferriere and Legendre 2013). Dans les modèles de cette thèse, la difficulté de l'implémentation de la fréquence-dépendance relève plus d'un problème conceptuel que méthodologique. En effet, le modèle de Fisher ne

permet pas directement de modéliser la fréquence-dépendance : le paysage est fixé pour un environnement donné, quels que soient les génotypes en présence. Il existe dans la littérature des formulations générales de dynamiques intégrant la fréquence-dépendance dans des paysages adaptatifs, via des kernels de compétition entre phénotypes différents, en plus d'une forme de sélection stabilisante ou directionnelle sur les phénotypes (Nordbotten and Stenseth 2016). Toutefois, les résultats qualitatifs de ces modèles sur l'existence ou l'unicité de masses de distributions phénotypiques (espèces multiples ou unique) ne sont donnés qu'à l'équilibre. Les dynamiques en temps, hors état stationnaire, utilisables dans le cadre du sauvetage évolutif ne sont pas traitées. Par contre, des modèles plus simples incluant une forme de densité-dépendance (type logistique) peuvent être implémentés dans le modèle du chapitre II. Toutefois, le couplage avec la dynamique démographique devrait être fait sur la base de la trajectoire déterministe des tailles de population, alors que celles-ci sont stochastiques dans le modèle (la stochasticité démographique n'était pas négligée jusqu'ici). Les résultats du chapitre II (Supplementary Figure 6) suggèrent que ces prédictions déterministes capturent assez bien la trajectoire de l'espérance de la taille de population parmi les réplicats stochastiques. Il est donc possible que l'approche soit pertinente dans les cas où cette espérance est suffisante pour prédire les effets de densité-dépendance.

Changement environnemental abrupt versus graduel

Au cours de cette thèse nous nous sommes focalisés sur la persistance de populations asexuées face à des changements environnementaux abrupts. D'après Estes et Arnold (2007), les modèles considérant un changement d'optimum abrupt sont les plus à mêmes de s'ajuster sur des données d'évolution à très long terme (données paléontologiques), mais il n'est pas assuré que le même patron soit observé dans des cas de sauvetage évolutif ayant lieu sur de courts pas de temps. En effet, ces changements abrupts font écho aux traitements antibiotiques créant des stress immédiats et très forts sur des populations de pathogènes. Cette vision simplifiée de l'effet d'un traitement anti-pathogène peut s'appliquer à des tests expérimentaux in vitro mais néglige une grande partie de la pharmacodynamique associée à l'effet d'un antibiotique au sein d'un hôte (Gunderson *et al.* 2001; Regoes *et al.* 2004). Afin de pouvoir rendre compte de l'effet de la variation dynamique de l'environnement sur la persistance de populations, il est nécessaire de considérer un optimum mobile (par ex. Burger and Lynch 1995; Ferrière *et al.* 2004; Bertram *et*

al. 2017). Il est possible de considérer un optimum mobile dans le contexte évolutif du chapitre II, mais ces développements restent à implémenter.

Optimum unique versus optimums multiples

Dans la littérature sur les traitements antibiotiques il est courant de considérer des combinaisons de plusieurs traitements dans le but d'éradiquer des populations de pathogènes. Dans le cadre de traitements successifs, le modèle du chapitre II permet de prédire les dynamiques évolutives et démographiques de la population en fonction du temps auquel apparaît le second traitement, tel que décrit dans le chapitre III. En revanche, la modélisation d'une combinaison de traitements appliqués conjointement implique de connaître les effets combinés de stress qui ne sont pas nécessairement additifs (synergisme ou antagonisme). Pour cela il est nécessaire de conceptualiser ces effets dans le cadre d'un modèle de paysage adaptatif, c'est-à-dire de déterminer comment les optimums associés à chaque traitement/concentration déterminent la fonction de valeur sélective résultant d'une combinaison de ces deux traitements/concentrations.

Conclusion générale

L'objet de cette thèse était l'étude de la capacité de persistance des populations asexuées face à des conditions environnementales fortement stressantes. Les changements environnementaux stressants peuvent être étudiés sur de nombreux organismes, dans des contextes de conservation ou d'éradication. Cependant, en prenant un peu de recul, on s'aperçoit rapidement que les conditions environnementales imposées aux pathogènes à travers des traitements antibiotiques, représentent des stress difficilement comparables à ceux, plus « doux », subis par d'autres organismes, par exemple étudiés dans le cadre de la conservation. En effet, les antibiotiques sont conçus pour éradiquer la quasi-totalité des individus des populations de pathogènes en seulement quelques générations, (sans pour autant être trop toxiques pour l'hôte). Néanmoins, dans ces deux situations, pour modéliser le sauvetage évolutif, il est nécessaire de prendre en compte les interactions entre le potentiel de résistance des populations et les effets stressants des changements environnementaux.

Nous avons choisi dans cette thèse de modéliser ces interactions essentielles dans la persistance ou l'éradication d'un pathogène en utilisant le paysage adaptatif de Fisher, afin de créer un cadre théorique réaliste pour l'étude des traitements antibiotiques (même si nos résultats n'excluent pas le cadre de la conservation). Nous focaliserons donc ici notre conclusion sur ce contexte.

Les résultats des modèles développés dans ce cadre nous ont permis de montrer des variations très fortes des capacités de persistance des populations asexuées face à de faibles variations dans les conditions environnementales. Ces résultats, appliqués aux traitements anti-pathogènes, suggèrent que de faibles variations dans les doses peuvent faire la différence entre innocuité et éradication. A l'inverse, les résultats des modèles montrent également que des conditions environnementales suffisamment stressantes peuvent empêcher l'apparition de résistance quel que soit le taux de mutation des organismes visés. Les traitements de virus ou de cancer, supposés rendus inefficaces par des taux de mutation très variables chez ces « organismes », sembleraient donc possiblement efficace, d'après ces résultats, si des traitements produisant effectivement ce niveau de stress existent et sont supportés par l'hôte. Cependant, les résultats de cette thèse, sans confrontation à des données empiriques, sont à nuancer, et restent loin des conditions des traitements antibiotiques du domaine médical, bien évidemment.

Néanmoins, ces résultats semblent indiquer que le développement d'un cadre théorique éco-évolutif, axé autour d'un paysage adaptatif, est un bon moyen de rendre compte de certains patrons d'interactions complexes entre les contextes génétiques et environnementaux. Il serait donc intéressant, dans l'explosion actuelle de la littérature traitant des dynamiques éco-évolutives, d'inclure les paysages adaptatifs comme « traducteurs » des « informations » échangées entre les processus écologiques et évolutifs. Ceci permettrait peut-être, en réponse à la citation récente de Hendry (2016) : *"Research initiatives in ecology and evolution have periodically dated but never married"* , de pousser l'un ou l'autre des deux partis à faire sa demande.

Bibliography

Balaban N. Q., Merrin J., Chait R., Kowalik L., Leibler S., 2004 Bacterial Persistence as a Phenotypic Switch. Science 305: 1622–1625.

Bansaye V., Simatos F., 2015 On the scaling limits of Galton-Watson processes in varying environments. Electron. J. Probab. 20.

Bertram J., Gomez K., Masel J., 2017 Predicting patterns of long-term adaptation and extinction with population genetics. Evolution 71: 204–214.

Burger R., Lynch M., 1995 Evolution and Extinction in a Changing Environment: A Quantitative-Genetic Analysis. Evolution 49: 151.

Chevin L.-M., Lande R., Mace G. M., 2010a Adaptation, Plasticity, and Extinction in a Changing Environment: Towards a Predictive Theory. PLOS Biol. 8: e1000357.

Chevin L.-M., Lande R., 2010 When Do Adaptive Plasticity and Genetic Evolution Prevent Extinction of a Density-Regulated Population? Evolution 64: 1143–1150.

Chevin L.-M., Martin G., Lenormand T., 2010b Fisher's Model and the Genomics of Adaptation: Restricted Pleiotropy, Heterogenous Mutation, and Parallel Evolution. Evolution 64: 3213–3231.

Chevin L.-M., Gallet R., Gomulkiewicz R., Holt R. D., Fellous S., 2013 Phenotypic plasticity in evolutionary rescue experiments. Philos. Trans. R. Soc. Lond. B Biol. Sci. 368: 20120089.

Débarre F., Ronce O., Gandon S., 2013 Quantifying the effects of migration and mutation on adaptation and demography in spatially heterogeneous environments. J. Evol. Biol. 26: 1185–1202.

Estes S., Arnold S. J., 2007 Resolving the Paradox of Stasis: Models with Stabilizing Selection Explain Evolutionary Divergence on All Timescales. Am. Nat. 169: 227–244.

Ferrière R., Dieckmann U., Couvet D., 2004 *Evolutionary conservation biology*. Cambridge University Press, Cambridge, UK; New York.

Ferriere R., Legendre S., 2013 Eco-evolutionary feedbacks, adaptive dynamics and evolutionary rescue theory. Phil Trans R Soc B 368: 20120081.

Ghalambor C. K., McKAY J. K., Carroll S. P., Reznick D. N., 2007 Adaptive versus non-adaptive phenotypic plasticity and the potential for contemporary adaptation in new environments. Funct. Ecol. 21: 394–407.

Gomulkiewicz R., Holt R. D., 1995 When does Evolution by Natural Selection Prevent Extinction? Evolution 49: 201.

Gunderson B. W., Ross G. H., Ibrahim K. H., Rotschafer J. C., 2001 What Do We Really Know About Antibiotic Pharmacodynamics? Pharmacother. J. Hum. Pharmacol. Drug Ther. 21: 302S–318S.

Harmand N., Gallet R., Jabbour-Zahab R., Martin G., Lenormand T., 2016 Fisher's geometrical model and the mutational patterns of antibiotic resistance across dose gradients. Evolution: n/a-n/a.

Hendry A. P., 2016 *Eco-evolutionary Dynamics*. Princeton University Press.

Legrand D., Cote J., Fronhofer E. A., Holt R. D., Ronce O., *et al.*, 2017 Eco-evolutionary dynamics in fragmented landscapes. Ecography 40: 9–25.

Lowe W. H., Kovach R. P., Allendorf F. W., 2017 Population Genetics and Demography Unite Ecology and Evolution. Trends Ecol. Evol. 32: 141–152.

Martin G., Lenormand T., 2006 A General Multivariate Extension of Fisher's Geometrical Model and the Distribution of Mutation Fitness Effects Across Species. Evolution 60: 893–907.

Martin G., Aguilée R., Ramsayer J., Kaltz O., Ronce O., 2013 The probability of evolutionary rescue: towards a quantitative comparison between theory and evolution experiments. Phil Trans R Soc B 368: 20120088.

Martin G., Lenormand T., 2015 The fitness effect of mutations across environments: Fisher's geometrical model with multiple optima. Evolution 69: 1433–1447.

Martin G., Roques L., 2016 The Non-stationary Dynamics of Fitness Distributions: Asexual Model with Epistasis and Standing Variation. Genetics: genetics.116.187385.

Nordbotten J. M., Stenseth N. C., 2016 Asymmetric ecological conditions favor Red-Queen type of continued evolution over stasis. Proc. Natl. Acad. Sci. 113: 1847–1852.

Orive M. E., Barfield M., Fernandez C., Holt R. D., 2017 Effects of Clonal Reproduction on Evolutionary Lag and Evolutionary Rescue. Am. Nat.: 000–000.

Pelletier F., Garant D., Hendry A. P., 2009 Eco-evolutionary dynamics. Philos. Trans. R. Soc. Lond. B Biol. Sci. 364: 1483–1489.

Regoes R. R., Wiuff C., Zappala R. M., Garner K. N., Baquero F., *et al.*, 2004 Pharmacodynamic Functions: a Multiparameter Approach to the Design of Antibiotic Treatment Regimens. Antimicrob. Agents Chemother. 48: 3670–3676.

Stewart G. S., Morris M. R., Genis A. B., Szűcs M., Melbourne B. A., *et al.*, 2017 The power of evolutionary rescue is constrained by genetic load. Evol. Appl. 10: 731–741.
Uecker H., Hermisson J., 2016 The Role of Recombination in Evolutionary Rescue. Genetics 202: 721–732.
Uecker H., 2017 Evolutionary rescue in randomly mating, selfing, and clonal populations. Evolution 71: 845–858.
Yourassowsky E., Van der Linden M. P., Lismont M. J., Crokaert F., Glupczynski Y., 1985 Correlation between growth curve and killing curve of Escherichia coli after a brief exposure to suprainhibitory concentrations of ampicillin and piperacillin. Antimicrob. Agents Chemother. 28: 756–760.

Bertram J., Gomez K., Masel J., 2017 Predicting patterns of long-term adaptation and extinction with population genetics. Evolution 71: 204–214.
Burger R., Lynch M., 1995 Evolution and Extinction in a Changing Environment: A Quantitative-Genetic Analysis. Evolution 49: 151.
Chevin L.-M., Lande R., Mace G. M., 2010a Adaptation, Plasticity, and Extinction in a Changing Environment: Towards a Predictive Theory. PLOS Biol. 8: e1000357.
Chevin L.-M., Lande R., 2010 When Do Adaptive Plasticity and Genetic Evolution Prevent Extinction of a Density-Regulated Population? Evolution 64: 1143–1150.
Chevin L.-M., Martin G., Lenormand T., 2010b Fisher's Model and the Genomics of Adaptation: Restricted Pleiotropy, Heterogenous Mutation, and Parallel Evolution. Evolution 64: 3213–3231.
Chevin L.-M., Gallet R., Gomulkiewicz R., Holt R. D., Fellous S., 2013 Phenotypic plasticity in evolutionary rescue experiments. Philos. Trans. R. Soc. Lond. B Biol. Sci. 368: 20120089.
Débarre F., Ronce O., Gandon S., 2013 Quantifying the effects of migration and mutation on adaptation and demography in spatially heterogeneous environments. J. Evol. Biol. 26: 1185–1202.
Drlica K., 2003 The mutant selection window and antimicrobial resistance. J. Antimicrob. Chemother. 52: 11–17.
Engelstädter J., 2014 Fitness landscapes emerging from pharmacodynamic functions in the evolution of multidrug resistance. J. Evol. Biol. 27: 840–853.
Estes S., Arnold S. J., 2007 Resolving the Paradox of Stasis: Models with Stabilizing Selection Explain Evolutionary Divergence on All Timescales. Am. Nat. 169: 227–244.
Ferrière R., Dieckmann U., Couvet D., 2004 *Evolutionary conservation biology*. Cambridge University Press, Cambridge, UK; New York.
Ferriere R., Legendre S., 2013 Eco-evolutionary feedbacks, adaptive dynamics and evolutionary rescue theory. Phil Trans R Soc B 368: 20120081.
Ghalambor C. K., McKAY J. K., Carroll S. P., Reznick D. N., 2007 Adaptive versus non-adaptive phenotypic plasticity and the potential for contemporary adaptation in new environments. Funct. Ecol. 21: 394–407.
Gomulkiewicz R., Holt R. D., 1995 When does Evolution by Natural Selection Prevent Extinction? Evolution 49: 201.
Gunderson B. W., Ross G. H., Ibrahim K. H., Rotschafer J. C., 2001 What Do We Really Know About Antibiotic Pharmacodynamics? Pharmacother. J. Hum. Pharmacol. Drug Ther. 21: 302S–318S.
Harmand N., Gallet R., Jabbour-Zahab R., Martin G., Lenormand T., 2016 Fisher's geometrical model and the mutational patterns of antibiotic resistance across dose gradients. Evolution: n/a-n/a.
Legrand D., Cote J., Fronhofer E. A., Holt R. D., Ronce O., *et al.*, 2017 Eco-evolutionary dynamics in fragmented landscapes. Ecography 40: 9–25.
Lowe W. H., Kovach R. P., Allendorf F. W., 2017 Population Genetics and Demography Unite Ecology and Evolution. Trends Ecol. Evol. 32: 141–152.
Martin G., Lenormand T., 2006 A General Multivariate Extension of Fisher's Geometrical Model and the Distribution of Mutation Fitness Effects Across Species. Evolution 60: 893–907.
Martin G., Aguilée R., Ramsayer J., Kaltz O., Ronce O., 2013 The probability of evolutionary rescue: towards a quantitative comparison between theory and evolution experiments. Phil Trans R Soc B 368: 20120088.
Martin G., Lenormand T., 2015 The fitness effect of mutations across environments: Fisher's geometrical model with multiple optima. Evolution 69: 1433–1447.
Martin G., Roques L., 2016 The Non-stationary Dynamics of Fitness Distributions: Asexual Model with Epistasis and Standing Variation. Genetics: genetics.116.187385.

Orive M. E., Barfield M., Fernandez C., Holt R. D., 2017 Effects of Clonal Reproduction on Evolutionary Lag and Evolutionary Rescue. Am. Nat.: 000–000.

Pelletier F., Garant D., Hendry A. P., 2009 Eco-evolutionary dynamics. Philos. Trans. R. Soc. Lond. B Biol. Sci. 364: 1483–1489.

Regoes R. R., Wiuff C., Zappala R. M., Garner K. N., Baquero F., *et al.*, 2004 Pharmacodynamic Functions: a Multiparameter Approach to the Design of Antibiotic Treatment Regimens. Antimicrob. Agents Chemother. 48: 3670–3676.

Stewart G. S., Morris M. R., Genis A. B., Szűcs M., Melbourne B. A., *et al.*, 2017 The power of evolutionary rescue is constrained by genetic load. Evol. Appl. 10: 731–741.

Uecker H., Hermisson J., 2016 The Role of Recombination in Evolutionary Rescue. Genetics 202: 721–732.

Uecker H., 2017 Evolutionary rescue in randomly mating, selfing, and clonal populations. Evolution 71: 845–858.

Résumé :

La capacité de persistance d'une population face à un changement environnemental stressant est une question complexe à l'interface entre l'écologie et l'évolution. Le processus par lequel une population échappe à l'extinction en s'adaptant aux nouvelles conditions environnementales stressantes est nommé sauvetage évolutif. Ce cas particulier de dynamique éco-évolutive est de plus en plus étudié autant théoriquement qu'expérimentalement, entre autres dans le contexte des changements environnementaux d'origines anthropiques. Cependant, les études modélisant ce processus négligent les interactions entre génotypes et environnements, qui impactent le potentiel évolutif des populations face aux changements environnementaux. Dans le cadre de cette thèse, j'ai développé des modèles intégrant ces interactions. Pour cela, j'ai modélisé le processus de sauvetage évolutif de populations à reproduction asexuée, face à des changements environnementaux abrupts, en utilisant le paysage adaptatif de Fisher (modèle géométrique de Fisher (1930)). Ce paysage nous a permis de modéliser ces interactions génotypes-environnements et leur impact sur la proportion de mutations pouvant sauver une population. A travers deux modèles, considérant soit le sauvetage d'une population par une mutation d'effet fort, soit par un grand nombre de mutations d'effets faibles, nous avons pu dégager des prédictions pour la probabilité de sauvetage évolutif en fonction des conditions environnementales et des caractéristiques de l'organisme étudié. Ces modèles peuvent être paramétrés sur des données d'évolution expérimentale et leurs prédictions comparées à des données de traitement antibiotiques visant des pathogènes asexués. Au-delà du sauvetage évolutif, les modèles développés nous ont également permis d'établir des outils permettant de modéliser d'autres dynamiques éco-évolutives, intégrant des interactions génotype-environnement et leurs effets sur la distribution d'effets des mutations.

Mots-clefs : Sauvetage évolutif – Paysages adaptatifs – Dynamiques éco-évolutives – Mutation – Asexué

Summary:

The ability of a population to persist when facing a stressing environmental change is a complex question at the interface between ecology and evolution. The process by which a population avoids extinction by adapting to the new stressing environmental conditions is termed evolutionary rescue. This particular case of eco-evolutionary dynamic is increasingly investigated both theoretically and experimentally, among other things in the context of the environmental changes caused by human activity. However, the studies modeling this process neglect the interactions between genotypes and environments that impact the evolutionary potential of the populations facing environmental changes. In the context of this thesis, I developed models integrating these interactions. To this end, I modeled the process of evolutionary rescue in asexual populations facing abrupt environmental changes, using the adaptive landscape of Fisher (Fisher's geometric model (1930)). This landscape allowed us to model the genotypes-environments interactions and their impact on the proportion of mutations needed to save a population. Using two models, considering either the rescue of a population by a single mutation of strong effect, orby a large number of mutations of small effect, we derived predictions for the probability of evolutionary rescue, which depends on the environmental conditions and the characteristics of the studied organism. These models can be parametrized on data from evolutionary experiments and their predictions compared to data of antibiotic treatments used against asexual pathogens. Beyond evolutionary rescue, the models developed in this thesis also give tools to model other eco-evolutionary dynamics, integrating genotype-environment interactions and their effects on the distribution of mutations effects.

Key-words: Evolutionary rescue – Adaptive landscapes – Eco-evolutionary dynamics – Mutation – Asexual